THE LIVING AORTIC VALVE

A thesis submitted to the University of London for the degree of

Doctor of Philosophy

by

Ismail El-Hamamsy

July 2010

Harefield Heart Science Center

National Heart and Lung Institute

Imperial College London

"If I have seen ~~further~~, it is by standing on the shoulders of giants"

- Adapted from Isaac Newton

ABSTRACT

Aortic valve disease represents a leading cause of morbidity and mortality for patients with cardiovascular disease. The number of patients requiring aortic valve replacement is in fact expected to triple within the next 40 years. To date, surgical valve replacement represents the only option for patients with aortic valve disease. No treatments exist to slow down or reverse the disease process. This is in large part due to the fact that for a long time, aortic valves were thought to be passive flaps which open and close in responses to changes in transvalvular pressures. However, recent data suggests that aortic valves are dynamic structures with a complex, yet well-preserved macro- and microstructure and unique features which differentiate it from surrounding structures. In light of these findings, we sought to further evaluate the intricate structure and function of the aortic valve. Our hypothesis was that as a living organ, aortic valves will have the capacity to modulate their own properties, to regulate structural changes within them, thus affecting their overall function.

The aims of this work were to investigate the structural complexity of the aortic valve at a cellular level, to evaluate the role of aortic valve endothelium in actively regulating valve calcification and modulating valve mechanical properties. We will also seek to evaluate the adaptive properties of heart valves in response to their biomechanical and biochemical environment and the role of a living valve substitute on aortic root flow dynamics. Finally, the clinical implications of a living valve will be highlighted through results of a clinical trial evaluating outcomes following the Ross procedure, the only operation which guarantees long-term viability of the aortic valve.

Our findings support the notion that the aortic valve is a dynamic and living structure. Its unique location which exposes it to a variety of side specific hemodynamic and mechanical stresses leads to significant structural and functional adaptive responses on either side of the valve. These responses are operative in physiological conditions but

also appear to affect pathological processes within the valve, which could partly explain the pathophysiology of aortic valve disease. In addition, our findings show that aortic valves adapt to their environment by modifying their mechanical properties, in particular their overall stiffness. This could have a major impact on the patterns of flow within the aortic root and stress distribution on the cusps. Using patient-specific computational modelling of aortic root flow dynamics, we show that a living aortic valve following aortic valve replacement such as with the Ross procedure, results in a pattern of flow which closely resembles that of normal subjects. In contrast, non-living valve substitutes such as homografts and xenografts do not provide similar results. Clinically, these differences play an important role as shown in a randomized clinical trial comparing autografts to homografts showing improved survival following autograft root replacement, along with other clinically-relevant endpoints.

In conclusion, the aortic valve is a living, dynamic organ with unique features and intricate complexity which allows it to adapt to its complex hemodynamic and biomechanical environment and ensure adequate function. The clinical relevance of a living valve substitute in patients requiring aortic valve replacement is confirmed and highlights the importance of developing tissue-engineered heart valve substitutes. Additional work is required to further understand the molecular complexity of heart valves and understand their immediate impact in the body through new in vivo functional imaging techniques.

TABLE OF CONTENTS

LIST OF FIGURES

LIST OF TABLES

ACKNOWLEDGEMENTS

No words can express my gratitude to my supervisors: Professor Magdi Yacoub, Dr. Adrian Chester and Dr. Patricia Taylor. Over the course of 4 fantastic years, I have learned more things than I could have imagined at the outset. The lessons learned extend beyond research practice. This section is too short to detail them; suffice to say I have learned by witnessing the passion for science, the dedication to hard work, the humanity at work and the humility in learning. These lessons transcend science and practice. I hope to be worthy of your trust in continuing this legacy.

As I write this page, many memories spring to mind of the long hours spent in the lab learning many new techniques. This would have been impossible without the dedication and selfless generosity of Lucy Clark and Padmini Sarathchandra. I am greatly indebted to them for every practical knowledge that I have acquired. In addition to being exceptional teachers, they were great company. I wish you all the best in your continuing endeavours and hope we can stay in touch for many years to come.

My thoughts and gratitude also go to my lab colleagues and friends, particularly Francesca Colazzo and Wenfang Meng, who made every day and every conversation a great entertainment. Their human qualities, their generosity and their work ethic were always a source of inspiration.

Finally, as I embark on a new stage in my career as a a surgeon-scientist, I look back at these 4 years with great pride and excitement to use the tools I was given and the drive to look further into my new practice.

Last but not least, none of this would have been possible without the love, support and encouragements from my beloved family and close friends. To all of them, a huge thank you!

DECLARATION

I hereby declare that this thesis is my own work and that it has not been submitted anywhere else for any award. Where other sources of information have been used they have been cited.

Ismail El-Hamamsy, June 2010

LIST OF PUBLICATIONS

1. ***El-Hamamsy I***, Eryigit Z, Stevens LM, Sarang Z, George R, Clark L, Melina G, Takkenberg JJM, Yacoub MH. Long-Term Outcomes Following Autograft versus Homograft Aortic Root Replacement in Adults - A Prospective Randomized Trial. *The Lancet (in press).*

2. Yacoub MH and ***El-Hamamsy I***. Intervention: The private life of tissue valves. *Nat Rev Cardiol (in press).*

3. ***El-Hamamsy I***, Clark L, Stevens LM, Sarang Z, Melina G, Yacoub MH. Late outcomes following Freestyle versus Homograft aortic root replacement: Results from a prospective randomized trial. *J Am Coll Cardiol* 2010;55:368-76.

4. Miragoli M, Moshkov A, Novak P, Shevchuk A, Nikolaev VO, ***El-Hamamsy I***, Potter C, Lyon A, HArding SE, Mitchell J, Chester AH, Lab M, Korchev Y, Gorelik J. The scanning ion conductance microscopy: a convergent high-resolution technology for multiparametric analysis of living cardiovascular cells. *Cardiovasc Res (submitted).*

5. ***El-Hamamsy I***, Yacoub MH. The cellular and molecular mechanisms of thoracic aortic aneurysms. *Nat Rev Cardiol* 2009;6:771-86.

6. ***El-Hamamsy I***, Zaki M, Stevens LM, Clark L, Rubens M, Yacoub MH. Rate of progression and functional significance of aortic valve and root calcification up to 8 years following total aortic root replacement using a homograft versus freestyle prosthesis: Results from a prospective randomized trial. *Circulation* 2009;120:S269-75.

7. ***El-Hamamsy I***, Balachandran K, Yacoub MH, Stevens LM, Sarathchandra P, Taylor PM, Yoganathan A, Chester AH. Endothelial-dependent regulation of aortic valve mechanical properties. *J Am Coll Cardiol* 2009;53:1448-55.

8. ***El-Hamamsy I***, Yacoub MH. A measured approach to the management of the aortic root in patients with bicuspid aortic valve disease. *Curr Cardiol Rep* 2009;11:94-100.

9. ***El-Hamamsy I***, Chester AH, Yacoub MH. Cellular regulation of the structure and function of aortic valves. *J Adv Res* 2009;1:5-12.

10. ***El-Hamamsy I***, Yacoub MH, Chester AH. Neuronal regulation of aortic valve cusps. *Curr Vasc Pharmacol* 2009;7:40-6.

11. ***El-Hamamsy I*** and Yacoub MH. Repair, AVR, Ross: How I approach the child with missed aortic stenosis/aortic insufficiency. *Semin Thorac Cardiovasc Surg Pediatr Card Surg Annu* 2009;1:133-8.

12. Chambers J, Zhao J, Terracciano C, Bezzina C, Zhang W, Kaba R, Navaratnarajah M, Lotlikar A, Sehmi J, Kooner M, Deng G, Siedlecka U, ***El-Hamamsy I***, WassM, Dekker L, de Jong J, Sternberg M, McKenna W, Severs N, de Silva R, Wilde A, Anand P, Yacoub M, Scott J, Elliott P, Wood J, Kooner J. Genetic variation in *SCN10A* influences cardiac conduction. *Nat Genet* 2010;42:149-52

13. ***El-Hamamsy I***, Willerson JT, Yacoub MH. Preserved homograft function 32 years following surgery in a young patient. *J Thorac Cardiovasc Surg* 2010;139:e141-2.

14. Melina G, ***El-Hamamsy I***, Sinatra R, Yacoub MH. Late fulminant pulmonary valve endocarditis after the Ross procedure. *J Thorac Cardiovasc Surg* 2010;139:e99-e100

ABSTRACTS

1. ***El-Hamamsy I***, Sarang Z, Patel R, Sarathchandra P, Taylor PM, Yacoub MH. Side-dependent regulation of aortic valve calcification. 4th Biennial Heart Valve Biology and Tissue Engineering Meeting – Hilton Head, USA 2009.

   (Nominated for the Young Investigator Award)

2. ***El-Hamamsy I***, Torii R, Eyrigit Z, Mittal T, Yacoub MH. Late aortic root biomechanics following the Ross procedure. 4th Biennial Heart Valve Biology and Tissue Engineering Meeting – Hilton Head, USA 2009.

3. ***El-Hamamsy I***, Clark L, Stevens LM, Sarang Z, Melina G, Yacoub MH. Late outcomes following Freestyle versus Homograft aortic root replacement: Results from a prospective randomized trial. Scientific Sessions, American Heart Association – Orlando, USA 2009.

4. ***El-Hamamsy I***, Eryigit Z, Kilner P, Mittal T, Yacoub MH. Evaluation of the shape and function of the pulmonary autograft root 10 or more years after the Ross procedure. Society for Heart Valve Disease – 5th Biennial Meeting – Berlin, Germany 2009.

5. ***El-Hamamsy I***, Balachandra K, Stevens LM, Sarathchandra P, Taylor PM, Yacoub MH, Chester AH. Aortic valve mechanical properties are regulated by the cellular components of the valve. 3rd Biennial Heart Valve Biology and Tissue Engineering Meeting – London, UK 2008.

6. ***El-Hamamsy I***, Zaki M, Stevens LM, Clark L, Rubens M, Yacoub MH. Rate of progression and functional significance of aortic valve and root calcification up to 8 years following total aortic root replacement using a homograft versus freestyle prosthesis: Results from a prospective randomized trial. Scientific Sessions, American Heart Association – New Orleans, USA 2008.

7. ***El-Hamamsy I***, Latif N, Meng W, Srathchandra P, Taylor P, Yacoub MH, Chester A. calcification potential of porcine aortic valves and identification of cells involved. Society for Heart Valve Disease – 4th Biennial Meeting – New York, USA 2007.

8. ***El-Hamamsy I***. Mechanical properties of heart valves. Bose Annual User Group Meeting – Keele University, UK 2007.

9. ***El-Hamamsy I***, Balachandra K, Sarathchandra P, Taylor PM, Yacoub MH, Chester AH. Endothelial-dependent biaxial regulation of aortic valves in response to endogenous

mediators. Canadian Cardiovascular Society – 60th Annual Scientific Meeting – Quebec City, Canada 2007.

LIST OF ABBREVIATIONS

5-HT	5-hydroxytryptamine (Serotonin)
AchE	Acetylcholinesterase
ANOVA	Analysis of variance
cAMP	Cyclic amine monophosphate
CyB	Cytochalasin B
DNA	Deoxyribonucleic acid
EDRF	Endothelial-derived relaxing factors
EDCF	Endothelial-derived contracting factors
EDHF	Endothelium-derived hyperpolarizing factor
EMT	Epithelial to mesenchymal transition
eNOS	Endothelial nitric oxide synthase
IBMX	Isobutylmethylxanthine
ICAM-1	Intercellular adhesion molecule
iNOS	Inducible NOS
sGC	Soluble guanylyl cyclise
cGMP	Cyclic guanosine monophosphate
5-HT	5-hydroxytryptamine

BSA	Bovine serum albumin
DMEM	Dulbecco's Modified Eagle Medium
ECM	Extracellular matrix
ET-1	Endothelin-1
FCS	Fetal calf serum
JNK	c-Jun terminal kinase
L-NAME	L-nitroarginine methyl ester
LVEF	Left ventricular ejection fraction
LVOT	Left ventricular outflow tract
NADPH	Nicotinamide adenine dinucleotide phosphate oxidase
NFKB	Nuclear factor KB
NO	Nitric oxide
NOS	Nitirc oxide synthatase
NPY	Neuropeptide Y
NYHA	New York Heart Association Classification
PBS	phosphate buffered saline
PCR	Polymerase chain reaction
PECAM-1 or CD31	Platelet endothelial cell adhesion molecule-1
RNA	Ribonucleic acid
SDS	Sodium dodecyl sulphate

SEM	Standard error of the mean
SF-36	Short-Form 36 Health Survey Questionnaire
SICM	Scanning ion conductance microscopy
SMA	Smooth muscle alpha actin
SNP	Sodium nitroprusside
TGF-β	Transforming growth factor-β
TNF-α	Tumour necrosis factor-α
VEGF	Vascular endothelial growth factor
VE cadherin	Vascular endothelial cadherin
vWF	von Willebrand Factor

I INTRODUCTION

THE HEART

The heart is a complex organ with a simple function: to pump the blood in one direction thus maintaining the circulation and ensuring adequate tissue oxygenation. To do so, it depends on the interplay between its structural components and a number of signalling pathways which ensure coordinated movements and maximum contractile efficiency. The heart is composed of fours chambers (2 atria and 2 ventricles) and four valves (2 atrioventricular valves and 2 ventriculo-arterial valves) (Figure 1.1). Functionally, it is divided into a "right" heart which pumps deoxygenated blood returning to the heart from the venae cavae into the pulmonary circulation to fill with oxygen and release carbon dioxide. Oxygenated blood then returns to the "left" heart via pulmonary veins and is ejected into the systemic circulation. The aortic valve lies at the junction between the left ventricle and the aorta and constitutes the last step before blood exits the heart into the systemic circulation.

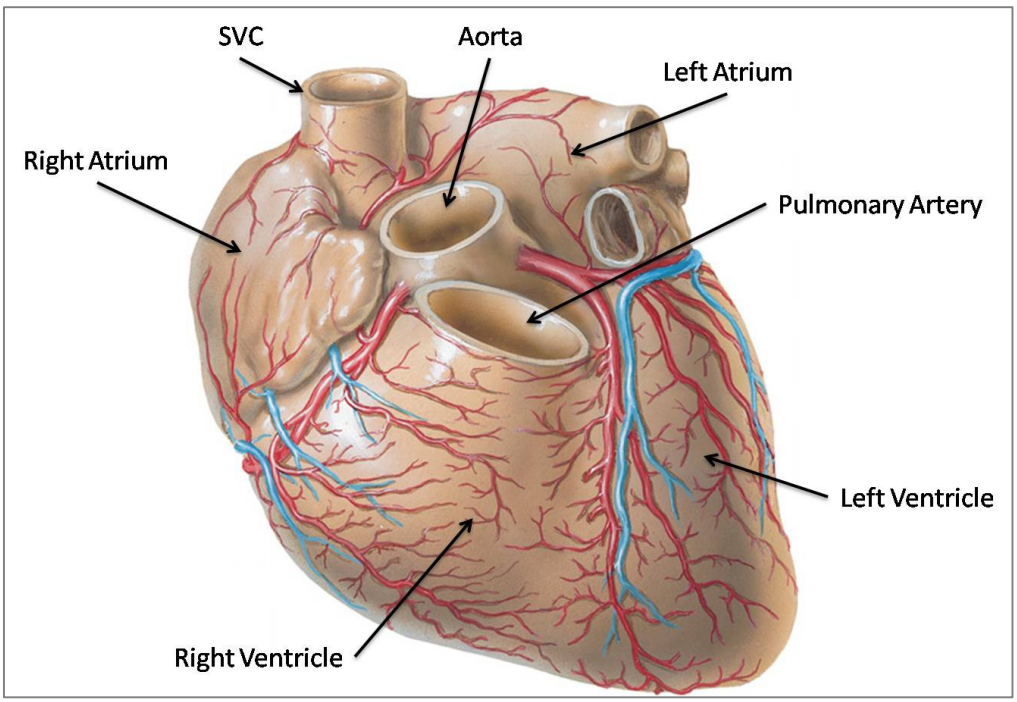

Figure 1.1 - Anatomy of the heart *(SVC, superior vena cava). Adapted from Netter's Atlas of Human Anatomy*

1.1 THE AORTIC VALVE

1.1.1 Developmental Biology of The Aortic Valve

The heart is the first organ to form during embryogenesis and develops via a series of complex steps involving simultaneous morphogenesis and differentiation (

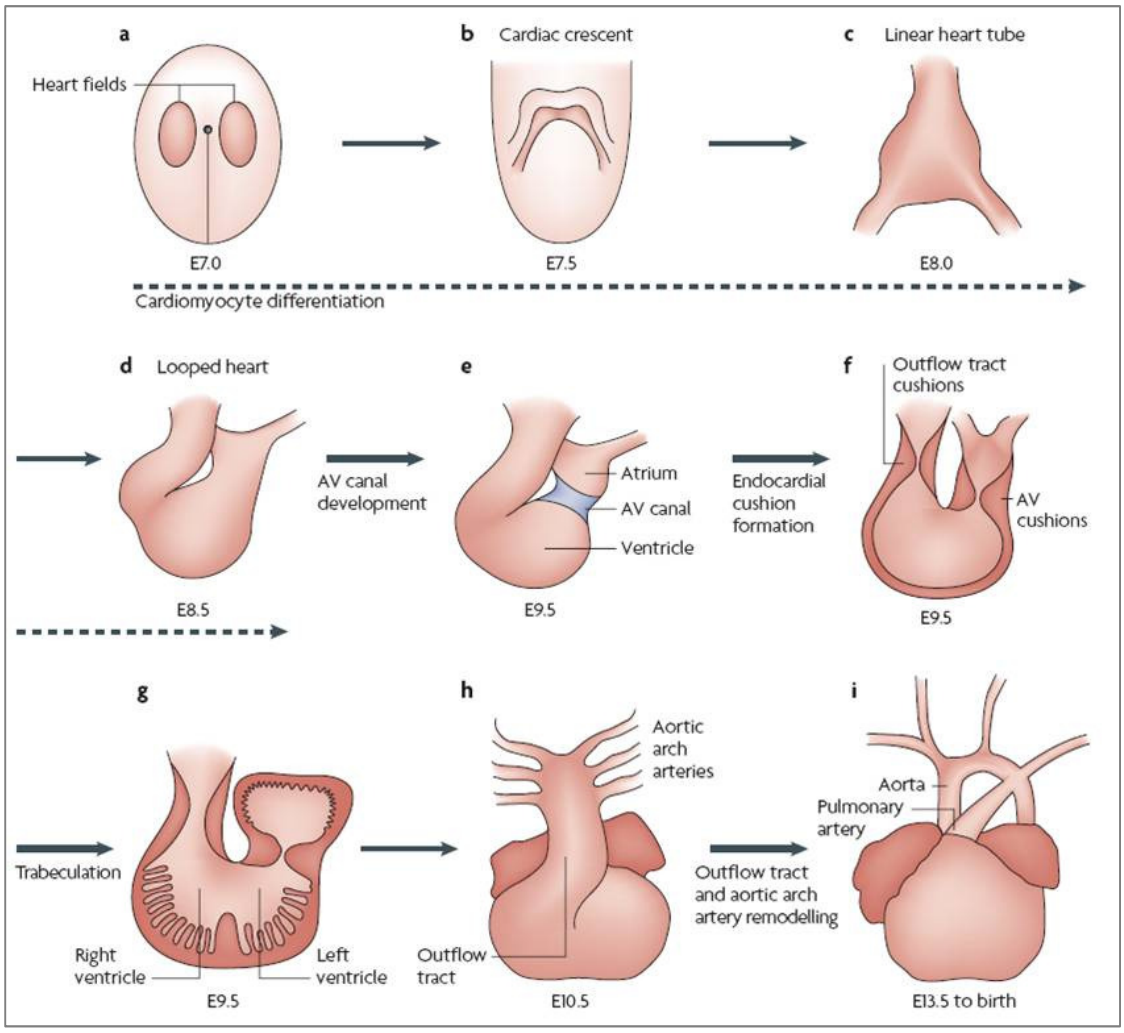

Figure 1.2). It has become increasingly clear that understanding the developmental biology of cardiac structures is essential to understanding their behaviour in adult life, both in health and disease. Indeed, several of the signalling pathways and molecular mechanisms involved in cardiac, and more specifically valve morphogenesis remain operative at later stages.

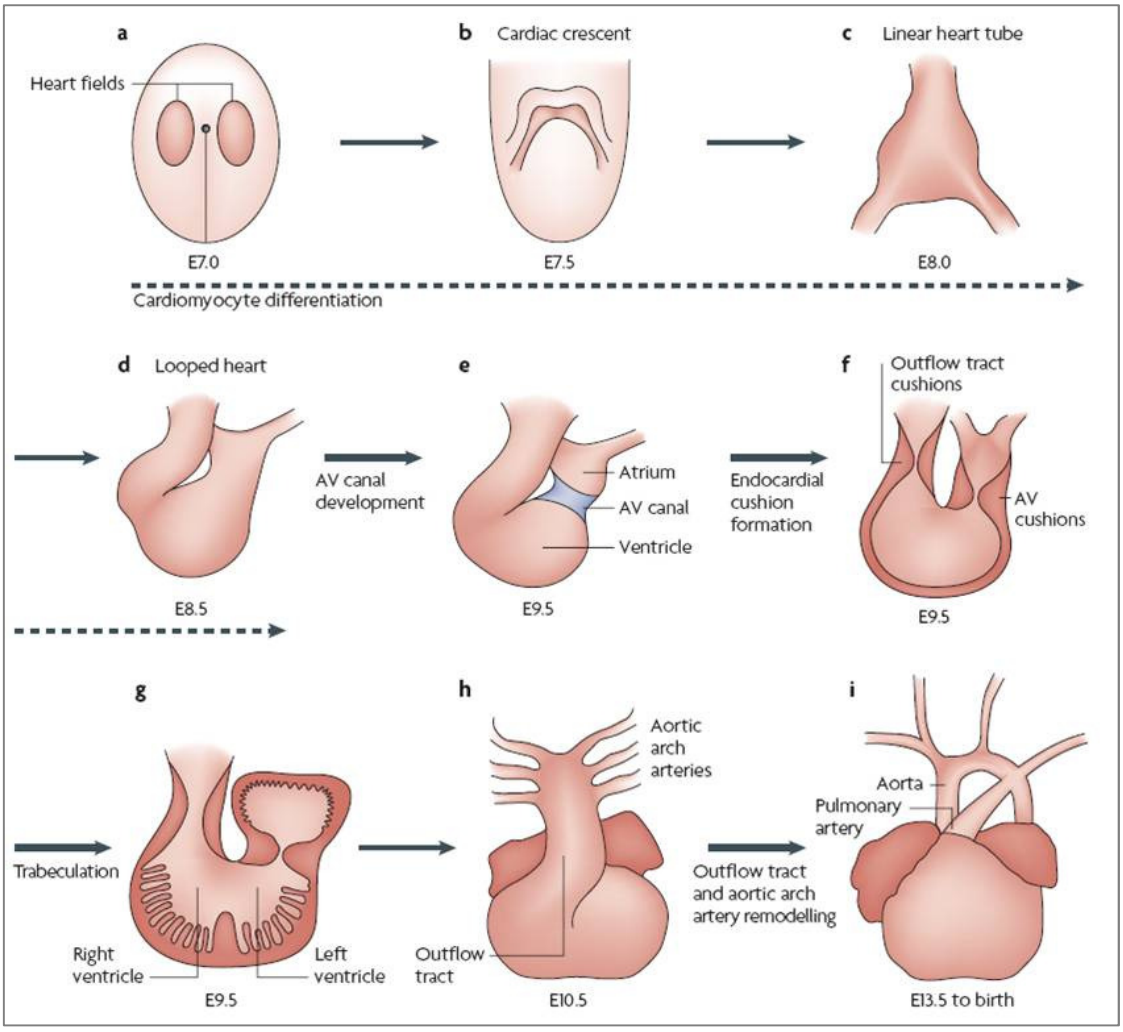

Figure 1.2 – Overview of Cardiac Development. *Adapted from High et al. (High & Epstein, 2008)*

1.1.1.1 Valve Development

Development of both the atrioventricular and semi-lunar valves consists of a series of delamination, migration, transdifferentiation and maturation of specific cells. At the time the heart goes from a tubular structure to a looped configuration, it is composed of 2 layers of cells: the endocardium and the myocardium. During the looping process, the primary myocardium secretes a hyaluronan-rich matrix, termed the *cardiac jelly* which forms gelatinous-looking swellings, the *endocardial cushions* at the site of the eventual atrioventricular junction and outflow tract (Figure 1.2). These cushions form the basis of what will become the heart valve cusps. Following signals from the adjacent myocardium, endocardial cells delaminate and

migrate into the cardiac cushions through activation of the Snail family of proteins which leads to downregulation of the cell adhesion molecule vascular endothelial cadherin (VE-cadherin). In addition, these cells undergo a process of *epithelial to mesenchymal transition* (EMT) characterized by the expression of smooth muscle α-actin (SMA), thus forming the major cell population of cardiac valves. It has been suggested that a subset of endocardial cells derived from a unique area of the anterior heart field are pre-determined to undergo EMT even prior to heart tube formation (Eisenberg & Markwald, 1995). Ex vivo studies have shown that 10% to 20% of endocardial cells undergo EMT. Once in the cardiac jelly, these cells digest the hyaluronan and start secreting an extracellular matrix (ECM) rich in collagens I, II and III, versican and other proteoglycans, making the original jelly significantly more rigid. Factors involved in migration and EMT of endocardial cells include the Notch signalling pathway, members of the transforming growth factor β (TGFβ) superfamily: TGFβ 1-3) and bone morphogenic proteins (BMP), the wnt/β-catenin signalling pathway, vascular endothelial growth factor (VEGF) and the NFAT family of proteins, a series of five related transcription factors. Recent work suggests that endothelial nitric oxide synthase (eNOS) signalling also plays an important role in the maturation of the cardiac cushions and the formation of the valve cusps. Full understanding of the complex network of interactions between the different signalling molecules and pathways during development remains to be determined. Nevertheless, it is clear that overexpression or underexpression of any of these elements can result in an abnormal EMT process and valvulogenesis.

1.1.1 Outflow Tract Development

The cardiac outflow tract encompasses the arterial pole of the heart where the right and left ventricles empty into the pulmonary artery and aorta. The predominant source of cells

populating the outflow tract derives from the neural crest. The neural crest is a multipotent population of precursor cells derived from the dorsal neural tube that give rise to melanocytes, nerve tissue, cartilage, muscle and bone among others. In addition, neural crest cells play an important role in the formation of the cardiac outflow tract. Although fate mapping studies using wnt-1 as a definitive marker of neural crest cells suggests the absence of neural crest cells in the aortic and pulmonary valves (de Lange et al., 2004), their role is critical for left ventricular outflow tract formation, aortic arch development and aorto-pulmonary septation (Figure 1.) (Jiang, Rowitch, Soriano, McMahon, & Sucov, 2000). Prior to migrating into the outflow tract, neural crest cells undergo EMT in the neural tube, a process mediated by Notch signalling (High et al., 2007; Niessen & Karsan, 2008). Migration of these cells into the outflow tract is mediated by BMP activation (Kaartinen et al., 2004; Kim, Robertson, & Solloway, 2001). In addition, recent evidence suggests that eNOS signalling also plays an essential role in mediating neural crest cell migration, proliferation and outflow tract septation (Fernández et al., 2009). A study performed on eNOS knockout Syrian hamsters showed an increased incidence of bicuspid aortic valves (BAV) characterized by right and left coronary cusp fusion. This is thought to be due to abnormal outflow tract septation due to abnormal behaviour of neural crest cells (Fernández et al., 2009).

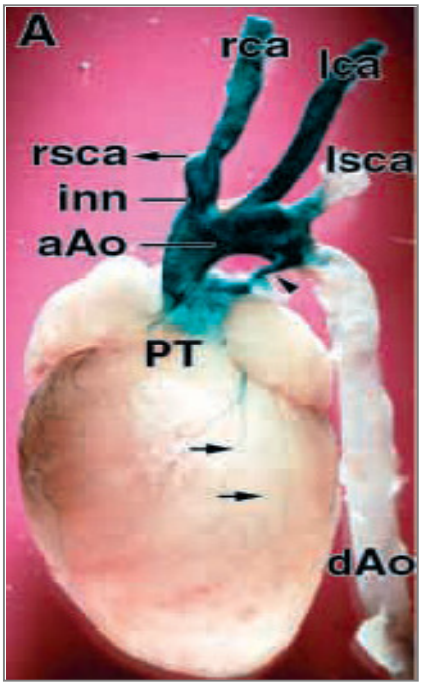

Figure 1.3 - Fate mapping of neural crest cells *(blue)* in adult hearts. *Taken from Jiang et al. (Jiang et al., 2000)*

1.1.1.3 From Developmental Biology to Clinical Applications

Understanding of the steps involved in valve and cardiac outflow tract development helps to explain a number of congenital cardiac malformations such as the tetralogy of Fallot, truncus arteriosus, transposition of the great arteries and more. Moreover, identification of the involved signalling pathways at various stages of development in conjunction with animal models of disease has allowed establishment of a direct link between specific mutations and cardiac anomalies. As mentioned previously, eNOS knockout animals have been associated with BAV and the phenotype of the fused cusps appears to be related to the site of action of eNOS in particular cases (Fernández et al., 2009). Mutations in Notch-1 illustrate the concept that pathways that are operative during cardiac development can also be responsible for valve disease in adult life. Garg et al. identified Notch-1 mutations in 2 families with an increased incidence of BAVs and outflow tract anomalies such as tetralogy of Fallot and hypoplastic left ventricles (Garg et al., 2005). Interestingly, unaffected subjects in these families developed early aortic valve calcification even in the presence of normal tricuspid valves,

Notch-1 signalling pathway in osteogenesis. Similarly, the wnt/β-catenin signalling pathway has been implicated in calcification. These pathways and their potential role in aortic valve calcification will be discussed later in further detail.

1.1.2 Macrostructure of the Aortic Valve

The aortic valve is formed of 3 semi-lunar cusps which attach to the aorta forming a crown-shaped annulus. The cusps are part of a functional unit: the aortic root, which lies at the junction between the left ventricular outflow tract and the ascending aorta. In addition to the aortic cusps, the aortic root is composed of the aortic annulus, the sinuses of Valsalva and the sinotubular junction. Changes in the shape or function of one or more of these components can lead to dysfunction of the aortic valve mechanism. At its base, the aortic root connects to the interventricular muscular septum along two-thirds of its surface and the remaining part connects to fibrous tissue forming the aortic-mitral continuity (Figure 1.). At both ends of the subaortic curtain lie the right (also called central fibrous body) and left fibrous trigones which act as hinge points between the aortic and mitral valves during the cardiac cycle. The sinuses of Valsalva constitute outpouches of aortic wall and correspond to the 3 aortic cusps. The coronary arteries originate from 2 of the sinuses, aptly termed the left and right coronary sinuses, while the remaining sinus is called the non-coronary sinus. Due to their semi-lunar attachment line to the aorta, the space between the cusps is triangular in shape and lies within the left ventricular outflow tract rather than the aorta. The highest point in these triangles corresponds to the highest point of leaflet attachment, referred to as the commissure. The circumferential line connecting these commissures is the so-called sinotubular junction. The inlet diameter usually exceeds the sinotubular junction diameter by a 15% to 20% (Dagum et al., 1999; Kunzelman, Grande, David, Cochran, & Verrier, 1994; Lansac, Lim, Shomura, Lim, Rice et al., 2002)).

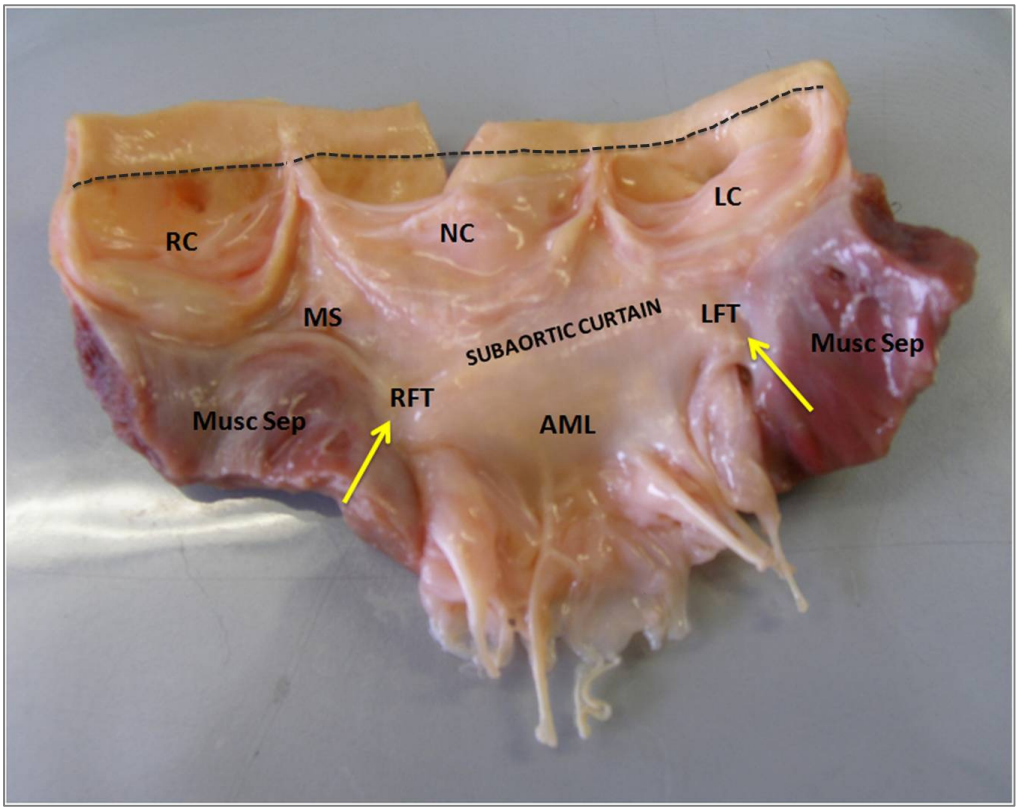

Figure 1.4 - Photograph of an open aortic root showing its structural components (annulus, cusps, sinuses of Valsalva and sinotubular junction [dashed line]) and their relationship with the left ventricular outflow tract and the mitral valve. *AML, anterior mitral leaflet; LC, left coronary cusp; LFT, left fibrous trigone; MS, membranous septum; Musc Sep, muscular septum; NC, non-coronary cusp; RC, right coronary cusp; RFT, right fibrous trigone. Adapted from Yacoub, El-Hamamsy et al. (M.H. Yacoub et al., 2009)*

Aortic valve competence depends on adequate cusp coaptation during diastole. The central point of cusp coaptation is characterized by the presence of raised nodules called the nodules of Arantius. These nodules are helpful to demarcate the midpoint along the free edge of the cusps. In each individual, cusp length and aortic root diameter are in direct relationship, which suggests there is variability in the size of cusps between individuals (Kunzelman et al., 1994). In addition, there is consistent asymmetry of individual cusp surface area within individuals. According to a study of 200 normal hearts, the right coronary cusp is most frequently the largest (43%), followed by the non-coronary cusp (37%) and the left coronary cusp (20%) (Vollebergh & Becker, 1977). Interestingly, a recent study has shown that variation

in aortic root size is associated with genetic variants between individuals, suggesting a degree of genetic predetermination of aortic root dimensions (Vasan et al., 2009).

1.1.3 Microstructure of the Aortic Valve

The aortic valve shows a highly preserved microstructural architecture across humans and different species, both from a cellular and extracellular composition. The aortic valve is a thin structure measuring 300μm - 700μm in thickness. Histologically, it is composed of 3 distinct superposed layers: the fibrosa, spongiosa and ventricularis (Figure 1.5). The fibrosa lies on the aortic side of the cusp while the ventricularis lies on the ventricular-facing side. The spongiosa lies in between these 2 layers. The fibrosa which represents about 45% of the cusp thickness is rich in circumferentially oriented collagen fibers providing structural strength to the cusps. In contrast, the ventricularis (20% of the thickness) is mainly composed of radially-aligned elastin fibers conferring elasticity to the leaflets. The spongiosa layer (35% of thickness) is rich in proteoglycans and glycosaminoglycans which have a high hydrous content allowing smooth sliding of the fibrosa and ventricularis during the various phases of the cardiac cycle, thereby minimizing repeated microtrauma related to valve deformation.

Aortic valve cusps are covered on both sides by a monolayer of endothelial cells which lies in direct continuity with the aortic endothelium on one side and the ventricular endocardium on the other side. The body of the cusp is populated by a mix population of cells commonly termed the interstitial cells. These cells are a dynamic population of cells comprising a minimum of 3 distinct cell types: smooth muscles cells, fibroblasts and myofibroblasts (Figure 1.5). In addition, a small but likely significant population of resident stem cells has recently been identified to reside within the body of the cusps (Chen, Yip, Sone, & Simmons, 2009). The precise role and contribution of these cells to aortic valve structure and physiology will be discussed in further detail in this section.

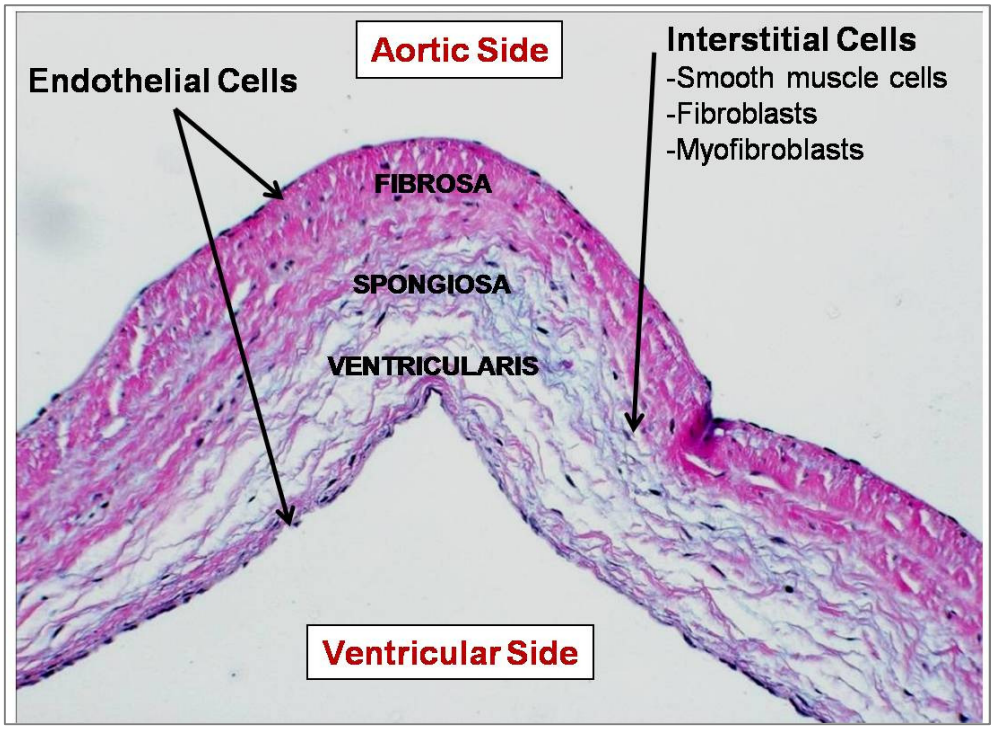

Figure 1.5 - Microstructure of aortic valve cusps showing the characteristic trilaminar architecture. *Adapted from El-Hamamsy et al. (El-Hamamsy, Chester, & Yacoub, 2010)*

Further characterization of heart valves has revealed the presence of an intricate and elaborate network of nerve cells populating the valves (Marron et al., 1996). Though The distribution of these nerve networks varies between the four valves, it is remarkably conserved between species. Aortic valve innervation arises from ventricular endocardial plexuses while some fibers originate from the aortic adventitial wall penetrating the leaflets through the raphe. These nerves are predominantly localized to the ventricularis (the lower part of the leaflet). The entire length of the leaflets is covered with nerves except for the coapting edge which is devoid of any nerve terminals. The left and right coronary cusps are equally innervated, whereas the non-coronary cusp is less extensively so. Due to its non-juxtaposition to the ventricular endocardium, it receives its nerve endings from both contiguous cusps (the right and left) which may account for the uneven nerve density. Interestingly, nerve cells are circumferentially aligned, mirroring the orientation of endothelial cells and collagen fibers (De Biasi & Vitellaro-Zuccarello, 1982). Nerve terminals present on the aortic valve express

immunoreactivity for tyrosine hydroxylase and neuropeptide Y, both markers of post-ganglionic sympathetic nerves as well as acetylcholinesterase activity. Using double immunostaining techniques, nerve endings are shown to be in close proximity to SMA-positive interstitial cells in the matrix, suggesting a direct role of these nerves on valve function. The precise role of these nerves on aortic valve structure and function is increasingly understood (El-Hamamsy, Yacoub, & Chester, 2009).

1.1.3.1 Aortic Valve Endothelial Cells

The endothelium forms a monolayer of cells throughout the body which separates blood components from underlying microstructural elements of various organs. For a long time, endothelial cells from different locations were considered to be similar both at the structural and functional levels. The vascular endothelium was therefore the most widely studied type of endothelium and assumptions were made about endothelial cells in other locations. However, it has now been clearly demonstrated that the endothelium is a superfamily of cells that share several common features but also express many differences which have an impact on their function (Yano et al., 2007). In light of these findings, aortic valve endothelial cells have gained significant interest in recent years both to understand normal valve physiology and more importantly in an attempt to elucidate valvular disease mechanisms. This has stemmed from a paradigm of the pathophysiology of aortic valve disease which suggests that aortic valve endothelial dysfunction is the first step in a series of events leading to valve calcification, similar to what happens in the vasculature (Otto, Kuusisto, Reichenbach, Gown, & O'Brien, 1994). The role of the endothelium is thus understood to be central to aortic valve function.

1.1.3.1.1 The Structure and Function of Normal Endothelium

Endothelial cells form a layer that separates the blood lumen from underlying structures. In blood vessels, vascular smooth muscle cells lie directly underneath the endothelium whereas in aortic valves, interstitial cells constitute the body of the cusp. Endothelial cells have a typical cobblestone-like appearance which distinguishes them morphologically from other types of cells. The main "traditional" roles of the endothelium are as follows:

- Inhibition of platelet aggregation
- Inhibition of the expression of adhesion molecules and hence the rolling and penetration of inflammatory cells into the wall, including macrophages
- Prevention of smooth muscle cell proliferation and contraction

The endothelium exerts these properties in response to a variety of different stimuli, which can be chemical, physical or mechanical, by secreting specific endothelium-derived substances as well as by regulating cell-cell and cell-matrix adhesions.

Endothelial-derived substances can be divided into 2 broad categories: endothelial-derived relaxing factors (EDRF) and endothelial-derived contracting factors (EDCF), both names derived from the role of the endothelium on vascular tone. The main relaxing factors are nitric oxide (NO), prostacyclin and endothelium-derived hyperpolarizing factor (EDHF).

- **Nitric Oxide**

NO is a soluble gas which is released by endothelial cells and acts in a paracrine fashion by acting on underlying smooth muscle cells in the vasculature. Autocrine effects of NO on endothelial cells have not been excluded. NO is produced in response to various stimuli such as acetylcholine, bradykinin, hypoxia and shear stress. L-arginine serves as a substrate for the production of NO in a reaction mediated by an intracellular enzyme, endothelial nitric oxide synthase (eNOS or NOS III), an NADPH-dependent oxidase that requires tetrahydrobiopterin (BH4), Fad and FMN as cofactors. Two more isoforms of NOS are found throughout the system:

neuronal NOS (nNOS or NOS type I) present among other locations in central and peripheral neurons, islets, endometrium and skeletal muscle and inducible NOS (iNOS or NOS type II) found in macrophages, liver, smooth muscle, heart and other sites (Murad, 2006). All 3 isoforms of NOS are encoded by 3 different genes on different chromosomes and have 50%-60% homology with each other (Murad, 2006). Once released by endothelial cells, NO diffuses into the subendothelial space and activates soluble guanylyl cyclase (sGC) in smooth muscle cells (Figure 1.). This leads to increased formation of cyclic guanosine monophosphate (cGMP). cGMP in turn activates cGMP-dependent protein kinase which results in protein phosphorylation and decreased cytosolic calcium by extrusion from the cell, thereby limiting contraction of the cell (Lincoln, Komalavilas, & Cornwell, 1994). In addition, dephosphorylation of myosin light chain occurs which also contributes to relaxation. Finally, activation of potassium channels leads to hyperpolarisation of the cell membrane, thereby preventing action potential formation. Biochemical mediators of eNOS activation include serotonin or 5-hydroxytryptamine (5-HT) which can be released by platelets. 5-HT stimulates endothelial 5HT1D receptors coupled to eNOS through pertussis toxin-sensitive Gi-coupled proteins. This results in NO production and release. Thus, 5-HT can act as a useful probe for endothelial NO-mediated activity.

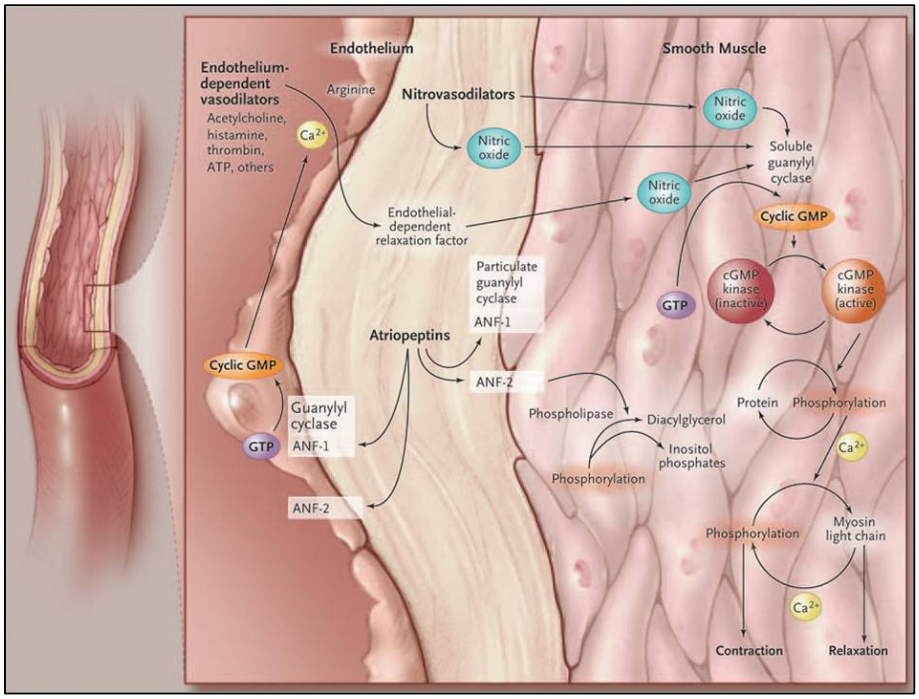

Figure 1.6 - Endothelium-Dependent Relaxation of Smooth Muscle. NO activates soluble guanylyl cyclise (sGC) to form cyclic guanosine monophosphate (cGMP). cGMP activates cGMP-dependent protein kinase, resulting in protein phosphorylation, decreased cytosolic calcium levels, myosin light chain dephosphorylation and relaxation. *Taken from Murad F. (Murad, 2006)*

- **Prostacyclin**

The action of prostacyclin (prostaglandin I_2, or PGI_2) depends on the presence of receptors coupled to adenylate cyclase which once activated lead to increased cyclic adenosine monophosphate (cAMP) in smooth muscle cells. cAMP in turn stimulates ATP-sensitive potassium channels leading to cell membrane hyperpolarisation and inhibition of contraction (Parkington, Tonta, Coleman, & Tare, 1995). Similar to the effect of cGMP, cAMP leads to extrusion of calcium from the cytosol (Abe & Karaki, 1992). In addition, prostacyclin facilitates the release of NO from endothelial cells, acting in a synergistic fashion (Shimokawa, 1998).

- **Endothelial-dependent hyperpolarizing factor (EDHF)**

In addition to NO and prostacyclin, a third mediator of smooth muscle relaxation has been recognized for many years but its exact identity remains to be defined. It is known as EDHF due to its mechanism of action.

- **Endothelial-dependent contracting factors (EDCF)**

Aside from its role as a smooth muscle relaxant, the endothelium can also release contractile elements, commonly termed EDCF. These comprise superoxide anions, endoperoxides, thromboxane A2 and endothelin-1 (ET-1) (Murad, 2006). In the normal vascular wall, there is a homeostatic balance between EDRFs and EDCFs favouring the former. However, the contracting agents are prominent in several pathophysiological conditions, including hypertension, atherosclerosis and plaque formation. Superoxide anions and endoperoxides are prominent in oxidative stress injuries.

ET-1 is a potent vasoconstrictor peptide which is stored and released by endothelial cells. There are 2 ET receptors, ET-A receptor and ET-B receptor. Both endothelial cells and smooth muscle cells have receptors to ET-1, with ET-B receptors being most prevalent on endothelial cells. Although ET-1 stimulation of smooth muscle cells results in contraction, stimulation of ET-B receptors on endothelial cells results in the release of NO, forming a negative feedback loop (Ahlborg & Lundberg, 1997; Flavahan & Vanhoutte, 1990, 1995). In addition, NO inhibits the expression and production of ET-1 (Boulanger & Luscher, 1990; Luscher, 1992; Luscher et al., 1990). In healthy vessels, ET-1 plays a minor role in constitutive vasomotor tone. However, as the endothelium becomes dysfunctional, it loses Gi protein-mediated responses (Flavahan & Vanhoutte, 1995), which leads to increased and unrestricted ET-1 production. The most convincing evidence of the role of NO on ET-1 activity is from experiments showing that vasoconstriction due to inhibition of NOS is inhibited by the addition of ET-A antagonists (Thorin, Cernacek, & Dupuis, 1998; Thorin, Nguyen, & Bouthillier, 1998).

In addition to their synthetic properties, endothelial cells act as a selective barrier to blood products through cell-cell and cell-matrix adhesions. Recent evidence suggests that these junctions act as more than barriers by participating in mechanosensing and mechanotransduction of mechanical stimuli. Two main types of junctions are found on the surface of endothelial cells: adherens junctions and tight junctions. In addition, platelet endothelial cell adhesion molecule-1 (PECAM-1 or CD31), though not considered adhesion or tight junctions, is found in intercellular spaces. Of the different adhesion molecules, PECAM-1, VE-cadherin and claudin-5 are proper to endothelial cells and not found on epithelial cells. Together, these cell surface proteins maintain cell connections and communication. Moreover, these junctional proteins are linked to the cytoskeleton and constitute the basis of mechanotransduction mechanisms.

1.1.3.1.2 Aortic Valve Endothelial Cells

Until recently, aortic valve endothelial cells were thought to play a minor role in valve physiology because valves were considered passive structures that opened and closed in response to changes in transvalvular pressure. More recently, several studies focusing on the structural and functional properties of aortic valve endothelial cells suggest that valvular endothelium possesses unique properties which distinguish it from other endothelial beds, particularly the endothelium lining the aorta with which it lies in direct continuity. The most striking difference between valvular and vascular endothelial cells is cell alignment with regards to flow orientation. Whereas the vascular endothelium throughout the body aligns with the long axis of the cell parallel to flow (Imberti, Seliktar, Nerem, & Remuzzi, 2002) (except in areas of turbulent flow) (Passerini et al., 2004), aortic valve endothelial cells are aligned perpendicular to the direction of flow (Butcher, Penrod, Garcia, & Nerem, 2004; Deck, 1986). This was first described by Deck et al. (Deck, 1986) by electron microscopic analysis of explanted aortic valves and further validated by in vitro studies (Butcher et al., 2004). Cultured

porcine aortic valve endothelial cells were compared to aortic (vascular) endothelial cells from the same animal in response to unidirectional non-pulsatile laminar flow at 20 dynes.cm^{-2}. Whereas vascular cells were aligned parallel to flow after 24 hours, instead, aortic valve endothelial cells aligned perpendicular to flow even without the presence of an aligned substrate (Butcher et al., 2006). These adaptations were dependent on cytoskeletal reorientation, a process involving different mechanotransduction pathways in each type of endothelium. Laminar flow induced activation of Rho-kinase, phosphatidylinositol-3-kinase and calpain pathways in vascular endothelial cells, whereas valve endothelial cells did not require activation of the latter for cytoskeletal reorganization (Butcher et al., 2004). In addition, aortic valve endothelial cells also appear to have a higher proliferation rate than vascular endothelial cells (Farivar et al., 2003).

Furthermore, both sets of cells possess different transcription profiles. In a study examining the transcription profiles of 847 genes, there was common expression of 55 activated genes whereas a further 48 genes were differentially activated. Among those genes with a higher activation in the valvular endothelial cells were transcription factors associated with higher proliferation rate such as jun D and protein kinase C (Farivar et al., 2003). Notably, both vascular endothelium and valve endothelial cells expressed markers linked with calcification such as osteonectin, bone morphogenic protein-7 and -9 (BMP-7 and BMP-9). Differences in gene expression profile between vascular and valvular endothelium were further validated by another study showing different gene expression profiles in response to shear stress stimulation of cultured porcine aortic endothelial cells or aortic valve endothelial cells (Butcher et al., 2006). In that study, Butcher et al. showed preferential expression of genes associated with chondrogenesis by aortic valve endothelial cells whereas vascular endothelial cells expressed more genes associated with osteogenesis. Shear stress reduced the expression of osteogenic genes (Butcher et al., 2006).

Aortic valve calcification is a major clinical problem in elderly patients and those with bicuspid aortic valve disease. In recent years, it has become increasingly clear that aortic valve calcification is an active cell-driven process that shares many similarities with atherosclerosis. Among those, early endothelial dysfunction has been shown to act as an initial occurrence in the cascade of events leading to valve calcification (Otto et al., 1994). Histologically, aortic valve calcification occurs almost exclusively on the aortic side of the valve. Simmons et al. developed an innovative technique to separately analyze gene expression of aortic valve endothelial cells from either side of the valve (Simmons, Zilberberg, & Davies, 2004). This modified Hautchen technique for en face isolation of aortic valve endothelial cells allowed extraction of mRNA for analysis of gene expression profiles between both aortic-side and ventricular-side aortic valve endothelial cells. The authors reported the differential expression of 584 genes in situ between both sides of the valve (Simmons, Grant, Manduchi, & Davies, 2005). However, the gene array used was a human array and only covered 12,000 genes. Currently, porcine gene arrays that cover >23,000 genes are commercially available and could provide additional clues into the functional side-specificity of aortic valve endothelial cells.

Differences in flow patterns between both sides of the valve as described later in the Introduction, are sensed by a thin layer of glycoproteins on the luminal surface of endothelial cells called the glycocalix, which communicates with the cytoskeleton and can activate several signalling pathways in response to flow (P. F. Davies, 1995; Lopez-Quintero, Amaya, Pahakis, & Tarbell, 2009; Pahakis, Kosky, Dull, & Tarbell, 2007; Wang, Butler, & Ingber, 1993). This process of translating mechanical stimuli into biological signals is commonly termed mechanotransduction. Studies on vascular endothelial cells have demonstrated that differences in shear stress translate into activation of different signalling pathways, illustrated by the presence of atherosclerotic plaques in areas of low wall shear stress in the vasculature such as the carotid artery bifurcation. One of the major activated signalling pathways is the nuclear factor-kB (NFkB), a highly conserved transcription factor which translocates to the nucleus when activated, triggering the production of pro-inflammatory molecules (Helderman et al.,

2007; Partridge et al., 2007). To date, the glycocalix has not been identified or characterized on the surface of aortic valves. Nevertheless, it is thought that flow characteristics at the level of the aortic valve have major implications in health and disease.

1.1.3.2 Aortic Valve Interstitial Cells

The matrix of aortic valve cusps is rich with a mixed population of cells commonly termed valve interstitial cells. Phenotypic studies suggest the presence of at least 2 distinct populations of cells within the matrix: a smooth muscle α-actin (SMA)-positive population of cells and fibroblasts. SMA-positive cells are themselves thought to include pure smooth muscle cells and an "activated" subset of fibroblasts which express contractile proteins, called myofibroblasts. Myofibroblasts are thought to be involved in some of the pathological mechanisms involving aortic valves, such as valve calcification or myxomatous valve degeneration (Rabkin et al., 2001; Walker, Masters, Shah, Anseth, & Leinwand, 2004). This dual cell population confers on valve interstitial cells 2 main properties: the ability to contract and the capacity to synthesize extra-cellular matrix (ECM) components, thereby constantly remodelling the valve. Valve interstitial cells are different from cells from other sources. We have previously shown that valve-derived fibroblasts have different properties than dermal fibroblasts or pericardial cells (Taylor, Allen, & Yacoub, 2000). In addition, valve interstitial cells express a range of specific skeletal and non-muscle cell markers such as β-myosin heavy chain and markers of the troponin complex (Brand, Roy, Hoare, Chester, & Yacoub, 2006).

Valve interstitial cells are a dynamic population of cells which can move from one phen-otype to another within a cell's lifespan. (Rabkin-Aikawa, Farber, Aikawa, & Schoen, 2004). It has been speculated that valve interstitial cells are composed of 5 identifiable phenotypes that define their molecular structure-function relationships (Table 1.1). These include embryonic progenitor endothelial/mesenchymal cells, quiescent VICs (qVICs), activated VICs (aVICs), pro-genitor VICs (pVICs), and osteoblastic VICs (obVICs). These phenotypes exhibit plasticity

allowing them to convert from one form to another. Indeed, work from our laboratory has recently shown the capacity of valve interstitial cells to transdifferentiate into other cell phenotypes including osteoblasts, adipocytes and chondrocytes (L. Osman, M. H. Yacoub, N. Latif, M. Amrani, & A. H. Chester, 2006).

Table 1.1 Structural-functional classification of aortic valve interstitial cells. *Adapted from Liu et al. (Liu, Joag, & Gotlieb, 2007)*

Cell type	Location	Function
Embryonic progenitor endothelial/ mesenchymal cells	Embryonic cardiac cushions	Give rise to qVICs through an activated stage or EMT
qVICs	Valve leaflet	Maintain valve structure and function and prevent angiogenesis
pVICs	Bone marrow, blood ± valve leaflet	Enter valve or are resident. Provide aVICs for valve repair. May be CD34-, CD133- and/or S100+
aVICs	Valve leaflet	SMA-containing VICs with activated cellular repair processes (proliferation, migration, remodelling). Respond to valve injury and abnormal hemodynamic or mechanical forces.
obVICs	Valve leaflet	Calcification, chondrogenesis and osteogenesis in the leaflet. Secrete ALP, osteocalcin, osteopontin and bone sialoprotein.

Valve interstitial cells actively respond to their local cellular, matrix and hemodynamic environment through a range of specific molecules which allow to adapt to its environment. Studies by Merryman et al. show that valve interstitial cells isolated from different valves have different mechanical properties, with cells from the left side of the heart significantly stiffer

(Merryman, Youn et al., 2006). This underlines the direct correlation between cells strcture and function. Cell-cell communication at the interstitial cell level occurs via cell-cell junction molecules such as cadherens, desmosomal junctions and gap-junction proteins (connexion-26 and -43) (Latif et al., 2006). Cell-matrix communication is thought to be a major component of valvular responses to changing mechanical conditions. Integrins are present in high concentrations in valve interstitial cells and are thought to contribute to linkage of force transmission between the ECM and the cellular components (Latif et al., 2007).

Aortic valve interstitial cells have recently been the focus of much attention because of the important role they are thought to play in valve disease. Some authors suggest valve interstitial behaviour is the main orchestrator of valve pathobiology. Studies from our group and others (J. N. Clark-Greuel et al., 2007; Mohler, 2004; Mohler et al., 1999; L. Osman et al., 2006) have shown that human aortic valve interstitial cells are directly involved in the calcification process of aortic valves. However, the precise mechanism by which calcification occurs through aortic valve interstitial cells action is still unclear. Some studies suggest that as a result of aortic valve interstitial cell apoptosis, calcium accumulates in matrix vesicles which are released by these apoptotic bodies, leading to mineralization. Other groups suggest a phenotypic transdifferentiation of aortic valve interstitial cells in osteogenic-like cells, capable of producing mineralized bone (L. Osman et al., 2006). Others have suggested the presence of resident stem cells within the valve matrix, which are capable of undergoing differentiation and bone formation, and could be the main culprits in valve disease (Chen et al., 2009). Though the precise mechanisms are yet to be fully understood, the combined evidence suggests an active participation of cells residing within the valve interstitial space in pathological processes affecting the function of the valve.

1.1.3.3 Nerves

A rich and highly preserved network of nerves is also found in aortic valves. To date, the precise function of these neural networks remains to be elucidated, but there is increasing evidence that they play an active role in normal valve physiology as well as a potential contributory role in valve disease (El-Hamamsy, Yacoub et al., 2009). Marron et al. (Marron et al., 1996) reported the most comprehensive anatomical study of the neural distribution in human heart valves. They showed that aortic valve innervation arises from ventricular endocardial plexuses (Marron et al., 1996) while some fibers originate from the aortic adventitial wall penetrating the leaflets through the raphe (Kawano, Shirai, Kawano, & Okada, 1996). These nerves are predominantly localized to the ventricularis (the lower part of the leaflet). The entire length of the leaflets is covered with nerves except for the coapting edge which is devoid of any nerve terminals. The left and right coronary cusps are equally innervated, whereas the non-coronary cusp is less extensively so. Due to its non-juxtaposition to the ventricular endocardium, it receives its nerve endings from both contiguous cusps (the right and left) which may account for the uneven nerve density. Although the mitral valve (which lies in continuity with the left and non-coronary cusps) is more densely innervated than the aortic valve, none of its nerve fibers extend into the aortic cusps (Kawano et al., 1996). Thus, each valve seems independently innervated and controlled. Most aortic valves studied showed no large nerve terminals. Rather, groups of thin nerve terminals originate from large individual nerves that cross the entire leaflet. These thin nerves have a dot- and brush-like ending whereas the thicker proximal nerves appear to have a varicose-like structure (Kawano, Kawai, Shirai, & Okada, 1993; Kawano et al., 1996). According to De Biasi et al. (De Biasi & Vitellaro-Zuccarello, 1982), they follow a circumferential distribution within the leaflets, mirroring the orientation of muscle fibers in the valve (Steele, Gibbins, & Morris, 1996). Nerve terminals present on the aortic valve express immunoreactivity for tyrosine hydroxylase and neuropeptide Y (NPY), both markers of post-ganglionic sympathetic nerves as well as acetylcholinesterase (AchE) activity (Marron et al., 1996). Previous studies from our laboratory have highlighted the functional significance of

nerves on aortic valve contractile properties (Chester, Kershaw, Sarathchandra, & Yacoub, 2008) and recent evidence suggests a role for the sympatho-adrenergic system in valve calcification (Osman et al., 2007).

1.1 AORTIC ROOT DYNAMICS

As mentioned by Zimmerman in his Hunterian Lecture to the Royal College of Surgeons of England in 1966, "...an understanding of the anatomical shape of the heart requires that we visualize it as a *structure-function continuum*" (Zimmerman, 1966). The aortic root is a fine example of this intricate relationship which remains to be fully understood. Nevertheless, it has become increasingly clear that the aortic root constitutes a structural and functional unit comprising several components, including the aortic valve cusps. Therefore, any study of the aortic valve cusp behaviour should include mention of the root as a whole.

1.2.1 Function of the Aortic Root

The aortic root lies in direct continuity with the LVOT proximally and gives origin to the tubular ascending aorta distally. In summary, the aortic root has 3 main functions: to ensure laminar unobstructed flow from the LVOT to the ascending aorta in systole in an energy-efficient manner, to facilitate the instantaneous opening and closing movements of the aortic valve cusps thus reducing stresses on them and to optimize coronary blood flow during both diastole and importantly systole.

1.2.2 Structure of the Aortic Root

The aortic root represents a structural unit composed of 4 pillars: the cusps, the annulus, the sinuses of Valsalva and the sinotubular junction. Each of these anatomic components is an essential and indispensable contributor to the normal function of the root. The aortic root is a 3-dimensional dynamic structure. The aortic annulus which constitutes the base of the aortic root corresponds to the tip of the LVOT. Part of its circumference is formed by thick ventricular myocardium and the other part is fibrous, representing the aortic-mitral continuity. The right and left fibrous trigones lie at both ends of this fibrous portion, also known as the subaortic curtain. During diastole, the aortic annulus assumes an oval or clover shape rather than a circular one and becomes fully circular during cardiac ejection (Lansac, Lim, Shomura, Lim, Rice et al., 2002; Tops et al., 2008). The area of the base of the aortic root corresponding to the annular level is larger than that at the sinotubular junction (Dagum et al., 1999; Lansac, Lim, Shomura, Lim, Rice et al., 2002). Longitudinally, this confers to the aortic root a "conical" shape which is important in generating a velocity gradient across the root because as blood flow moves from a larger cross section to a smaller cross section, conservation of mass dictates that velocity must increase proportionally.

The sinuses of Valsalva lie between the annulus and the sinotubular junction. Their diameter and area significantly exceeds those of the base or sinotubular junction of the root. Their importance has been highlighted by several recent studies using computational flow dynamics and computer simulations showing the importance of the sinuses in facilitating smooth closure of the aortic valve cusps starting in late systole and into early diastole. In addition, their 3-dimensional configuration allows for recirculation of blood in the sinuses during systole (Grande-Allen, Cochran, Reinhall, & Kunzelman, 2000; Grande, Cochran, Reinhall, & Kunzelman, 1998; Katayama, Umetani, Sugiura, & Hisada, 2008), which can flow into the coronaries, an element which is often disregarded in terms of coronary flow physiology (J. E. Davies, Parker, Francis, Hughes, & Mayet, 2008). Beyond the physiological interest of

understanding the role of each of the components of the aortic root on its function, these considerations are of major importance for surgical decision-making as will be discussed later.

1.2.3 Structure-Function Dynamics

Using a closed-chest ovine model with radiopaque markers placed at key points in the aortic root, Dagum et al. studied aortic root deformations during the cardiac cycle (Dagum et al., 1999). Interestingly, changes in aortic root shape are asymmetric and dictated both by structure and changes in transvalvular pressure. For instance, during the early isovolumic contraction phase, circumferential expansion of the base was greatest in the left annular region and least in the non-coronary (NC) annular region which is continuous with the anterior mitral annulus (aortic–mitral continuity and right fibrous trigone) and primarily composed of fibrous tissue. Importantly, this is accompanied by a simultaneous increase in circumferential diameter at the level of the commissures. This conformational change is proportional to the end-diastolic volume. In other terms, before the aortic valve opens, the aortic root prepares to accommodate a large volume of blood exiting from the LV thereby improving transvalvular hemodynamics and reducing turbulent damage to the aortic cusps (Dagum et al., 1999; Lansac et al., 2005).

Additional evidence for Zimmerman's structure-function continuum is apparent during ventricular systole. It is known that aortic root expansion is asymmetric but importantly, it generates precise changes in its tilt angle. The aortic root tilt angle (between the basal plane and the commissural plane) is ~16° degrees at end-diastole (angle oriented posteriorly and to the left) (Lansac et al., 2005). During systole, it is reduced by ~7°, aligning the LV outflow tract with the ascending aorta (Lansac et al., 2005). This tilt angle reduction results in a straight cylinder which undoubtedly facilitates ejection; whereas during diastole, the tilt angle increased, probably reducing leaflet stress.

Of particular importance in our case are the dynamics of aortic valve opening and closing. Valve instantaneous movements can impose major stresses on the cusps, especially closing velocity during end-systole. It has been clearly demonstrated that aortic valve cusps

initiate the closure movement during the second half of systole. From a dynamic perspective, the conformational change of the aortic root from a conical shape generating a velocity gradient to a cylindrical shape, negates any gradient. In terms of fluid dynamics, when the velocity gradient disappears, the pressure across the aortic valve reverses as the blood flow begins to decelerate. Deceleration of flow implies a negative value for $\delta v/\delta t$, and consequently a positive pressure gradient $\delta p/\delta z$ must exist in moving across the valve from LV to aorta. This gradient applied to the leaflets begins to move them towards closure. If the velocity gradient across the aortic root persists, flow deceleration is offset by the positive velocity gradient and pressure reversal occurs later in ejection, which means that the leaflets begin to close later in systole. Considering the leaflet edges must traverse the same distance within a shorter time period, this results in an increase in the speed at which the leaflets close, therefore increasing the closing stress on the cusps. Furthermore, the generation of vortex patterns of flow in the sinuses of Valsalva early in systole generate momentum which allows timely initiation of valve closure during systole (Katayama et al., 2008; Robicsek & Thubrikar, 1999; M. J. Thubrikar, Nolan, Aouad, & Deck, 1986).

1.2.4 Mechanical Stresses in the Aortic Root

The aortic root itself is exposed to 2 main stresses: normal radial stress or pressure, and a shear stress tangential to the aortic root structures, which is caused by blood flow. Characterizing the patterns of flow and measuring shear stress levels in vivo remain significant challenges which can only be overcome through computational fluid dynamics in idealized models of aortic root geometry.

In addition, aortic valve cusps are subjected to unique stress profiles for 2 reasons. First, they are subjected to a range of stresses consisting of shear stress, leaflet strain in both the radial and circumferential directions, mechanical pressure during diastole and bending forces. Second, both sides of the valves are exposed to different forces, particularly shear stresses. The

ventricular side of the valve is exposed to a high-velocity high-shear stress whereas the aortic side is exposed to a low-velocity complex pattern of shear. Combined with the microstructural differences between ventricularis and fibrosa as discussed earlier, defining precise stress maps for aortic valve cusps represents a major challenge. Nevertheless, early work by Thubrikar et al. using in vivo fluoroscopy to image radiopaque markers placed on the valve cusps demonstrated the presence of important dynamic strains on the cusps during diastole, reaching 10% in the circumferential axis and 30% in the radial direction (M. Thubrikar & Eppink, 1982; M. Thubrikar, Skinner, Aouad, Finkelmeier, & Nolan, 1982; M. J. Thubrikar, Aouad, & Nolan, 1986). This corresponds to strain rates of 440%/s and 1240%/s in the circumferential and radial directions, respectively. Additional studies have further characterized the behaviour of aortic valve cusps: they exhibit a highly non-linear stress-strain relationship, undergo large deformations, are anisotropic tissues, have complex viscoelastic properties and undergo complex axial coupling behaviours (Sacks & Yoganathan, 2007). In terms of stress on the cusps, Grande-Allen et al. have produced finite element models of aortic roots, specifically looking at the stresses and strains on the cusps. They showed that the magnitude of stresses on the cusps varies across the surface of the cusp, reaching a maximum at the level of the free margin and belly and a minimum at its basal attachment to the aortic wall (Grande-Allen et al., 2000; Grande et al., 1998). In addition, right and non-coronary sinus stresses were 21% and 10% greater than the left sinus and in all sinuses, stresses near the annulus were higher than near the sinotubular junction (Grande et al., 1998).

From the present data, it is clear that the aortic root is a highly dynamic structure which forms a highly regulated structural and functional unit. Understanding the normal physiology of aortic root function in addition to its adaptation to changing hemodynamic conditions can have a major impact on the management of patients with aortic valve or root disease.

1.2 AORTIC VALVE DISEASE

1.2.1 Natural History of Aortic Valve Disease

Aortic valve disease represents a major source of morbidity and mortality both in the developed and the developing worlds. The increase in overall life expectancy, the improvements in cardiac imaging techniques and the increased accessibility to primary health care all contribute to the increasing prevalence of this affliction. Estimates suggest that the prevalence of aortic valve disease requiring aortic valve replacement will triple by 2050 (M. H. Yacoub & Takkenberg, 2005). Aortic valve disease can result from different structural abnormalities which cause valve dysfunction. Valve dysfunction manifests as either valve stenosis or regurgitation, thus imposing in either case, an important hemodynamic burden on the left ventricle. In the case of valve stenosis, the increased resistance at the outlet causes left ventricular pressure overload, left ventricular hypertrophy, and an increase in energy demand. In neglected cases this can lead to severe irreversible ventricular dilatation which carries a very poor prognosis for the patient. Similarly, aortic valve regurgitation results in left ventricular volume overload because of the regurgitant volume at each cardiac cycle.

Patients with aortic valve disease can range from asymptomatic to severely symptomatic. The principal symptoms are dyspnea at rest or with effort, chest pain and syncope. The presence of any of these symptoms in patients with aortic valve stenosis is associated with a markedly decreased vital prognosis, with most patients being deceased at 5 years from the onset of symptoms (Figure 1.7) (Ross & Braunwald, 1968).

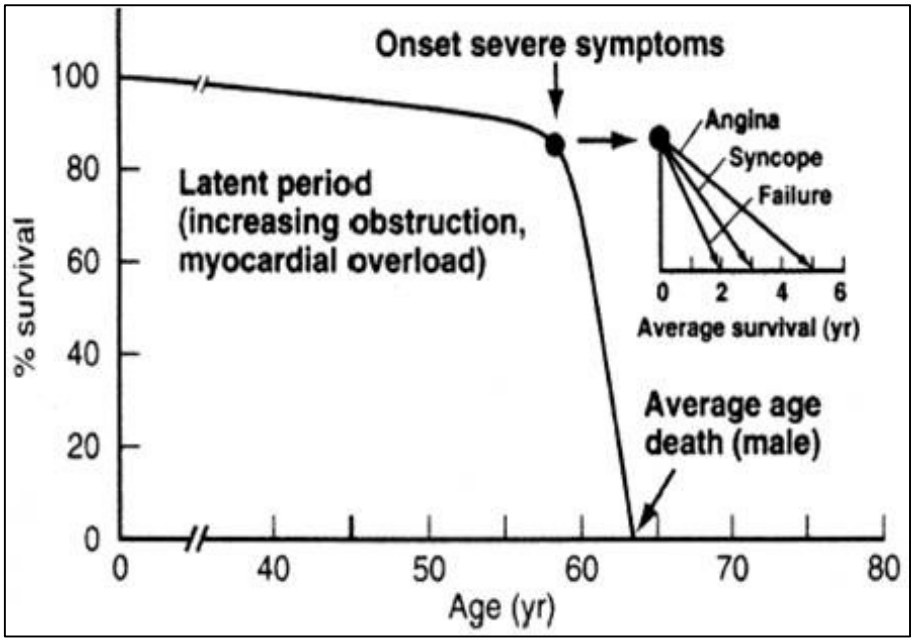

Figure 1.7 – The natural history of patients with aortic valve stenosis. Survival is markedly reduced with the onset of cardinal symptoms: angina, dyspnea or syncope. *Adapted from Ross and Branwald (Ross & Braunwald, 1968).*

1.2.2 Current Therapies for Aortic Valve Disease

Currently, the only treatment for patients with symptomatic aortic valve disease remains replacement of the aortic valve. Traditionally, aortic valve replacement remains a surgical procedure, though in recent years, percutaneous methods for aortic valve implantation have also been developed. Irrespective of the method to substitute the native valve, it remains that native aortic valves require substitution, highlighting the fact that to date, no treatments have been developed to alter the natural history of the disease or to slow the progression of aortic valve disease, which most often presents as aortic valve calcification. Various clinical trials assessing the role of different medications have produced disappointing results in terms of disease progression or patient outcomes, most notably studies involving the use of statins (Hermans et al., 2010). Considering recent advances into the understanding of aortic valve calcification as an active cell-mediated process involving inflammatory mechanism and the fact that aortic valve stenosis shares many epidemiological risk factors with atherosclerosis such as hypertension, smoking and dyslipidemia, it was hoped that statins could be as effective in aortic

valve disease. These findings underline the need for increased research into understanding the pathophysiological mechanisms behind aortic valve calcification as will be addressed in this thesis.

1.2.3 Surgical Options for Aortic Valve Replacement

Several options are available for surgical replacement of the aortic valve. Detailed discussion of the technical aspects of each valve substitute are beyond the scope of this thesis. Nevertheless, important differences exist between the different substitutes which will be addressed in Chapters 5 and 6. Native aortic valves can be replaced using homografts (aortic root from a different human being), xenografts (using porcine or bovine tissues), mechanical valves or pulmonary autografts (the patient's own pulmonary root placed in the aortic position while substituting the pulmonary root with a pulmonary homograft), also known as the Ross procedure (Figure 1.8).

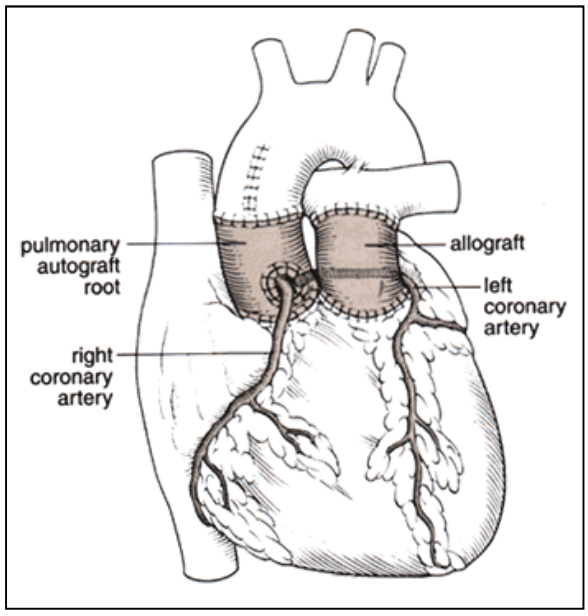

Figure 1.8 – Schematic representation of autograft aortic root replacement, also known as the Ross procedure. The pulmonary autograft is placed in the aortic position while a pulmonary homograft is used to replace the pulmonary root. This technique has the advantage of placing a living substitute in the aortic position.

The most important difference in the intrinsic properties of these different valve substitutes is the fact that all represent non-living aortic valves, except pulmonary autografts. This includes homografts which become acellular within weeks after implantation, even when used as "homovital" homografts. Various studies examining the outcome of patients following aortic valve replacement show lower survival following surgery than the general population matched for gender and age (Figure 1.10) (van Geldorp et al., 2009).

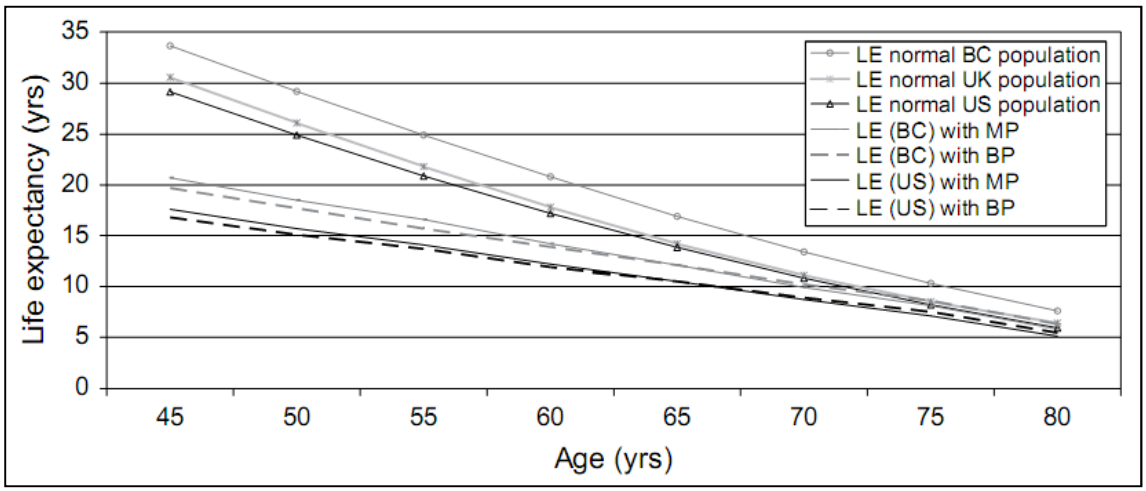

Figure 1.10 – Survival following biological or mechanical aortic valve replacement compared to survival of the general population showing reduced patient survival after surgery compared to the general population. *Adapted from von Geldorp et al. (van Geldorp et al., 2009).*

In contrast, the pulmonary autograft is the only substitute which has been shown to remain viable over many years after implantation. We believe that in light of the sophisticated structure and functions of the aortic valve which we will further examine in this thesis, implantation of a living pulmonary autograft in the aortic position should translate into improved clinically-relevant patient outcomes, including survival.

1.3 HYPOTHESIS

The aortic valve has unique structural features which allow it to function adequately in a highly dynamic mechanical environment. As a living organ, it is capable of actively adapting its shape,

structure and function to changing local conditions. As a result, a living valve substitute is thought to translate into significantly better clinically relevant outcomes.

1.4 AIMS AND OBJECTIVES

In recent years, the complex structure and function of the aortic valve is slowly being elucidated at the cellular, molecular and genetic levels. Nevertheless, many questions remain unanswered, particularly with regards to the role of the endothelium in regulating valve structure and function. The aim of this thesis was to unveil more of the specific and unique features of aortic valves in order to better understand their physiology in health and disease. It is hoped that the present work could add important blueprint information into the requirements for tissue-engineered heart valves.

The specific aims of this work were:

1- To develop a reliable and reproducible technique to separately isolate aortic valve endothelial cells from either side of the valve in order to evaluate side-specific heterogeneity with a particular focus on cell markers, single-cell mechanical properties and gene expression profiles.

2- To assess the differential role of aortic valve endothelium from either side of the valve on modulating aortic valve calcification in vitro.

3- To determine the role of the endothelium in regulating aortic valve mechanical properties using a biaxial micromechanical testing system. Importantly, one of the aims was to evaluate the communication between endothelial and interstitial cells in regulating aortic valve mechanical properties.

4- To determine the importance of a living valve on aortic root biomechanics through functional imaging techniques by comparing results following aortic root replacement using living versus non-living aortic valve substitutes.

5- To determine the impact of a living aortic valve substitute on clinically relevant endpoints.

II Aortic Valve Endothelial Cell Heterogeneity

2.1 BACKGROUND

As mentioned earlier, although most endothelial cells throughout the body share the same basic anti-thrombogenic, anti-adhesive and anti-proliferative properties, there is a considerable amount of heterogeneity between the endothelium from different regions of the body both at the structural and functional levels (Aird, 2006). Structurally, although most endothelial cells have a typical cobblestone appearance, they can vary significantly in thickness. Endothelial cells in the aorta can reach up to 20 times the thickness of those from capillaries or veins. The number, distribution and properties of tight and adherens junctions between endothelial cells also varies considerably from one vascular bed to another. These structural differences result from the adaptation of endothelial cells to local biochemical (pH, oxygen tension, growth factors, cytokines etc...) and biomechanical factors (mechanical and shear stress). In addition, this heterogeneity reflects epigenetic factors which are dynamic in nature. Importantly, these structural variations translate into functional differences which serve to adapt specifically to the local environment.

Based on these assumptions, the aortic valve represents a compelling model of endothelial cell heterogeneity. As previously mentioned, the valve is lined with endothelial cells on both sides. Yet, despite the thinness of the valve and its small overall surface area, both sides are exposed to vastly different biomechanical environments, suggesting that if one were able to study both sides independently, differences should be observed in their structural and functional properties. This is further supported by the fact that aortic valve calcification, the most common valve pathology, occurs almost exclusively on the aortic surface of the valve. Defining the differences between endothelial cells from either side of the valve could therefore provide valuable insight into disease mechanisms and suggest potential therapeutic avenues.

Previous work from Simmons et al. looking at endothelial cells extracted from porcine aortic valves shows significant differences in gene expression profiles between cells from either side of the valve (Simmons et al., 2005). A total of 516 genes were differentially expressed. This

side-specific heterogeneity of endothelial cells was in addition to concurrent studies from other groups showing site-specific structural and functional differences between valvular and vascular endothelial cells (Butcher et al., 2004; Butcher et al., 2006; Farivar et al., 2003). Together, these data confirm the unique properties of valve endothelial cells and highlight the necessity of exploring both sides of the valve separately in order to understand the intricate mechanisms in health and disease.

Aortic valve endothelium has been shown to play an important role in valve function. Thus far, our understanding of this role is derived from observations linking aortic valve disease to endothelial dysfunction, both from a histological standpoint in explanted calcified aortic valves (Otto et al., 1994)and a clinical standpoint showing an association between systemic endothelial dysfunction and aortic valve disease (Huseyin Bozbas et al., 2008; Chenevard et al., 2006; Poggianti et al., 2003). Considering the suspected role of valve endothelium in valve disease, it is therefore imperative to further investigate the differences between both sides.

In order to analyze endothelial cells in vitro, a technique to isolate endothelial cells from both sides of the valves separately is required. In their study, Simmons et al. used a novel and innovative technique to obtain mRNA from endothelial cells using an ice-cold rod to induce endothelial cells from an explanted valve to stick to a glass coverslip (Simmons et al., 2004). This method proved very effective in obtaining mRNA from pure populations of endothelial cells; however it did not allow obtainment of live primary cultures of endothelial cells from both sides of the valve. It should also be mentioned that due to the absence of porcine gene arrays at the time of their study, a human array was used to assess gene expression profiles. Though the homology between both genomes is thought to exceed 90%, this represents a limitation which requires further investigation.

2.2 AIMS

The overall aims of this work were to develop methods and to perform studies to characterize differences between endothelial cells from the aortic and ventricular sides of the aortic valve. Specifically, the aims were as follows:

- To develop a reliable and reproducible technique of selective isolation of aortic valve endothelial cells from either side of the valve
- To evaluate differences in responses of cultured endothelial cells from both sides of the aortic valve to similar stimuli
- To compare the gene expression profiles of aortic valve endothelial cells from either side following in vitro isolation and culture
- To compare structural differences in the biomechanical properties of endothelial cells from both sides and determine their functional responses to similar stimuli

2.3 METHODS

2.3.1 Aortic valve endothelial cell isolation

Isolation of endothelial cells from whole aortic valve cusps is based on a technique of enzymatic digestion. This method was initially described for isolation of vascular endothelial cells and subsequently adapted for valve endothelial cells (Butcher et al., 2004; Paranya et al., 2001). The technique herein described represents a modified version of these methods.

2.3.1.1 Isolation of Aortic Valve Endothelial Cells

Porcine hearts (12-18 months old) were obtained within 12 hours from animal sacrifice from a commercial abattoir (Cheale Meats, Essex, UK). Hearts were immediately placed in cold-buffered Hanks solution for transport. Under sterile technique, aortic valve cusps were dissected and washed in 1% phosphate-buffered saline (PBS) at room temperature, and kept in

cold, serum free M-199 (Sigma UK) until use. Care was taken during dissection to avoid excessive cusp manipulation which could damage the cellular structure of the cusps. Only fine forceps were used to handle them and gentle traction was exercised only by holding the nodule of Arantius. Various methods were tested to obtain aortic valve endothelial cells in a reliable and reproducible manner. These will be discussed in detail in the Results. The favoured technique consists of selective "clonal" expansion of aortic valve endothelial cells to ensure their purity. All 3 cusps from a single heart were placed in a 50mL Falcon tube containing 10mL of sterile-filtered Collagenase type II solution (*Clostridium histolyticum,* Sigma UK [PN: C6885]) diluted in PBS (600U/mL) and maintained at 37C. The tube was placed in a 37C incubator ($95\%0_2$, $5\%CO_2$) for 12 minutes to extract the endothelial cells. Following this period, an equal volume of cold serum-free M199 solution (10 mL) was added to the tubes. The tubes were vigorously vortexed for a period of 60 seconds to dislodge the endothelial cells from the surface of the valve following weakening of their attachments to the basal membrane. The cusps were then removed from the tubes in a sterile fashion using fine forceps. The resultant medium was placed in a centrifuge at 1000g for 5 minutes. The supernatant was discarded and the pellet resuspended in 1 mL of endothelial growth medium (EGM 2, Promocell, UK). Cells were counted and a volume equivalent to ~150-200 cells was aspirated and diluted in 25 mL of final endothelial growth medium which consisted of EGM 2 solution mixed with a supplement rich in growth factors (epidermal growth factor, basic fibroblast growth factor, insulin-like growth factor, vascular endothelial growth factor, ascorbic acid, heparin and hydrocortisone), 10% heat-inactivated fetal calf serum, 100 U/mL (1%) penicillin (Life Technologies, UK), 100 μmol/L (1%) streptomycin (Life Technologies, UK) and 4 mmol/L (1%) L-glutamine (Invitrogen, UK). This volume was then distributed in five 96-well plates with a volume per well of 50 μL, to achieve a density of 0.3 cells/well (or 1 cell per 3 wells). All wells were coated with a thin layer of sterile 1% gelatine (Sigma UK) which was maintained for 60 minutes in a 37C incubator before use. Following cell seeding, the dishes were maintained in a $95\%0_2$, $5\%CO_2$ incubator at 37C for a period of 48 hours. All wells were then examined daily and wells exhibiting cells

morphologically suggestive of endothelial cells were marked. The medium in these wells was then replaced every 3 days until the cells reached confluence. At confluence, cells were passaged by detaching them using a 1% trypsin/EDTA solution for 2 minutes. In order to dislodge the cells, a 100 µL pipette was used to vigorously aspirate the medium and mobilize the cells. Cells from each well were then seeded into 12-well plates coated with 1% sterile gelatine. Each well's contents were transferred to a single well, so that no mixing of the cells was performed in the early passages to avoid cross-contamination. Once confluent, cells were then moved to a T25 flask (25 cm^2) and used between passages 3 and 7 or frozen until further use.

2.3.1.2 Aortic Valve Endothelial Cell Characterization

Cells were characterized by immunocytochemistry. Cells staining positive for PECAM (CD31) and von Willebrand factor (vWF) while showing negative staining for smooth muscle α-actin (SMA) were considered pure endothelial cell colonies. In cases where >1-2% of the cells stained positive for SMA, the isolate was discarded because of cross-contamination with interstitial cells. To perform immunocytochemistry, cells were seeded on small gelatine-coated glass cover slips at a density of 30,000 cells per cover slip. Once reaching 80% confluence, the cover slips were washed 3 times in PBS and fixed for 5 minutes in ice-cold acetone. They were then air-dried and either frozen for later staining or used immediately. In both cases, this was followed by incubation with 2% bovine serum albumin (BSA) in 0.05% Tween PBS (PBST-BSA) for 30min to block nonspecific binding sites. Cells on cover slips were incubated separately with primary antibodies against mouse anti-CD31 (1/40) (Serotec, UK), goat anti-vWF (1/200) (Dako, UK) and mouse anti-SMA (1/200) (Dako, UK) in PBST-BSA for 1hr. A control of PBST-BSA was also used. The cover slips were washed 3 times in PBS before incubation with a secondary antibody for 30min, either alexa 594/488 goat anti-mouse (1/500) or alexa 594/488 goat anti-rabbit (1/500) (both Invitrogen, UK). Excess secondary antibodies were removed by washing with

PBS containing DAPI for nuclear staining (1/10000; Sigma, UK). Cover slips were blotted to dry and mounted using PermaFluor aqueous mounting medium (Thermo-Scientific, UK). Cells on cover slips were then visualised using the Ziess Axioskop microscope (x20 and x40 objective). Digital micrographs were taken using Nikon DMX1200 camera.

2.3.1.3 Selective Side-Specific Aortic Valve Endothelial Cell Isolation

Following development of a successful technique to isolate aortic valve endothelial cells, we sought to develop a method to isolate them separately from the aortic and the ventricular sides. To do so, aortic valve cusps freshly obtained from the abattoir were placed in a custom plate normally used for our bioreactor flow simulation system (discussed in the following Chapter). As shown in Figure 2.1, cusps from a single heart were placed in the same orientation, so that either the aortic or the ventricular surfaces would face upwards. A glass plate was then superposed and firmly tightened, creating a tight seal, so that only a single surface was exposed to enzymatic digestion. The same protocol for selective isolation of valve endothelial cells as previously described, was performed. In order to ensure the side-specificity of the cells isolated, cusps were immediately fixed and en face immunohistochemical staining was performed on both sides to ensure side selectivity (data not shown).

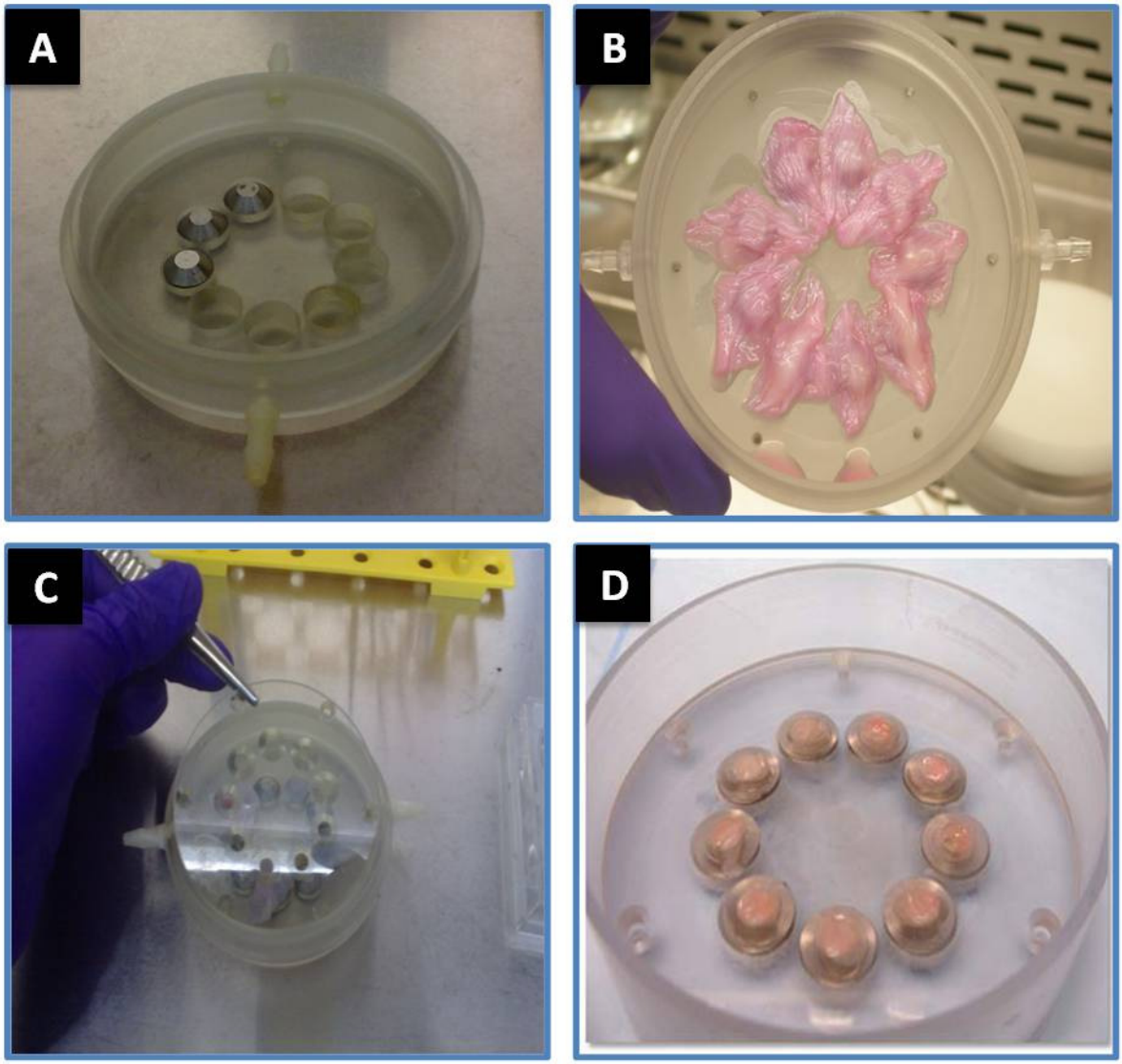

Figure 2.1 – Photographs depicting the different steps leading to selective isolation of aortic valve endothelial cells. **A)** The custom-made plate used for cell isolation. The slots are fitted with stainless steel plugs that bulge up from the level of the holes. **B)** Up to 3 aortic valve cusps from the same heart are laid on the stainless steel plugs. Each cusp sits on a single plug. All cusps are placed so that a single side (aortic or ventricular) is facing upward. [*NB: in this photograph, a total of 9 cusps are plated. However for cell isolation, only 3 cusps are plated so that the cells correspond to a single animal at a* time]. **C)** A glass plate with 9 circular holes to fit the tips of the plugs is placed on top of the cusps. **D)** The glass plate is screwed thereby sealing any gaps. The plate is then filled with collagenase so that only the side facing up is exposed to enzymatic digestion.

2.3.2 Differences Between Aortic and Ventricular Side Aortic Valve Endothelial Cells

2.3.2.1 Immunocytochemistry

Immunocytochemical analysis of primary cultures of aortic versus ventricular-side aortic valve endothelial cells in vitro was performed as described above. The different markers examined were CD31 (1/40) (Serotec, UK), vWF (1/200) (Dako, UK), eNOS (1/100) (BD Biosciences, UK), VE-Cadherin (1/100) (Serotec, UK), TGF-β receptor 1 (1/100) (Sanata Cruz, UK), TGF-β receptor 2 (1/100) (Sanata Cruz, UK), nuclear factor KB (NF KB) (1/50) (BD Biosciences, UK) and vimentin (1/200) (Dako, UK).

2.3.2.2 Endothelial Cell Activation

Primary cultures of endothelial cells from either side of the cusp were seeded on gelatine-coated glass cover slips. At 80% confluence, the medium was supplemented with porcine tumour necrosis factor-α (TNFα, 1 ng/mL) for 12, 24 and 48 hours. Cells from the same animal were always compared to each other. A control group was always included in the analysis. In addition, similar experiments were performed by adding 10ng/mL of porcine TGFβ1 (R&D Biosystems, UK) and examining the cells at similar time points. Markers used to evaluate endothelial cell activation were intercellular adhesion molecule-1 (1/100) (ICAM-1, Southern Biotech, USA), vascular adhesion molecule-1 (1/100) (VCAM-1, SanatCruz, USA), NF KB (1/50) (BD Biosciences, UK), phosphorylated JNK (1/100) (Cell Signaling, UK) and phosphorylated p38 (1/100) (Cell Signaling, UK). Relative expression of the various markers was semi-quantitatively evaluated to compare groups.

2.3.3 Analysis of Gene Expression Profiles

2.3.3.1 RNA Extraction

RNA extraction was achieved using the RNeasy extraction kit (Qiagen Ltd, UK). The lysates were removed from storage and transferred to a clean sterile 1.5 mL eppendorf. This was mixed with 350µL of 70% ethanol (ETOH) (made with RNase free water and High grade ETOH). 700µL of the 70%ETOH/lysate mixture was transferred to an RNeasy mini column sitting in a 2mL collection tube and then centrifuged for 15sec at full speed. The flow through was discarded as the RNA binds to the silica gel membrane in the column. To remove contaminants, the column was washed with 350µL of buffer RW1 (ethanol based). A DNase treatment was then performed on the lysate. 80µL of DNaseI (Qiagen Ltd, UK) made according to manufacturer's guidelines, was added to the RNeasy mini spin column for 15min at room temperature. This was then followed by 1 wash with 150µL RW1 buffer, the column was spun for 15sec at full speed and the flow through was discarded. This was followed by two further washes with 500µL of buffer RPE. The last wash with RPE buffer was centrifuged for 2min to help remove all traces of ethanol which would inhibit subsequent enzyme reactions. To elute the RNA, the mini column was transferred to a new sterile 1.5mL eppendorf, 40µL of RNase-free water was added. The column was left for 10min at room temperature and then was centrifuged for 1min at full speed. The eluted RNA was put on ice prior to analysis of the purity and concentration of the RNA.

2.3.3.2 RNA Quantification

Absorption spectroscopy was performed to assess the purity and the concentration of the isolated RNA in each sample, using the GeneQuant II spectrophotometer (Pharmacia Biotech, UK). 5µl of sample was diluted in 70µl of TE buffer (10mM Tris, 1mM EDTA; pH 8.0) and optical density (OD) readings were taken at 260nm and 280nm using a double beam spectrophotometer. The spectrophotometer was corrected for background absorbance by

comparing the 75µl chamber test cuvette, containing dH_20, with a reference cuvette containing only TE buffer. RNA concentration was calculated using the rule that at 260nm an OD of 1.0 represents an RNA concentration of 40µg/ml. It is important to note that absorbance readings cannot discriminate between DNA and RNA since single and double-stranded DNA also absorbs at 260nm. Thus, to minimise DNA contamination, the RNA extraction protocol included a DNase I step. RNA purity was measured using OD at 280nm. In a pure RNA sample, the OD at 280 nm is twice that at 260nm and the sample has an A_{260}/A_{280} ratio of 2.0. Proteins absorb at 280nm and an A_{260}/A_{280} ratio lower than 2.0 indicates protein contamination. Additionally the A_{260}/A_{280} ratio is dependent on pH and ionic strength. As pH increases from 5.4 to 7.5, the A_{280} decreases whilst the A_{260} is unaffected, resulting in an increased A_{260}/A_{280} ratio. To ensure accurate readings, TE buffer (pH 8.0) was used as a diluent. The obtained RNA was placed in a -80C fridge and kept until use.

2.3.3.3 Gene Expression Analysis

Gene expression analysis was performed using a commercial porcine gene chip containing more than 23,900 genes obtained from Affymetrix (GeneChip Porcine Genome Array, Affymetrix, UK). A total of 6 RNA samples of aortic valve endothelial cells obtained from 3 animals (3 aortic side, 3 ventricular side) were sent in dry ice to the EMBL labs in Heidelberg, Germany for DNA extraction and performance of the gene chip analysis.

2.3.4 Analysis of Endothelial Cell Mechanical Properties

2.3.4.1 Principle of Scanning Ion Conductance Microscopy (SICM)

SICM is a non-optical method which uses a nanopipette as a scanning probe to image cell surface structures with nanometer resolution (Gorelik et al., 2008; Korchev et al., 2000; Novak et al., 2009). The probe used is a sensitive glass nanopipette which detects ion current and uses

the current as an interaction signal to control the vertical (z axis) position of the cell relative to the pipette tip (Gorelik et al., 2006). The hardware used is manufactured by Ionscope (UK), whereas acquisition and analysis software were custom-made. Several imaging modalities are available with SICM such as split mode and hopping mode imaging. Hopping probe SICM allows imaging of convoluted cell surfaces at nanoscale resolution by ensuring the pipette always approaches the cell surface from above (Figure 2.2) (Novak et al., 2009). Briefly, at each imaging point, the pipette approaches the sample from a starting position that is above any of the surface features. The reference current is measured while the pipette is well away from the surface and the position of z-dimension actuator when the current achieves this reduction is recorded as the height of the sample at this imaging point. The z-dimension actuator then withdraws the pipette away from the surface and the sample is moved laterally to the next imaging point. By continuously updating the reference current while the pipette is away from the surface, the method automatically adjusts for any slow drifts in the pipette current.

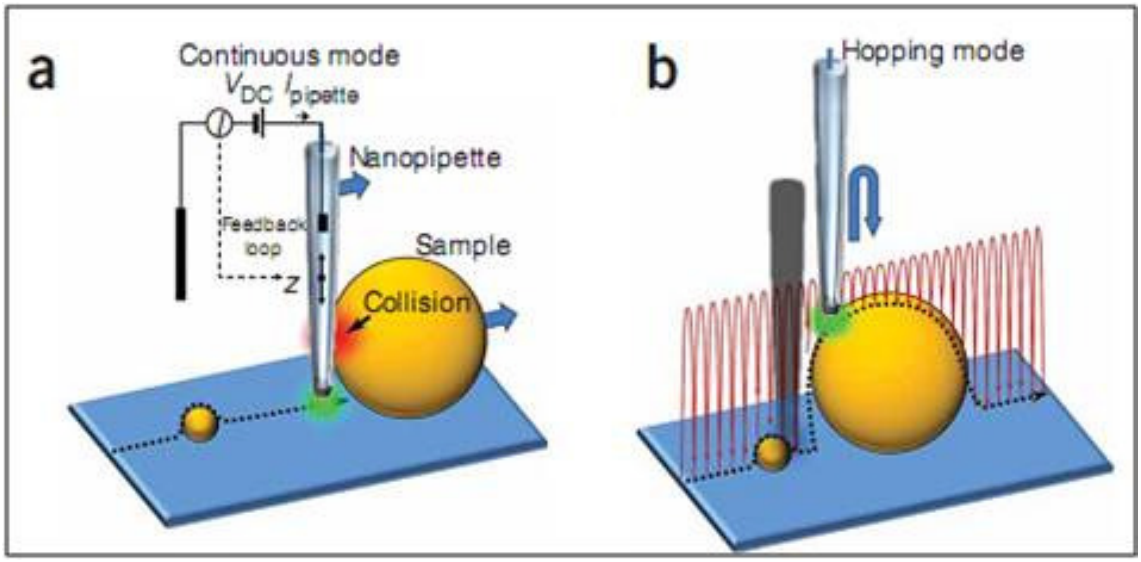

Figure 2.2 – Illustration of the principle of hopping mode SICM. In a), the nanopipette scanning in continuous mode collides with the sample to be imaged, whereas in b) the nanopipette is constantly withdrawn to a position well above the level of the sample at each scanning point, thus allowing better resolution and functional imaging. Adapted from Novak et al. (Novak et al., 2009).

2.3.4.2 Measurement of Single-Cell Mechanical Properties

We recently developed a SICM modification permitting to apply quantified positive and negative force at defined positions to the surface of cells. With this method hydrostatic pressure (0.1–50 kPa) was applied through a pipette. To prevent any surface contact or contamination of the pipette, the distance between the pipette and cell surface was kept constant using ion conductance-based distance feedback, allowing fast and repeated measurements (Sanchez et al., 2008).

2.3.4.3 Experimental SICM Protocol

Aortic valves (n=30 cusps) were obtained from porcine hearts obtained from a commercial abattoir (Cheale Meats, Essex). The cusps were pinned under basal stretch inside a 30mm diameter plastic dish with careful attention to the aortic versus ventricular orientation of the cusp. A total of 3 mL of growth medium was added inside the dish to cover the cusp. The dish is then placed under the scanning microscope and a nanopipette with pre-determined internal diameter is prepared and mounted for the scanning. An initial scan is performed to visualize the surface topography of the tissue over an 80x80 nm area. This allows clear visualization of the nucleus, cytoplasm and cell junctions. Based on this, specific points are chosen with fine precision to measure localized cell stiffness. A controlled and quantifiable pressure is applied using the nanopipette tip is applied to the cell surface and the resultant displacement is quantified. Based on this, stress-displacement maps can be determined, thus reflecting cell stiffness.

Basal stiffness of endothelial cells was initially compared between the aortic and ventricular sides of the aortic valve. Each cusp served as its own control by splitting the cusps in half and exposing both sides to SICM testing. In addition, changes in response to sodium nitroprusside (SNP, 10^{-5}M), endothelin-1 (ET-1, 10^{-10} to 10^{-8}M) and L-nitroarginine methyl ester

(L-NAME, 10^{-4}M) were evaluated. For each measurement, a minimum of 20 cells were randomly examined from the belly of the cusp.

2.3.5 Statistical Methods

Data are expressed as mean ± standard error of the mean (SEM) for continuous data and analyzed using paired or unpaired Student's t-test as indicated. Categorical variables are expressed as a percentage and compared using Fisher's exact test. Differences between groups for each assay were assessed using either a one-way ANOVA followed by a Dunn's multiple comparison post-test or an un-paired students t-test. All analyses were performed using SAS software (SAS Institute, Cary, NC). P-values <0.05 were considered statistically significant.

2.4 RESULTS

2.4.1 Development of a Side-Selective Endothelial Cell Isolation Technique

2.4.1.1 Isolation of Valve Endothelial Cells

The initial objective was to develop a means of isolating valve endothelial cells (aortic and ventricular sides combined) in a reliable and reproducible way. Previous work from other groups had described isolation techniques which all relied on enzymatic digestion of the tissue using collagenase followed by selective clonal explansion or cell-sorting using flow cytometry (Butcher et al., 2004; Farivar et al., 2003; Hoerstrup et al., 1998; Paranya et al., 2001). Based on the previously described methods in the literature, we set out to evaluate the most reliable technique for isolation of endothelial cells from healthy porcine aortic valves freshly obtained within 4 hours of animal sacrifice from a local abattoir (Cheale Meats Inc., UK). Four criteria were evaluated in comparing different isolation protocols: purity of the cells after several

passages, rate of infection ease of the method and reproducibility of the technique. Different protocols were used as summarized in Table 2.1.

Table 2.1 – Summary of the different aortic valve endothelial cell isolation protocols tested.

Protocol	Collagenase concentration	Duration of digestion	EC removal after digestion	Growth medium	Purification technique
A	600 U/mL vs. 1000U/mL	5min. vs. 10 min. +Gentle shaking at 37C	Shaking of the cusps using forceps	-EGM -10% FCS -1% L-glut -1% Pen -1& Strep	None
B	600 U/mL vs. 1000U/mL	5min. vs. 10 min. +Gentle shaking at 37C	Shaking of the cusps using forceps	-EGM -10% FCS -1% L-glut -1% Pen -1& Strep	Cell-sorting Using flow cytometry
C	600 U/mL vs. 1000U/mL	5min. vs. 10 min. +Gentle shaking at 37C	Shaking of the cusps using forceps	-EGM -10% FCS -1% L-glut -1% Pen -1& Strep	Dynabeads using CD-31-positive magnetic beads
D	600 U/mL vs. 1000U/mL	7min vs. 12 min at rest at 37C	Gentle vortex for 1 min.	-EGM -10% FCS -1% L-glut -1% Pen -1& Strep	Selective clonal explansion

EC, endothelial cell; EGM, endothelial growth medium; FCS, fetal calf serum; L-glut, L-glutamine; Pen, penicillin; Strep, streptomycin

The following table shows results obtained following each of the different isolation protocols used (Table 2.2).

Table 2.2 – Summary of the efficacy of different aortic valve endothelial cell isolation protocols tested. Evaluation criteria used were purity of the obtained cells, risk of infection, ease and reproducibility of the technique.

Protocol*	Purity of the cells	Risk of infection	Ease of	Reproducibility

			technique	
A1	-	+	+++	+++
A2	-	+	+++	+++
B1	+	+++	++	+++
B2	-	+++	++	+++
C1	-	+	++	+++
C2	-	+	++	+++
D1ǂ	+++	+	+	++
D2	++	+	+	++
D3	+	+	+	++
D4	+	+	+	++

** Refers to the protocols presented in the previous Table. Each protocol was subdivided into "1" and "2" where "1"=600U/mL and "2"=1000U/mL.*
ǂ D1, 600U/mL for 7 min; D2, 600U/mL for 12 min; D3, 1000U/mL for 7 min and D4, 1000U/mL for 12 min

Following these various iterations of enzymatic digestion of aortic valve cusps to isolated endothelial cells, the following can be concluded. Obtaining a pure population of endothelial cells is a particularly challenging technique due to the high risk of contamination with interstitial cells using any of the mentioned techniques. In our case, cell sorting using flow cytometry proved unsuccessful because of the high risk of infection associated with the technique. This might simply be due to the fact that the cell-sorting flow cytometer in our lab is a multi-user apparatus that is most often used for non-sterile techniques. Therefore, preventing infectious contamination of the cell samples was almost impossible which made this technique highly impractical in our context. Magnetic bead separation of the cells was disappointing in that interstitial cell contamination was surprisingly high immediately after separation which inevitably led to complete overtake of the cultures by interstitial cells.

The technique of isolating cells using static exposure to collagenase for a longer period of time followed by gently vortexing the cusps to detach the endothelial cells from the underlying matrix to which they've become weakly attached represents the most successful technique. This is followed by selective clonal expansion based on cell morphology. Valve endothelial cells are cuboidal in shape although they sometimes assume a more elongated shape. Endothelial cells tend to grow in little clusters as shown in Figure 2.3.

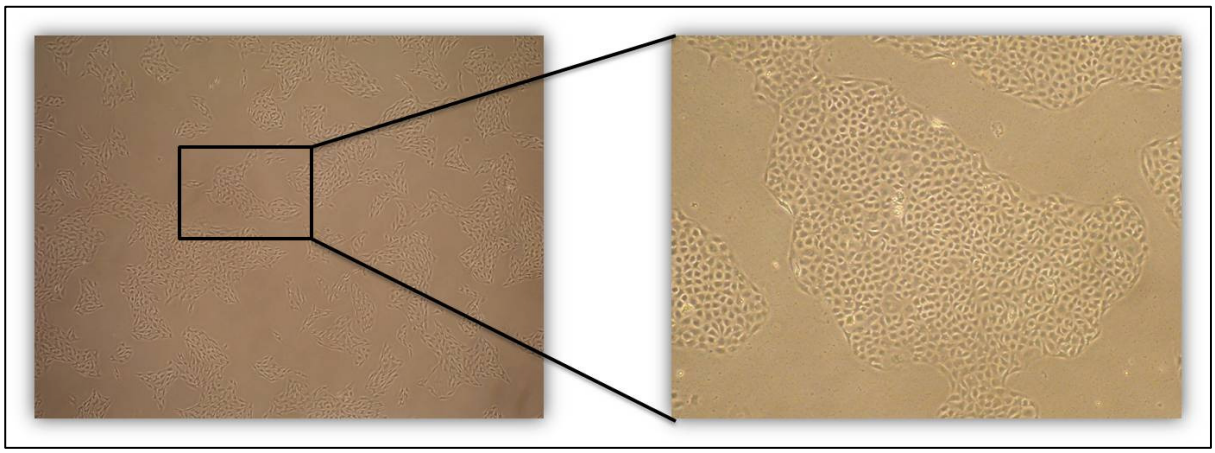

Figure 2.3 – Light microscopy photographs of cultured aortic valve endothelial cells showing their typical appearance in vitro. Cells are small, cuboidal in shape and tend to grow in clusters as shown on the left and right panels.

In addition, valve endothelial cells are easily distinguishable from valve interstitial cells which are significantly longer and wavier than endothelial cells (Figure 2.4). In addition, interstitial cells grow much faster than endothelial cells.

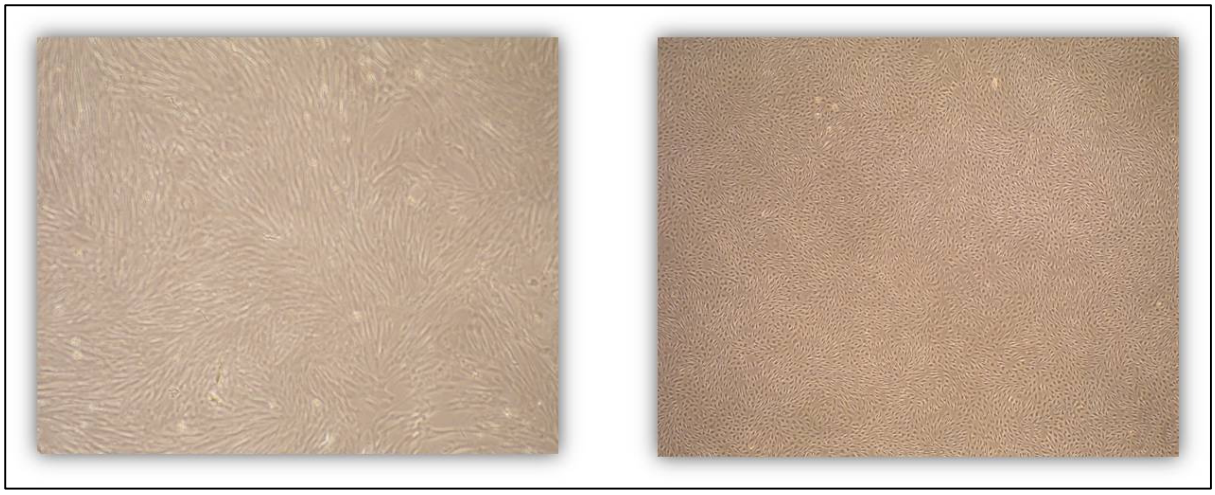

Figure 2.4 – Light microscopy photographs illustrating the morphological differences between cultured porcine aortic valve interstitial *(left)* and endothelial cells *(right)*. Interstitial cells are elongated and wavy. In addition, they tend to grow much faster than endothelial cells.

Table 2.3 Summary of the morphological differences between aortic valve endothelial and interstitial cells.

	Valve Endothelial Cells	**Valve Interstitial Cells**
Shape	Cuboidal (sometimes elongated but much less than interstitial cells)	Very elongated and wavy
Proliferation rate	Slow	Rapid
Growth pattern	Clusters	Uniformly across plate
Distribution in culture	Monolayer even when confluent	Can grow in multi-layers when over-confluent
Ease of detachment when passaging with EDTA	Easy	Easy

2.4.1.2 Separate Isolation of Aortic and Ventricular Side Endothelial Cells

Following the successful application of a reproducible technique to isolate valve endothelial cells, a side-selective endothelial cells isolation technique was developed using the same principles, but exposing only a single side of the aortic valve to the collagenase. The setup consisted of a plate which only allowed exposure of the aortic or the ventricular side to solution while the other side was totally excluded (Figure 2.1).

2.4.2 Phenotypic and Morphological Differences Between Aortic and Ventricular Side Aortic Valve Endothelial Cells

2.4.2.1 Morphological Differences

Primary cultures of aortic versus ventricular-side aortic valve endothelial cells were compared. From a morphological standpoint, cells on the ventricular side appeared more elongated than those on the aortic side as shown in Figure 2.X with vimentin staining. (Figure 2.5). The shape of cells from the ventricular side in culture sometimes mimicked that of valve interstitial cells, although much less swirly than the latter. However, cells were positive for endothelial markers (CD31 and vWF) and negative for SMA.

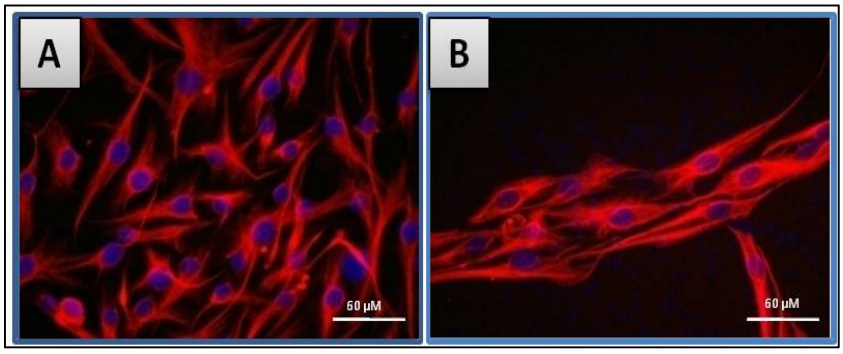

Figure 2.5 – Vimentin expression *(red)* in primary cultures of porcine aortic valve endothelial cells from the aortic (A) and ventricular side (B) of the cusp. Aortic-side endothelial cells have a more typical cobblestone appearance than cells from the ventricular side which often appeared elongated in culture under static conditions.

2.4.2.2 Immunocytochemistry

The only differences observed in the expression of various phenotypic markers between endothelial cells isolated from the aortic and ventricular sides of aortic valve cusps were observed in vWF and eNOS expression. Primary cultures of porcine aortic valve endothelial cells showed more vWF expression in cells isolated from the aortic side than the ventricular side of the cusp (Figure 2.6; *vWF=green, CD31=red*).

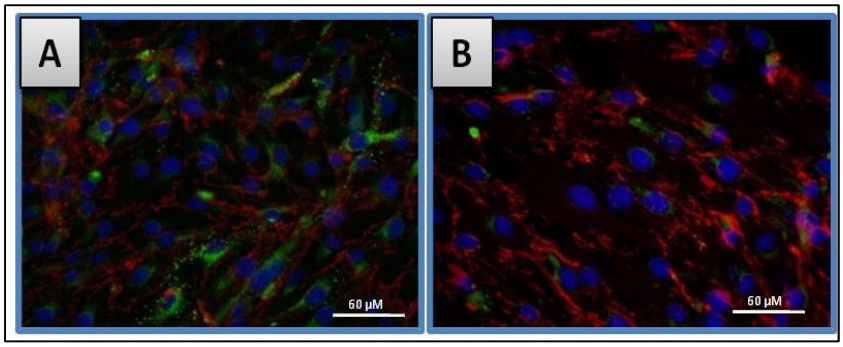

Figure 2.6 – vonWillebrand factor expression *(green)* in primary cultures of porcine aortic valve endothelial cells from the aortic (A) and ventricular side (B) of the cusp. Aortic-side endothelial cells express more vWF than their ventricular counterparts.

In addition, cultured cells from the aortic side of the cusps express more eNOS than their ventricular counterparts (Figure 2.7; *eNOS=red*).

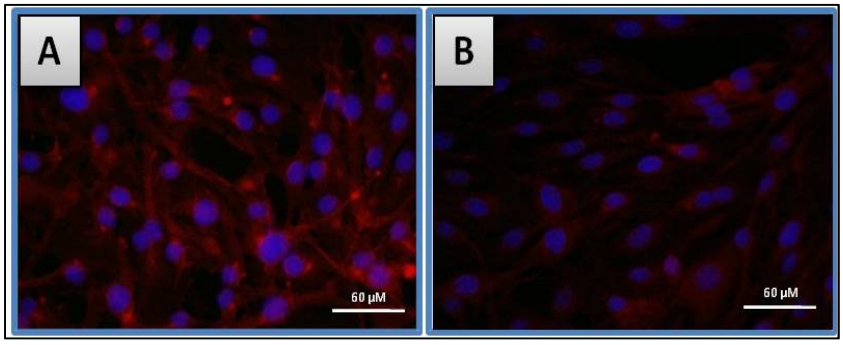

Figure 2.7 – Endothelial nitric oxide synthase (eNOS) expression *(red)* in primary cultures of porcine aortic valve endothelial cells from the aortic (A) and ventricular side (B) of the cusp. Aortic-side endothelial cells express more eNOS than their ventricular counterparts.

2.4.3 Functional Responses to Inflammatory Stimulation

No differences were observed in the expression of inflammatory markers (ICAM-1, VCAM-1, NFKB, phosphorylated p38 and phosphorylated JNK) with the addition of TNFα or TGFβ1 for 12, 24 or 48 hours, on endothelial cells from either side of the valve.

2.4.4 Differences in Gene Expression Profiles

The pig genome was expected to be released in December 2009. Unfortunately, to this day, it remains unpublished, therefore precluding any definitive conclusions of the gene array performed. Nevertheless, preliminary analysis of the data shows a total of 61 genes that are differentially expressed with a p-value <0.001 and a total of 423 genes with a p-value <0.01. This data represents a unique comparison of primary cultures of live aortic valve endothelial cells and may hold important clues into the functional and pathological differences observed between both sides of the aortic valve.

2.4.5 Structural and Functional Differences in Biomechanical Properties

2.4.5.1 Baseline Stiffness of Aortic Valve Endothelial Cells

Baseline analysis of aortic valve endothelial cell mechanical properties using SICM showed a significant difference between cells from either side of the cusp. AVECs on the ventricular surface of the aortic valve are significantly stiffer than cells on the aortic side of the valve (mean displacement: 11 ± 2 nm/kPa versus 32 ± 4 nm/kPa; $p<0.01$) (Figure 2.8).

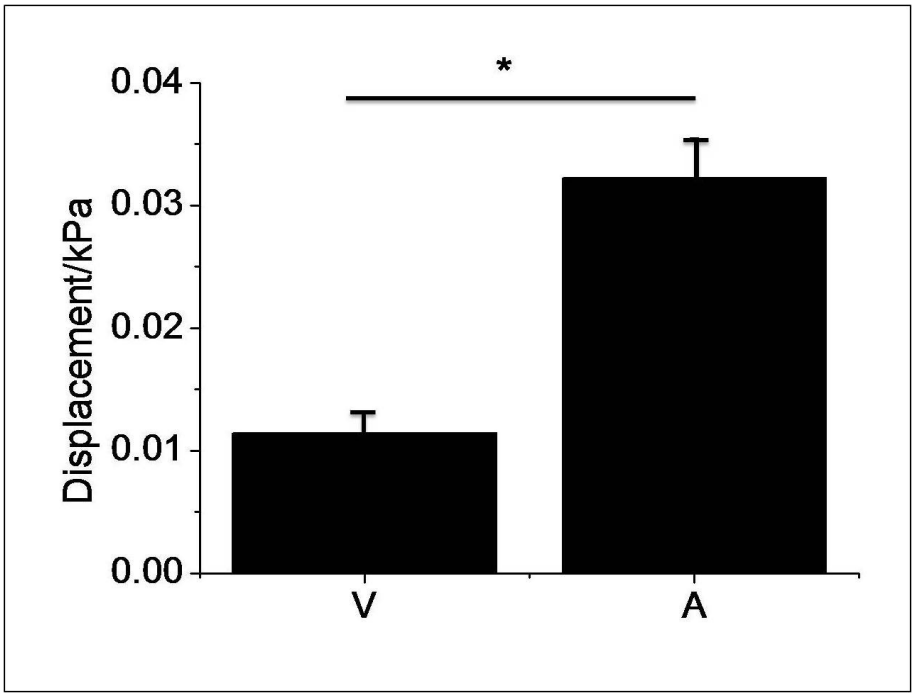

Figure 2.8 – Mean baseline stiffness of aortic valve endothelial cells from the ventricular and aortic sides of the aortic valve. Endothelial cells on the ventricular side are significantly stiffer than their aortic counterparts as evidence by reduced displacement in response to pressure.
*p<0.01
A: Aortic; V: Ventricular

2.4.5.2 Changes in Stiffness of Aortic Valve Endothelial Cells from the Aortic Surface of the Cusp in Response to Different Mediators

Changes in the stiffness of aortic valve endothelial cells from the aortic surface of the cusp in response to various mediators was assessed (Figure 2.9). Addition of SNP (10^{-5}M) did not affect the stiffness of endothelial cells. However, addition of ET-1 (10-8M) resulted in a significant increase in cell stiffness (mean displacement: 13 ± 1 nm/kPa following ET-1 administration versus 32 ± 4 nm/kPa in controls; *p<0.01*). The presence of L-NAME when adding ET-1 did not affect these results (mean displacement: 16 ± 3 nm/kPa with ET-1 and L-NAME versus 32 ± 4 nm/kPa; *p<0.01*). Furthermore, inhibition of NO production by adding L-NAME alone (10^{-5}M) resulted in similar findings with a significant increase in the stiffness of the tissue in the same range as addition of ET-1 (mean displacement: 11 ± 1 nm/kPa in the presence of L-NAME versus 32 ± 4 nm/kPa; *p<0.01*).

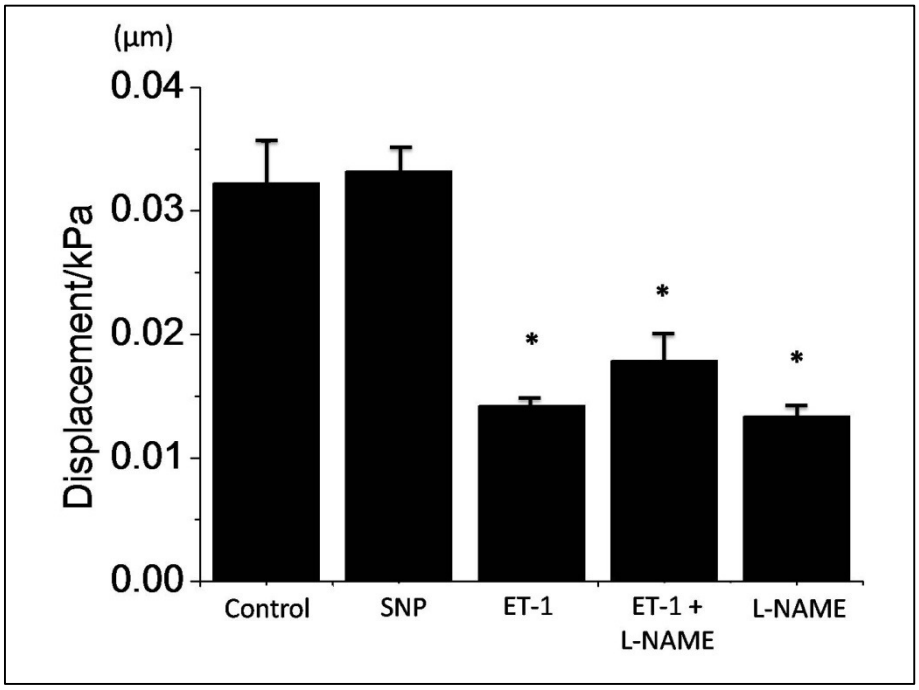

Figure 2.9 – Mean changes in stiffness of aortic valve endothelial cells on the aortic surface of the valve in response to different vasoactive agents. There was no change in stiffness following SNP administration. Addition of ET-1, L-NAME significantly increased the stiffness of endothelial cells. Addition of L-NAME to ET-1 did not change the results.
*p<0.01 vs. Control
SNP, sodium nitroprusside; ET-1, endothelin-1; L-NAME, L-Nitroarginine methyl ester.

In order to determine the direct role of ET-1 in inducing changes in cell stiffness, concentration-dependent responses to increasing concentrations of ET-1 were analyzed. As shown in Figure 2.10, there was an almost linear relationship between ET-1 concentrations and the degree of stiffening of endohtelial on the aortic surface of the cusps (ANOVA $p<0.05$).

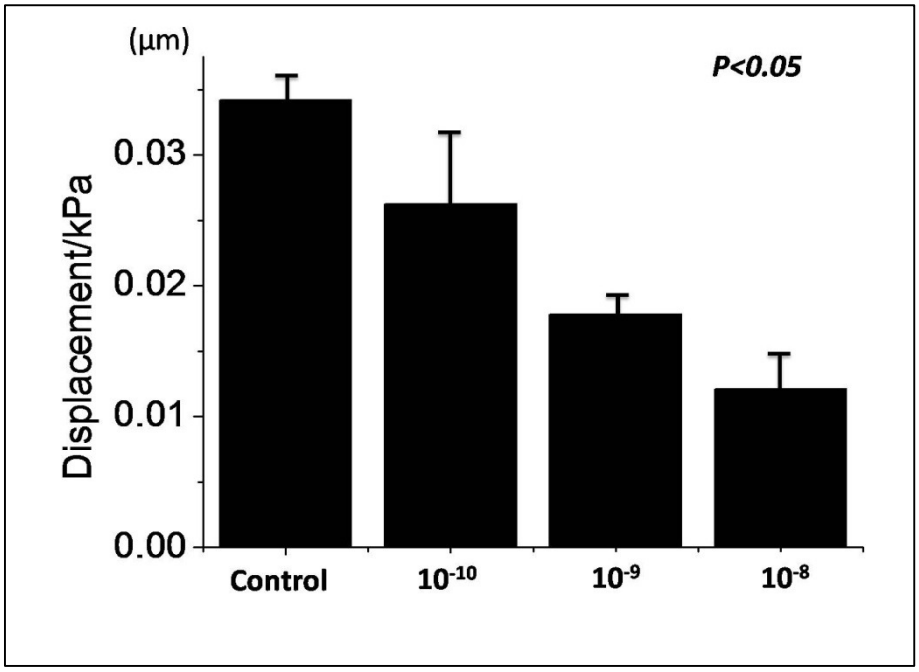

Figure 2.10 – Concentration-dependent changes in aortic valve endothelial cells on the aortic surface of the valve in response to increasing concentrations of ET-1.
*ANOVA $p<0.05$

Changes in cell stiffness in response to ET-1 administration are more clearly depicted in Figure 2.11 where individual measurements are each depicted by a seprate line. Black lines represent control cusps showing baseline cell stiffness. The slope of the curve is indicative of cell stiffness. The less steep the slope is, the less stiff the cells are. This figure shows a quasi-linear relationship between increasing pressure and displacement of cell surface. In contrast, after addition of ET-1 to the solution (red lines), increasing applied pressure on the cells resulted in little change in cell surface displacement, indicating increased stiffness.

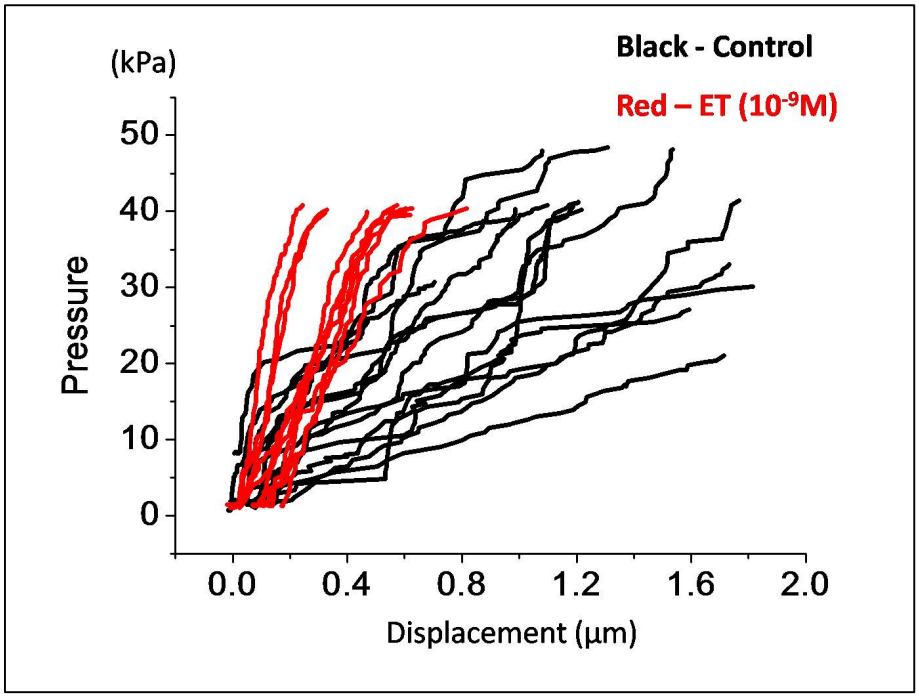

Figure 2.11 – Relationship between pressure and displacement of cell membrane in endothelial cells from the aortic surface of the aortic valve at baseline *(black)* and after addition of ET-1 *(red)*. *ET-1, endothelin-1*

2.4.5.3 Changes in Stiffness of Aortic Valve Endothelial Cells from the Ventricular Surface of the Cusp in Response to Different Mediators

Similarly, changes in aortic valve endothelial cell stiffness in response to similar agents were studied on the ventricular surface of the cusps. Figure 2.12 shows that, in contrast to cells from the aortic side, addition of SNP resulted in a significant decrease in endothelial cell stiffness (mean displacement: 32 ± 2 nm/kPa after addition of SNP versus 11 ± 2 nm/kPa in control cusps; $p<0.01$). However, addition of maximum concentrations of ET-1 (10^{-8}M) resulted in no significant change in the stiffness of endothelial cells (mean displacement: 9 ± 2 nm/kPa after addition of ET-1 versus 11 ± 2 nm/kPa in control cusps; $p<0.01$). Similarly, addition of L-NAME induced no significant change in cell stiffness (mean displacement: 13 ± 2 nm/kPa after addition of L-NAME versus 11 ± 2 nm/kPa in control cusps; $p<0.01$).

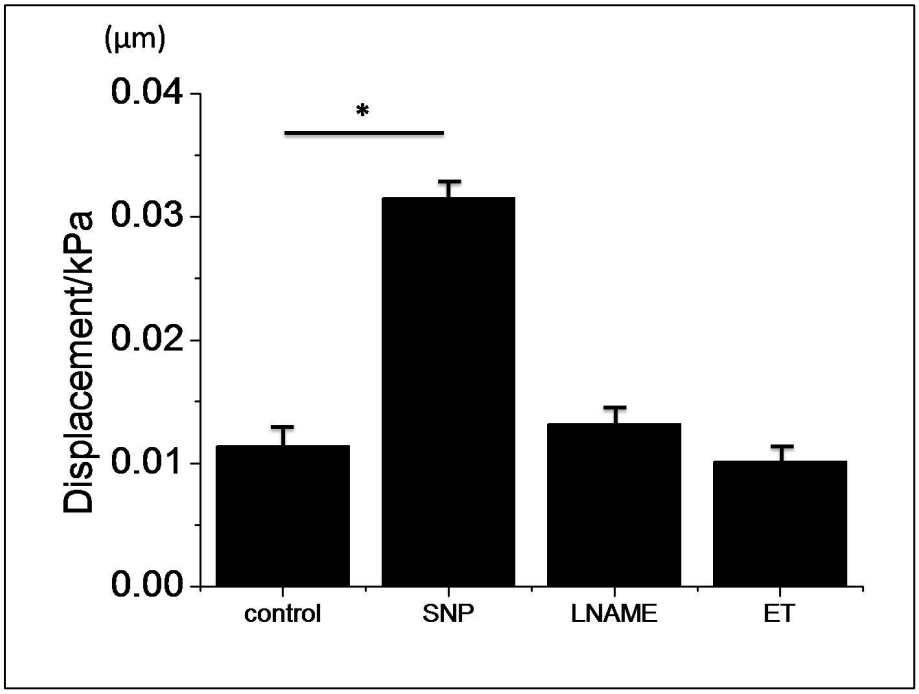

Figure 2.12 – Mean changes in stiffness of aortic valve endothelial cells on the ventricular surface of the valve in response to different vasoactive agents. There was a significant increase in stiffness following SNP administration ($p<0.01$). Addition of ET-1 or L-resulted in no changes in the stiffness of endothelial cells.
*$p<0.05$ vs. Control
SNP, sodium nitroprusside; ET-1, endothelin-1; L-NAME, L-Nitroarginine methyl ester.

Figure 2.13 illustrates the decrease in cell stiffness through various measurements in response to SNP *(red lines)* versus control *(black lines)*.

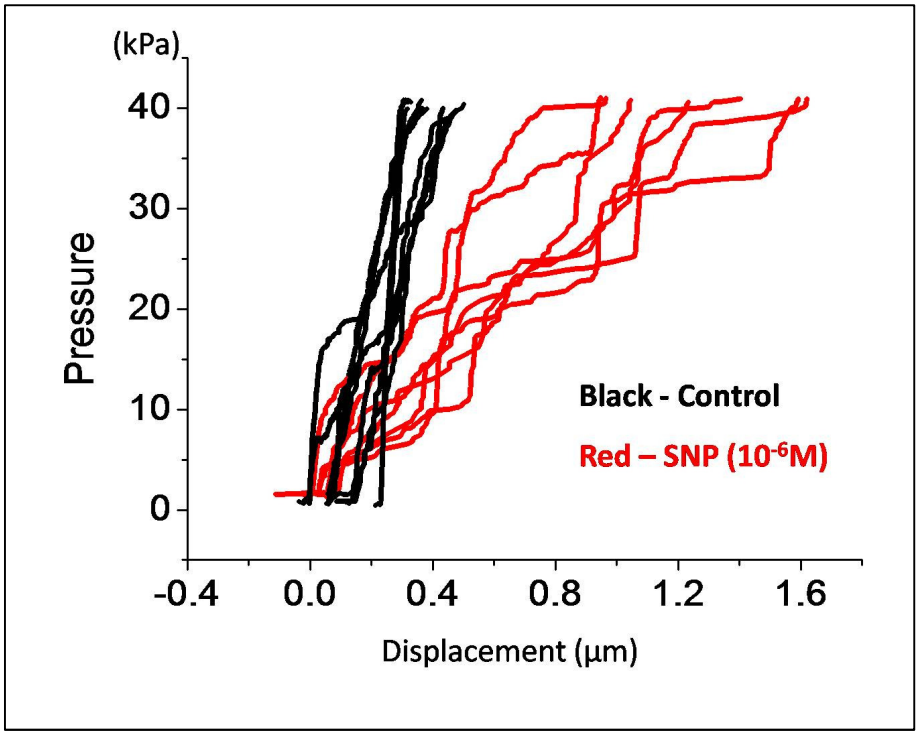

Figure 2.13 – Relationship between pressure and displacement of cell membrane in endothelial cells from the ventricular surface of the aortic valve at baseline *(black)* and after addition of SNP *(red)*.
SNP, sodium nitroprusside

2.5 DISCUSSION

In this chapter, we have described a novel, reliable and easily reproducible technique to selectively isolate primary cultures of aortic valve endothelial cells from either side of the valve in vitro. This has allowed to study morphological and phenotypic differences between cells from either side of the valve as well as analysis of gene expression profiles, confirming significant differences between the 2 sides, though precise knowledge of these differences awaits full identification of the pig genome. In addition, in the present chapter, we have shown that endothelial cells from either side of the valve analyzed in situ using SICM, have different baseline mechanical properties and exhibit different responses to the same vasoactive agents.

As mentioned previously, there is very compelling evidence that endothelial cells across the body have different properties on many levels, ranging from structure (size, shape), molecular composition, gene expression and ultimately, function. In this set of experiments, we have demonstrated that endothelial cells from either side of the aortic valve also further differ in terms of their in situ mechanical properties. Endothelial cells on the ventricular surface of the valve are significantly stiffer than cells on the aortic side. In addition, they exhibit different responses to similar vasoactive agents. The stiffness of eukaryotic cells is mainly determined by the cytoskeleton. Although the name suggests a static structure, the cytoskeleton is a highly dynamic and adaptive structure whose components are in constant flux. In addition to determining the stiffness of the cells, the cytoskeleton has 3 main functions: it physically and biochemically connects the cell to the extracellular environment, it allows the cell to move and change shape through coordinated movements and it spatially organizes the contents of the cell (Fletcher & Mullins, 2010). The cytoskeleton consists of 3 main polymers: actin filaments, microtubules and a group of polymers collectively known as intermediate filaments. They differ mainly in their mechanical stiffness, their assembly dynamics, their polarity and the molecular motors they associate with. Microtubules are the stiffest of the 3 polymers while intermediate filaments are the least rigid. Most cells in the cardiovascular system are mainly exposed to pressure-type mechanical forces. However, endothelial cells are additionally exposed to shear stress which is defined as the frictional force per unit area from flowing blood. The magnitude of shear stress can be estimated in most of the vasculature by Poiseuille's law stating that wall shear stress is proportional to blood flow viscosity and volumetric flow rate and inversely proportional to the third power of the internal radius (P. F. Davies, 1995). While actual wall shear stress is very difficult to estimate, mean shear stress along an artery is estimated at 20 dynes/cm^2. Unlike blood vessels, the aortic valve is not a cylindrical structure, therefore estimation of shear stress levels on either side of the valve requires more complex modelling. A number of potential mechanotransducers thought to mediate endothelial cell responses to shear stress have been described such as integrins, ion channels, apical glycocalix, the primary

cilia, heterotrimeric G-proteins, CD31 and VE-cadherin. A question that remains however is: What is the value of determining the mechanical properties of single cells?

A cell is more than the sum of its individual components. It is a hierarchically ordered system which lies within a dynamic environment. The cytoskeleton is an integral part of this structural, molecular and functional continuum. Cellular mechanosensing is based on force-induced conformational changes in mechanosensitive proteins that result in opening of membrane channels or altered affinities to binding partners, thereby activating signalling pathways. Therefore, any differences in intrinsic mechanical properties or any changes in the normal intracellular force transmission through changes in cellular (or extracellular) structure and organization can lead to altered molecular forces acting on these proteins, resulted in attenuated or increased mechanosensitive signals (Jaalouk & Lammerding, 2009). Our findings indicate that endothelial cells on both sides of the aortic valve have different baseline mechanical properties with cells on the ventricular surface being significantly stiffer than their counterparts on the aortic side. Whether these differences are present from the developmental origins of the cells or represent an evolutionary adaptation to their local mechanical environments remains to be determined. Endothelial cells on the aortic surface of the valve are exposed to low shear disturbed flow mainly during diastole whereas the ventricular side is exposed to high shear laminar systolic flow. This inevitably translates into different mechanical signals and requires distinct adaptive changes. Differences in the expression of vWF and eNOS were observed between both sides, with cells on the aortic side expressing more of both in static culture conditions. In addition, morphological differences were also observed. Although cells in static culture do not align in a particular orientation, yet cells from the ventricular side show a significantly more elongated shape which likely reflects the type of flow they are exposed to in vivo. Cytoskeletal form meets function in vivo and cytoskeletal arrangement in vitro can certainly serve as a map of the cell's previous mechanical environment (Fletcher & Mullins, 2010). A point of major importance will be to evaluate the effect of various clinical risk factors for aortic valve disease such as hypertension (increased pressure and strain),

smoking/dyslipidemia (endothelial dysfunction) or high circulating 5-HT levels (carcinoid disease) on the mechanical properties of the cells. It might be that some of these factors can directly alter cytoskeletal prestress which controls the stiffness of tensed cytoskeletal filaments (such as stress fibers and intermediate filaments), thereby modulating the fidelity and speed of intracellular mechanical signalling responses (Janmey, Euteneuer, Traub, & Schliwa, 1991; Kumar et al., 2006; Luo, Xu, Lele, Kumar, & Ingber, 2008).

Another important element to take into consideration when evaluating differences in cell mechanobiology is the fact that the ECM composition differs between the fibrosa and the ventricularis. Changes in the mechanical properties of the substrate or the matrix has been demonstrated to have major effects on cell behaviour (Engler, Sen, Sweeney, & Discher, 2006). The fibrosa is rich in collagen whereas the ventricularis contains most of the elastin. Knowing that the cytoskeleton interacts directly or indirectly with ECM components during mechanotransduction and that collagen and elastin have different elastic moduli and importantly have important functional roles, studying aortic valve endothelial cell mechanobiology has to take these elements into account. Finite element modelling using acquired mechanical information of the different elements and incorporating shear stress and strain data represents a plausible approach at this stage (Charras & Horton, 2002).

There are several available techniques to assess the mechanical properties of cells, whether in culture or in situ, including SICM, atomic force microscopy (AFM), optical trapping, magnetic bead microrheometry and micropipette aspiration. Of these, SICM and AFM allow studying non-fixed living cells in an aqueous environment. As described in the Methods, SICM is based on the differences in electrical charge between the scanning nanopipette and the medium, while maintaining the distance between the pipette and the sample constant. Because of that difference in charge, there is a constant flux of ions through the nanopipette. Any reduction in the distance between the pipette tip and the sample will automatically translate into reduced flow of ions through the pipette. This determines cell surface deformations during

testing. On the other hand, AFM uses a tapered probe, typically made of silicon or silicon nitride, which is attached to a cantilever arm. When the probe tip interacts with the sample, the arm is deflected. Deflections are simultaneously measured by sensing the position of a laser beam that reflects off the cantilever arm. Displacements of less than 1nm can be accurately detected. Both techniques can provide morphological data of cell topography as well as mechanical and molecular information of living cells (Charras & Horton, 2002; Gorelik et al., 2008; Horton, Charras, & Lehenkari, 2002; Nikolaev et al., 2010; Novak et al., 2009).

The pig represents an excellent model to study normal cellular and molecular physiology due its close similarity with human beings. In fact, porcine aortic roots are used everyday in cardiac surgery as valves or roots (eg., Medtronic Freestyle®, Medtronic, Minneapolis, MN, USA). Nevertheless, there are significant differences between the pig and the human species at several levels. Anatomically, the pig heart presents some differences compared to the human heart: there is a significant muscle shelf below the subcoronary cusp, the height of the coronary arteries and the intercoronary angle are consistently different from humans. At the immunological level, the swine leucocyte antigen (SLA) system is different from the human leukocyte antigen (HLA). Importantly, from a clinical relevance standpoint, it has always been thought that pigs do not develop aortic valve calcification, though that remains to be determined in a scientific fashion. Along with these differences between pigs and humans, it is expected that differences in the human and pig genomes are inevitable. Though there are many similarities between both genomes and the separation between the pig and human genomes is less than between the mouse and human ones (Wernersson et al., 2005), yet it would be inaccurate to analyze porcine gene arrays using the human genome. In a previous study, Simmons et al. had however accepted this extrapolation and sued a human gene array on pig-derived aortic valve endothelial cells (Simmons et al., 2005). Their findings were interesting because they showed differences in gene expression profiles between both sides. However, the specific pattern of differences remains to be confirmed using pig-specific tools. There are several collaborative projects currently in progress attempting to map the full porcine genome,

but to date, the it remains incompletely mapped. Therefore, until this is completed, it was thought more accurate to delay analyzing the gene array data obtained.

The observed heterogeneity in endothelial cell properties could have important implications in the understanding of aortic valve disease. As will be discussed in the following chapter, aortic valve calcification (the most common aortic valve pathological presentation) occurs almost exclusively on the aortic side of the cusp. In addition, it is proposed that mechanisms similar to those involved in atherosclerosis are operative in aortic valve calcification. As is well demonstrated, endothelial dysfunction is a first step in the sequence of events leading to plaque formation and rupture. Endothelial dysfunction which was once thought to be restricted to the inability of the endothelium to produce and release vasodilatory agents such as NO, could also represent alterations in cell mechanobiology, mechanosensing or mechanotransduction.

2.6 LIMITATIONS

This set of experiments has several limitations. First, we used a pig model both to isolate aortic valve endothelial cells as well to study their mechanical properties in situ. As mentioned in the Discussion, there are inter-species differences which could make our results invalid in humans. However, the lack of availability of healthy human valves for research purposes makes it almost imperative to undertake such studies on an animal model. The pig is well suited for such experiments since the cardiac anatomy and the hemodynamics are largely comparable to humans. Although gene expression profiles were examined in aortic and ventricular endothelial cells, the absence of full porcine genome mapping makes it yet difficult to fully exploit this data. Once the genome is fully sequenced, this data will provide significant insight into differences between cells on either side of the valve. Mechanotransduction implies by definition the presence of mechanical stimuli. In the case of aortic valves, theses stimuli are mainly strain,

shear stress, compression and bending forces. Though we have demonstrated significant differences in the mechanical properties of cells from both sides of the valve, these experiments were performed in static conditions. This, in itself, may constitute a pathological state. Nevertheless, experiments were always performed within hours of animal sacrifice at which time it is thought that cells still carry their in vivo cytoskeletal arrangement memory.

2.7 Conclusions and Future Directions

In conclusion, the present experiments demonstrate for the first time the feasibility of separately isolating primary cultures of aortic valve endothelial cells from either side of the aortic valve. In addition, in situ analysis of the mechanical properties of endothelial cells shows they have significantly different baseline stiffness and their responses to vasoactive agents differ significantly. These findings can have important research implications in allowing better understanding of the cellular and molecular differences between both sets of endothelial cells. This could help understand the pathophysiology of aortic valve calcification and allow testing different therapeutic strategies in vitro, such as the use of statins. Ongoing and future studies will focus on 2 parallel sets of experiments. In vitro study of endothelial cells will focus on better characterization of the molecular pathways activated in response to different stimuli as well as the role of various agents on endothelial cells in vitro, such as statins and angiotensin-converting enzyme inhibitors (ACE-I). In addition, using an in vitro flow system which has been adapted for use with cultures cells, we will examine the response of endothelial cells to different patterns of shear stress. Obtained conditioned medium from these experiments will be tested on valve interstitial cells grown in osteogenic medium to test the proposed protective effect of endothelial cells against valve calcification. Another set of experiments will be focused on endothelial cells in situ using SICM. Aortic valve cusps will be exposed to different degrees, durations and pattern of shear stress and changes in the mechanical properties of endothelial

cells will be examined. More importantly, using a tissue model of aortic valve calcification (discussed in the following chapter), we will evaluate the role of mechanotransduction on aortic valve calcification in response to altered shear stress.

III Modulation of Aortic Valve Calcification

3.1 BACKGROUND

Aortic valve calcification is a major source of morbidity and mortality from cardiovascular causes. Treatment of aortic valve calcification remains limited to surgical replacement of the severely calcified valve if the patient is symptomatic or develops left ventricular dysfunction (Bonow et al., 2006). Until recently, aortic valve calcification was thought to be due to "wear and tear" of the cusps due to opening and closure leading to repetitive areas of microtrauma with subsequent degeneration and formation of calcium nodules. Nevertheless, careful evaluation of the calcified aortic valve cusps suggested that calcification is likely due to active cell-mediated mechanisms which could be similar in nature to vascular calcification phenomena (Mohler et al., 1999; Otto et al., 1994; Reynolds et al., 2004). It is thought that similar to atherosclerosis, aortic valve calcification is characterized by early endothelial dysfunction, an initial step in the cascade of events leading to valve calcification (Otto et al., 1994). This hypothesis is corroborated by clinical assessment of patients with aortic valve disease showing systemic endothelial dysfunction measured by brachial flow analysis (Poggianti et al., 2003). Similar to atherosclerotic vessels, the site of calcium formation in the valve cusps is the body of the cusp, ie., the subendothelial region. This suggests that if the endothelium is implicated in calcification, it necessarily communicates with the underlying interstitial cells, sending pro- or anti-calcification signals. Interestingly, calcified nodules occur almost exclusively on the aortic side of the valve (Figure 3.1), prompting us to evaluate the potential regulatory effect of the endothelium from either side of the cusps on aortic valve calcification.

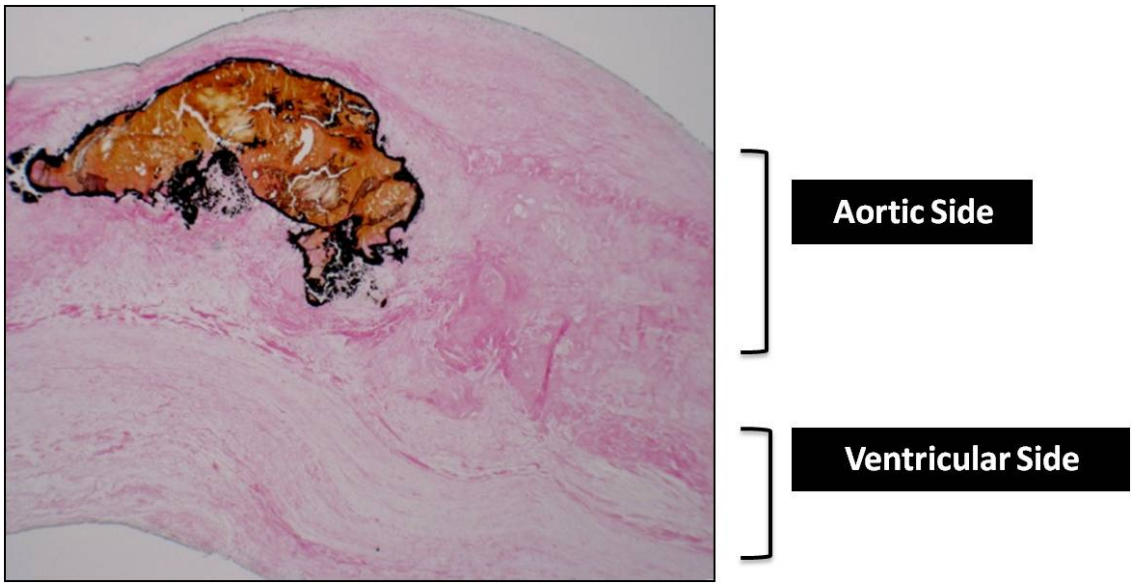

Figure 3.1 - Histological section across a human calcified aortic valve showing the presence of a von Kossa-positive nodule. The calcium nodule is characteristically located on the aortic side of the valve (fibrosa).

Previous work from our group and others, focusing on human valve interstitial cell calcification suggested that aortic valve interstitial cells undergo a process of transdifferentiation into osteoblast-like cells demonstrating alkaline phosphatase activity after exposure to osteogenic medium (Mathieu et al., 2005; Lana Osman, Magdi H. Yacoub, Najma Latif, Mohamed Amrani, & Adrian H. Chester, 2006). Nevertheless, because of the difficulty of obtaining healthy human aortic valves, it is important to develop a reliable and reproducible model of in vitro aortic valve interstitial cell calcification. Various groups had previously published data describing such results using aortic valves from different sources including pigs, dogs and sheep (Jocelyn N. Clark-Greuel et al., 2007; Mathieu et al., 2005; Mohler et al., 1999). All the studies based their findings on the in vitro formation of cell nodules, similar to those observed in vascular smooth muscle cell cultures following exposure to osteogenic medium. However, the precise composition and characterization of these nodules has never been properly tested beyond the demonstration that they stain positively to Alizarin red or von Kossa.

3.1.1 Aims

The aims of the present series of experiments were to develop a reliable and reproducible in vitro whole tissue model of aortic valve calcification. Using this model, we aim to evaluate the differential propensity of either side of the cusp to aortic valve calcification and determine the role of endothelium-derived NO in regulating the calcification process.

3.2 METHODS

3.2.1 Aortic Valve Interstitial Cell Isolation and Culture

Porcine hearts (12-18 months old) were obtained within 12 hours after sacrifice from a commercial abattoir (Cheale Meats, Essex, UK). Hearts were immediately placed in cold-buffered Hanks solution for transport. Under sterile technique, aortic valve cusps were dissected and washed in 1%phosphate -buffered saline (PBS) at room temperature, and kept in cold serum free M-199 (Sigma UK) until use. Care was taken during dissection to avoid excessive cusp manipulation which could damage the cellular structure of the cusps. All 3 cusps from a single heart were then placed in a 50mL Falcon tube containing 10mL of Collagenase type II solution (*Clostridium histolyticum,* Sigma UK [PN: C6885]) diluted in PBS (600U/mL) and maintained at 37C and the tube was placed in a 37C incubator (95%0_2, 5%CO_2) for 12 minutes to extract the endothelial cells. Following this initial period of digestion, the tube was place on a vortex at high velocity and kept for 1 minute. The cusps were then individually removed from the solution and placed in a new 50mL Falcon tube containing fresh Collagenase II (10mL at 600U/mL) at 37C. The tubes were put in a tube shaker with their bottom dipping in a 37C waterbath to maintain the collagenase temperature and enzymatic activity. After shaking the tubes for 1 hour, an equal volume (10mL) of cold high glucose Dulbecco's Modified Eagle

Medium (DMEM) was added to inactivate the collagenase. The digested cusps at this stage have a gelatinous texture and are removed from the solution under sterile conditions. The mixture is centrifuged for 5 minutes at 1000g. The supernatant was discarded and the pellet is resuspended in growth medium (high-glucose DMEM [Sigma UK] with 10% heat-inactivated fetal calf serum, 100 U/mL (1%) penicillin, 100 µmol/L (1%) streptomycin [Life Technologies, UK] and 4 mmol/L (1%) L-glutamine [Invitrogen, UK]) and plated in T75 flasks (75 cm^2). One T75 flask was used for each heart (ie, 3 cusps). Tissue plates were placed in an incubator at 37^0C in 5% CO_2 in air with medium changes after 24hr then every three days thereafter. When confluent, cells were passaged by adding a trypsin/EDTA solution for 2 minutes. When cells started detaching, the flask was gently shaken and enzymatic activity interrupted by adding an equal volume of cold DMEM to the flask. The cells were aspirated and centrifuged at 1000g for 5 minutes. For experiments, cells were used between passages 3 and 7.

3.2.2 In vitro Aortic Valve Calcification Model

3.2.2.1 Cell-Based In Vitro Calcification

In vitro calcification was tested by placing aortic valve interstitial cells in osteogenic medium. Osteogenic medium consisted of normal growth medium supplemented with 50 µg/mL ascorbate-2-phosphate (Sigma, UK), 10 nmol/L dexamethasone (Sigma, UK), 10 mmol/L β-glycerol phosphate (Sigma, UK) and 10 ng/mL porcine TGF-β1 (R&D Systems, UK). The medium was changed every 3 days and cells were examined at 7, 14 and 21 days. All isolates cultured in osteogenic medium were compared to a control population from the same isolate grown in normal growth medium.

3.2.2.2 Histochemical Staining for Calcium Detection

Alizarin Red Staining

Cells grown on cover slips were washed 3 times in PBS then fixed using 4% paraformaldehyde for 10 minutes at room temperature. Alizarin red S solution was then added for 5 minutes and the cover slips were then washed vigorously 3 times with ultra-distilled water to remove any unbound stain. The cover slips were then examined under light microscopy. Red-brown stains were considered positive markings. Alizarin red-positive nodules were quantified in terms of number and size.

Von Kossa Staining

Cells grown on cover slips were washed 3 times in PBS then fixed using 4% paraformaldehyde for 10 minutes at room temperature. Silver nitrate solution (2%) was then added to the cover slips which were maintained under direct light for 45 minutes. After 45 minutes, the silver nitrate was washed off using ultra-distilled water and the cover slips were counterstained with van Giesson stain. Cover slips were then examined under light microscope. Black stains were considered positive marking. Von Kossa-positive nodules were quantified in terms of number and size.

3.2.2.3 Tissue-based In Vitro Calcification

Using the same plate used for selective isolation of aortic valve endothelial cells as previously described, aortic valve cusps were placed in control growth medium versus osteogenic growth medium: normal growth medium supplemented with 50 μg/mL ascorbate-2-phosphate (Sigma, UK), 10 nmol/L dexamethasone (Sigma, UK), 10 mmol/L β-glycerol phosphate (Sigma, UK) and 10 ng/mL porcine TGF-β1 (R&D Systems, UK) for up to 21 days. The presence of Alizarin Red staining, von Kossa staining and markers of osteogenic differentiation were used to evaluate the validity of this model in mimicking aortic valve calcification in situ.

After dehydration, formalin samples were embedded in paraffin wax and cut into 0.5μm sections using a microtome. Sections were collected on glass slides and heated for 24 hours at

60°C. The tissue samples were then dewaxed, rehydrated and incubated in Alizarin red S for 5 minutes or 2% silver nitrate for 1 hour under direct light followed by van Giesson counterstaining. Samples were blot dried and dehydrated. The slides were viewed on Nikon light microscope. Calcium nodules were quantified in terms of number and size. The overall distribution was also assessed.

3.2.3 Role of the Endothelium on Aortic Valve Calcification

3.2.3.1 Side-Specific Aortic Valve Calcification Model

Using the same plate used for selective isolation of aortic valve endothelial cells, aortic valve cusps were placed in culture medium under control or osteogenic conditions for a period of 10 days. The aortic and ventricular sides of porcine aortic valve cusps were selectively exposed to control growth medium or osteogenic medium. The presence of Alizarin red-positive nodules on histological sections of the aortic cusps was the primary endpoint. The aortic and ventricular sides were compared to each other as well as their respective controls (cusps kept in normal growth medium). All 3 aortic valve cusps were obtained from each animal. Each aortic valve cusp was used for a specific subset of experiments. Each cusp was cut into 3 pieces, forming the 4 study groups as shown below (Figure 3.2):

- ***Cusp #1 – Aortic side osteogenic vs. control***
    i. Baseline control (day 0)
    ii. Aortic side in control medium for 10 days (day 10)
    iii. Aortic side in osteogenic medium for 10 days (day 10)
- ***Cusp #2 – Ventricular side osteogenic vs. control***
    i. Baseline control (day 0)
    ii. Ventricular side in control medium for 10 days (day 10)
    iii. Ventricular side in osteogenic medium for 10 days (day 10)

- ***Cusp #3 – Aortic side osteogenic vs. Ventricular side osteogenic***
    i. Baseline control (day 0)
    ii. Aortic side in osteogenic medium for 10 days (day 10)
    iii. Ventricular side in osteogenic medium for 10 days (day 10)

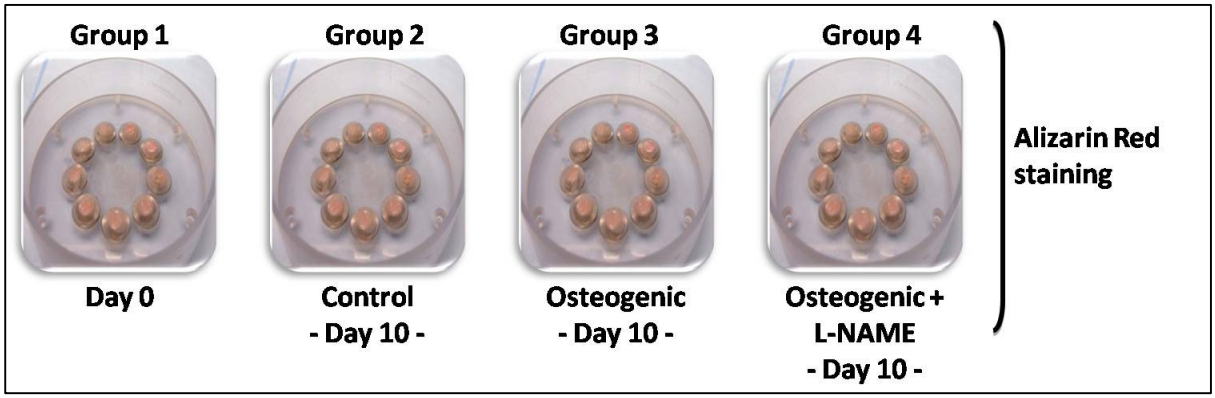

Figure 3.2 - Figure illustrating the different groups in the study. For each group, the aortic and the ventricular surfaces of aortic valve cusps were exposed. The same cusp was cut in two pieces so that each cusp served as its own control. Experiments were carried for a period of 10 days and Alizarin red staining was used to verify the presence of calcium nodules.

3.2.3.2 Evaluation of the Role of the Endothelium

3.2.3.2.1 Pharmacological Inhibition of the Endothelium

The capacity of the endothelium to produce NO was inhibited by adding L-NAME (100 μM), an inhibitor of nitric oxide synthase (NOS) activity, to the control or osteogenic medium. L-NAME was replaced every 3 days while replacing the growth medium.

3.2.3.3 Evaluation of Nitric Oxide Production by Aortic Valve Endothelium

NO production from either side of the valve (n=8 for each side) was evaluated under static (n=4) and physiological flow conditions (n=4) using a cone and plate apparatus (as described below). To evaluate side-specific production of NO, a commercially available kit to measure the

levels of cyclic guanosine monophosphate (cGMP) was used as a surrogate for NO production (K372-100, BioVision, UK). Experiments were performed in the presence of isobutylmethylxanthine (IBMX), a non-specific inhibitor of phosphodiesterase (PDE), to prevent degradation of cGMP in the tissue.

All tissues were excised, flash frozen and crushed in liquid nitrogen and then homogenized in 0.1M HCl. After centrifuging the homogenate at 3600g for 10 minutes, the supernatant was collected and immediately frozen at -80C for later use to perform the cGMP analysis. Reagents, supernatant and the standard solution (for the standard curve) were prepared as per the manufacturer's protocol (see below). The supernatant was acetylated to increase the sensitivity of cGMP detection. After completion, the Protein G Coated Plate was read in an optical spectrometer at 450nm.

cGMP Analysis protocol:

1. Prepare re-agents as advised in the protocol leaflet.
2. Prepare sample by freezing in liquid nitrogen, crush into powder and homogenise in 5-10 volume of 0.1m HCL.
3. Centrifuge and collect supernatant.
4. Prepare standard solution for the standard curve
5. Acetylate the mixture to increase the sensitivity of the assay
6. Add acetylated standard cGMP and samples to protein G coated well plates
7. Add antibody, and later cGMP-HRP and one hour later the cGMP-HRP developer
8. Stop reaction by adding 0.1M HCL
9. Read OD at 450nm

10. Construct standard curve and calculate amount of cGMP/well

3.2.3.4 Cone and Plate Apparatus for Reproduction of Aortic and Ventricular Waveforms

In order to perform studies on aortic valve tissue while exerting physiological flow and shear stress patterns on the aortic and ventricular side of the cusps, we used a cone and plate device developed by the biomedical engineering team at the Georgia Institute of Technology (Sucosky et al., 2008). As mentioned in the Introduction, the aortic and ventricular sides of the cusps are exposed to vastly different shear stress patterns, which could have an important effect on endothelial cell responses. Figure 3.3 depicts the variations in physiological shear stress across the cardiac cycle on either surface of a living aortic valve according to their calculations.

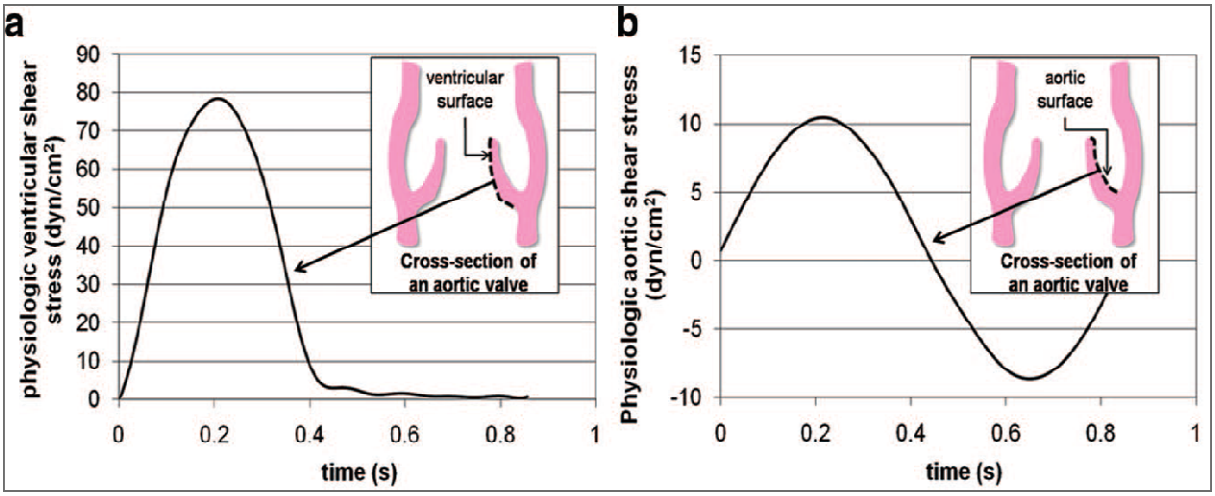

Figure 3.3 – Computed physiological shear stress variations across time as experienced by the aortic valve endothelial cells on a) the ventricular surface of the cusps and b) the aortic surface of the cusps. Adapted from Sucosky et al. (Sucosky, Balachandran, Elhammali, Jo, & Yoganathan, 2009)

Aortic valve cusps were mounted in the previously mentioned plate while ensuring that all cusps were oriented in the same direction, thus exposing only the aortic or the ventricular side of the cusps to a particular condition. Cusps were exposed to their physiological flow then analyzed at 2 time points: 30 minutes and 4 hours. Individual cusps could only be analyzed at a

single time point. Once cusps were obtained, they were immediately flash frozen and the steps described in the previous section for cGMP quantification were undertaken.

3.3 RESULTS

3.3.1 In Vitro Aortic Valve Calcification

3.3.1.1 Cell Culture Model of Valve Calcification

Primary porcine aortic valve interstitial cell isolates were used between passages 4 and 7 for these experiments. Two groups were compared: control medium and osteogenic medium. Cells were cultured for a period of 21 days without passaging, and analyzed using different techniques at baseline, 7, 10, 14 and 21 days. Control cultures showed the formation of spontaneous nodules starting at 1 week and showing a steady but slow increase up to 3 weeks. When grown in osteogenic medium, cells started forming nodules within 1 week of exposure to osteogenic medium (Figure 3.4 and 3.5).

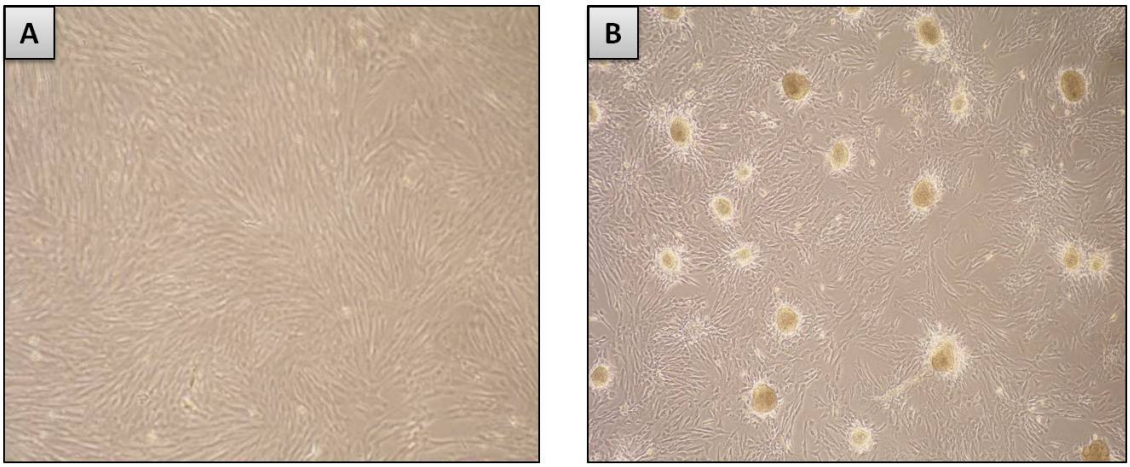

Figure 3.4 – Light microscopy pictures of primary cultures of porcine aortic valve interstitial cells in A) control growth medium and B) osteogenic medium for 1 week, showing the presence of dense nodules.

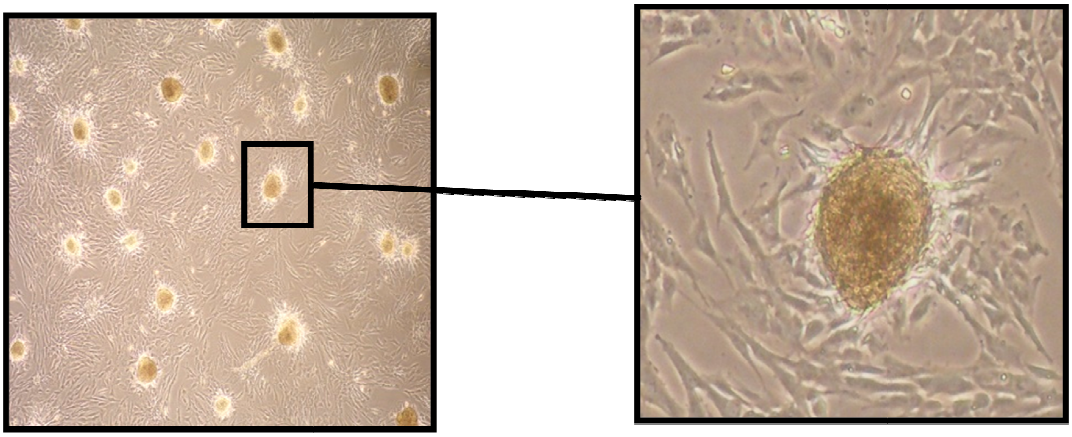

Figure 3.5 – Higher magnification (100x) of in vitro aortic valve interstitial cell nodules following exposure to osteogenic medium showing a coalescence of cells in and around the nodule.

The number and density of nodules increased with length of exposure. The number of nodules was significantly higher in osteogenic cultures than control cultures at 14 and 21 days ($p<0.05$) (Figure 3.6).

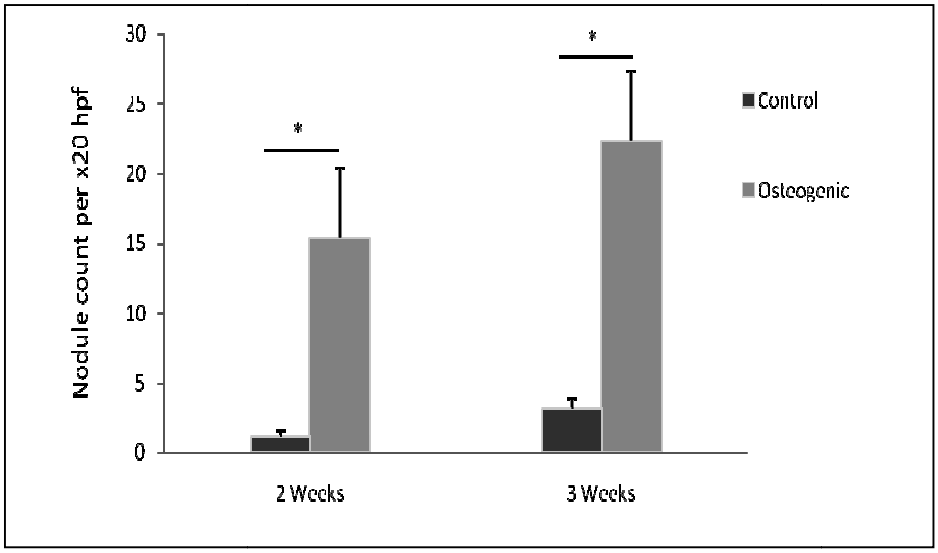

Figure 3.6 – Histogram showing a significant increase in the number of porcine aortic valve interstitial cell nodules following exposure to osteogenic medium for 2 and 3 weeks. **p<0.05*

In order to determine the presence or absence of mineralization in cell nodules, Alizarin red and von Kossa were performed as previously described. As shown in Figure 3.7, nodules

grown in osteogenic medium stained showed positive Alizarin red staining. In contrast, von Kossa staining was more difficult to elicit (Figure 3.8). The positive Alizarin red staining suggests the presence of calcium and early mineralization in these nodules.

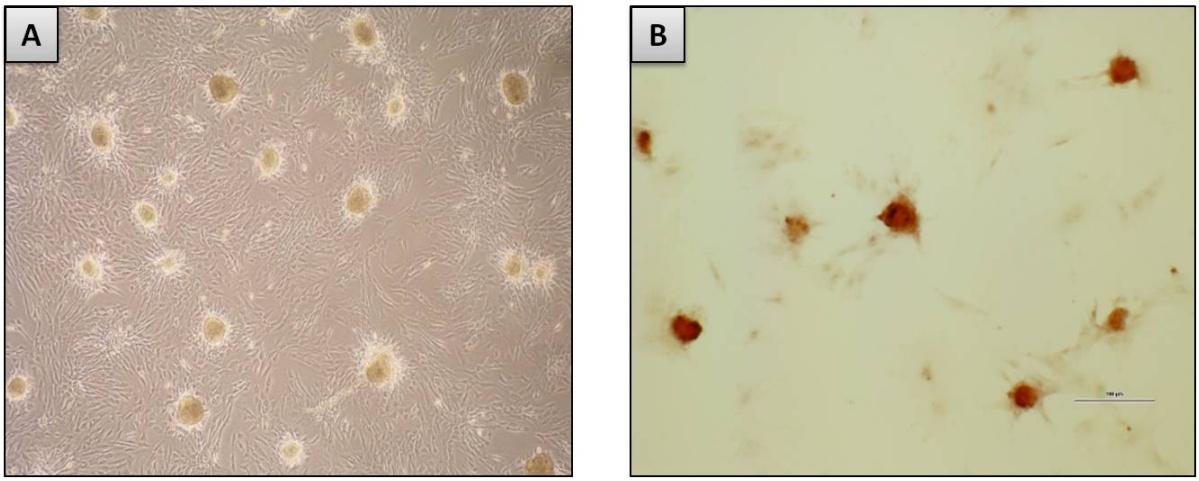

Figure 3.7 – Alizarin Red staining of cultured aortic valve interstitial cells grown in osteogenic medium showing positive red staining, indicative of the presence of calcium in the nodules.

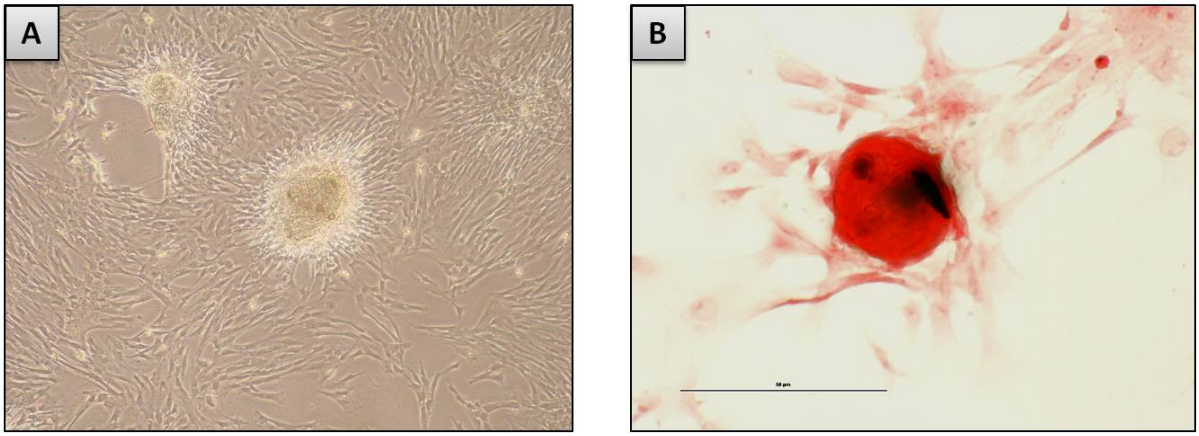

Figure 3.8 – von Kossa staining of cultured aortic valve interstitial cells grown in osteogenic medium showing faint positivity as characterized by the presence of black staining inside the nodules.

3.3.3.2 Tissue Culture Model of Valve Calcification

We hypothesized that the mechanisms that were operative in nodule formation and mineralization of aortic valve interstitial cells in culture should also be operative if whole aortic

valve cusps were put in culture under the same conditions. Using a custom-made tissue culture chamber for aortic valve cusps, 2 groups were compared as previously: control group and osteogenic group. Each cusp was cut in two pieces, with each half being exposed either to control or osteogenic medium for a period of up to 21 days. Thus, each cusp served as its own control. Cusps were removed at 7, 10, 14 and 21 days and fixed according to the appropriate protocols. Histochemical evidence of mineralization was assessed using Alizarin red and von Kossa staining as well as immunohistochemical evidence of osteogenic transdifferentiation.

Aortic valve cusps placed in osteogenic medium showed the presence of Alizarin-red positive nodules after 7-10 days in culture. Cusps grown in control medium did not demonstrate the presence of nodules within the matrix. Furthermore, the nodules were almost exclusively located on the aortic side of the cusp as shown in Figure 3.9.

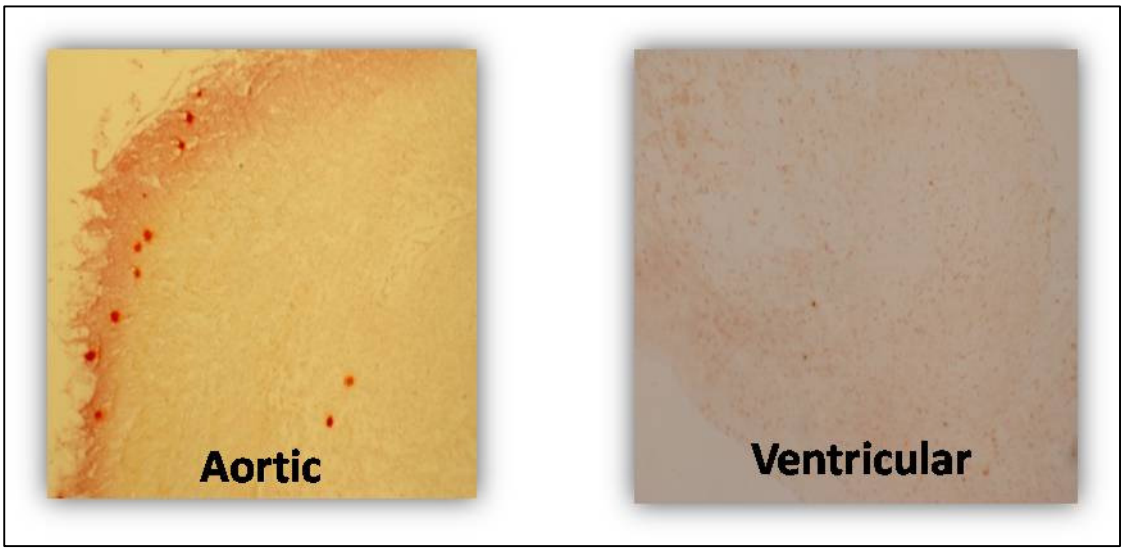

Figure 3.9 Representative histological sections of porcine aortic valve cusps placed in osteogenic medium containing TFG-beta1 for 10 days. Alizarin-red positive nodules are seen on the aortic side of the cusp whereas no nodules are observed on the ventricular side

Similar to cell cultures, von Kossa staining did not yield positive results in either group. In addition, immunohistochemical analysis of the cusps was performed to evaluate the presence of osteogenic transdifferentiation within the interstitial cell population. Bone-specific markers

used were osteopontin, osteocalcin, cbfa-1 and bone-specific alkaline phosphatase. Cusps were stained at baseline and at different time points. No evidence of osteogenic differentiation was observed in aortic valve cusps including after 21 days of exposure to osteogenic medium.

3.3.2 Side-Specificity of Aortic Valve Calcification

No differences were observed between the aortic and ventricular control groups at baseline and after 10 days in growth medium. Exposure of the ventricular surface of the cusp to osteogenic medium for a period of 10 days produced no increase in the number of Alizarin red-positive nodules (Figure 3.10). In contrast, exposure of the aortic surface to osteogenic medium for 10 days resulted in a statistically significant increase in the number of Alizarin red-positive nodules compared to its respective control group (Figure 3.11).

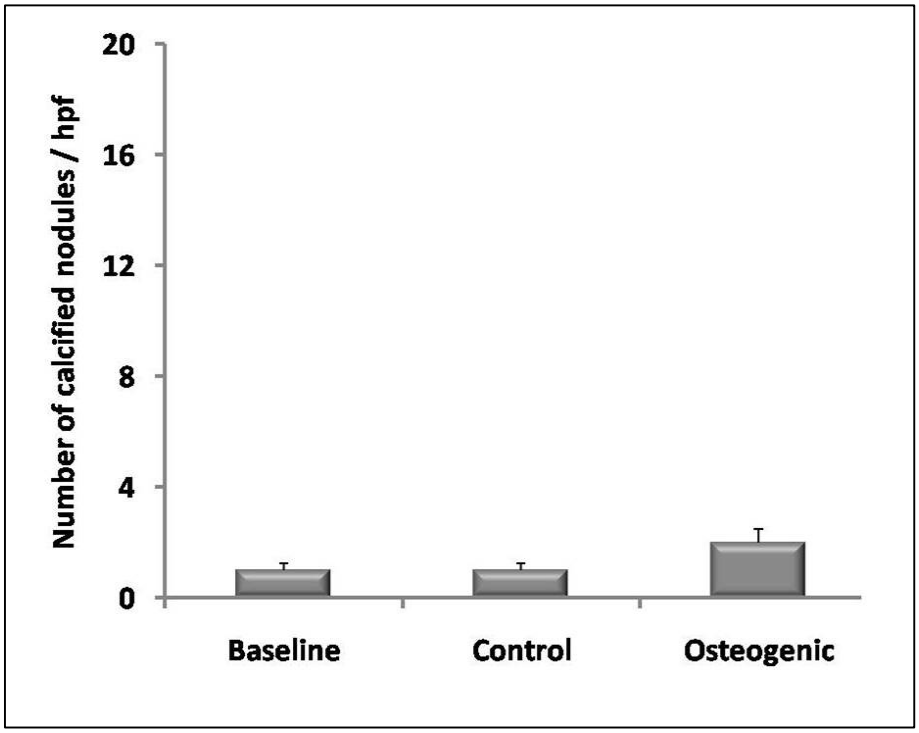

Figure 3.10 Exposure of the ventricular surface of aortic cusps to osteogenic medium - No statistically significant differences in the numbers of Alizarin-red positive nodules were observed

between baseline aortic valve cusps (Day 0) and following exposure to control or osteogenic medium for 10 days. (*hpf; high-power field).*

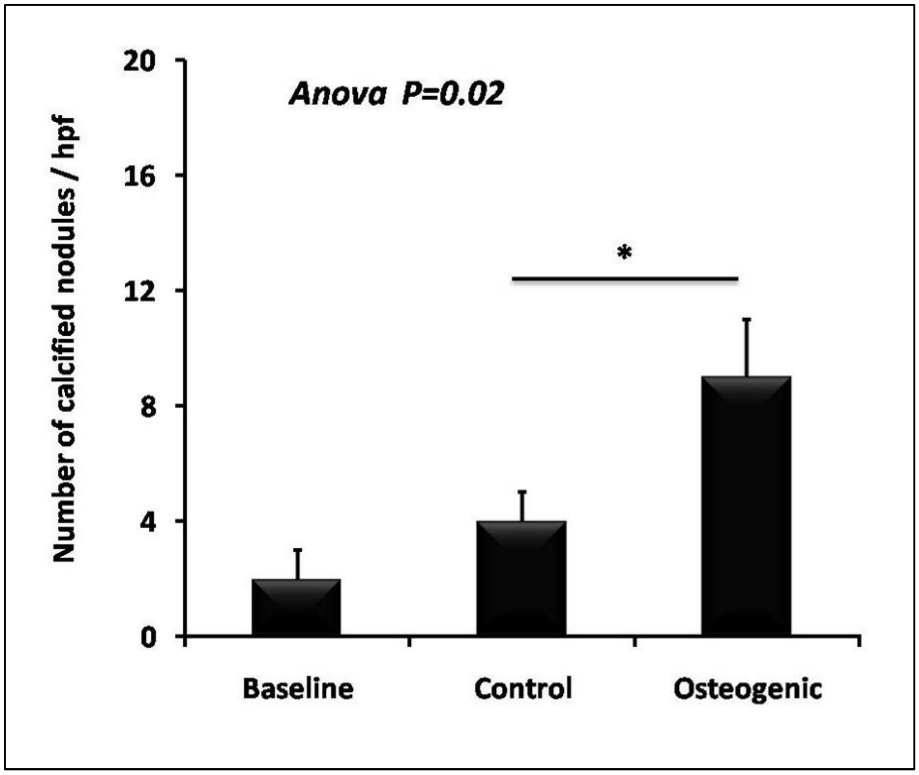

Figure 3.11 Exposure of the ventricular surface of aortic cusps to osteogenic medium – There was a significant increase in the number of Alizarin-positive nodules following exposure of the aortic surface of the cusps to osteogenic medium for 10 days compared to control medium or baseline cusps (Day 0) (p=0.02). *P<0.05*

When comparing the aortic and ventricular surfaces of the same cusp to osteogenic medium for 10 days, there was a significantly increase in the number of Alizarin red-positive nodules on the aortic side (Figure 3.13).

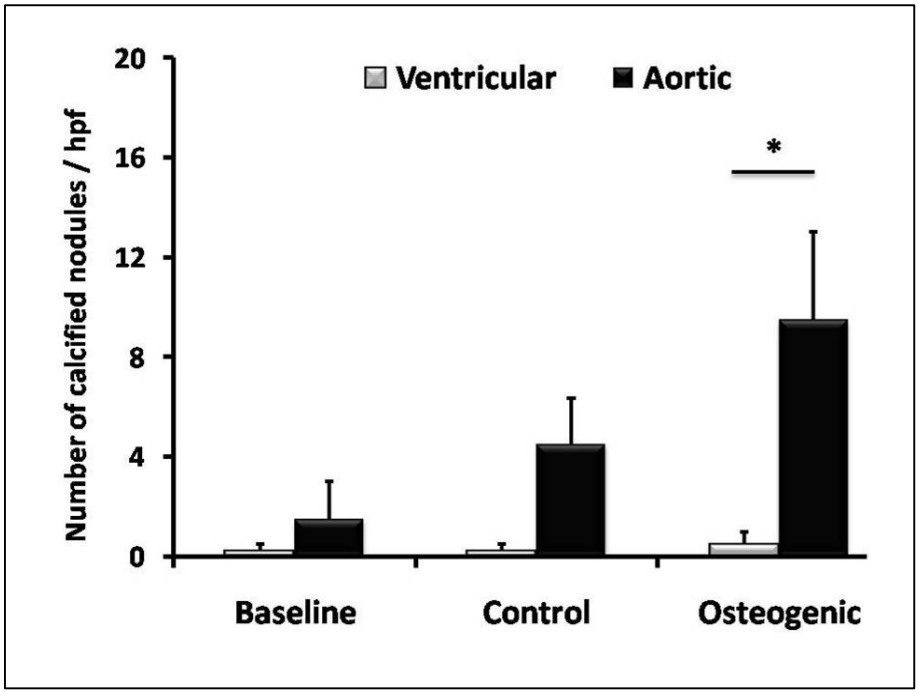

Figure 3.13 Comparison of the number of Alizarin red-positive nodules between the aortic and ventricular surfaces of aortic valve cusps at baseline (Day 0) and following exposure to control and osteogenic medium for 10 days. Each cusp served as its own control. Following exposure of the aortic side to osteogenic medium, there was a significant increase in the number of calcifying nodules. **P<0.05*

3.3.3 Role of the Endothelium on Aortic Valve Calcification

We sought to investigate the potential role of the endothelium in modulating aortic valve calcification, and importantly the role of side-specific inhibition of endothelial function on nodule formation. The same side-specific model of cusp exposure to osteogenic medium was used. As described in section 3.2.3.2, the endothelium was inhibited using pharmacological agents (L-NAME) or mechanical denudation.

3.3.3.1 Effect of Pharmacological Inhibition of the Endothelium on Valve Calcification

Inhibition of NOS using L-NAME resulted in a significant increase in the number of Alizarin red-positive nodules on the aortic side of the cusp compared to cusps kept in control medium or in osteogenic medium alone (Figure 3.14). Similarly, addition of L-NAME to the ventricular side

resulted in a statistically significant increase in the number of nodules, although the increase was less pronounced (Figure 3.15). When comparing the aortic and ventricular sides of the same cusp to L-NAME, there were significantly more nodules on the aortic side than the ventricular side (Figure 3.16).

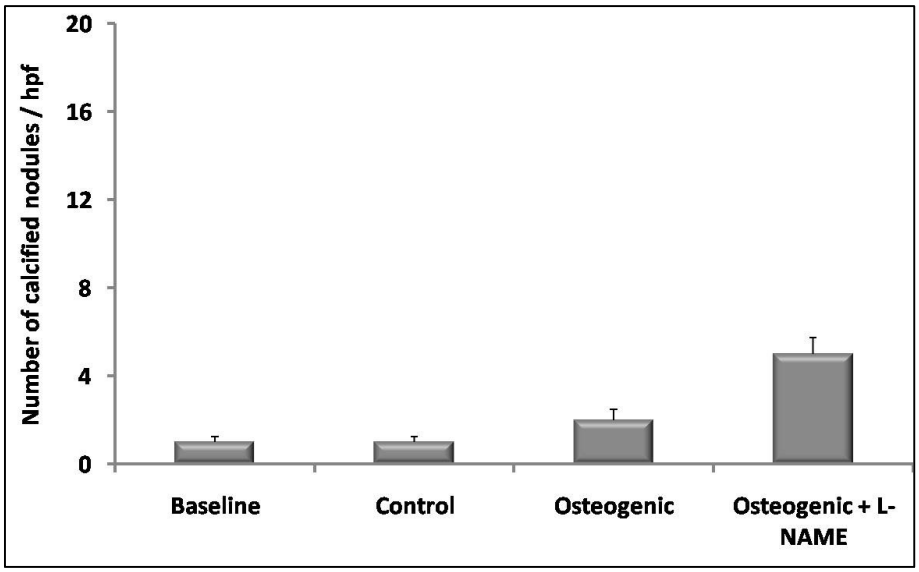

Figure 3.14 Effect of the inhibition of NO production by adding L-NAME to osteogenic medium for 10 days on the ventricular side of aortic valve cusps. There was a non-significant trend towards an increase in the number of calcifying nodules.

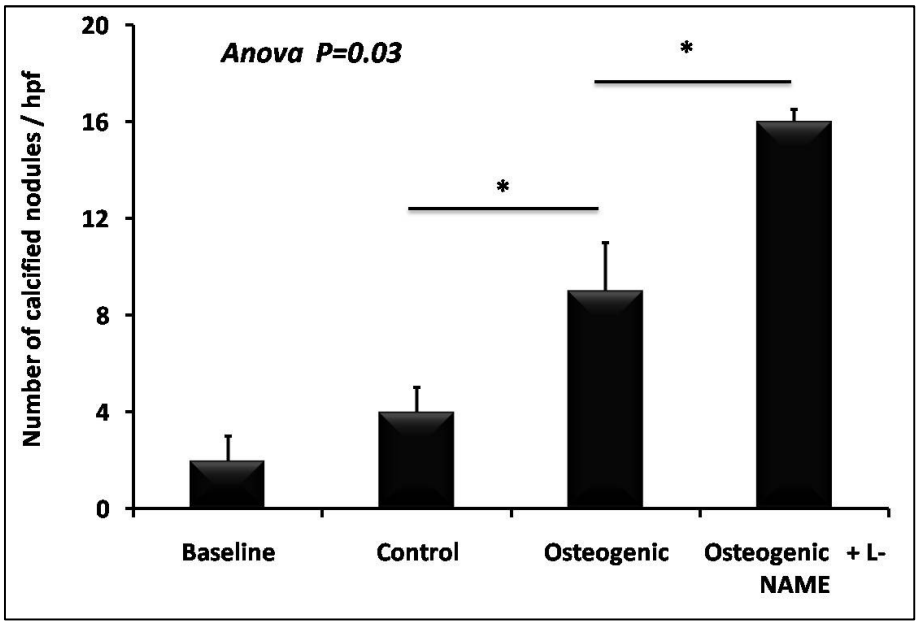

Figure 3.15 Effect of the inhibition of NO production by adding L-NAME to osteogenic medium for 10 days on the aortic side of aortic valve cusps. There was a significant increase in the number of calcifying nodules. **P<0.05*

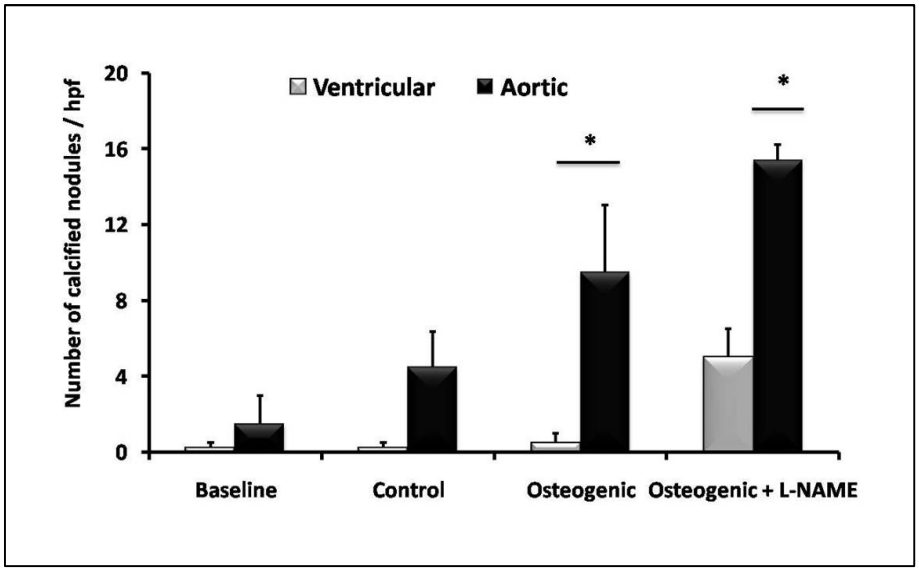

Figure 3.16 Comparison of the role of L-NAME on the formation of calcifying nodules on the aortic and ventricular sides of aortic valve cusps grown in osteogenic medium for 10 days. There was a significant higher number of calcifying nodules on the aortic side than the ventricular side. **P<0.05*

3.3.4 Side-Specific Evaluation of NO Production by Aortic Valve Endothelium

The capacity of the endothelium to synthesize NO was assessed by evaluating the production of cGMP using a commercially available kit. Following side-specific exposure of the aortic valve cusps to control medium *(as described in section 3.2.3.3)*, baseline cGMP production was assessed. There was significantly more cGMP production from the ventricular side of the cusp in static conditions than the aortic side (Figure 3.16).

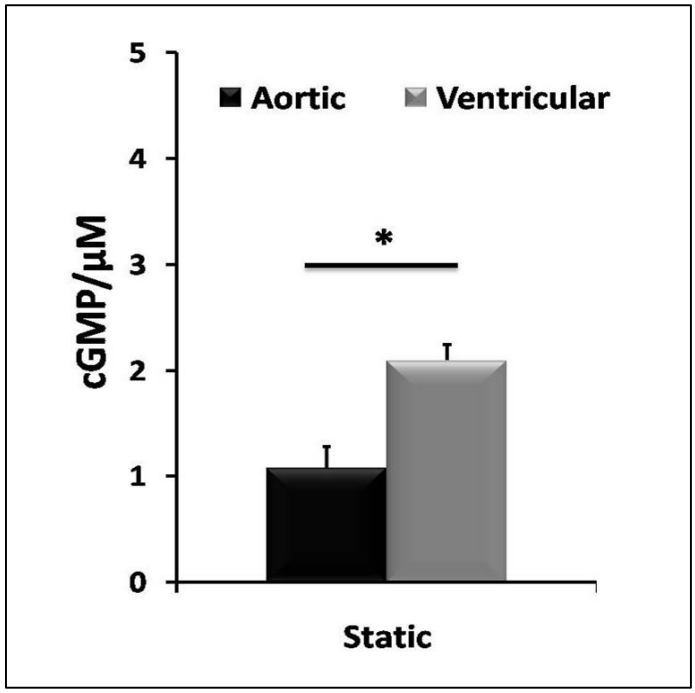

Figure 3.16 Histogram showing NO production as demonstrated using a cGMP assay on the aortic and ventricular sides of the aortic valve. The figure shows a significantly higher levels of NO production on the ventricular side under static conditions. **P<0.05*

In order to assess the response of endothelial cells to native flow conditions, aortic valve cusps were selectively exposed to physiological aortic or ventricular flow waveforms in a cone and plate apparatus previously described (Sucosky et al., 2008). Each side of the valve was exposed to its in vivo physiological flow pattern. Aortic and ventricular flow induced a significant increase in the production of NO by each respective side, as suggested by an increase in cGMP production. In comparison, the ventricular produced significantly more cGMP than the aortic side in response to flow (Figure 3.17).

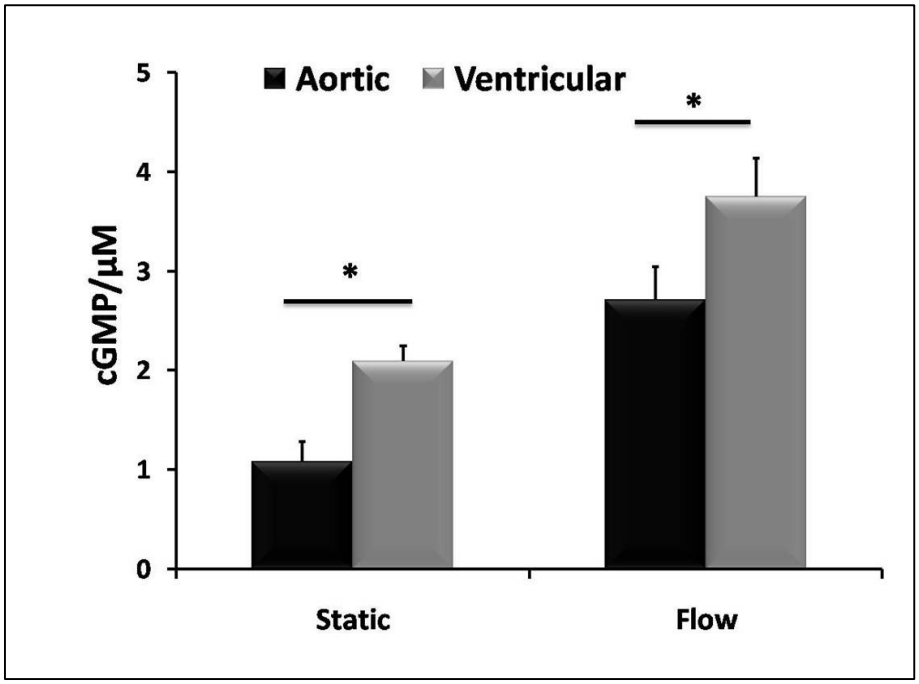

Figure 3.17 Histogram showing changes in NO production in response to physiological sheart stress patterns on the aortic and ventricular sides of the aortic valve. The figure shows an increase in NO production on both sides, but a maintained statistical difference in NO production between both sides. **P<0.05*

3.4 DISCUSSION

In this chapter, we have described an adapted model of porcine in vitro aortic valve calcification, both at the cellular and tissue levels. In both models, the presence of Alizarin red-positive nodules was considered a surrogate for calcification, a method which is widely accepted and used clinically in other settings such as detection of calcium in synovial fluid aspirates. In addition to forming calcium nodules in response to osteogenic mediators, the side-specificity of aortic valve calcification to the aortic side of the valve (fibrosa) was preserved using our model. In light of studies suggesting structural and functional differences between endothelial cells on both sides of the valve, we assessed the role of the endothelium in regulating the calcification process. Our results suggest that the endothelium plays a protective role against calcification through an NO-mediated process. Inhibition of NO production through

inhibition of NOS activity led to a significant increase in the number of calcified nodules. This effect was particularly pronounced on the aortic side of the valve. In addition, the ventricular side of the valve exhibits significantly more NO production than the ventricular side (using cGMP as a surrogate marker), both in baseline conditions as well as following exposure to physiological flow patterns. Together, these data strongly support a protective role of NO in reducing aortic valve calcification.

3.4.1 The Role of the Endothelium on Aortic Valve Calcification

Most of the studies examining cellular and molecular mechanisms of aortic valve calcification have focused almost exclusively on aortic valve interstitial cells because calcium nodules in aortic valve cusps occur in the interstitial space. However, from studies on atherosclerosis as well as a number of studies on valve calcification, it is clear that the endothelium plays an important role in the disease process. The role of NO in preventing calcification, as shown in this chapter, can be due to several potential mechanisms. These are the subject of ongoing and future research.

3.4.1.1 Clinical Evidence for the Role of Endothelial Dysfunction in Aortic Valve Disease

While the role and prognostic significance of endothelial dysfunction in atherosclerosis is well accepted, its importance in aortic valve disease was largely overlooked until recently. A number of studies looking at different clinical cohorts suggest a strong relationship between systemic endothelial dysfunction and aortic valve disease. Poggianti et al. compared subjects with aortic valve sclerosis to a control patient population showing a significant decrease in systemic endothelial function in patients with aortic valve sclerosis, evidenced by a decrease in flow-mediated brachial artery dilatation (Poggianti et al., 2003). In a separate study, coronary flow reserve was assessed as a marker of microvascular endothelial function in a population of

patients with aortic valve calcification but no hemodynamically significant stenosis (peak transvalvular gradient <25mmHg) versus a cohort of normal subjects (Huseyin Bozbas et al., 2008). Patients with aortic valve calcification were found to have significantly lower coronary flow reserve compared to controls. In addition, patients with aortic valve stenosis were found to have increased circulating levels of asymmetric dimethylarginine (ADMA), an endogenous inhibitor of NOS (Ngo, Heresztyn, Mishra, Marwick, & Horowitz, 2007). Similar results were reproduced in animal models of aortic valve calcification (Ngo et al., 2008). Interestingly, endothelial dysfunction in this patient population persists despite aortic valve replacement suggesting that the dysfunction is part of a wider systemic process (Chenevard et al., 2006).

Other studies have examined the presence of local endothelial dysfunction at the level of the aortic valve itself. Increased numbers of ET-1-positive cells and ET_A receptor mRNA levels as well as a downregulation of eNOS gene expression in human stenotic valves was observed (Peltonen et al., 2009). Interestingly, an eNOS knockout mouse model was reported to be associated with an increased incidence of bicuspid aortic valves (Lee, Zhao, Courtman, & Stewart, 2000). The decrease in eNOS in this patient population has been confirmed in humans by comparing the expression of eNOS in explanted bicuspid and tricuspid aortic valves showing reduced expression of eNOS in valves and aortas of patients with bicuspid valves (Aicher, Urbich, Zeiher, Dimmeler, & Schafers, 2007). The pathogenesis of bicuspid valves in eNOS-knockout animal models has been further elucidated in accordance to phenotype. Right and non-coronary cusp fusion is thought to be the product of a morphogenetic defect that happens before outflow tract septation and that probably relies on an exacerbated NO-dependent epithelial-to-mesenchymal transformation (Fernández et al., 2009). In contrast, right-left cusp fusion results from the anomalous septation of the proximal portion of the outflow tract, likely caused by abnormal behaviour of neural crest cells (Fernández et al., 2009). Interestingly, bicuspid aortic valves are associated with early valve calcification. Though some of that might be due to mechanical factors related to abnormal stress distribution and flow patterns on the cusps, decreased levels of eNOS might play an important pathophysiological role.

3.4.1.2 Restoration of Endothelial Function Mitigates Aortic Valve Calcification

Our findings are corroborated by a few studies showing positive results both in vitro and in vivo in reducing or preventing aortic valve calcification support a critical role for the endothelium or endothelial-derived products in mitigating the calcification process. Using an in vitro model of porcine aortic valve interstitial cell calcification such as the one described in this chapter, Kennedy et al. showed that supplementation of cultures maintained in osteogenic medium (conatinaing TGFβ) with NO donors or agents that increase intracellular cGMP (8-bromo cGMP, C-type natiuretic peptide [CNP] and brain natiuretic peptide [BNP]), result in a significant decrease in calcifying nodules (Kennedy et al., 2009). This suggests that NO mitigates calcification through a direct effect on aortic valve interstitial cells. In a study examining the role of statins on aortic valve calcification in a chronic high cholesterol diet rabbit model, treatment of the animals with atorvastatin significantly reduced the incidence of aortic valve calcification (Rajamannan et al., 2005). This was associated with an increase in eNOS protein concentration in aortic valves from statin-treated animals, as well as a significant increase in the levels of circulating nitrites, suggesting preserved or improved endothelial function in these animals (Rajamannan et al., 2005). These findings confirm earlier studies demonstrating the role of statins in upregulating eNOS expression through posttranscriptional mechanisms (Laufs, La Fata, Plutzky, & Liao, 1998; Laufs & Liao, 1998). Exercise training was also shown to simultaneously preserve endothelial integrity and limit progression of aortic valve calcification in a low density lipoprotein receptor-deficient mouse model (Matsumoto et al., 2010). These recently published studies shed light on a once neglected but increasingly recognized role of the endothelium in preserving aortic valve structural and functional integrity. Our findings using a novel experimental model, confirm the protective role of the endothelium, and specifically endothelium-derived NO, against valve calcification. But more importantly, our data propose a potential explanation for the side-selective localization of calcium nodules in human aortic valve cusps. Although no differences in baseline eNOS expression were observed using

immunocytochemistry between the aortic and ventricular surfaces of aortic valve cusps, it is more likely that differences would be observed after 10 days of exposure to osteogenic medium. These studies are currently ongoing. These findings are in slight contradiction with findings from Simmons et al. showing increased eNOS gene expression in endothelial cells isolated from the aortic surface of freshly-obtained porcine aortic valve cusps (Simmons et al., 2005). This could be due to their use of a human gene array on porcine endothelial cells owing to the absence of dedicated porcine arrays at the time as well as the age of the animals which might play an important role in endothelial integrity and expression of eNOS. It could also be explained by posttranscriptional regulation of eNOS protein expression in endothelial cells or the ratio of coupled/uncoupled eNOS. Some pathological conditions are associated with an absolute increase in eNOS with closer inspection showing an increase in uncoupled eNOS,a major source of oxidative stress (Hong, Mohamad, & Chris, 2007).

3.4.1.3 Potential Mechanisms of Action of NO on Aortic Valve Calcification

3.4.1.3.1 NO and Oxidative Stress

Oxidative stress is an important mediator of pathological processes both in the valve and the vasculature. Several studies have identified the presence of reactive oxygen species (ROS) in calcified aortic valves (H. Bozbas et al., 2008; Liberman et al., 2008; Miller et al., 2008; Ngo et al., 2008; Towler, 2008). In addition, many of the clinical conditions that predispose to the development of aortic valve calcification are associated with oxidative stress and endothelial dysfunction, such as hypertension, hypercholesterolemia, diabetes and smoking. ROS include free oxygen radicals, oxygen ions and peroxides. Oxidative stress is potentially mediated by several enzyme systems present in endothelial cells including the nicotinamide adenine dinucleotide phosphate oxidase-dependent (NADPH oxidase), uncoupling of eNOS (in which oxygen reduction is uncoupled from nitric oxide synthesis) and the xanthine oxidase system (Forstermann, 2008). Although it remains unclear whether oxidative stress is both necessary

and sufficient for aortic valve calcification, it is undoubtedly an aggravating factor in disease progression, causing reduced NO bioavailability, upregulation of adhesion molecules and chemokines and apoptosis (Bedard & Krause, 2007; Cote et al., 2008). Furthermore, in vitro studies show an increase in calcifying nodules in response to oxidative stress (Kennedy et al., 2009).

Studies examining the role of NO on oxidative stress have shown the ability of NO to reduce ROS generation and related cell injury. Using cultured human microvascular endothelial cells, Selemidis et al. have shown that NO causes sustained suppression of NADPH oxidase-dependent superoxide production by S-nitrosylation of the organizer subunit p47phox, one of the major subunits of NADPH oxidase (Selemidis, Dusting, Peshavariya, Kemp-Harper, & Drummond, 2007). In a separate study examining porcine aortic valve interstitial cells grown in osteogenic medium supplemented with TGFβ1, supplementation of NO resulted in decreased production of superoxide anions, possibly through superoxide scavenging, an effect which was independent of NADPH oxidase activity (Kennedy et al., 2009). Thus, it appears that however small NO's contribution is to reducing oxidative injury, it is likely a contributing factor which requires further study, both experimentally and clinically.

3.4.1.3.2 Inhibition of TGFβ Signalling by NO

The TGFβ signalling pathway is involved in many cellular processes in both the adult organism and the developing embryo including cell growth, cell differentiation, apoptosis, matrix regulation and other important functions. It has also been implicated in different pathological processes ranging from aortic aneurysms to myocardial fibrosis (Leask, 2007; Loeys et al., 2006; Neptune et al., 2003). TGFβ is part of a superfamily of proteins: the TGFβ superfamily which also includes bone morphogenetic proteins (BMP) and growth and differentiation factors (GDF). Different TGFβ ligands signal by binding to a TGFβ type II receptor on the cell surface which recruits and phosphorylates a type I receptor. The activated receptor then phosphorylates

receptor-regulated SMADs (R-Smad), most commonly Smad2, which bind the co-Smad (or Smad4). R-Smad/Smad4 complexes translocate to the nucleus where they act as transcription factors regulating gene expression.

The role of the TGFβ pathway in the pathogenesis of human aortic valve calcification has recently been recognized both in human valve explants and in vitro aortic valve interstitial cell cultures (Jian, Narula, Li, Mohler Iii, & Levy, 2003; Lana Osman et al., 2006). As shown in our in vitro studies, addition of TGFβ1 to osteogenic medium resulted in acceleration of calcifying nodule formation, a finding similar to other investigators using comparable in vitro models (Jocelyn N. Clark-Greuel et al., 2007; Kennedy et al., 2009). TGFβ1 can contribute to aortic valve calcification through several mechanisms, none of which has been clearly identified. TGFβ1 can induce valve interstitial cell apoptosis which might lead to formation of calcium nodules (Jocelyn N. Clark-Greuel et al., 2007; Jian et al., 2003). Indeed, in a model of vascular atherosclerosis, it was shown that apoptotic bodies are formed following vascular smooth muscle cell apoptosis (Reynolds et al., 2004). These apoptotic bodies act as sources of calcium as well as trapping the calcium in the ECM. Histological analysis of human calcified aortic valves consistently shows the presence of apoptotic markers in regions close to foci of calcification. Alternatively, increased TGFβ1 activity can result in calcification by stimulating the release of various ECM proteins, including collagen I and III, essential elements in the formation of bone or cartilage, two elements found in sclerotic and calcified valves. This can be further accentuated in the presence of transdifferentiation of valve interstitial cells into osteoblast-like cells, as seen following osteogenic stimulation in vitro (Mathieu et al., 2005; L. Osman et al., 2006). In addition, TGFβ1 can also "activate" fibroblasts to express SMA, a phenotype known as myofibroblasts, which are thought to be directly involved in the aortic valve pathogenesis (Walker et al., 2004). In our experiments, we performed immunohistochemical analysis of the aortic valves exposed to osteogenic medium and did not observe expression of osteoblatic markers such as osteopontin, Runx-2 or osteocalcin. However, this could be due to the early time point chosen to analyse the specimens, which was strongly dictated by the cost of replacing

the TGFβ1-rich osteogenic medium twice weekly. It remains to be determined whether longer exposure to osteogenic medium would result in osteoblastic differentiation of valve interstitial cells or whether the early calcifying nodules observed are the product of apoptosis and accumulation of calcium-rich matrix vesicles, as suggested by Reynolds et al. (Reynolds et al., 2004). Finally, TGFβ1 has been shown to directly affect endothelial function by disrupting adhered junctions and inducing endothelial barrier dysfunction (Lu et al., 2006). This suggests that TGFβ1 not only has a direct effect on the underlying interstitial cells, but can also directly affect permeability of the endothelial layer, thereby potentially facilitating transmigration of inflammatory cells from the blood.

NO has recently been shown to directly interfere with the TGFβ signalling pathway by inhibiting TGFβ-induced phosphorylation of Smad2/3 in cultured vascular smooth muscle cells (Kanno, Into, Lowenstein, & Matsushita, 2008). This direct effect of NO is cGMP-dependent and also results in inhibition of the differentiation of smooth muscle cells into osteoblasts (Kanno et al., 2008). In a separate study comparing aortas from wild-type mice versus eNOS knockout mice, NO was shown to inhibit TGFβ signalling by enhancing the proteosomal degradation of Smad2 in a cGMP/protein kinase 1 (PKG-1) dependent fashion (Saura et al., 2005). In addition, aortas from eNOS-deficient mice showed enhanced collagen type I expression (in addition to enhanced TGFβ1 expression and nuclear translocation of Smads) (Saura et al., 2005).

3.4.1.3.3 Effect of NO on Valve Mechanical Properties

As shown in our previous work, the valve endothelium can regulate aortic valve stiffness through NO-dependent mechanisms, which likely involve the contribution of valve interstitial cells (El-Hamamsy, Balachandran et al., 2009). Changes in valve mechanical properties, particularly in valve stiffness can affect valve structure and function in 2 ways. First, cusp compliance is an important factor determining the amount and distribution of stress on the cusps. Thus, localized changes in cusp stiffness accompanied by elevated mechanical stresses

could result in repeated microtrauma, particularly during periods of high hemodynamic stress. Microtrauma can lead to disruption of the endothelial cell barrier as well as initiating active cell-mediated dystrophic changes in the interstitial space. Second, in vitro studies have recently demonstrated that the calcifying potential of valve interstitial cells is partly dictated by the stiffness of the surrounding matrix. Aortic valve interstitial cells grown on non-compliant matrices (mimicking calcified valves) in osteogenic medium differentiated to myofibroblasts and formed calcified aggregates that contained apoptotic cells (Yip, Chen, Zhao, & Simmons, 2009). Interestingly, in that same study, cells grown on a compliant matrix readily formed calcified aggregates of viable cells that expressed osteoblast-related transcripts and proteins, suggesting that the myofibrogenic and osteogenic process in aortic valves might constitute 2 distinct processes (Yip et al., 2009).

ET-1 is often associated with pathological vascular and valvular remodelling. We have previously shown that ET-1 can significantly increase the stiffness of aortic valves, which could be on the pathogenic mechanisms (El-Hamamsy, Balachandran et al., 2009). In contrast, endothelium-dependent NO release resulted in decreased stiffness of the cusps, possibly contributing to the significantly lower calcification potential of healthy aortic valves, and more importantly of the ventricular surface of the aortic valve, where NO is more readily synthesized, both at rest and with flow stimulation.

3.4.1.3.4 NO and the Adrenergic System

Aortic valves contain a rich and highly preserved network of afferent and efferent nerves, both intrinsic and extrinsic, whose role on valve structure and function remains poorly understood (El-Hamamsy, Yacoub et al., 2009). We have recently demonstrated the presence of β2-adrenergic receptors on valve interstitial cells from human aortic valves. Furthermore, treatment with β2-adrenergic receptor antagonists significantly reduced the risk of interstitial cell osteogenic differentiation (Osman et al., 2007). In a separate study examining the link

between NO and β-adrenergic stimulation, Hare et al. showed a direct effect of NO bioavailability on the inotropic response to β-adrenergic stimulation (Hare, Givertz, Creager, & Colucci, 1998). Although this does not imply an effect of NO on β-adrenergic receptors in aortic valves, it represents a potential important area of investigation. Indeed, no trials have yet looked at β-adrenergic receptor antagonists in animal models of subjects with early aortic valve calcification.

3.4.2 Side-Selectivity of Aortic Valve Calcification

In human calcified aortic valves, calcium nodules occur almost exclusively on the aortic surface of the cusp. This has long been an intriguing finding which had, until recently, received little attention. We believe that this side-selectivity is the combined result of several factors, some of which have already been discussed. These include the fact that the ventricular side is exposed to high shear laminar flow during each ventricular ejection phase. In contrast, the aortic surface is exposed to a low shear disturbed flow pattern, which is thought to cause endothelial activation, triggering a cascade of events leading to myofibroblast generation and osteoblast differentiation. The different flow patterns also result in unequal NO production between cells from either side as shown in these experiments. The increased release of NO from the ventricular side might play an important protective role. In addition, the basic ECM composition differs significantly between both sides of the aortic cusp: the fibrosa and the ventricularis. Indeed, as discussed in the Introduction, the fibrosa in particularly rich in collagen, whereas the ventricularis contains a high amount of elastin. Although attempts have been made to analyze their individual mechanical properties, no definitive answer results are yet available (Stella & Sacks, 2007). Nonetheless, in light of the role of matrix composition and stiffness on the potential of valve interstitial cells to calcify, it is likely that this may be an important contributor to the observed side-selectivity (Karien & Kristyn, 2009; Yip et al., 2009). It should also be emphasized that ECM acts as more than a scaffold. It can also regulate the

activity and function of interstitial cells as has been shown in vascular walls. This cross-communication regulates many of the functions of interstitial cells in health and disease and explains the pathophysiology of vasculopathies in subjects with mutations in collagen or elastin (El-Hamamsy & Yacoub, 2009a).

3.5 LIMITATIONS

This study has several limitations. Though the nodules obtained stain positively for Alizarin red staining, it remains to be determined whether this model represents a valid model of in vitro aortic valve calcification. Nevertheless, the consistency and reproducibility of the results suggests that the observed results are indeed valid. Porcine aortic valves are commonly thought to be resistant to calcification although this has never been formally studied. The use of pig valves as a model of aortic valve calcification raises important questions. Nevertheless, pig valves are very similar to human valves in terms of macro- and microstructure and hemodynamic environment. Due to the ethical and practical difficulties of obtaining healthy human heart valves for research purposes, we believe that pig valves constitute a useful model for aortic valve calcification.

3.6 CONCLUSION AND FUTURE DIRECTIONS

In conclusion, this study demonstrates the role of endothelium-derived NO in regulating aortic valve calcification in a porcine model of in vitro calcification. NO exerts a protective effect against the production of calcifying nodules in the valves. Inhibition of NO production, a sign of endothelial dysfunction resulted in a significant increase in the rate and degree of aortic valve calcification. In addition, results from this study suggest that the side-selectivity of aortic valve calcium nodules could be partly due to differences in basal and flow-stimulated NO production.

These findings suggest that NO supplementation using agents like L-arginine or tetrahydrobiopterin (BH4) might be beneficial in the treatment of subjects with early rather than late signs of aortic valve calcification. Further work is also required to assess the mechanisms of action of NO on valve cells as well as the overall effect on valve function. In addition, advanced chemical characterization techniques such a bio-Raman spectroscopy should be performed to assess the precise composition of in vitro nodules and compare them to native aortic valve calcification (Cloyd et al., 2010).

IV Regulation of Aortic Valve Mechanical Properties

4.1 BACKGROUND

The aortic valve lies in a unique hemodynamic environment which exposes it to a variety of mechanical stimuli including pressure, stretch, bending and shear stress (Figure 4.1). These forces can reach very high magnitudes in absolute terms. Considering the thickness of aortic valve cusps (300μm - 700μm), it is remarkable that the cusps function adequately while opening and closing uninterruptedly over 3 billion times in an average lifetime, in constantly varying hemodynamic conditions.

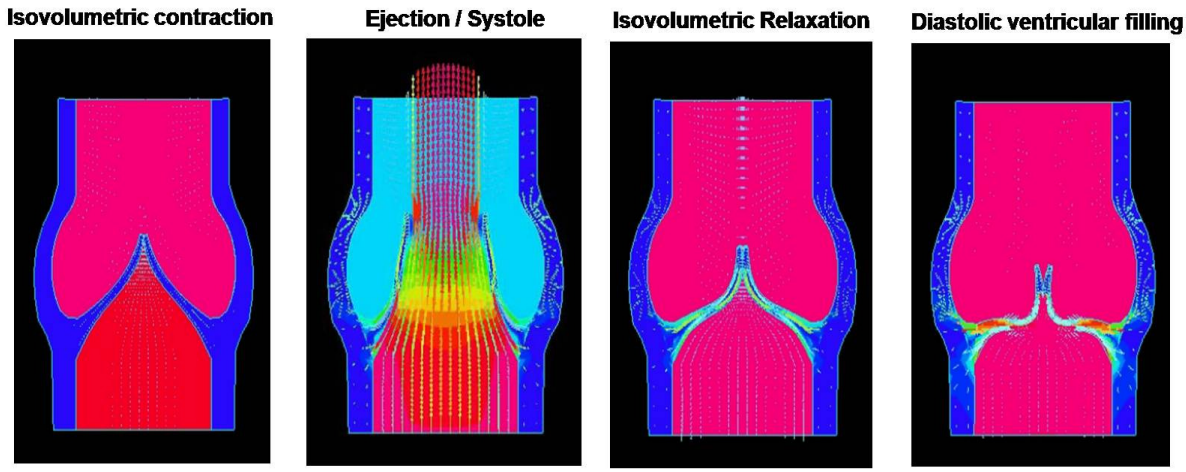

Figure 4.1 - Schematic diagram showing the various forces exerted on aortic valve cusps during the cardiac cycle, consisting of stretch, pressure, bending and shear stresses.

For a long time, the aortic valve was considered a passive structure that opens and closes in response to changes in ventricular pressure and its mechanics were only considered from an engineering standpoint. However, recent findings into the complex interplay between valve cells, matrix, neural network and surrounding environment has generated new insights into valve mechanics both at a cellular level as well as tissue level.

Aortic valve biomechanics include several aspects such as cusp stiffness and instantaneous movements of the cusps. These are thought to have important clinical

implications both in health and disease. In this chapter, we will focus on aortic valve stiffness as a key component of valve mechanical properties. Changes in cusp stiffness can potentially modulate several parameters such as the pattern of flow in the aortic root which dictates coronary flow, particularly in systole (J. E. Davies et al., 2008) as well as stress distribution on the surface of the individual cusps (Grande-Allen, Cochran, Reinhall, & Kunzelman, 2001). Aortic valves can translate mechanical cues into biological stimuli, a process termed mechanotransduction, leading to changes in cell proliferation and migration, apoptosis and matrix remodelling. Changes in cusp stiffness therefore hold the potential of modulating the response of the aortic valve to mechanical stimuli and allow it to adapt to varying hemodynamic conditions.

Stiffness of the aortic valve cusps can be measured by deriving the Young's modulus from the stress-strain relationship of the tissue, as shown in these experiments. Thus far, studies examining the mechanical properties of aortic valves have determined that aortic valve cusps possess properties of viscoelastic materials (Billiar & Sacks, 2000a, 2000b; Stella, Liao, & Sacks, 2007). Another important property of aortic valve cusps is anisotropy. Anisotropy is the property of having directionally dependent mechanical properties, which in the case of the aortic valve refers to the radial and circumferential axes of the cusps. Indeed, it has been shown that aortic valve cusps are significantly stiffer in their circumferential axis than the radial one. This could be due to the specific content and alignment of ECM proteins or cells in each axis, as will be discussed later. Because both axes of the aortic valve are part of a single unit, they inevitably influence each other in an inter-dependent manner. Nevertheless, published reports have thus far predominantly analyzed aortic valve cusps one axis at a time, using uniaxial tensile testing methods. In addition, most studies have mainly focused on the baseline mechanical properties of the cusps, leaving aside the potential contribution of its cellular components.

As discussed earlier, the endothelium forms a monolayer on the surface of aortic valve cusps and as such is exposed to all mechanical stimuli including shear stress. It is now well

accepted that valve endothelial cells have unique signalling and gene expression profiles, different from endothelial cells in other parts of the body, including aortic-derived vascular endothelial cells (Butcher & Nerem, 2006; Butcher et al., 2004; Farivar et al., 2003). While in the vasculature, endothelial cells are responsible for regulating vascular tone, the role of valve endothelial cells on valve mechanical properties remains completely undetermined. As mentioned in our hypothesis, the definition of a living structure is its capacity to adapt its structure and function in response to different stimuli.

4.1.1 Aims

The aims of this series of experiments is to evaluate the mechanical properties of aortic valve cusps using a biaxial micromechanical tensile testing apparatus. Importantly, the capacity of the cusp to modify its mechanical properties in response to various stimuli will be specifically examined, with a particular focus on the role of endothelium-derived signals.

4.2 METHODS

4.2.1 Tissue Procurement

Porcine hearts (18-24 months) were obtained from a commercial slaughterhouse (Cheale Meats, UK). Hearts were immediately placed in a cold Hanks solution prior to transport. All 3 aortic cusps were then isolated from each heart by careful dissection, ensuring minimal manipulation of the cusp surface to avoid damaging the endothelial cells. Aortic cusps were placed in ice-cold Kreb's buffer solution (in mM: KCl 2.7, NaCl 136.9, $CaCl_2$ 2.5, $NaHCO_3$ 11.9, NaH_2PO_4 0.4, $MgCl_2$ 2.5, Dextrose 11.1, Na_2EDTA 0.04) and used within 12 h of sacrifice. A

square-shaped cutter was used to isolate identical 10 x 10 mm sections from the "belly" of each cusp in a radial-circumferential direction (Figure 4.2).

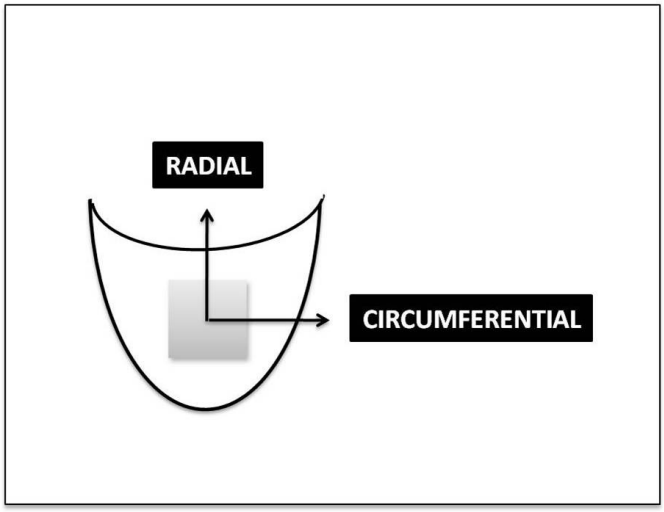

Figure 4.2 - Figure showing the belly region of the aortic valve cusp (grey) which was used for all mechanical testing experiments. The radial and circumferential axes were noted for each cusp to evaluate tissue anisotropy

4.2.2 Biaxial Micromechanical Testing System

The Bose micromechanical tensile testing system (Bose Electroforce, Eden Prairie, MN) allows for the evaluation of the mechanical properties of a solid structure through a variety of protocols. It is composed of 4 orthogonally-placed load-cells which can be individually controlled. The motors can be used under load control or strain control, ie, controlling the amount of tension applied to a tissue or the degree of "stretch". By performing controlled experiments, stress-strain relationship of the tissue can be determined, which forms the basis for determining the elastic modulus of the tissue. The Bose system allows applying and measuring biaxial data, which in our case, provides specific data for the circumferential and radial axes separately, all the while taking into account the interdependence of tissue mechanics in both directions. Figure 4.3 shows a representative stress-strain curve from a porcine aortic valve illustrating 2 important elements. First, the anisotropic nature of aortic valve cusps, ie, the mechanical properties of the tissue vary significantly between both axes. Second, it

illustrates a typical stress-strain curve, which can be decomposed into 3 parts: the toe, the transition and the linear region. To derive the elastic modulus of a given tissue, data from the linear region of the stress-strain relationship is used.

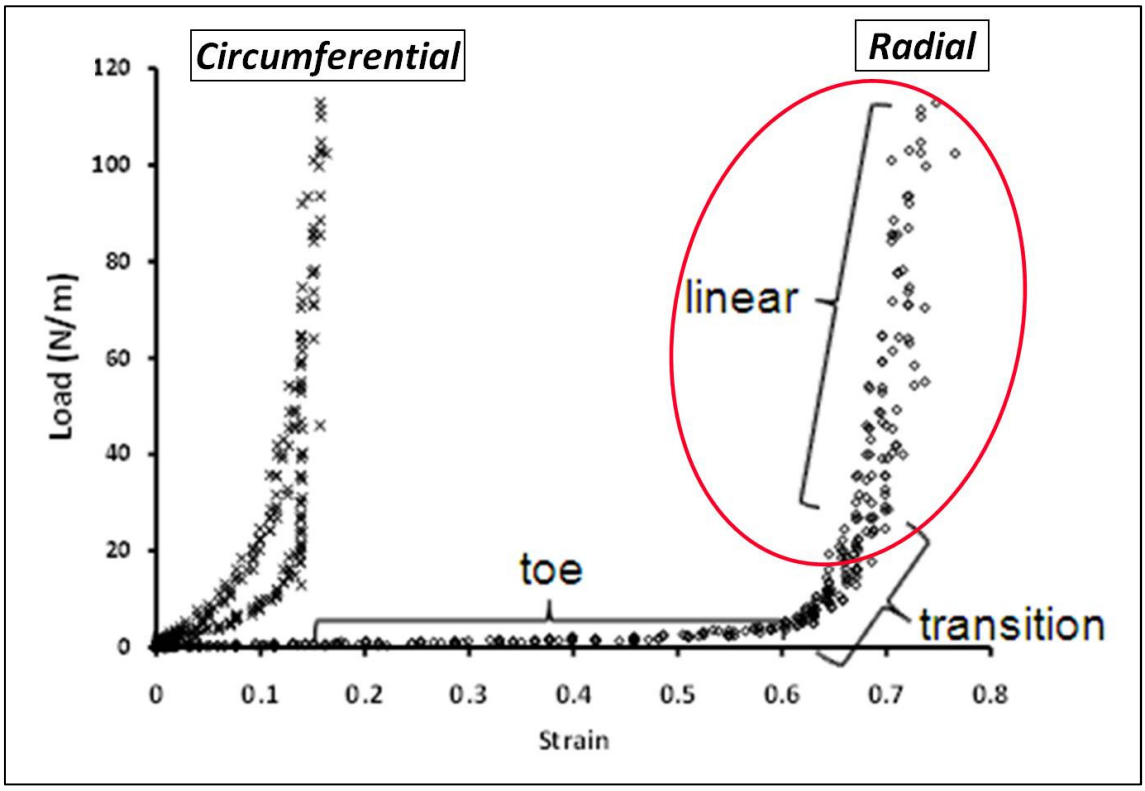

Figure 4.3 – Representative figure showing typical stress-strain relationship in an aortic valve cusp in the radial and circumferential direction. The anisotropic nature of aortic valve cusps is illustrated by the differences in elasticity between both directions. As shown, circumferential stiffness is significantly higher than radial stiffness (load increases rapidly with strain increments). In addition, this figure illustrates the 3 phases of stress-strain curves, with the linear phase being the region used to derive the elastic modulus (stiffness).

4.2.3 Experimental Protocol

Stainless steel springs (McMaster-Carr, Atlanta, GA) were threaded through each side of the leaflet sections. Care was taken to preserve the valve endothelium while mounting the springs. Four dots were marked on the central region of the specimen forming a square. The specimens were then mounted in a biaxial micromechanical testing device (Bose Electroforce, Eden Prairie, MN) in a Kreb's bath maintained at 37°C and continuously gassed with 95% O_2 / 5% CO_2 (Figure 4.4).

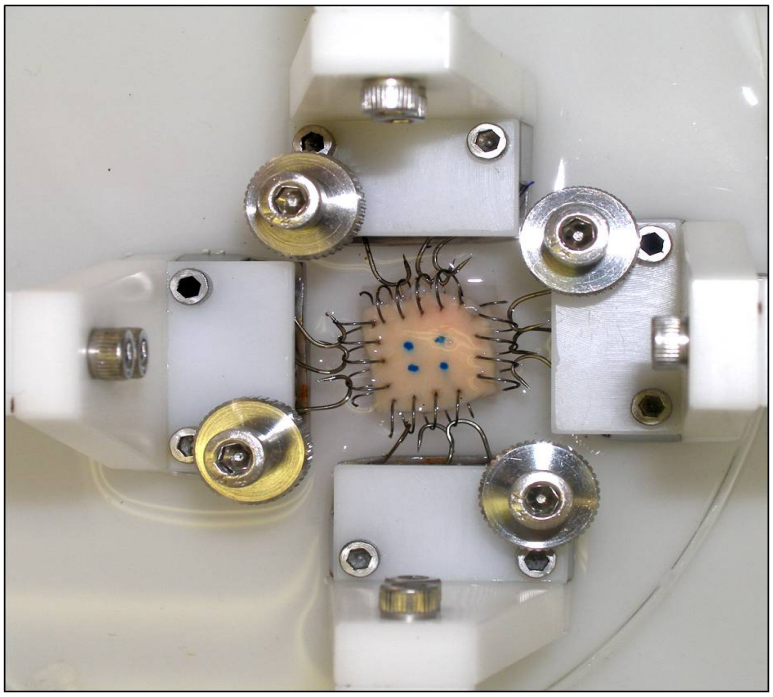

Figure 4.4 – Overhead picture showing a square sample of aortic valve belly region mounted between the four loads of the Bose biaxial tensile testing system using springs passed through all four edges of the cusp and hooked to hooks attached to the load cells.

The pH of the solution was tested before and after every experiment and held constant between 7.35 and 7.45. Strain gauge force transducers (Bose Electroforce®) were mounted along the two orthogonal axes to continuously monitor the changes of force in the radial and circumferential directions. A single camera two-dimensional measuring system (Bose Electroforce®) was used to track the movement of the four dots, measuring real-time strains on the specimen (Figure 4.5). Samples were initially allowed to stabilize in the bath for 5 min before being preloaded to 10 mN. In order to maintain the stability of the entire setup, all protocols were conducted under displacement control. All mechanical tests were conducted equibiaxially.

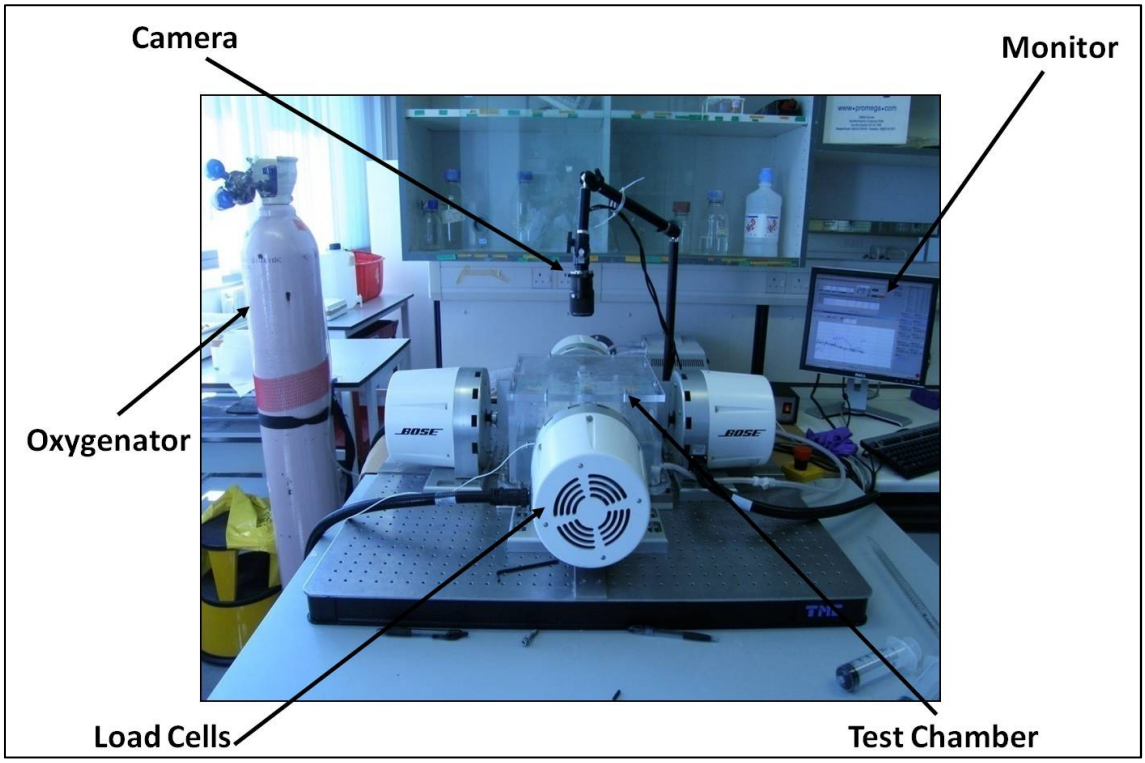

Figure 4.5 – Photograph showing the overall setup for the Bose micromechanical tensile testing system. The sample is placed in the test chamber in a Krebs solution maintained at 37C. The solution is continuously oxygenated by inserting a cannula in the bath, attached to an oxygenator. The load cells are separately controlled to apply equibiaxial strain on the tissue. Tissue deformations are recorded by an overhead high-resolution camera and transmitted to a computer monitor where live data is readily displayed.

Aortic valve physiological load was estimated using Laplace's law for cylinders (T=Pr), where T is mean valve membrane tension, P is transvalvular pressure and r is radius. A transvalvular pressure of 80mmHg (106.7 kPa) was used. Figure 4.6 illustrates the experimental protocol. Each sample was first preconditioned to this level at a frequency of 0.1 Hz for twenty cycles to allow the load-strain response of the valve to become repeatable. If the mechanical data at this point were not consistent, the specimen was subjected to twenty further preconditioning cycles. Following this, three cycles of load versus strain measurements were recorded (baseline elastic modulus). The sample was then stretched to 55 N/m (half the maximum physiological load) on both its axes to approximate diastolic conditions, and allowed to relax with the load held constant for 10 min. The tissue was then challenged with increasing concentrations of the selected vasoactive agent while load measurements were carried out every 0.1 s. Three more

cycles of load versus strain were then recorded and the resultant elastic modulus was compared to baseline. Thus, each sample served as its own control. Each sample served as its own control and was used only once. Load data was plotted against areal strain (calculated using the radial and circumferential strains obtained above) for baseline and treated groups. Percentage change in cusp stiffness in response to different agents is reported.

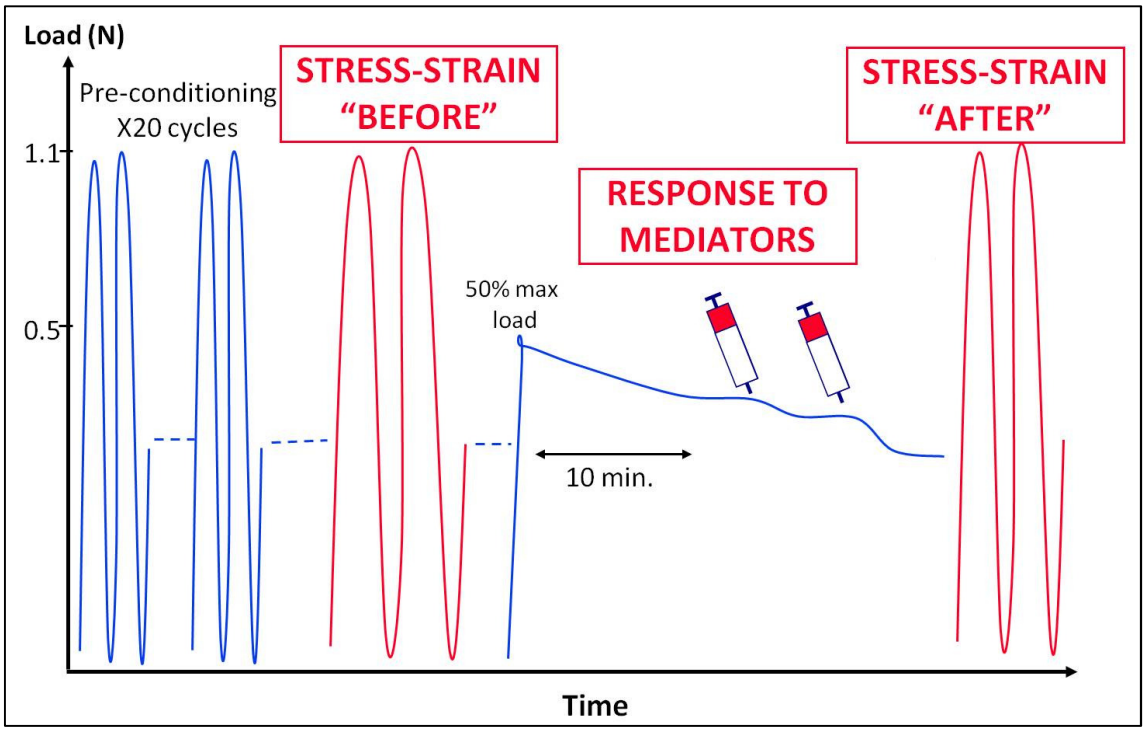

Figure 4.6 – Diagram illustrating the experimental protocol. After mounting the cusps in the test chamber, they were preconditioned through a series of 20 strain cycles. Baseline stress-strain was then measured by averaging 3 cycles. The tissue was then stretched to 50% of maximal load, then allowed to reach equilibrium over a period of 10 minutes, and increasing concentrations of a specific mediator were added to the Krebs solution. Tissue contractions or relaxations were measured during that period. This was then followed by another series of 3 cycles of stress-strain to measure the post-exposure elastic modulus of the tissue.

4.2.3.1 Evaluation of Tissue Stiffness

To account for the coupling between the radial and circumferential axes in determining valve mechanical properties, areal strain was used as a measure of cusp tissue stiffness. Areal strains are calculated by incorporating simultaneously measured radial and circumferential strains as

detailed below. The gradient of the linear portion of the load-areal strain curve was used as a measure of the stiffness/modulus of the valve leaflet. This is the region where the collagen fibers are fully uncrimped and the load-bearing components of the valve cusp are recruited. In the following sections, the terms stiffness, modulus and elastic modulus are used interchangeably.

Areal Strain Calculation

Areal (Green's) strain: $E_A = \frac{1}{2}([\lambda_R \lambda_C]^2 - 1)$

$\lambda_R = (2E_R + 1)^{\frac{1}{2}}$
$\lambda_C = (2E_C + 1)^{\frac{1}{2}}$
λ_R = *Radial stretch ratio*
λ_C = *Circumferential stretch ratio*
E_C *= Radial (Green's) strain*
E_R *= Circumferential (Green's) strain*

4.2.3.2 Evaluation of Contraction and Relaxation Responses

Contraction and relaxation responses of the tissue were also measured to evaluate concentration-dependent tissue responses to the addition of various endothelial-dependent mediators.

4.2.4 Study Groups

4.2.4.1 Experimental Groups

Aortic valve cusps were randomly allocated to four different groups according to the vasoactive agent used: 5-HT (10^{-8} to 10^{-5}M; n=6; Sigma-Aldrich, UK), ET-1 (10^{-10} to 10^{-8}M; n=6; Sigma-Aldrich, UK), sodium nitroprusside, (SNP; 10^{-7} to 10^{-5}M; n=6; Sigma-Aldrich, UK), and control (n=4). 5-HT was chosen for several reasons: it has been shown to induce nitric oxide (NO) release from coronary endothelium (Tschudi, Richard, Buhler, & Luscher, 1991). Additionally,

5-HT receptors have previously been characterized in aortic valve tissue (Roy, Brand, & Yacoub, 2000), and importantly 5-HT is also capable of inducing valve contractions (Chester, Misfeld, & Yacoub, 2000) by inducing release of intracellular calcium in valve interstitial cells (Taylor et al., 2000). Therefore, it is perfectly suited to evaluate relaxation or contraction responses in aortic valves. ET-1 is an endothelium-derived peptide that has previously been localized in valvular endothelial cells (Misfeld, Morrison, Sievers, Yacoub, & Chester, 2002). Each tissue section was only exposed to a single vasoactive agent to avoid interactions between various agents.

4.2.4.2 Role of the Endothelium

The role of the endothelium was evaluated by pharmacological and mechanical means. Cusps were exposed to L-NAME (100 μM; Sigma, UK), a nitric oxide synthase inhibitor, to evaluate the role of endothelial-derived NO responses (n=4) . In other cusps, the endothelium was mechanically removed using a cell-scraper as previously described in Chapter 2, before exposing the tissue to vasoactive agents (denuded group; n=4).

4.2.4.3 Contribution of Interstitial Contractile Responses

In order to evaluate the contribution of interstitial cell contractions to changes in cusp mechanical properties, specimens (n=4) were incubated for 4 hours in cytochalasin B (CyB; 2 μM; Sigma-Aldrich, UK), an actin depolymerizing agent, prior to testing (Carter, 1967).

4.2.4 Tissue Imaging

Valve cusps were fixed in formalin and stained for von Willebrand factor (endothelial cells) and smooth muscle α-actin ([SMA]; smooth muscle cells) to evaluate the integrity and distribution of the endothelium before and after testing (as previously described). Intact and denuded

specimens were fixed in glutaraldehyde and scanning electron microscopy was also performed to assess cellular composition.

4.2.5 Statistical Analysis

Data are expressed as mean ± standard error. For each valve specimen, the percentage change in load from pre-test values was calculated in the radial and circumferential axes, as a function of the vasoactive agent concentration. Mixed effect models were used to account for the correlation between measurements in the radial and circumferential directions and between repeated measurements in each valve specimen (the MIXED procedure in SAS software, version 9.1; SAS Institute, Cary, NC). Valve percentage changes in load versus control, were tested in order to assess if any of the mean responses were different from control. If this test was significant, we tested the percentage change at each concentration using a Dunnett correction. To further characterize the concentration-response relationship, more parsimonious models were fitted using linear trend over the log of the concentrations with or without an interaction term, i.e. allowing different slopes for the linear trend in radial and circumferential directions. Additionally, 2-sided Student t-tests for independent samples were used to compare the changes in elastic modulus between groups. P values < 0.05 were considered statistically significant. The statistical analyses were performed using SAS version 9.1.

4.3 RESULTS

4.3.1 Cellular Integrity of the Cusps Before and After Experiments

4.3.1.1 Endothelium

Endothelial integrity of all aortic valve cusps was assessed by immunohistochemistry. In addition, electron microscopy was performed on randomly selected specimens to ensure presence of the endothelial monolayer. Figure 4.7A is a representative section showing positive vWF staining, a marker of endothelial cells whereas as Figure 4.7B is an electron micrograph showing preserved endothelial cell integrity on the cusp surface after biaxial testing.

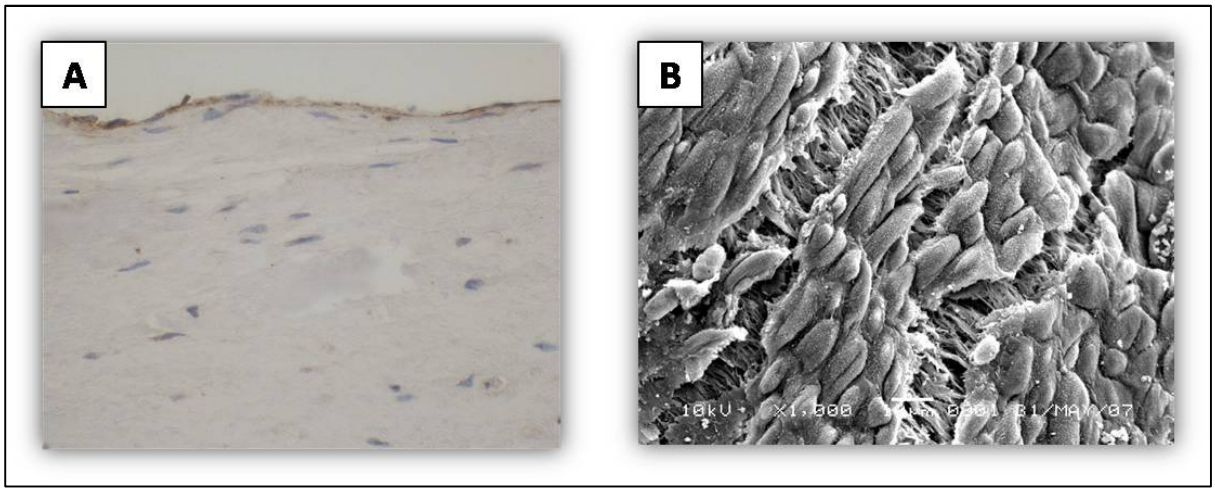

Figure 4.7 - A) Histological section (original magnification x40) showing preservation of the endothelial cells after biaxial testing by positive von Willebrand factor staining *(brown)*. B) Scanning electron micrograph (x1000) of aortic cusp before biaxial testing, showing preserved endothelial monolayer *(Note: areas of apparent endothelial denudation are due to air drying of specimens with hexamethyldisilazane. Both ridges of the endothelium are juxtaposable).*

lectron micrographs were also performed on all cusps undergoing mechanical denudation. If more than 10% of the cusp surface was covered by intact endothelial cells, cusps were dismissed from analysis (n=0). Figure 4.8 shows a representative cusp following mechanical denudation of the endothelium. Only the underlying matrix is apparent.

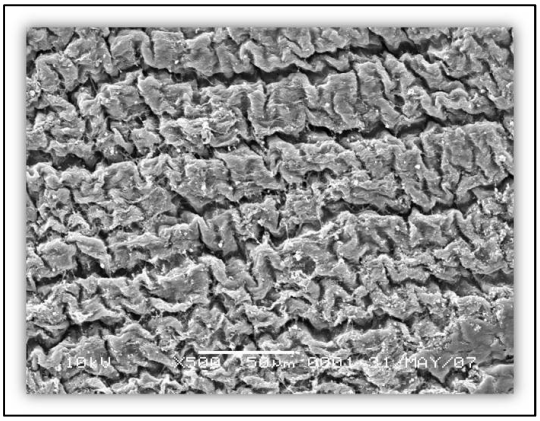

Figure 4.8 - Scanning electron micrograph of a mechanically denuded aortic valve cusp showing complete absence of endothelial cells and intact subendothelial matrix (x500).

4.3.1.2 Smooth Muscle Cells

All cusps showed intact SMA expression before testing. No differences in expression or distribution of SMA were observed after stretching, including in cusps presenting contractile responses (Figure 4.9).

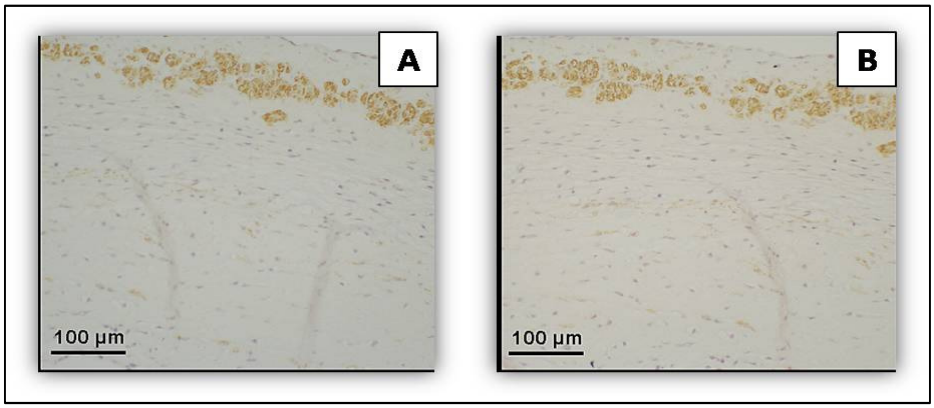

Figure 4.9 – A) Representative immunohistochemical analysis of smooth muscle α-actin (SMA) expression before stimulation with ET-1 (x20); B) SMA expression after stimulation with ET-1 showing no changes in overall SMA expression (x20).

4.3.2 Endothelial Regulation of Aortic Valve Relaxation and Contraction

4.3.2.1 Endothelial-Dependent Relaxation

When challenged with 5-HT, the valve specimens relaxed in a concentration-dependent manner (-0.29% ± 0.1% change in load per 10-fold increase in 5-HT concentration; *p=0.03*; Figure 4.10).

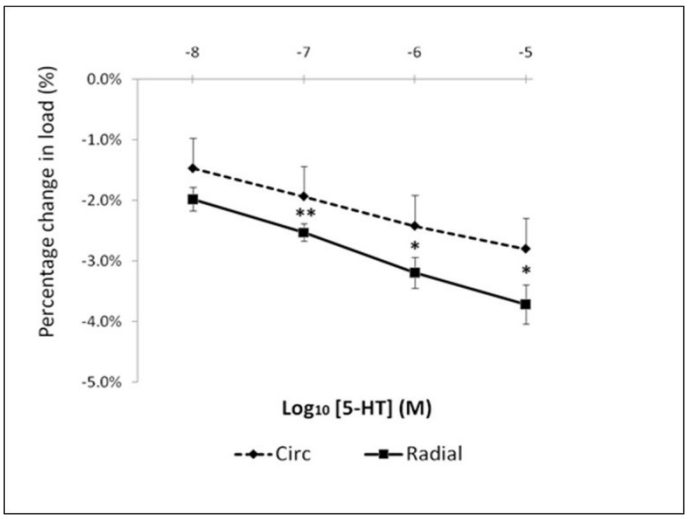

Figure 4.10 - Concentration-dependent changes in contraction or relaxation (±SE) of porcine aortic valve cusps in the radial and circumferential directions in response to 5-HT alone.
** Dunnett-adjusted p<0.05 vs. control*
*** Dunnett-adjusted p<0.01 vs. control*

In the denuded specimens (Figure 4.11), the cusps exhibited significant concentration-dependent contractions to 5-HT in both axes (+0.29% ± 0.06% change in load per 10-fold increase in 5-HT concentration; *p=0.02*).

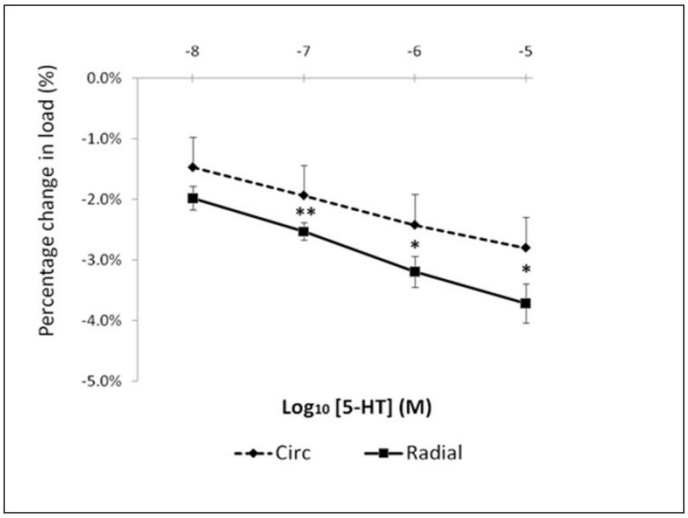

Figure 4.11 - Concentration-dependent changes in contraction or relaxation (±SE) of porcine aortic valve cusps in the radial and circumferential directions in response to 5-HT following mechanical endothelial denudation of the cusps.
** Dunnett-adjusted p<0.05 vs. control*
*** Dunnett-adjusted p<0.01 vs. control*

Similarly, in the presence of L-NAME, the cusps exhibited a significant concentration-dependent contraction in response to 5-HT in both axes (Figure 4.12).

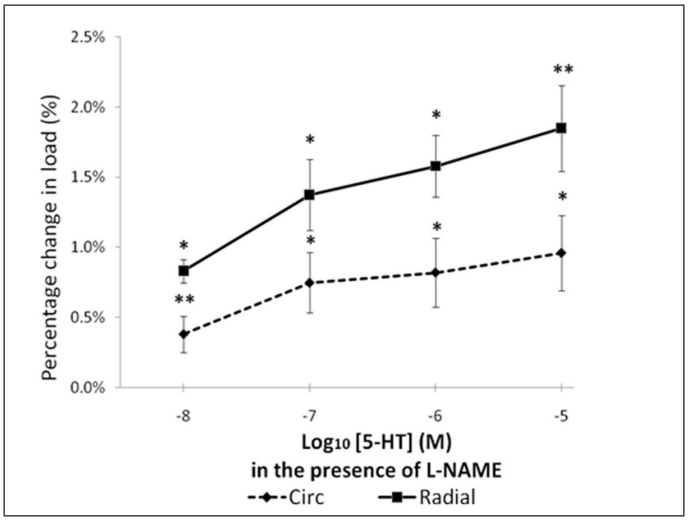

Figure 4.12 - Concentration-dependent changes in contraction or relaxation of porcine aortic valve cusps in the radial and circumferential directions in response to 5-HT in the presence of L-NAME, a specific inhibitor of NOS.
** Dunnett-adjusted p<0.05 vs. control*
*** Dunnett-adjusted p<0.01 vs. control*

4.3.2.2 Endothelial-Independent Relaxation

Valve specimens relaxed in a concentration-dependent fashion when challenged with SNP confirming the capacity of contractile cells to relax (*p=0.02*; data nor shown).

4.3.2.3 Tissue Contractility

Aortic valve cusps significantly contracted in response to increasing concentrations of ET-1 (+0.29% ± 0.08% change in load per 10-fold increase in ET-1 concentration; *p=0.02*; Figure 4.13A). When valve specimens were pre-incubated in CyB, the contractile response to ET-1 was mitigated (Figure 4.13B).

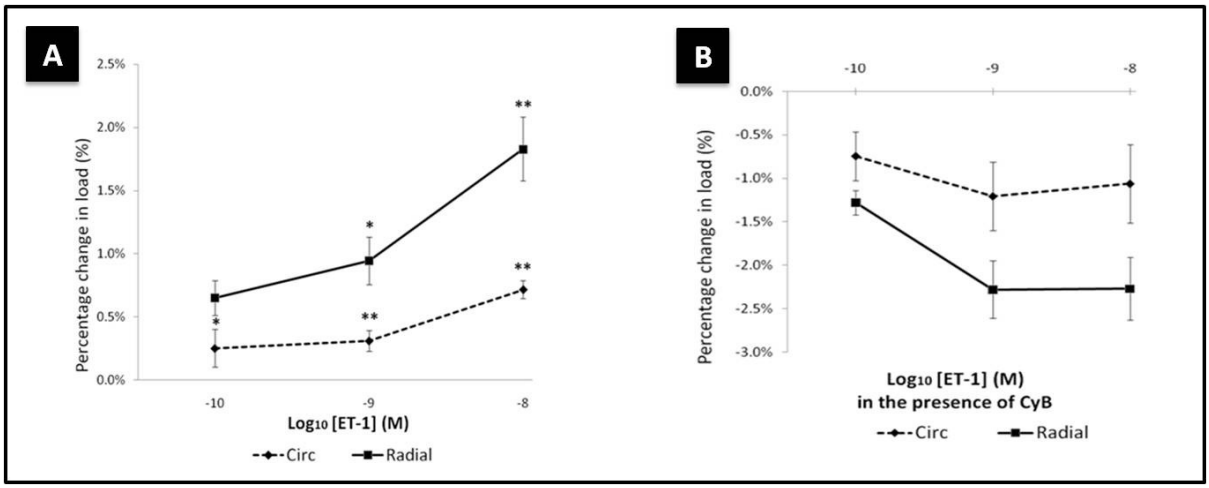

Figure 4.13 - Concentration-dependent changes in contraction or relaxation of aortic cusps in the radial and circumferential axes in response to A) ET-1 and B) ET-1 + cytochalasin B, an inhibitor of actin polymerization.
** Dunnett-adjusted p<0.05 vs. control*
*** Dunnett-adjusted p<0.01 vs. control*

4.3.3 Aortic Valve Stiffness

4.3.3.1 Baseline Aortic Valve Stiffness

Baseline stiffness was evaluated for 4 initial groups with respect to areal strain: control, endothelial denudation, L-NAME alone, and CyB alone (Table 4.1). Mean baseline stiffness for control aortic cusps was 0.82±0.08 kN/m. The modulus was not affected by endothelial denudation (0.72 ± 0.09 kN/m; p=0.4 vs. control) nor by the addition of L-NAME (0.66±0.18; p=0.5 vs. control). Addition of CyB to control cusps significantly reduced the baseline stiffness compared to control (0.36±0.11; *p<0.05 vs. control)*.

Table 4.1 Baseline aortic valve elastic modulus in the radial and circumferential axes and following treatments with L-NAME, endothelial denudation and CyB.

	Circumferential (kN/m)	Radial (kN/m)
Normal (n=6)	3.47±0.38	0.97±0.11
L-NAME alone (n=4)	1.73±0.17	1.30±0.22
Denuded leaflet (n=4)	2.13±1.05	1.00±0.30
CyB alone (n=4)	3.32±0.99	1.16±0.12

4.3.3.2 Endothelial Regulation of Uniaxial Aortic Valve Elastic Modulus

Individual variations in the radial and circumferential moduli in response to various stimuli are presented in Table 4.2. Tissue stiffness was significantly decreased by 5-HT in both the circumferential and radial directions (-28.3 ± 7.6% and-16.1 ± 5.4% versus control, respectively). In endothelium-denuded aortic valve cusps, addition of 5-HT resulted in a significant increase in the circumferential elastic modulus (+19.4. 1% versus control) and trend towards increased stiffness in the radial direction (+8.1 ± 5.6% versus control). Similarly, in the presence of L-NAME, there was a marked increase in the circumferential elastic modulus

(+58.3 ± 9.4% versus control), however was no significant change was observed in the radial direction (-4.6 ± 5.8% versus control).

Table 4.2 - Percentage change from baseline of aortic valve elastic modulus in the radial and circumferential axes following treatment with 5-HT alone, 5-HT following L-NAME administration and 5-HT following endothelial mechanical denudation.

	Circumferential	Radial
5-HT (n=6)	-28.3±7.6 %	-16.1±5.4 %
5-HT + Denudation (n=4)	+19.9±4.1 %	+8.1±5.6 %
5-HT + L-NAME (n=4)	+58.3±9.4 %	-4.6±5.8 %

4.3.3.3 Role of the Contractile Elements on Uniaxial Aortic Valve Elastic Modulus

Addition of ET-1 to aortic valve cusps resulted in a significant increase in tissue elastic modulus in both the circumferential (+21.4 ± 6.4% versus control) and the radial directions (+19.6 ± 4.7% versus control). Addition of CyB to inhibit actin polymerization resulted in a decrease in stiffness in both axes individually (-12.1 ± 4.6% versus control in the circumferential axis and -19.5 ± 2.1% in the radial axis) (Table 4.3).

Table 4.3 - Percentage change from baseline of aortic valve elastic modulus in the radial and circumferential axes following treatment with ET-1 and ET-1 + CyB, an inhibitor of actin polymerization.

	Circumferential	Radial
ET-1 (n=6)	+21.4±6.4 %	+19.6±4.7 %
ET-1 + CyB (n=4)	-12.1±4.6 %	-19.5±2.1 %

4.3.3.4 Overall Changes in Aortic Valve Stiffness

As mentioned in the introduction, due to the interdependence between both the radial and circumferential axes of the aortic valve, it is necessary to evaluate total areal strain which is a

measure of overall tissue stiffness. Using the same study groups, changes in aortic valve stiffness were compared to normal controls. Figure 4.14 demonstrates changes in tissue stiffness following different study protocols. Addition of 5-HT alone results in a decrease of stiffness by 25.0 ± 4.0% ($p<0.01$ vs. control). In contrast, in endothelium-denuded specimens, addition of 5-HT resulted in a significant increase in cusp areal strain compared to control (+14.7 ± 1.8%; $p<0.05$ vs. control). Similarly, when L-NAME was present in the tissue bath, there was a trend towards an increase in cusp areal strain after addition of 5-HT (+17.5 ± 5.3%; $p=0.07$ vs. control). Furthermore, the changes in elastic modulus in response to 5-HT in denuded cusps or after addition of L-NAME were each statistically different from the changes following addition of 5-HT alone (both $p<0.01$). ET-1 significantly increased the areal stiffness of aortic valve cusps (+34.4 ± 13.8%; $p<0.05$ vs. control). After incubation of the cusps in CyB, addition of ET-1 did not result in a significant difference in cusp stiffness (p=0.29 vs. control). However, direct comparison of changes following ET-1versus ET-1 and CyB was statistically significant ($p<0.05$).

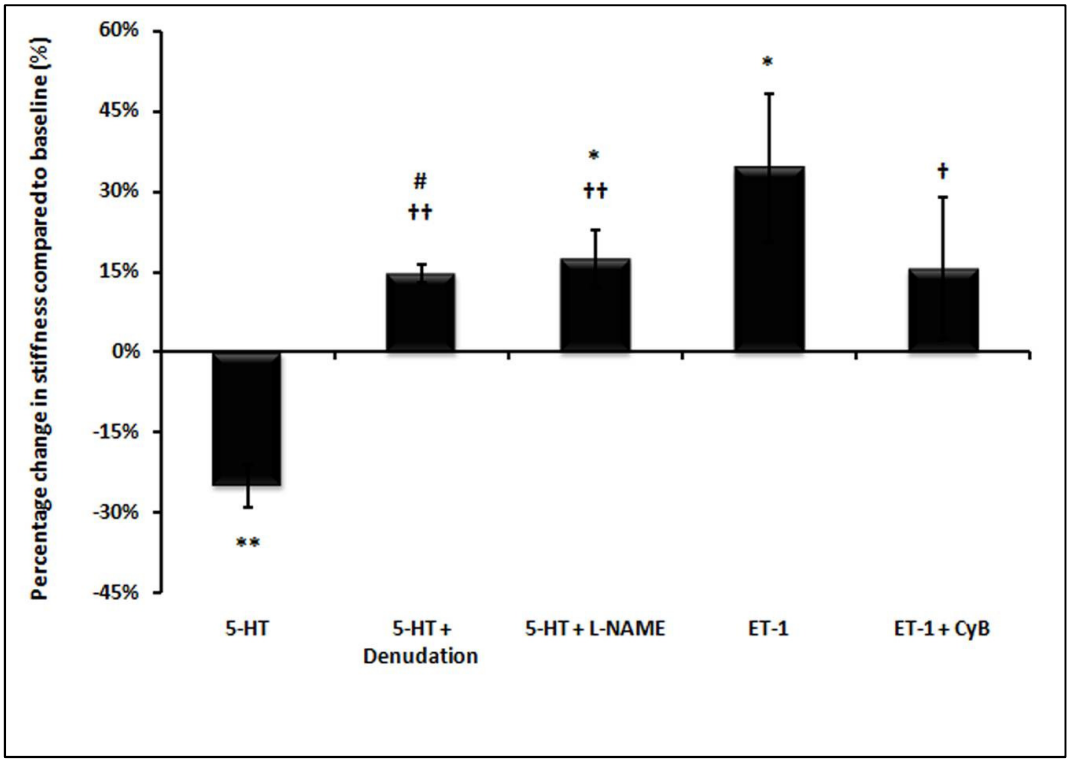

Figure 4.14 - Percentage change in aortic valve areal strains versus control in response to various agents. The percentage change in areal strain (±SE) of aortic cusps (normal and denuded) in response to the various vasoactive agents and their inhibitors. Areal strains were measured before and after addition of the compounds (each valve served as its own control).

* *Dunnett-adjusted p<0.05 vs. control*
** *Dunnett-adjusted p<0.01 vs. control*
\# *Dunnett-adjusted p<0.1 vs. control*
† *p<0.05 vs. ET-1 alone*
†† *p<0.01 vs. 5-HT alone*

4.4 DISCUSSION

Findings from the present series of experiments provides evidence for the critical role of endothelial-derived NO in regulating the stiffness of aortic valve cusp under physiological loading conditions. In addition, this work demonstrates direct communication by paracrine mechanisms between endothelial-derived NO and underlying valve interstitial cells, in particular SMA-positive cells. These findings represent the first evidence of the presence of active cell-mediated pathways regulating valve mechanical properties.

4.4.1 Rationale for Study Design

4.4.1.1 Choice of Mediators

The endothelium releases a number of bioactive substances in vivo, notably NO and ET-1. Whereas NO is a smooth muscle relaxant, ET-1 is a one of the most potent endogenous vasoconstrictor peptides causing contraction of smooth muscle cells via stimulation of specific receptor subtypes (Yanagisawa et al., 1988). ET-1 is stored and released by endothelial cells, a process strongly controlled (inhibited) by NO under normal conditions (Boulanger & Luscher, 1990; Luscher et al., 1990), creating a balance between both mediators. There are 2 ET receptors: ET_A and ET_B receptors. Both endothelial cells and smooth muscle cells have receptors to ET-1 and both receptors subtypes have been shown to be functional in aortic valves (Misfeld et al., 2002). Use of exogenous ET-1 serves to demonstrate the effect of this peptide if released in high quantities by endothelial cells such as observed in pathological conditions associated with aortic valve disease such as coronary artery

In this study, 5-HT was used to stimulate NO release by endothelial cells (Shimada et al., 1999; Tschudi et al., 1991; Vanhoutte, 1991). There are multiple known 5-HT receptor subtypes, a number of which have been characterized in aortic valve tissue (Rothman et al., 2000; Roy et al., 2000). They can be present on endothelial cells as well as smooth muscle cells. The overall effect of 5-HT stimulation represents the balance of receptor stimulation in both types of cells. With the addition of L-NAME however, the non NO-dependent effects of 5-HT was highlighted. Interestingly, this showed that under the present experimental conditions, it appears that the endothelium does not release basal NO or keep the tissue in a constitutively relaxed tone as evidenced by the absence of change in valve stiffness after pharmacological inhibition or mechanical denudation of the endothelium. However, after addition of 5-HT under these conditions, valve responses are reversed. The observed increase in stiffness suggests that 5-HT acts on normal endothelium by inducing a release of NO. By inhibiting NO synthesis, the

direct effect of 5-HT on valve interstitial cells is left unopposed and results in valve contraction and stiffening.

4.4.1.2 Experimental Setup

Though the experimental setup is not perfect to reproduce the full mechanical environment of aortic valves, it represents significant progress compared to previously published experimental models in terms of the actual study protocol (Merryman, Huang, Schoen, & Sacks, 2006; Stella et al., 2007; Stella & Sacks, 2007). Hearts were immediately placed in cold preservation solution following explantation. Aortic valve cusps were dissected and handled gently to avoid injuring the endothelium. Unlike other studies where experiments were performed in the days following animal sacrifice, all experiments were performed within 12 hours in this case, which we think has an important role in preserving cell-mediated responses. In addition, the organ chamber was filled with oxygenated Krebs solution maintained at 37C and at physiological pH. These elements are worth mentioning because they could individually or collectively account for differences in observations between various studies in the literature.

Nevertheless, the model fails to address several mechanical and hemodynamic elements which are relevant in vivo such as shear stress, bending and blood viscosity among other factors. These various components can each activate the endothelium into releasing different mediators through specific mechanotransduction pathways. Thus, the overall state of the aortic valve cusp in vivo remains to be defined. In order to do so, we are currently collaborating with a team of engineers from the Georgia Institute of Technology to develop a bioreactor which would combine both stretch and shear stress through flow.

In this study, the belly region from each aortic valve cusp was used to assess mechanical properties of the aortic valve. The choice of the belly region was related to the fact that it is the major load-bearing region of the cusp (Grande-Allen et al., 2000; Grande et al., 1998). However, histological analyses of aortic valve cusps often show a non-homogeneous distribution of interstitial cells, particularly SMA-positive cells (data not presented), which are predominantly

found closer to the base of the cusps. Thus, global mechanical properties of the valve could be ascertained through an in vivo model using microsonometric crystals, as was previously used to evaluate the 4-dimensional dynamics of the aortic root (Dagum et al., 1999; Lansac, Lim, Shomura, Lim, Rice et al., 2002).

4.4.2 Physiological Significance of Changes in Valve Stiffness

The precise physiological significance of changes in aortic valve stiffness are yet to be fully determined. It remains however undoubtable that a living valve capable of adapting its structure and function to the surrounding environment bears major clinical importance, both in terms of patient quality of life, survival as well as the ability of the cusps to withstand major hemodynamic forces over many years. Changes in stiffness can optimize stress distribution across the surface of the cusps. Although the belly region is thought to be the major load-bearing region, in the absence of regulation of the mechanical properties of the cusps, this might be accentuated, which can inevitably lead to cellular and molecular changes. Indeed, one can speculate that early valve calcification observed in some patients with bicuspid aortic valves could be in part due to the inability of the cusps to adapt their stiffness to changing hemodynamic and humoural conditions due a deficiency in eNOS (Aicher et al., 2007; Lee et al., 2000). Changes in valve mechanical properties can also be beneficial in hypertensive patients with high diastolic pressure. Increasing the stiffness of the cusps could maintain an adequate surface of coaptation and ensure valvular competence despite the elevated afterload.

Along with the aortic annulus, the sinuses of Valsalva ad the sinotubular junction, aortic valve cusps are one of the component parts of the aortic root. These different parts operate in harmony to ensure adequate function of the aortic root, thereby minimizing ventricular workload and optimizing coronary flow (J. E. Davies et al., 2008; M. H. Yacoub, Kilner, Birks, & Misfeld, 1999). Because of the extreme mechanical forces in that region, tissue stress is distributed between the sinuses and the cusps (Grande-Allen et al., 2000; Katayama et al., 2008; Robicsek & Thubrikar, 1999; M. J. Thubrikar, Nolan et al., 1986). Therefore, the stiffness of the

cusps could have a direct impact on the function of the sinuses of Valsalva and the magnitude of stresses at that level, which could contribute to changes in its structure (El-Hamamsy & Yacoub, 2009a), such as observed in bicuspid aortic valve disease for instance (El-Hamamsy & Yacoub, 2009b). Indeed, Grande-Allen *et al.* (Grande-Allen et al., 2001) showed that with every change in leaflet dimension, elastic modulus and surface of coaptation, there is a significantly altered distribution of strains over the aortic leaflet with a marked increase at the free edge. This increase in strain is thought to contribute to the observed aortic regurgitation in these patients.

An important consideration for in vivo mechanical properties is that the half-life of NO in the cellular environment is very short and thus it may have an impact on the beat-to-beat regulation of valve biomechanics. On the other hand, ET-1, which has much longer duration of action is more likely to affect the general tone of the valve, allowing it to adapt to its environment over a longer period of time. In addition, the impact of other endothelial-derived mediators such as prostacyclin and endothelium-independent mediators certainly have an impact on valve mechanics. Therefore, the true functional significance of these findings will be fully understood once 4 - dimesional functional imaging techniques which can track the instantaneous movements of the cusps and changes in Young's modulus are available.

4.4.3 Link Between Tissue Relaxation/Contraction Responses and Tissue Stiffness

One of the striking findings of our study was the significant disproportion between the magnitude of tissue relaxation or contraction responses to the different treatment conditions (<5%) and the magnitude of changes in cusp stiffness (up to 35%). It is likely that both sets of responses are related to each other since in all cases, relaxation responses resulted in a decrease in tissue stiffness and vice versa. The small magnitude of relaxation/contraction responses is physiologically expected since larger responses would in effect compromise valve function by reducing coaptation. However, the large changes in stiffness were unexpectedly large. From a mathematical standpoint, this might be explained by the fact that tissue stress (σ) is inversely proportional to the surface area (A) of the tissue ($\sigma \propto 1/A$). Therefore, small

changes in the leaflet area (A) through contraction or relaxation cause much larger changes in stresses and consequently in the elastic modulus. Nevertheless, this could not explain the full extent of the response. Tissue contraction or relaxation is a result of cellular contractions or relaxations in response to ET-1 or NO. Changes in tissue stiffness are thought to be the result of changes in cell-cell interactions or cell-matrix interactions in response to the various agents. This could be evaluated by assessing the number and distribution of cell adhesions. As it is now well understood that interstitial cells are intimately linked to the ECM through the cytoskeleton, it is likely that changes in cell shape or tone would also affect the ECM proteins. The differential changes in stiffness between the radial and circumferential directions strongly suggests that these factors are operative, in light of the specific orientation of collagen and elastin fibers in both axes. It is hoped that current work using scanning ion conductance microscopy on valve interstitial cells following addition of different mediators could shed light into the underlying mechanisms.

4.4.4 Clinical Significance of Current Findings

The current findings introduce a new paradigm into the role of the endothelium in aortic valve pathology. It is well accepted that endothelial damage or dysfunction – through the loss of anti-inflammatory and anti-oxidant mediators - is an early occurrence in the cascade of events leading to structural valve disease (Otto et al., 1994). This work suggests that endothelial dysfunction can additionally result in changes in mechanical responses to different stimuli, which could potentially contribute to the pathophysiology of valve disease. In our experiments, following pharmacological inhibition or mechanical denudation of the endothelium, changes in valve elastic modulus in response to endogenous mediators was significantly altered. As mentioned earlier, this may expose specific regions of the cusps to abnormally high stresses, increasing the risk of local microtrauma, which in turn leads to further endothelial damage and structural degeneration. A loss of the capacity of aortic valves to adapt to their mechanical environment can significantly compound and possibly accelerate structural valve degeneration.

Aside from its role as an endothelium-dependent agonist, 5-HT has been directly linked to valve pathologies, namely the carcinoid syndrome (Rajamannan et al., 2001) and secondary to treatment with fenfluramine and phentermine, two appetite suppressants which have since been withdrawn by the Food and Drug Administration (FDA) (Connolly et al., 1997; Gustafsson et al., 2005). In both instances, 5-HT appears to play an important role in valve pathology. The valvular pathologies reported in both these entities have focused on the structural changes in the valves which include plaque-like encasement of the leaflets and chordal structures (Connolly et al., 1997). Although these are the major determinants of disease manifestation, no studies have evaluated the mechanical properties of these valves, but in light of our findings, they are expected to be altered which can have an important on their function and response to changing hemodynamics.

4.5 Limitations of the Study

The local mechanical and hemodynamic environment of the aortic valve is extremely complex which makes any attempt at studying these factors ex vivo a major challenge. The current study represents one such example and at best, constitutes an approximation of the actual in vivo loading conditions. However, while actual values of the mechanical parameters may differ from in vivo values, ex vivo mechanical testing offers the advantage of being extremely sensitive to small changes between test groups, and is ideal for a study of this nature. In this report, we focused on the immediate changes related to administration of different mediators. This acute experimental setup does not account for the trophic effects of these agents or their ability to modulate the extracellular matrix following longer exposure (Hafizi, Taylor, Chester, Allen, & Yacoub, 2000; Jian et al., 2002). Finally, in vivo, aortic cusps are simultaneously exposed to a number of mechanical stimuli in addition to strain, such as bending and shear stress. Our present experimental setup does not yet allow us to combine these stimuli into a single setup. Nevertheless, decomposing the response of valve cusps to each stimulus is useful in singling out

their unique effects on the tissue. The biaxial testing system used in this work has 2 major limitations: the volume of medium required for each experiments is relatively high (~200mL) and chronic experiments (>24 hours) are difficult because it is only a semi-sterile system. The total volume represents an obstacle if one is to study the effect of expensive molecules such as TGFβ1 on valve mechanical properties, a study which would be particularly helpful considering its effect on valve pathophysiology.

4.6 Conclusion and Future Directions

In conclusion, we have demonstrated that the mechanical properties of aortic valve cusps are actively regulated through endothelial-dependent pathways. The valve endothelium exerts its effects by modulating aortic valve cusp relaxation and contraction to different mediators, but most importantly by regulating the changes in the stiffness of the cusps. Changes in valve mechanical properties, especially its elastic modulus, could explain the unique ability of aortic valves to withstand severe mechanical stresses during each cardiac cycle. These findings introduce a new paradigm in the understanding of aortic valve disease in patients with risk factors associated with endothelial dysfunction. In addition, they further our understanding of valve physiology and establish a more complete blueprint of adaptive responses of valve mechanical properties for future tissue-engineered heart valves.

Further work is required to assess the effects of these changes on the function of the valves in an in vivo setting. Work from another group looking at the mechanics of the mitral valve in an in vivo ovine model was performed using small radio-opaque videofluoroscopic markers placed at predefined points on the mitral leaflets (Itoh et al., 2009). In particular, it would be interesting to assess the effect of chronic endothelial dysfunction (with or without treatment with NO donors) in an animal model on aortic valve mechanical properties. In addition, we are currently working with our collaborators from the Georgia Institute of

Technology to develop in vitro testing systems that allow a combination of strain and flow on the tissue, while minimizing the overall volume of medium necessary in the apparatus.

V Adaptation Capacity of a Living Aortic Valve

5.1 BACKGROUND

One of the salient features of a living structure, organ or being is their ability to adapt to changing environmental conditions. In the case of heart valves, hemodynamics represent the main environmental stimulus to heart valves, characterized by changes in the mechanical forces the valves are subjected to, such as pressure, shear stress opening and closing velocities and bending forces. Adaptation is not only a reaction to the environment but is also aimed at improving the function of the involved organ. Examples of adaptation abound in the body and in nature. A compelling example of adaptation in nature is the capacity of swifts to morph their wings to control their glide performance (Lentink et al., 2007). Swifts are capable of modifying the size and shape of their wings to exploit the profound effect of wing morphology on aerodynamic performance. Though these adaptations are acute and temporary during the bird's flight, long-term changes in the structure of an aortic valve can have important effects on its function and represent an important feature of a living organ.

To date, no data is available to evaluate changes in valve structure during the cardiac cycle similar to those observed in the swifts' wings, mainly due to the absence of sensitive imaging techniques to detect such intricate changes. Nevertheless, the adaptation capacity of heart valves can be tested in vivo in the context of the Ross procedure. The Ross procedure consists of replacing the patient's aortic root with his own pulmonary root (autograft) while placing a pulmonary homograft in the pulmonary position. It is the only valve replacement operation which guarantees very long-term viability of the aortic root. Even homovital homografts which were once thought to maintain long-term viability, have been shown to become acellular within a few weeks after implantation. Retrospective series using the Ross procedure suggest excellent long-term clinically relevant outcomes such as survival (Elkins, Thompson, Lane, Elkins, & Peyton, 2008; Kouchoukos, Davila-Roman, Spray, Murphy, & Perrillo, 1994; M. H. Yacoub et al., 2006). We hypothesized that these observed outcomes are in large part a result of the capacity of the autograft root to adapt to changing hemodynamic conditions.

Opening and closing dynamics of the aortic valve are essential determinants of ventricular workload and the pattern of flow at the outlet which can strongly influence downstream systemic flow propagation, as well as affecting coronary flow (Bellhouse & Bellhouse, 1968; Bellhouse, Bellhouse, & Reid, 1968; J. E. Davies et al., 2008).

5.1.1 Aims

The aims of the present work was to evaluate the adaptation capacity of a living aortic root by 2 means:

- Assessing the structural adaptation of the autograft root following the Ross procedure at a microstructural level. It is well known that the number of elastic lamellae is maximal in the ascending aorta in response to strong radial mechanical forces. The capacity of the much thinner pulmonary root to modify its structure in response to these external forces would represent evidence of adaptation.
- Evaluating the pattern of flow across the aortic valve and in the aortic root following the Ross procedure. These results will be compared to a set of normal controls in addition to a number of patients undergoing aortic root replacement using non-living aortic substitutes (homografts and xenografts). The pattern of flow through the aortic is a function of the instantaneous movements of the aortic cusps and of the multidimensional expansion movements of the aortic root components during the cardiac cycle. Flow patterns mirroring the normal aortic root would suggest adequate adaptation capacity.

5.2 METHODS

5.2.1 Long-Term Viability of the Autograft Root

A total of 6 explanted autograft roots from patients who had undergone the Ross procedure were collected at the time of surgery after obtaining patient consent and immediately fixed in 1% formalin. Tissue sections from the wall of the autograft wall and autograft cusps were obtained and stained using hematoxylin and eosin, elastin van Giesson and alcian blue/sirius red staining protocols. Immunohisteochemical staining using vWF and CD31 for endothelial staining and SMA was used to evaluate the cellular composition of the sections.

5.2.2 Assessment of Aortic and Pulmonary Wall Elastic Laminae Count

Using the same sections stained with van Giesson, the number of elastic lamellae of the autograft cusps and root wall was assessed. This was compared to normal control aortic roots obtained from patients undergoing cardiac transplantation as well as pulmonary roots from the same individuals.

5.2.3 Aortic Root Biomechanics

To evaluate the role of a living aortic valve and root on overall aortic root biomechanics, patients undergoing 3 types of aortic root replacement procedures were evaluated using functional imaging techniques and compared to a total of 15 normal individuals. All patients underwent imaging 10 or more years after aortic root replacement to allow for adaptation and remodelling of the implanted aortic valve and root (if any). The 4 different groups were as follows:

- Autograft root replacement: n=13 patients
- Xenograft aortic root replacement: n=10 patients
- Homograft aortic root replacement: n=6 patients

- Normal individuals: n=15 patients

All the patients analyzed had normal or near-normal echocardiographic valve function. Written consent was obtained from all patients to undergo these studies prior to imaging. Functional analyses comprised 2 main areas: tissue mechanics and fluid mechanics. Tissue mechanics provides tensile stress maps of the aortic root during the cardiac cycle whereas fluid mechanics provide information on the pattern, shape and velocity of flow across the aortic valve and root as well as endothelial shear stress on the aortic wall. This work was performed in collaboration with Dr. Ryo Torii, PhD, a post-doctoral research fellow at Imperial College London.

5.2.3.1 Tissue Mechanics

Tissue (or solid) mechanics were obtained by performing multislice gated CT studies. Only patients undergoing autograft root replacement and normal individuals underwent CT imaging as described. Thus, comparison of tissue mechanics were limited to these 2 groups. Gated CT images of the aortic root (pulmonary autograft or native aorta) were obtained. Images were acquired at 10 timepoints (phases) during the cardiac cycle, ie, on average, images were obtained every 100 msec (for a hear rate of 60 beats/min). Slice thickness is 2mm, with in-plane resolution of 0.4-0.5mm/pixel. Patient peripheral blood pressure was simultaneously recorded for all patients and used for calculations. The first step to analyze tissue mechanics is to record the temporal variation in inner and outer diameter of the aortic wall at each phase of the cardiac cycle as shown in Figure 5.1.

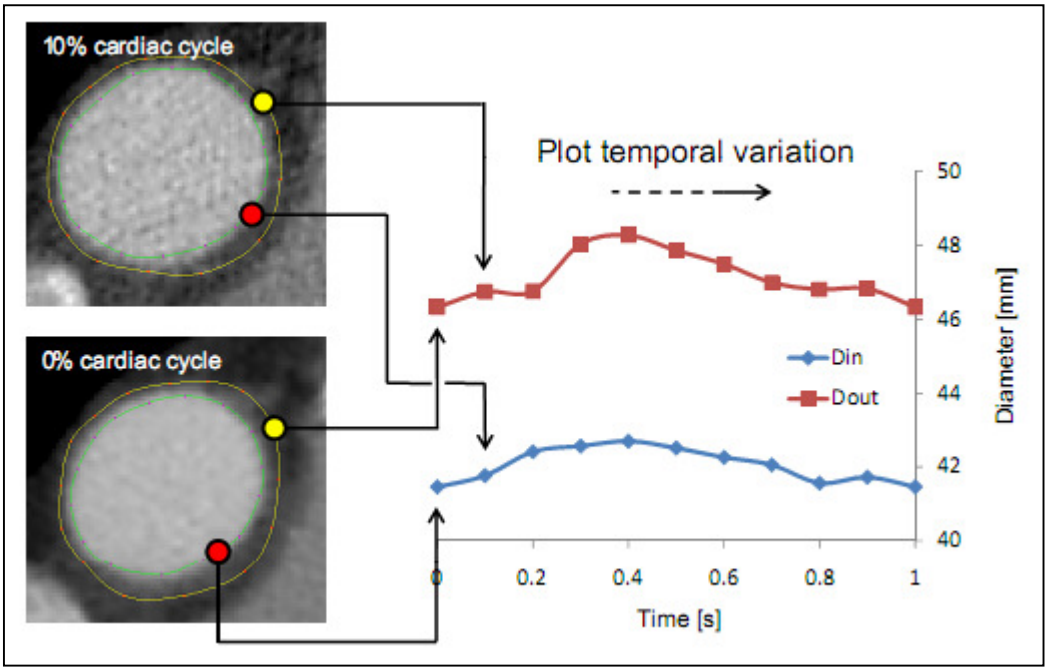

Figure 5.1 Figure showing the first step in evaluating tissue mechanics. Temporal variations in inner and outer diameter are measure at each phase of the cardiac cycle and plotted against time.

Based on data obtained, aortic wall stiffness (Young's modulus) and pressure waveform can be calculated using the following formulae and displayed as in Figure 5.2:

- Stiffness (Young's modulus):

$$E = \frac{r_i \Delta p}{u_i (r_o^2 - r_i^2)} \{(1-\nu) r_i^2 + (1+\nu) r_o^2\}$$

- Pressure waveform estimation:

$$\Delta p = \frac{E u_i (r_o^2 - r_i^2)}{\{(1-\nu) r_i^2 + (1+\nu) r_o^2\} r_i}$$

where:

E: Young's modulus
N: Poisson's ration (0.5)
Dp: inner pressure ($P_{systole}$-$P_{diastole}$)
r_i : inner wall diameter
r_o : outer wall diameter
u: inner wall displacement

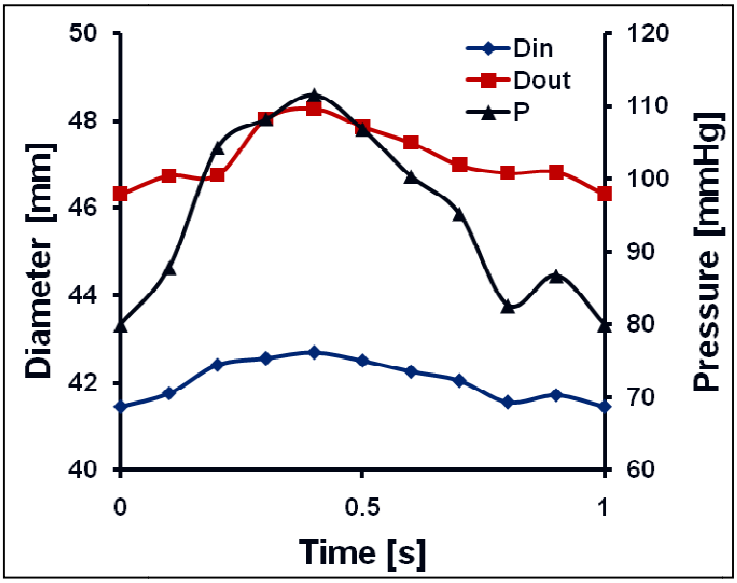

Figure 5.2 Temporal variation in inner *(blue)* and outer diameter (red) and pressure waveform estimation *(black)* in the aortic root.

Next, using the elastic modulus and the temporal pressure variation, the temporal and spatial variation in tensile stress in the aortic root wall can be estimated.

5.2.3.2 Fluid Mechanics

For fluid mechanics analysis, gated time series of phase-contrast MR images were acquired at the level of the aortic valve. Each cardiac cycle was divided into 20 phases (or timepoints). First, patient-specific aortic geometry was reconstructed based on the acquired stacked images. Next, velocity maps were calculated at the level of the aortic valve based on the phase-contrast data obtained, which then allowed flow simulation in the aorta (Figure 5.3).

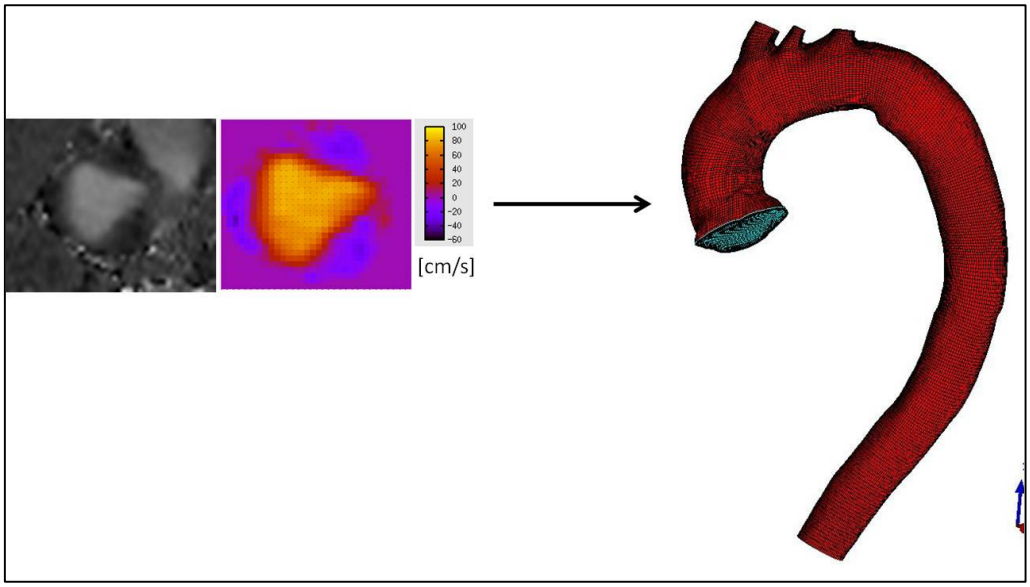

Figure 5.3 Velocity maps are obtained from the phase-contrast images at the level of the aortic valve. These results are then projected onto the 3-D reconstruction of the aorta based on the obtained stacked images of the aorta. Based on these data, flow simulation profiles can be obtained providing information on endothelial shear stress levels and velocity profiles.

5.3 RESULTS

5.3.1 Long-Term Viability of the Autograft Root Following the Ross Procedure

5.3.1.1 Trilaminar Structure

All explants obtained showed a trilaminar structure similar to that of the native aortic root, both at the level of the aortic wall and the aortic valve cusps. Normal aortic valve cusps are composed of a collagen-rich fibrosa, an elastin-rich ventricularis and a spongiosa rich with glycosaminoglycans. Autograft explants show a similar overall architecture along with a few differences. The first observation is a marked thickening of the ventricularis in autograft cusps and the adventitia in the aortic wall as observed in Figure 5.4. In addition, the amount of glycosaminoglycans appeared to be lower than in native aortic valve cusps. Due to the lesser thickness of both the native pulmonary cusps and wall compared to the aortic cusp and wall, this thickening represents an adaptive process to the higher mechanical loads in the left-sided

circulation. The adventitia is the layer of the vascular wall responsible for providing mechanical strength. In the cusp however, the collagen-rich fibrosa is typically the strength provider. Therefore a thickening of the elastin-rich ventricularis is counterintuitive, but could be due to an effort to provide more elasticity to the cusp in the face of higher diastolic loads.

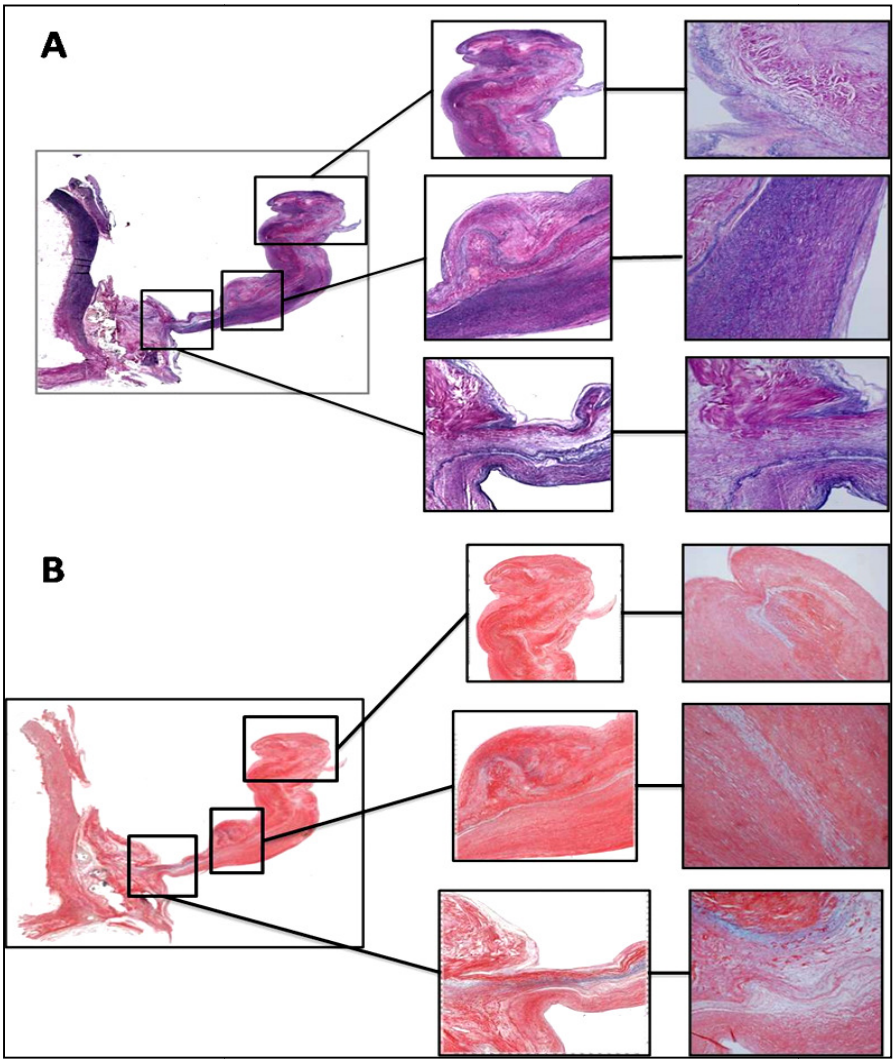

Figure 5.4 Immunohistological section of the autograft cusps at explantation (42 years after surgery) showing preservation of the trilaminar structure of the cusp. A) Elastin van Giesson staining showing the presence and distribution of collagen *(dark pink)* and elastin *(purple)*. B) Alcian blue/Sirius red staining showing the presence and distribution of glycosaminoglycans *(blue)* and collagen *(pink)*.

5.3.1.2 Cellular Composition

All samples were stained for the presence of endothelial cells (CD31 and vWf), smooth muscle cells (SMA) and inflammatory infiltrates (CD45 and CD68). Naturally, native aortic and pulmonary specimens were positive for endothelial and smooth muscle cell markers. No inflammatory cells were observed in healthy native aortic and pulmonary cusps or wall.

Explanted aortic autografts showed preservation of the endothelial cell layer and the presence of interstitial cells in the thickness of the tissue (Figure 5.5). However, in contrast to native tissue, inflammatory infiltrates were present in the explanted roots, suggesting an active chronic remodelling process.

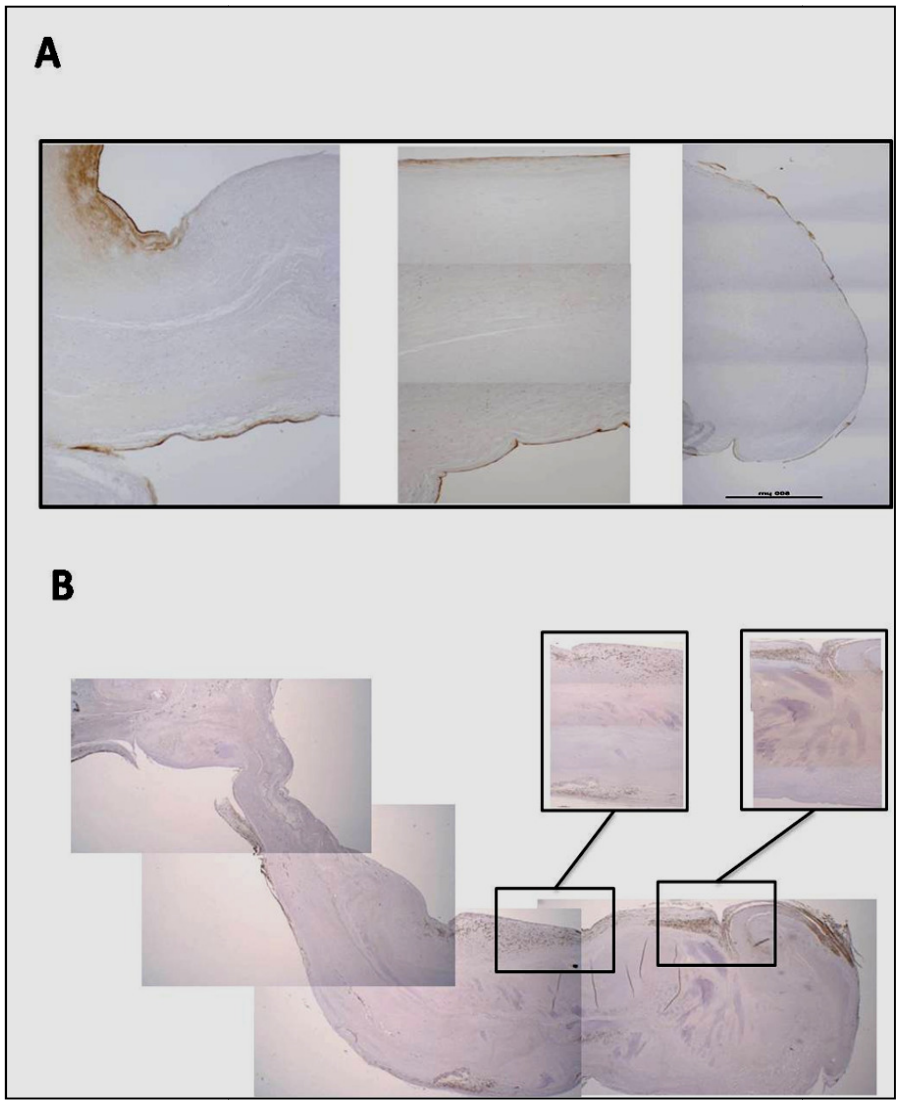

Figure 5.5 Immunohistological section of the explanted autograft cusp 42 years after implantation showing preservation of cusp cellularity as shown by A) positive von Willebrand factor staining, a marker of endothelial cells and B) smooth muscle α-actin staining in the body of the cusp, a marker of interstitial cells.

5.3.2 Adaptation of the Autograft Root to Local Mechanical Conditions

As clearly demonstrated by Wolinsky and Glagov (Wolinsky & Glagov, 1967), the lamellar unit represents the structural and functional unit of any vascular wall. The number of lamellar units varies between different segments of the vascular tree as a reflection of the different biomechanical and biochemical environments (Wolinsky, 1970). In the specimens examined by counting the number of lamellar units using elastin van Giesson staining, there were no observed differences in the number of lamellae between native aortic sinus wall, native pulmonary sinus wall and explanted autograft sinus wall (number of lamellae: 64±17, 59±12 and 62±22, respectively; p=NS) (Figure 5.6).

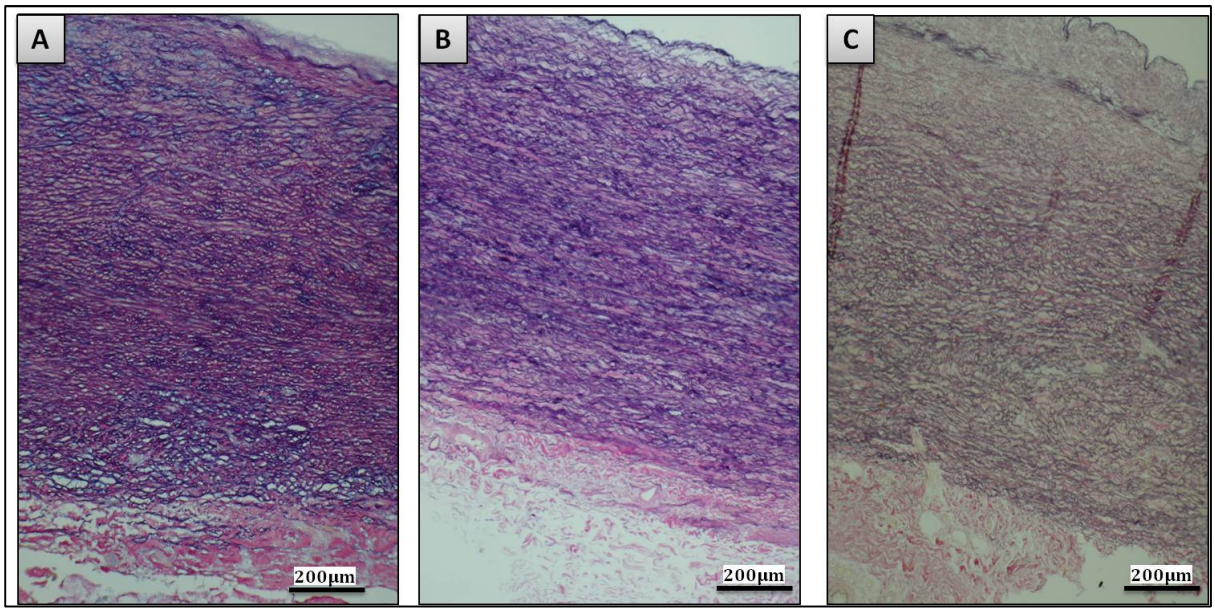

Figure 5.6 – Representative histological sections stained with elastin van Giesson showing the number of elastic laminae in A) native aortic sinus wall, B) native pulmonary sinus wall and C) autograft sinus wall. No significant differences were observed between the 3 groups.

5.3.3 Role of a Living Aortic Root on Aortic Root Biomechanics

5.3.3.1 Patient Characteristics

All patients studied for evaluation of aortic root biomechanics had undergone aortic root replacement using homografts, xenografts (Medtronic Freestyle porcine bioprosthesis implanted as a total root, Medtronic Inc, Minneapolis, USA) or autografts. All patients had undergone surgery 10 or more years before the study and all had normal or near-normal aortic valve function assessed by echocardiography (maximum trivial to mild aortic insufficiency). Patients were randomly selected to undergo these studies from a pool of patients that had been randomized in two different studies to evaluate clinical outcomes following aortic root replacement surgery. Patients were comparable for most aspects but differed significantly in terms of age. Patients in the homograft and the xenograft groups were significantly older than those in the autograft group. Similarly, they were significantly than normal individuals (Table 5.1).

Table 5.1 – Age and gender of individuals undergoing functional imaging studies. Note that homograft and xenograft recipients only underwent MR imaging whereas autograft recipients and normal individuals underwent both MR and CT imaging.

	Autograft	Homograft	Xenograft	Normal
n	13	6	10	15
Age (years)	47 ± 9	71 ± 11	76 ± 8	32 ± 5
Sex (M:F)	11 : 2	4 : 2	6 : 4	11 : 4
BSA (m^2)	2.05 ± 0.27	1.92 ± 0.20	2.06 ± 0.13	1.98 ± 0.15
HR (beats/min)	71.6 ± 15.7	75.8 ± 18.1	67.8 ± 19.9	72.1 ± 10.2
BP (mmHg)	117/68	118/86	127/75	122/66

M:F, male:female; BSA, body surface area; HR, heart rate; BP, blood pressure

5.3.3.2 Aortic Wall Tensile Stresses

Mean autograft aortic root stiffness measured at the level of the sinuses of Valsalva was higher than normal individuals, thought his did not reach statistical significance because of the high variability of results in the autograft group. Mean Young's modulus in the autograft group was 1364 ± 1231 kPa versus 492 ± 191 kPa in normal individuals (p=0.3). There was also a trend towards higher strain levels in native healthy aortas compared to autograft roots, with a mean strain of 7.6 ± 4.1 % in the autograft group and 12.9 ± 3.5 in the normal group (p=0.2). Nevertheless, importantly, maximum tensile stress levels at the level of the root were comparable between both groups (Figure 5.7). Mean maximal tensile stress in the autograft wall was 248 ± 66 kPa versus 218 ± 72 kPa. These figures are well below suggested values for aortic wall rupture or dissection (~800 kPa).

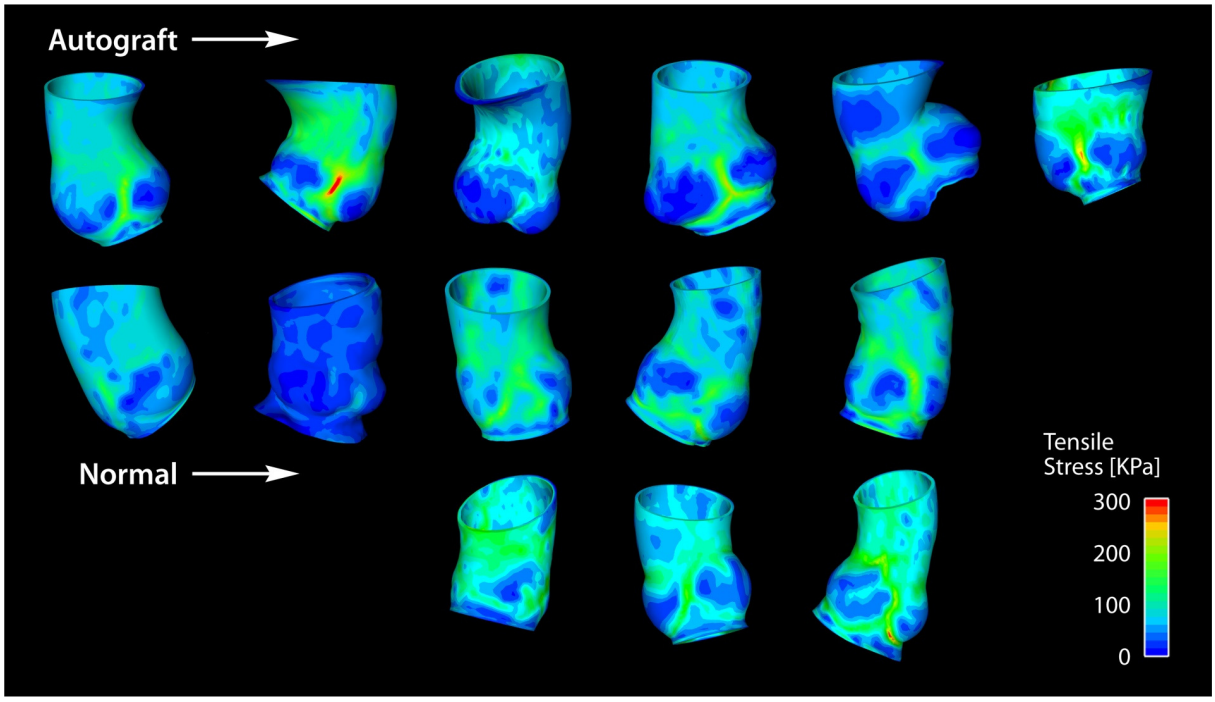

Figure 5.7 – Representative examples of 3-D stress maps following autograft aortic root replacement versus native healthy aortic roots showing comparable levels of aortic wall stresses in both groups despite the wide variability in aortic root shape in the autograft group and the differences in stiffness between the groups.

5.3.3.3 Pattern, Shape and Velocity of Flow in the Aortic Root

Relative orifice area was estimated as the ratio between the opening area at the level of the valve and the area at the mid-sinus level. There was no difference between relative orifice area in the autograft group or normal individuals (Figure 5.8 and 5.9). In contrast, relative orifice area was significantly smaller in the homograft group ($p<0.05$ versus normal individuals) and xenograft group ($p<0.01$ versus normal individuals).

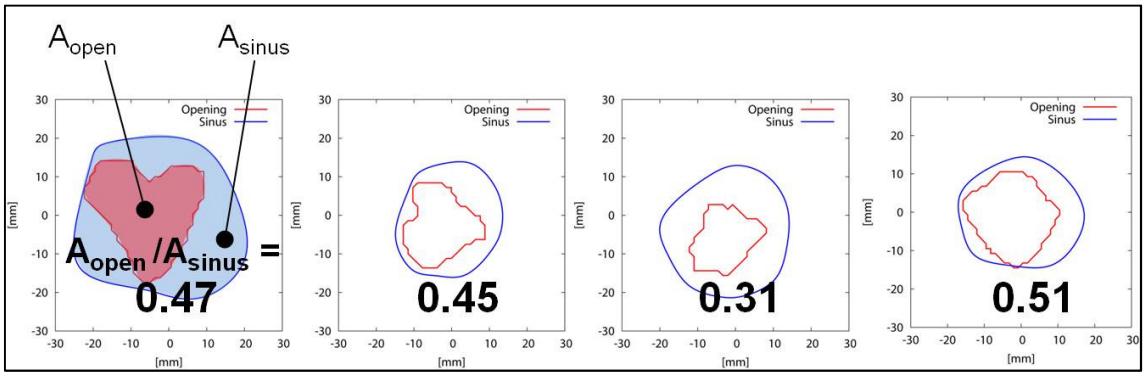

Figure 5.8 – Representative example of the relative orifice area measurement as the ratio between open aortic orifice area *(Aopen)* and the area of the mid-sinus of Valsalva *(Asinus).*

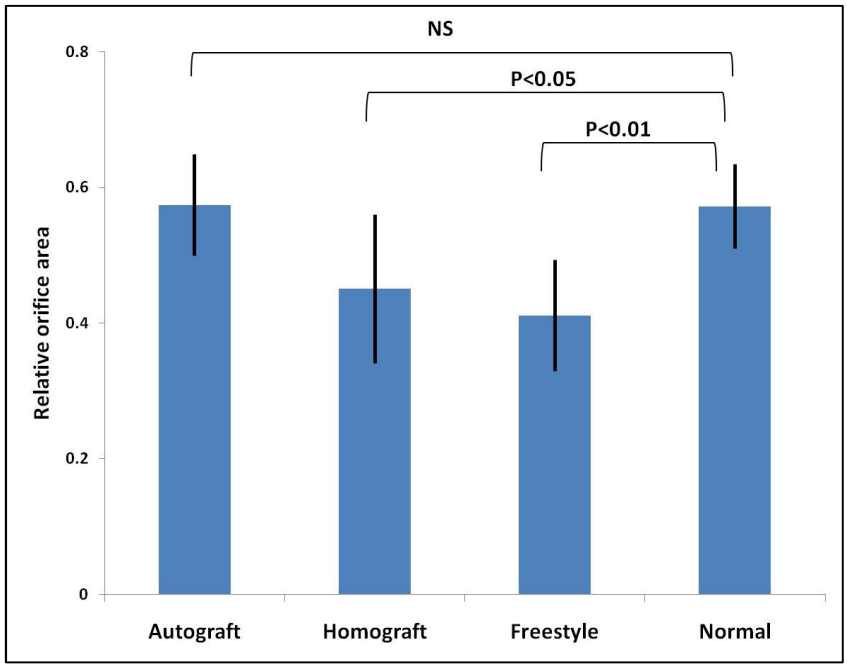

Figure 5.9 – Relative orifice area following autograft, homograft or xenograft (Freestyle) aortic root replacement, compared to normal individuals. The figure shows no differences between the autograft and normal groups, whereas the homograft and xenograft groups have significantly lower relative orifice areas.

In addition, the shape profiles of blood flow through the aortic valve and root were compared between all 4 groups. As shown in Figure 5.10, the shape of flow through the aortic valve in the autograft most closely reproduced the normal triangular shape when exiting the left ventricular outflow tract. In contrast, in the homograft and xenograft groups, the shape of the outflowing blood was more circular, suggesting less optimal movements of the aortic cusps in both groups.

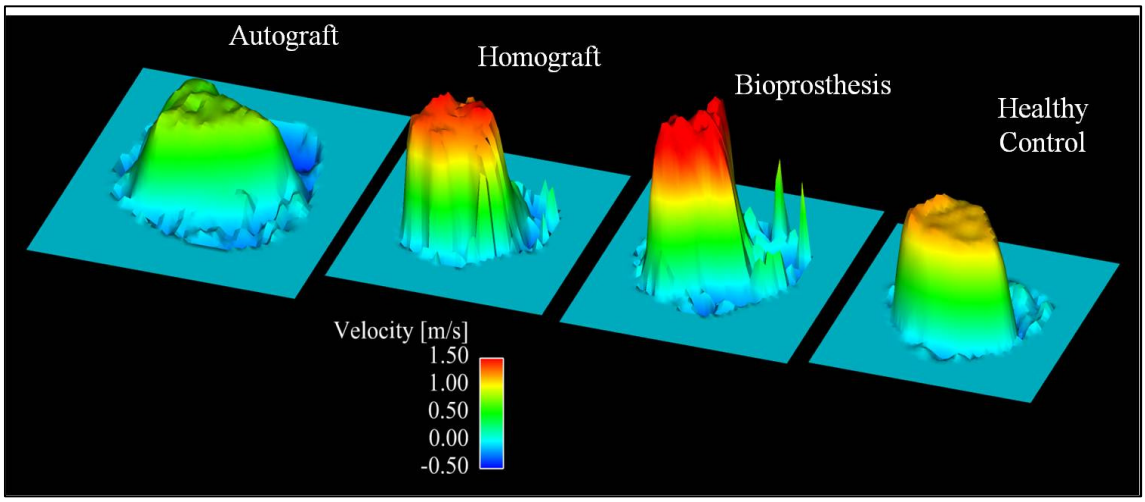

Figure 5.10 – Shape and velocity of aortic flow across the aortic root following autograft, homograft and xenograft aortic root replacement, compared to healthy controls. Autograft root replacement best reproduces normal aortic root flow dynamics both in terms of shape and velocity.

Blood flow velocity profiles were also compared between the different groups. Individual velocity profiles across the cardiac cycle in all 4 groups are presented in Figure 5.11. Interestingly, flow profiles in the autograft group show negative flow velocities in early diastole, reflecting the presence of recirculating flow in the sinuses, an important contributor to coronary blood flow. Negative blood flow could also be a result of aortic regurgitation. However, 3-dimensional cine reconstructions of aortic root flow patterns demonstrates the backward flow in the periphery, rather than in the center of the root, as would be expected in the presence of central aortic regurgitation.

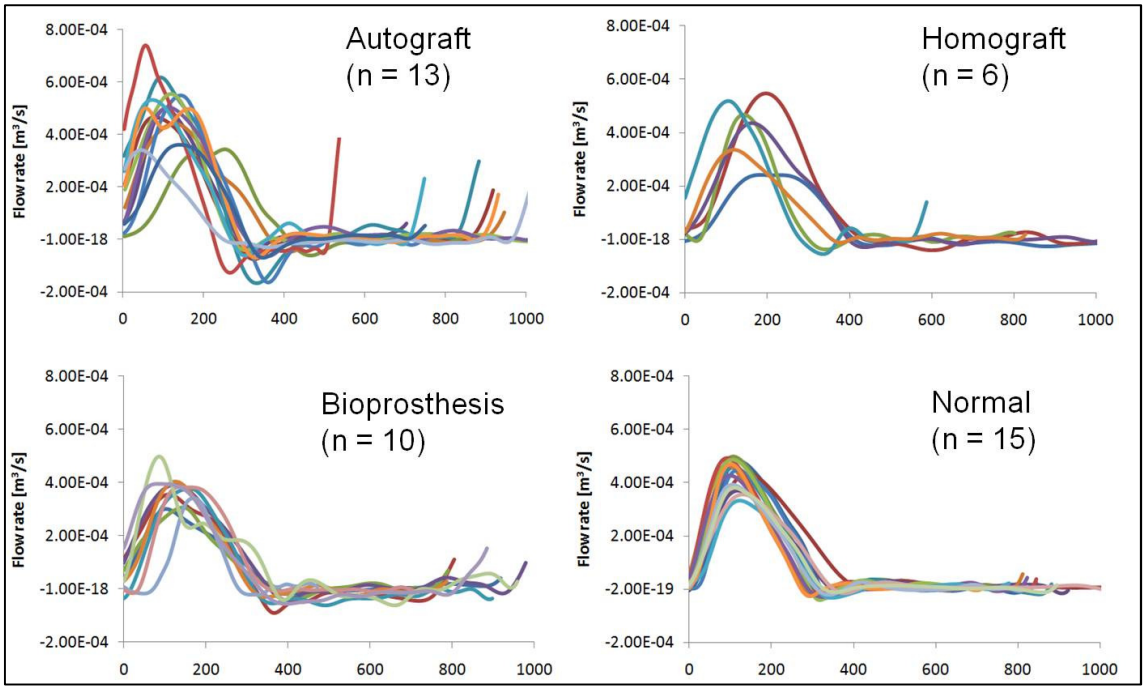

Figure 5.11 – Individual variability in flow velocity profiles across the cardiac cycle in the 4 study groups. Notice the negative flow rate in early diastole in the autograft group, indicating the presence of recirculating flow in the sinuses of Valsalva.

Comparison of the maximum velocity profiles in the 4 groups shows no differences between the autograft group and normal individuals. Similarly, there were no statistical differences between the homograft group and normal individuals, although this might be due to the small number of patients in the homograft group, as there was a clear trend towards higher velocities in the homograft group. In contrast, velocities following xenograft root replacement were significantly higher than in normal individuals as shown in Figure 5.12.

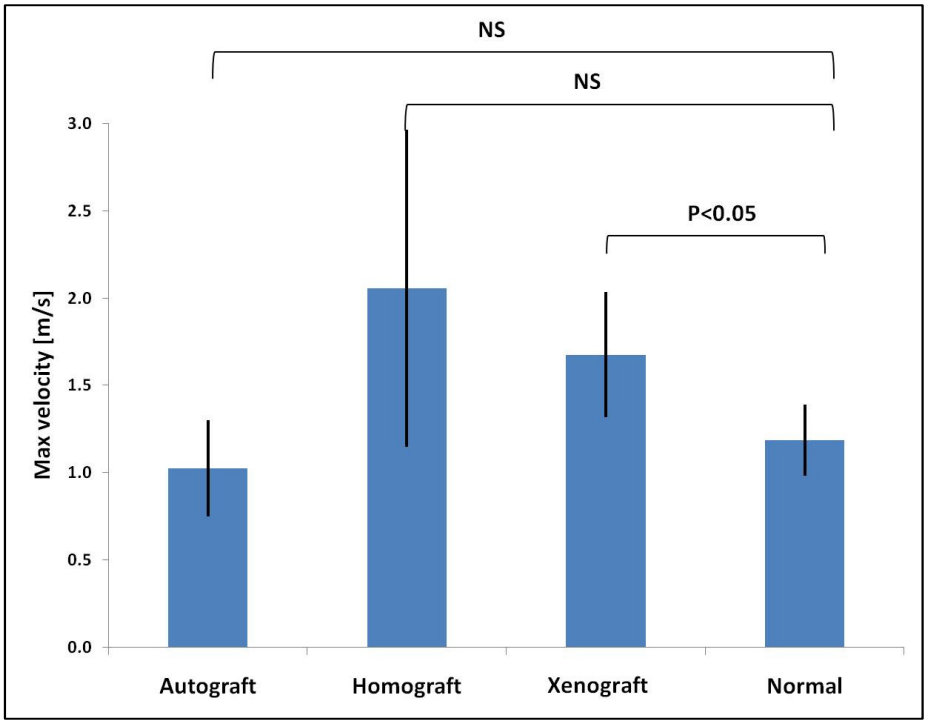

Figure 5.12 – Comparison of mean maximum flow velocity in the 4 study groups. Maximum flow velocity was significantly higher in the xenograft roots compared to normal individuals. Although homografts showed higher velocities, these were not statistically significant. There were no differences between the autograft and normal individuals.

Figure 5.13 shows a representative sagittal view through the aortic root of flow shape and velocity in the 4 different groups, summarizing the previous findings.

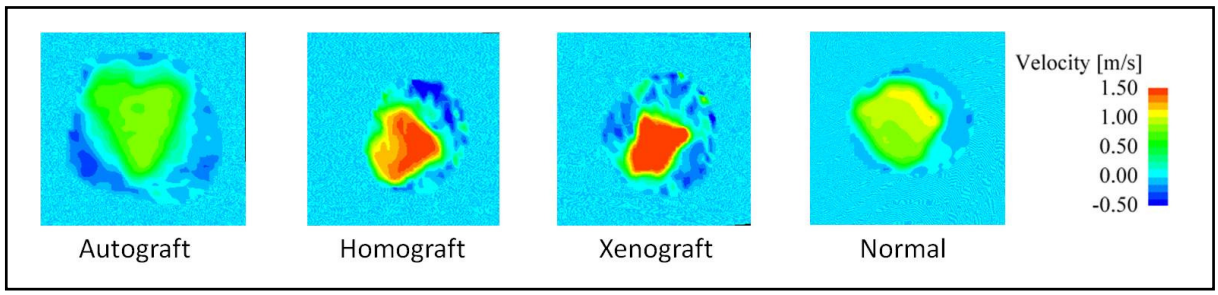

Figure 5.13 – Representative sagittal view of flow shape and velocity across the aortic valve in the 4 different groups, illustrating the triangular shape of the outflow and the low velocities in the autograft group, comparable to normal individuals. In contrast, homograft and xenograft roots show a more circular flow profile and higher velocities.

The 3-dimensional flow velocity profile across the ascending aorta was estimated using the 3-dimensional reconstruction of individual aortic geometry. The data obtained are similar to the

data already described, with lower and more homogeneous velocity profiles in the autograft group compared to the homograft and xenograft groups (Figure 5.14).

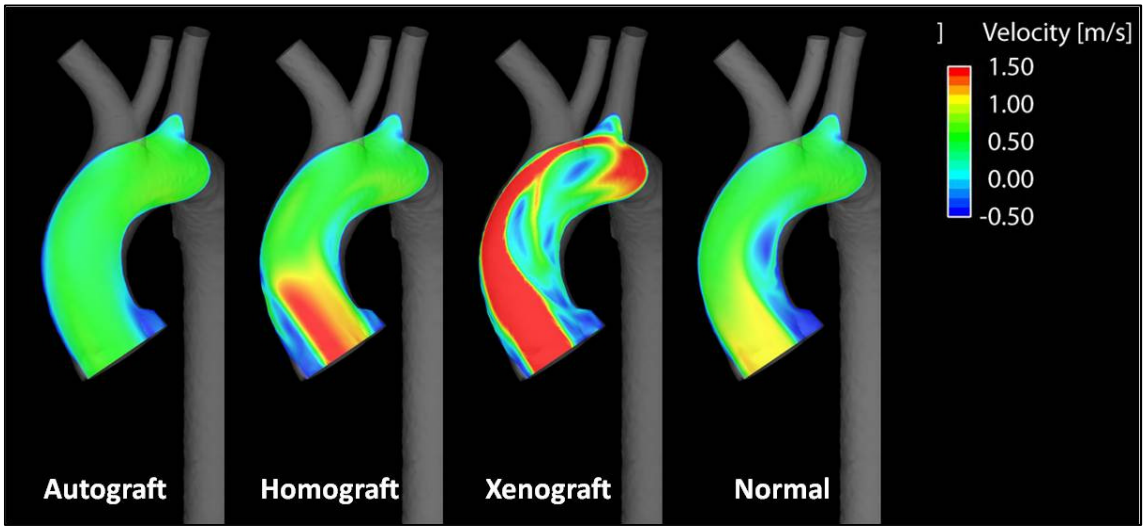

Figure 5.14 – Flow velocity profiles across the aortic root and ascending aorta in the 4 study groups. The autograft group shows more homogeneous and lower flow velocity profiles than the homograft and xenograft groups.

5.3.3.4 Endothelial Shear Stress

Endothelial wall shear stress values were estimated in the entire aorta based on the velocity profiles obtained from the MR images. Data obtained show that shear stress levels in the autograft are lower than values obtained in normal individuals. In contrast, shear stress levels were significantly higher in the xenograft group compared to healthy subjects. Homograft recipients showed areas of increased shear stress in the ascending aorta. However, the overall pattern of shear stress distribution was similar to healthy controls (Figure 5.15).

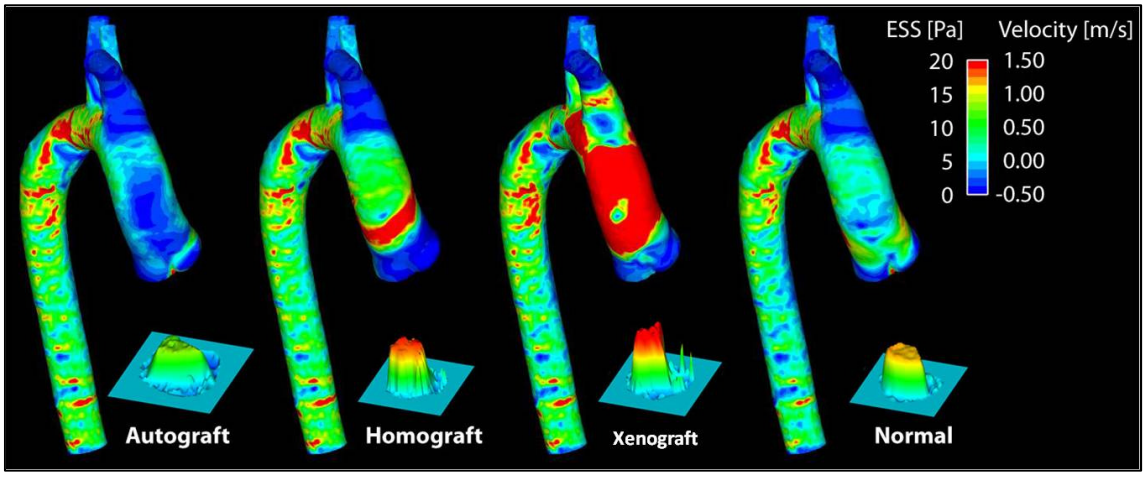

Figure 5.15 – Endothelial shear stress profiles across the aortic root and ascending aorta in the 4 study groups.

5.4 Discussion

In this chapter, we have attempted to examine the capacity of living human valves to adapt to their hemodynamic and biochemical environments. The Ross procedure represents a unique means of assessing the capacity of a living valve to adapt to its host hemodynamic environment. All other currently available surgical valve substitutes consist of non-living tissues, including homovital homografts which have been shown to become completely decellularized within weeks following implantation.

The changes observed in explanted autografts have previously been characterized as degenerative changes by some authors (Mookhoek, de Heer, Bogers, Takkenberg, & Schoof, 2010). It appears from the current data that the changes observed represent an adaptation to the hemodynamic and biochemical environment at the level of the left ventricular outflow. Indeed, in its native location, the pulmonary root is exposed to significantly lower systolic and diastolic blood pressures. The pulmonary valve cusps are exposed to lower mechanical loads (lower diastolic pressure). In addition, venous blood differs markedly from systemic blood: it has a lower oxygen content and a lower pH, it is warmer, it has lower concentrations of glucose

and other nutrients, and has higher concentrations of urea and other waste products. Nevertheless, in their native environment, pulmonary roots (cusps and wall) whose microstructural composition is very similar to aortic roots, function normally and are very rarely involved in acquired heart valve pathologies. Although most of this might be due to the "gentler" hemodynamic conditions that pulmonary valves lay in, its biochemical environment might also play a contributory role. For instance, hydroxyapatite is 1.99 times more soluble in venous blood pH than arterial blood pH which could explain the absence of calcification on the venous side.

Once exposed to systemic pressures such as in the arterial circulation, pulmonary autografts undergo a process of remodelling mainly characterized by an increase in the thickness of the ventricularis at the level of the cusps and the fibrosa at the level of the pulmonary wall. This is secondary to deposition of collagen fibers which provide mechanical strength to both the cusp and wall. Indeed, the elastic modulus of collagen is significantly higher than elastin, indicating that collagen is much stiffer than elastin. In vitro studies from our group and others have demonstrated that cyclic stretching of aortic valve interstitial cells or vascular smooth muscle cells mainly results in increased synthesis of collagen (Ku et al., 2006; Shyu, 2009). Although our policy following the Ross procedure is to ensure a tight control over patient blood pressure to maintain systolic pressure below 110mmHg, this still represents a significant increase in stretch for all of the of the root, both in systole and diastole (especially for the valve cusps). Although in the present analysis we did not observed any significant changes in the number of elastic lamellae between native aortic and pulmonary roots and autograft roots, this could be attributable to several elements. The specimens were not obtained from the same patients. Therefore, individual variability at various levels: genetic, developmental, epigenetic and hemodynamic could constitute significant biases. In addition, the autografts obtained also represent an important selection bias considering they originated from patients in whom a reoperation is required. As has been shown in several retrospective series, autografts have very good long-term performance (T. E. David, Woo, Armstrong, & Maganti, 2010; Elkins et

al., 2008; Kouchoukos et al., 2004; M. H. Yacoub et al., 2006). A more representative analysis would include post-mortem specimens from patients with well functioning autograft roots, though that may prove difficult. Nevertheless, in a separate study examining young and adult heart to compare the structure of aortic and pulmonary walls, Hokken et al. determined that the number of elastic lamellae in the sinus region did not differ between both trunks, both in children and in adults (Hokken, Bartelings, Bogers, & Gittenberger-de Groot, 1997). In contrast, there was a significantly larger number of lamellae in the ascending aorta (above the sinotubular junction) compared to the pulmonary artery at the same level (78 lamellae in the aorta versus 59 lamellae in the pulmonary artery). All autograft wall specimens obtained corresponded to the sinus region because all autografts are implanted as total aortic roots and only 2-3mm of supra-sinotubular junction autograft wall is left for the distal anastomosis. This could be an important contributing factor to the long-term stability of the autograft roots as will be discussed in the next chapter. Beyond the histological changes to the autograft root, the main question we tackled in this chapter was to analyze the functional impact of these adaptive changes. In conjunction with the computer engineering and imaging team at Imperial College, we were able to address this issue using advanced imaging techniques and computer simulation. Our findings show that in autografts implanted >10 years after surgery, thus representing a phase where they are fully remodelled, there are differences in the intrinsic mechanical properties of the autograft wall. This is characterized by reduced elasticity, distensibility and circumferential strain at the level of the autograft wall compared to the native aortic wall. Nevertheless, maximum wall stress in the autograft root was not statistically different from that seen in the native aortic wall (244 ± 71 kPa versus 208 ± 55kPa). In addition, these values are markedly below levels commonly thought to result in dissection or rupture of the aorta, ie ~800-900kPa (Elefteriades J., personal communication). These data represent novel insight into the mechanical behavior of autograft wall, although their clinical applicability remains yet to be determined. We are currently undertaking more studies in different patient populations in an effort to test the correlation between these intrinsic wall

biomechanics and other predictors of high-risk aortas (e.g., rapid rate of progression of root diameter and root diameter >45mm) as well as the role of biomechanics in prediciting clinical events.

In addition to the mechanical properties of the autograft, another important issue is the ability of the living autograft root to reproduce the sophisticated functions of the aortic root. One of the major functions of the aortic root is to ensure laminar and unobstructed blood flow through the aortic valve and into the aorta. This has a major impact on coronary and systemic blood flow patterns and distribution. It also constitutes a reflection of left ventricular function. Unobstructed flow translates into optimal ventricular dynamics and optimizes ventricular workload. The data obtained from the 3D phase contrast MRI studies performed on the patients suggest that the flow pattern following the Ross procedure best reproduces that of the native aortic root. Several physiological studies of aortic root dynamics over the last decades have clearly demonstrated the active participatory role of all aortic root component parts during the cardiac cycle to optimize cardiac function (Cheng, Dagum, & Miller, 2007; Dagum et al., 1999; Lansac, Lim, Shomura, Lim, Goetz et al., 2002; Lansac, Lim, Shomura, Lim, Rice et al., 2002; Lansac et al., 2005). The most prominent feature is the role of the root in anticipating events during the isovolumic contraction phase as well as in the second half of systole, where the cusps start their gentle excursion back towards a closed position, to reduce impact between shutting cusps. The pattern of flow in the autograft root showed a laminar, low-velocity, triangular-shaped flow through the aortic valve. The shape and velocity gradient of the flow was qualitatively comparable to native aortic flow. In contrast, following xenograft or homograft root replacement, both of which constitute a non-living aortic substitute, flow shape was more square- or circle-shaped, with a higher velocity of flow and more flow gradient. Importantly, there appeared to be increased vortex formation in the autograft root compared to xenograft or homograft roots, despite the fact that all 3 were implanted using a full root technique. This may be in part due to the larger autograft root diameter, but also could constitute the ability of the living sinuses to approximate normal function.

The clinical consequences of differences in aortic root flow pattern remain to be defined. However, our preliminary work examining the impact of these differences on endothelial wall shear stress levels represents an important finding. As mentioned previously, shear stress represents the most important mechanical signal to which endothelial cells respond through activation of various receptors and signalling pathways (P. F. Davies, 1995; Hahn & Schwartz, 2009; Pahakis et al., 2007; White & Frangos, 2007). Histological analysis of aortas explanted at the time of surgery from patients with bicuspid aortic valve disease (in whom flow pattern through the aortic root is different from normal tricuspid valves) show spatial differences at the cellular and extracellular matrix levels (Cotrufo et al., 2005; Della Corte et al., 2008). In addition, differences in the expression pattern and levels of matrix proteins is spatially-dependent, suggesting that mechanical forces from jet orientation, as well as differences in shear stress levels along the aorta can have immediate impact into matrix metabolism, leading to structural changes such as aortic dilatation (Della Corte et al., 2006).

One of the major challenges in terms of functional imaging using MRI is imaging of coronary artery flow pattern and velocity. This is mainly due to the position of the coronaries, their small diameter and the complexity of the flow pattern through them. Various authors have repeatedly raised the importance of the sinuses of Valsalva in modulating coronary artery flow (Bellhouse, Bellhouse, & Reid, 1968; J. E. Davies et al., 2008). In fact, Leonardo da Vinci was the first to model the importance of the sinuses in redirecting flow into the coronaries. Currently, there is ongoing research to try to reproducibly obtain phase-contrast flow images in the coronaries and to validate these results. These could help explain in large part the survival benefit observed in patients following the Ross procedure.

5.5 LIMITATIONS

This study has several limitations. As mentioned earlier, histological examination of explanted autograft roots inevitably bears a selection bias since these roots are always removed for dysfunction or dilatation. Nevertheless, this provides insight into the adaptive mechanisms of autograft roots. The imaging studies comparing different aortic root replacement procedures comprised patients that varied in age. Autograft recipients were significantly younger than homograft and xenograft recipients. Healthy individuals were themselves younger than autograft recipients. It is an established fact that the mechanical properties of the tissues change with increasing age, therefore this could have an impact on the observed flow patterns. Nevertheless, besides their age, all patients were similar in terms of demographics, hemodynamics and echocardiographic valve function. Therefore, the observations still represent a valid look into the role of the valve substitute itself on flow through the aortic root.

5.6 Conclusions and Future Directions

In conclusion, living heart valves are capable of adaptation in response to changes in their hemodynamic and biochemical environment, which reflects the dynamic nature of heart valves. Adaptation of heart valves is illustrated by the changes in the structure of pulmonary roots implanted in the aortic position (Ross procedure). These roots undergo structural changes as a result of activation of different mechanotransduction pathways. Although the autograft root differs from the native aortic root in its intrinsic mechanical properties, its adaptation translates into wall stress levels remarkably close to the native aorta. In addition to the mechanical adaptation, viability of the aortic root apparatus appears to have a direct impact on aortic flow pattern, a major determinant of coronary and systemic flow. Combined, these different elements are thought to translate into clinically relevant outcomes as will be seen in the following chapter. In addition, these studies underline the importance of having living heart valve substitutes capable of reproducing the sophisticated functions of the native valve. In the

future, continued work aimed at developing a tissue-engineered living heart valve remains the ultimate objective. In the immediate future, ongoing work is currently underway to examine patients with moderately dilated aortic roots following the Ross procedure, in order to evaluate the clinical sensitivity of in vivo assessment of aortic wall biomechanics in clinical decision-making. Furthermore, we are currently comparing patterns of flow through the aortic root following stented aortic valve replacement versus stentless aortic root replacement to evaluate the role of maintaining the structural unity of the aortic root on flow dynamics.

VI Clinical Implications of a Living Aortic Valve

6.1 BACKGROUND

Aortic valve replacement has been shown to improve the natural history of severe symptomatic aortic valve disease(Iivanainen, Lindroos, Tilvis, Heikkilä, & Kupari, 1996; Ross & Braunwald, 1968). The degree of improvement depends, at least in part, on the type of aortic valve substitute. However, to date, there are very few randomized trials comparing different surgical options with regards to survival and quality of life. Recent work has shown that the aortic valve performs several sophisticated functions which depend on its viability(Dagum et al., 1999; El-Hamamsy, Balachandran et al., 2009; M. Yacoub & Nerem, 2007). The Ross operation is the only operation which provides continued long-term viability of the valve tissue. We hypothesized that the regulatory and adaptive properties of a living substitute can translate into improved long-term patient outcomes.

6.1.1 Aims

The aims of this prospective randomized trial were to evaluate late outcomes following Autograft (Ross procedure) versus Homograft aortic root replacement.

6.2 METHODS

6.2.1 Study Population

From 1994 to 2001, 228 patients undergoing aortic root replacement were randomly assigned to receive a Homograft or an Autograft (Ross procedure). All patients with aortic valve disease requiring surgery were considered. Exclusion criteria were the presence of Marfan syndrome, rheumatoid arthritis, Reiter's syndrome and age >69 years. Patients presenting with bicuspid aortic valve disease, active endocarditis, rheumatic heart disease, ascending aortic aneurysms,

decreased ejection fraction or emergent surgery were not excluded from the study. In the initial study period, children <18 years were included (n=12). Due to early homograft failure in 2 of those patients, all patients <18 years of age were excluded from the trial. The present analysis therefore includes 216 adult patients (n=108 in each group; Figure 6.1). Sample size was calculated based on an estimated survival following homograft root replacement of 80% at 10 years (Lund et al., 1999), a population survival of 97% at 10 years (ONS) and the assumption that the Ross procedure would restore population survival. A total of 85 patients in each group would be needed to show a 15% survival difference at 10 years, with $\alpha<0.05$, $\beta>0.80$ and a dropout rate of 10%. The primary endpoint was long-term survival. Secondary endpoints were freedom from reoperation, valve-related morbidity, quality of life and changes in valvular and ventricular function determined echocardiographically. Approval for the study was obtained from the local ethics committee and all patients gave written informed consent to the study before enrolment.

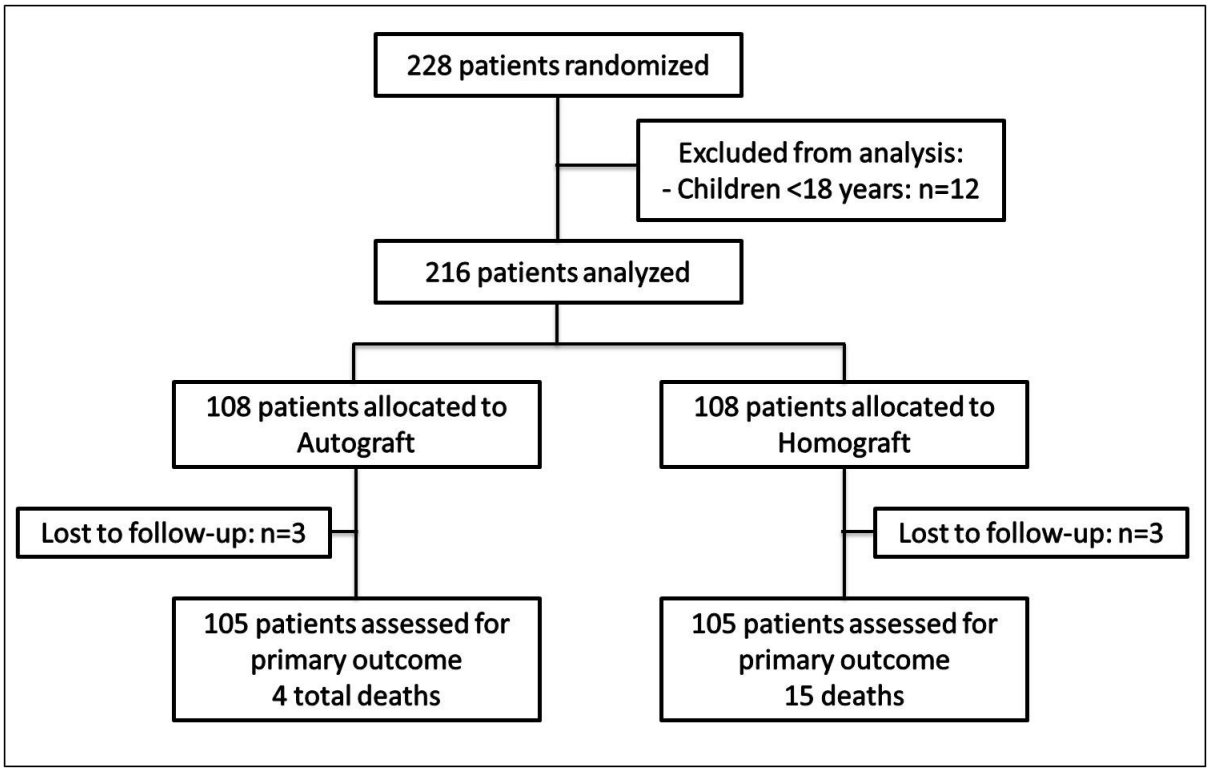

Figure 6.1 Trial profile

6.2.2 Surgical Technique

All procedures were performed by a single surgeon (MY) using the same technique over the study period. Total aortic root replacement was performed in all patients. For autograft root replacement, the pulmonary root was harvested in a scalloped fashion, leaving 1-2mm below the attachment of the cusps. The proximal aortic anastomosis was performed using close interrupted sutures. The left-facing sinus was positioned in the left coronary sinus and the autograft was placed in an intra-annular position to provide external fibrous support to the muscular pulmonary root. The coronary ostia were anastomosed to their respective sinuses. The distal anastomosis was performed 2-3mm above the level of the commissures to reduce the risk of autograft dilatation. No foreign material was used to support the proximal or distal anastomoses. A pulmonary homograft was placed in the pulmonary position using the largest available size. Strict blood pressure control (systolic blood pressure <110mmHg) was maintained perioperatively and for the first 6 months, to allow adaptive remodelling of the autograft. For patients undergoing homograft aortic root replacement, a standard previously described technique was performed (M. Yacoub et al., 1995).

6.2.3 Clinical Follow-up

Follow-up was actively conducted on a yearly basis and consisted of outpatient appointments, patient call-ups or contact with the patient's family physician. Mean duration of clinical follow-up was 10.2±3.2 years (total: 2173 patient-years) and was 97% complete within 12 months of study closure. Indications for reintervention were symptomatic valve dysfunction (moderate or severe) and/or progressive ventricular dilatation. Perioperative death was defined as hospital mortality or death <30 days after operation.

6.2.4 Echocardiographic Follow-up

Serial echocardiographic examinations were performed. These studies were performed every 2 years if patients were asymptomatic and last echocardiography showed no signs of valvular or ventricular dysfunction, and more frequently in the remaining patients. Completeness of echocardiographic follow-up was 80% within 24 months of study closure. A total of 1505 complete echocardiographic examinations were analyzed to produce mixed effect models of aortic valve function, ventricular dimensions and function and aortic sinus diameter. Aortic regurgitation was quantified by measuring the ratio of the maximal regurgitant jet diameter to the systolic left ventricular outflow tract diameter directly under the aortic valve in the parasternal long-axis view (jet diameter ratio) (Perry, Helmcke, Nanda, Byard, & Soto, 1987).

6.2.5 Quality of Life Assessment

Short-Form 36 Health Survey Questionnaires (SF-36) were used to assess patients' quality of life (Annex 1). Questionnaires were sent to all living patients between September and December 2008. Questionnaires were resent to non-responders. Response rate was 75% in the Autograft group (76/102 eligible patients) and 71% in the Homograft group (64/90 eligible patients) at a mean 11±2 years after surgery.

6.2.6 Statistical Analysis

Data are expressed as mean ± standard deviation for continuous variables and analyzed using Student's t-test. Categorical variables are expressed as a number (percentage) and compared using Fisher's exact test. Survival analyses were performed using the Kaplan-Meier method and the log-rank test was used to compare curves. Kaplan-Meier survival estimates were compared to survival of the general population matched for age, gender and year of surgery using 1996-1998 to 2005-2007 United Kingdom interim lifetables (ONS). Variables with a $P<0.2$ in the

univariable analyses were considered in the multivariate analyses. The effect of each variable was assumed to be constant over time. A stepwise backward elimination process was used and as for all other analyses, variables with a $P<0.05$ were considered statistically significant. Mixed effects models were used to assess changes in echocardiographic measures over time and account for the correlation between repeated follow-up measurements (the MIXED and NLMIXED procedures in SAS software, version 9.1; SAS Institute, Cary, NC). Fully parameterized mixed effect models were built including a coefficient for each time point for each group (baseline preoperatively "B", postoperatively prior to discharge "A", and yearly thereafter). Since most patients underwent echocardiography every 2 years, piecewise linear random effect models using time as a continuous measure were constructed with time knots at 1 month, 1 year and every 2 years. For aortic regurgitation grade, piecewise multinomial ordinal random effect model was performed using the same time knots. Between-group differences as well as changes over time were assessed. For patients with missing echocardiographic measurements at a given time point, the outcome data were considered to be missing at random.

SF-36 scores for all 8 domains were normalized using the Oxford Healthy Life Survey UK population estimates(Jenkinson, Coulter, & Wright, 1993) with a mean at 50 and a standard deviation at 10. Physical Component Scores (which correlate with 6 of the 8 domains) and Mental Component Scores (which correlate with 5 of the 8 domains) were computed using UK corrected weights (Jenkinson et al., 1993). Scores were expressed as median and interquartile range and group differences assessed using the Wilcoxon signed-rank test.

6.3 RESULTS

6.3.1 Patient Characteristics

Mean age of the patients was 39±13 years in the Autograft group versus 41±13 years in the Homograft group (P=0.312; Table 6.1). Active endocarditis was the indication in 8% of the patients in each group (P=0.816); and 42% of Autografts and 44% of Homografts had undergone prior surgery (P=0.784).

Table 6.1 Patient characteristics

Variable	Homograft (n=108)	Autograft (n=108)	P-value
Age	41 ± 13	39 ± 13	0.312
18-34	46 (43%)	47 (44%)	
35-49	28 (26%)	39 (36%)	
50-59	24 (22%)	13 (12%)	
≥60	10 (9%)	9 (8%)	
Sex (% male)	89 (82%)	92 (85%)	0.712
BSA (m^2)	1.9 ± 0.2	1.9 ± 0.2	0.823
Smoking			0.193
Current	23 (21%)	18 (17%)	
Previous	26 (24%)	18 (17%)	
No	59 (55%)	72 (66%)	
Comorbidities			
Hypertension	29 (29%)	21 (20%)	0.193
Dyslipidemia	4 (4%)	3 (3%)	0.717
Diabetes	2 (2%)	1 (1%)	0.616
Renal failure*	7 (8%)	6 (6%)	0.776
Preoperative AR			0.248
0	14 (13%)	8 (7%)	
1	5 (5%)	1 (1%)	
2	16 (15%)	21 (19%)	
3	28 (26%)	34 (31%)	

4	44 (42%)	44 (41%)	
Preoperative AR grade 3-4	72 (67%)	78 (72%)	0.460
Surgical Indication			0.652
Primary isolated AS	35 (32%)	30 (28%)	
Primary isolated AR	46 (43%)	49 (45%)	
Mixed AS/AR	27 (25%)	29 (27%)	
Thoracic Aortic Aneurysm	1 (1%)	2 (2%)	
Etiology			>0.99
Degenerative	48 (44%)	48 (44%)	
Congenital	54 (50%)	53 (49%)	
Rheumatic	6 (6%)	7 (6%)	
Endocarditis			0.816
None	86 (80%)	89 (83%)	
Active	9 (8%)	9 (8%)	
Treated	13 (12%)	10 (9%)	
Previous Intervention‡ (%)	48 (44%)	45 (42%)	0.784
Homograft	31	22	
Mechanical/Tissue prosthesis	11	12	
Aortic valve repair	8	11	
Coarctation repair	2	8	
NYHA			0.206
I	22 (20%)	33 (31%)	
II	48 (45%)	49 (45%)	
III	29 (27%)	21 (19%)	
IV	9 (8%)	5 (5%)	
Heart Rhythm			0.144
Sinus rhythm	101 (94%)	103 (95%)	
Atrial fibrillation	5 (5%)	1 (1%)	
Pacemaker	1 (1%)	4 (4%)	
Type of Operation			0.488
Emergent	8 (7%)	5 (5%)	
Urgent	8 (7%)	5 (5%)	
Elective	92 (85%)	98 (91%)	

6.3.2 Operative Results

There was one perioperative death in the Autograft group (0.9%) and 3 in the Homograft group (2.8%; P=0.621) (Table 6.2). Three of the 4 perioperative mortalities were due to low output syndromes in patients operated for acute infectious endocarditis. The fourth patient had undergone successful homograft root replacement and died suddenly at home on postoperative day 6. Post-mortem examination revealed no valvular dysfunction, but severe left ventricular hypertrophy and intramyocardial fibrosis.

Table 6.2 Operative data and results

Variable	Homograft (n=108)	Autograft (n=108)	P-value
Perioperative Deaths†	3 (2.8%)	1 (0.9%)	0.621
Concomitant Procedures			
CABG	3 (3%)	2 (2%)	>.999
Mitral valve	4 (4%)	5 (5%)	>.999
Bypass time (min)	117 ± 49	163 ± 37	<0.001
Ischemic time (min)	85 ± 23	110 ± 21	<0.001
Cardioplegia			>.999
Blood	41 (38%)	42 (39%)	
Crystalloid	67 (62%)	66 (61%)	
Aortic Homograft			
Homovital	36 (33%)		
Antibiotic sterilized	41 (38%)		
Cryopreserved	32 (30%)		
Inotropes			0.961
<24 h	68 (63%)	69 (64%)	
24-48 h	23 (21%)	21 (19%)	
>48 h	17 (16%)	18 (17%)	

Ventilatory support			0.815
<24 h	93 (86%)	96 (89%)	
24-48 h	5 (5%)	4 (4%)	
>48 h	10 (9%)	8 (7%)	
Complications			
Reexploration for bleeding	4 (4%)	13 (12%)	0.041
Pacemaker	2 (2%)	2 (2%)	>.999
Atrial fibrillation	17 (16%)	17 (16%)	>.999
CVA/TIA	3 (3%)	2 (2%)	0.682
Renal failure	2 (2%)	3 (3%)	>.999
Sternal wound infection	1 (1%)	4 (4%)	0.369
ICU length of stay (d)	1 [0, 9]	1 [1, 14]	0.774
Hospital length of stay (d)	9 [0, 46]	9 [4, 44]	0.451

6.3.3 Survival

Actuarial survival in the Autograft group was 97±2% and 95± 3% at 10 and 13 years, respectively (1 early death and 3 late deaths: 1 cardiac, 1 non-cardiac and 1 unknown cause) versus 83±4% and 78±5%, respectively in the Homograft group (*P=0.002*; Figure 6.2). There were 3 early deaths and 12 late deaths in the Homograft group (2 valve-related, 3 cardiac, 4 non-cardiac and 3 of unknown cause). Autograft group survival was comparable to an age- and sex- matched UK population (Figure 6.2). On multivariate analysis, the only independent predictor of late mortality was homograft use (hazard ratio 8.64 [2.76 – 27.06]) whereas higher creatinine clearance was protective (hazard ratio 0.97 [0.96 – 0.99]).

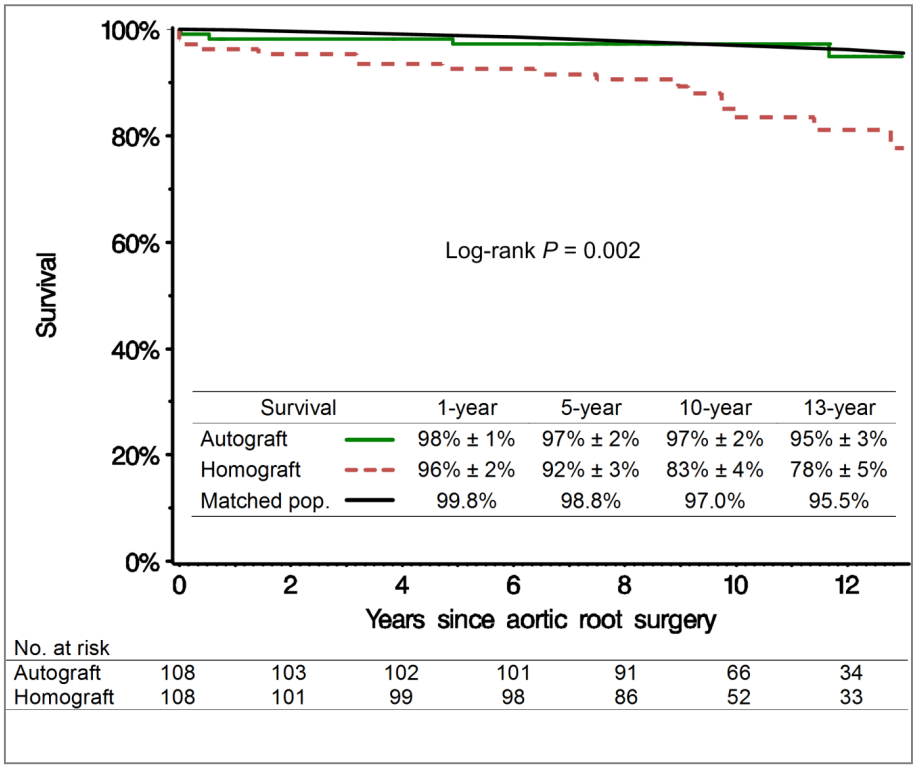

Figure 6.2 Actuarial survival following Autograft *(green)* versus Homograft *(red)* aortic root replacement *(P=0.002).*

6.3.4 Freedom from Reoperation

One patient in the Autograft group who had undergone surgery for prosthetic valve dysfunction required pulmonary autograft reoperation 9.5 years after surgery. The indication was mild autograft dilatation (44mm) with moderate aortic regurgitation and progressive left ventricular enlargement. Overall, actuarial freedom from aortic valve reoperation in the Autograft group was 99±1% at 13 years (Figure 6.3).

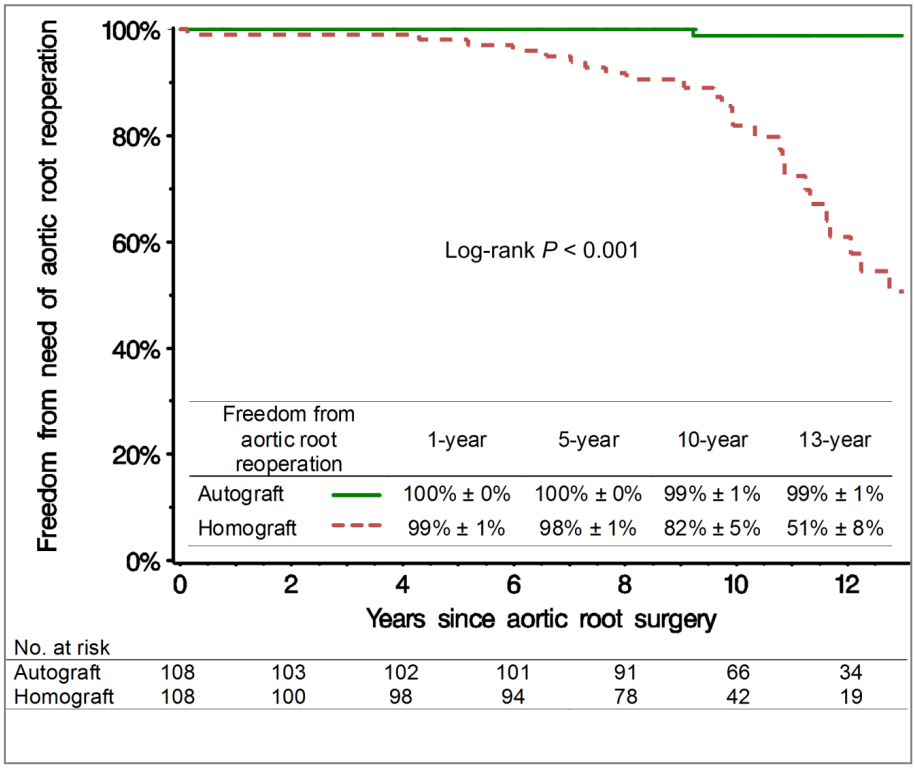

Figure 6.3 Actuarial freedom from aortic valve reoperation for patients following Autograft *(green)* versus Homograft *(red)* aortic root replacement *(P<0.001).*

In addition, there were 8 pulmonary homograft reoperations in 7 patients due to stenosis (n=6) and endocarditis (n=2). Four of the 8 pulmonary reoperations (50%) occurred within the first 18 months after surgery. Freedom from pulmonary homograft reoperation in the Autograft group was 95±2% and 94±3% at 10 and 13 years, respectively (Figure 6.4). Overall freedom from any reoperation in the Autograft group was 95±2% and 94±3% at 10 and 13 years, respectively (Figure 6.5).

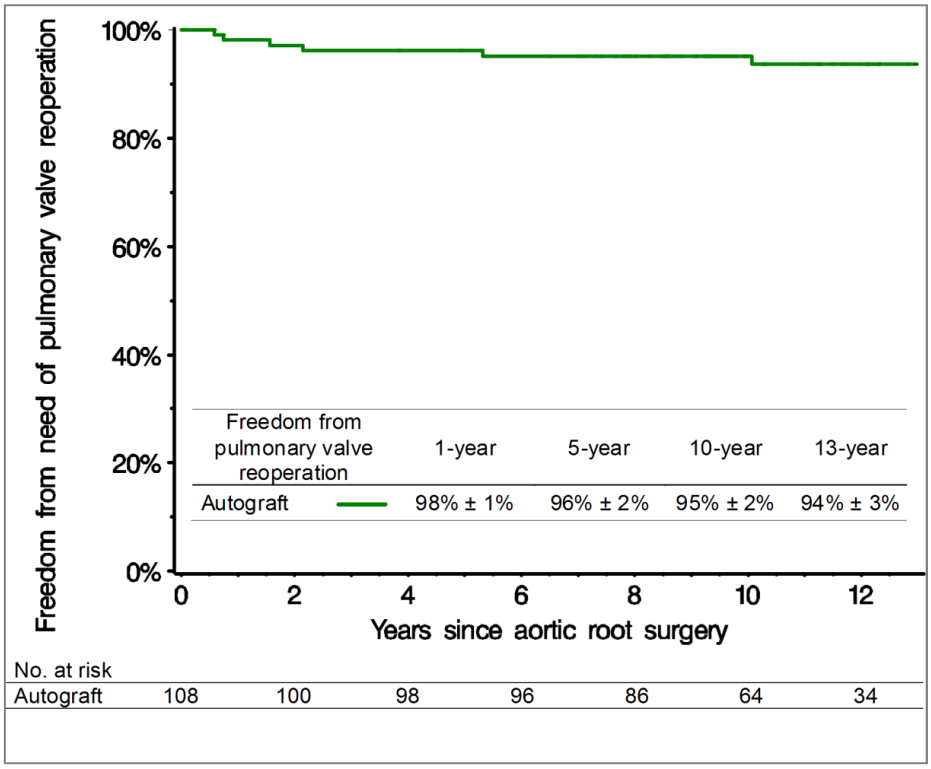

Figure 6.4 Actuarial freedom from pulmonary homograft reoperation in patients undergoing the Ross procedure.

Figure 6.5 Actuarial freedom from any valve reoperation following Autograft *(green)* versus Homograft *(red)* aortic root replacement *(P<0.001).*

In contrast, actuarial freedom from reoperation in the Homograft group was 82±5% and 51±8% at 10and 13 years, respectively (*P<0.001* versus all Autograft reoperations). Of the 27 total reoperations in the Homograft group, 18 were due to structural valve deterioration and 9 were due to infective endocarditis. Use of a homograft was an independent predictor of the need for reoperation on multivariate analysis (hazard ratio 5.69 [2.46 – 13.15]), whereas older age at surgery was a negative predictor (hazard ratio 0.74 [0.57 – 0.97]).

6.3.5 Long-Term Morbidity

There were no cases of aortic endocarditis and 2 late cases of pulmonary homograft endocarditis in the Autograft group. In contrast, 9 cases of infective endocarditis occurred in the Homograft group at a median time of 10 years after surgery (range 2 – 12 years). Actuarial freedom from all endocarditis was 98±1% and 97±2% in the Autograft group at 10 and 13 years, respectively versus 94±3% and 82±6% in the Homograft group (P=0.002) (Figure 6.6).

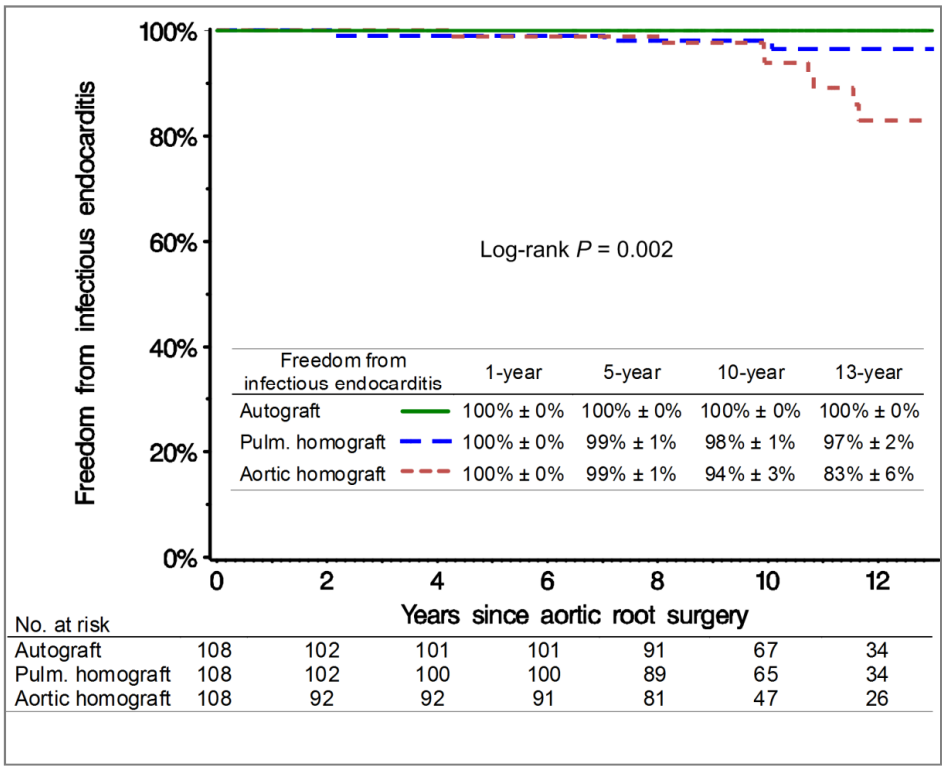

Figure 6.6 Actuarial freedom from endocarditis following Autograft (*green*=aortic valve and *blue*=pulmonary valve) and Homograft (*red*) aortic root replacement (*P=0.002*).

One patient in the Autograft group (59 years old) suffered a stroke 4 years after surgery versus 3 patients in the Homograft group at 2, 10 and 11 years after surgery *(*Figure 6.7*)*.

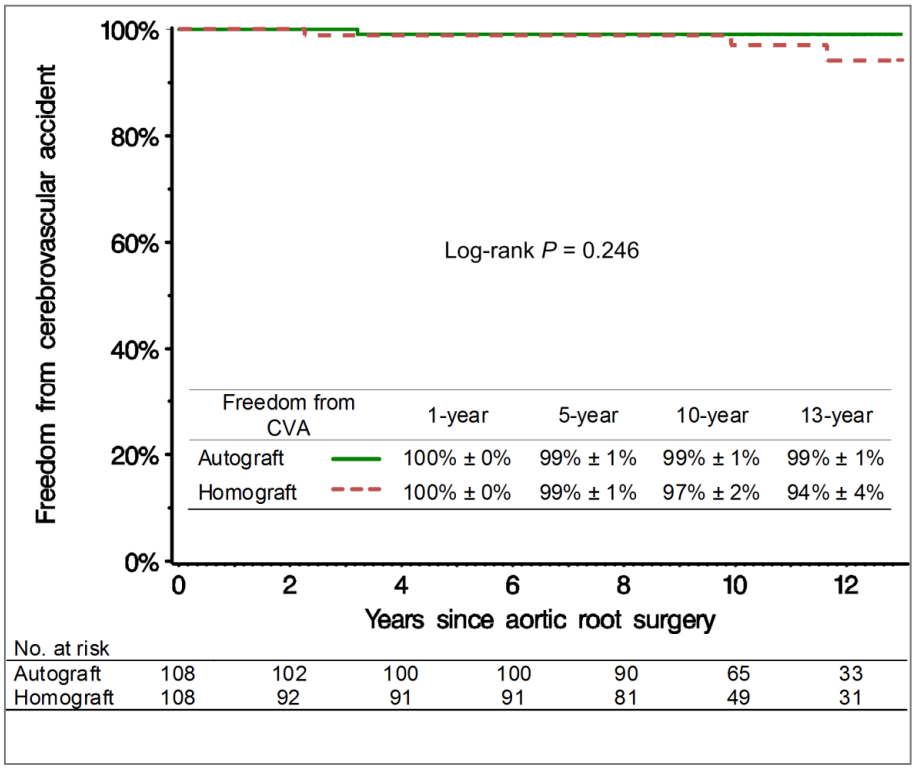

Figure 6.7 Actuarial freedom from cerebrovascular accident following Autograft *(green)* versus Homograft *(red)* aortic root replacement (*P=0.246*).

One of those cases occurred in the perioperative period following redo surgery for homograft endocarditis. No cases of bleeding or thrombosis were reported in both groups. Overall, freedom from the composite endpoint of endocarditis, stroke, bleeding or thrombosis was 97±2% and 96±2% in the Autograft group at 10 and 13 years, respectively versus 93±3% and 82±6% in the Homograft group (P=0.075; Figure 6.8).

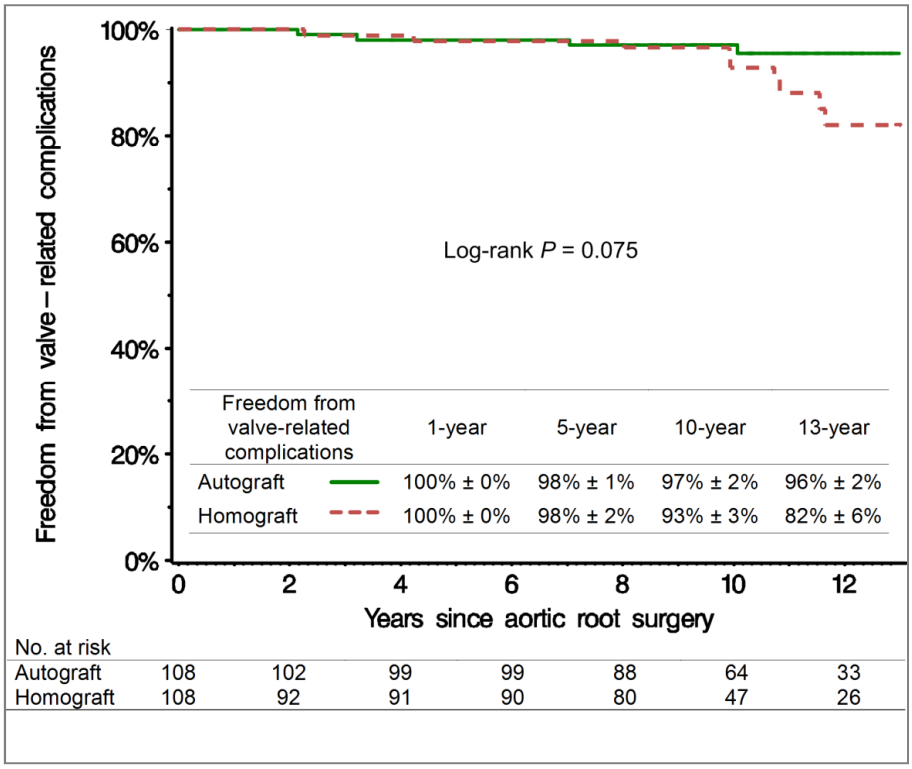

Figure 6.8 Actuarial freedom from the composite endpoint of endocarditis, cerebrovascular accident, bleeding or thrombosis following Autograft *(green)* versus Homograft *(red)* aortic root replacement (*P=0.075*).

6.3.6 Echocardiographic Data

6.3.6.1 Aortic and Pulmonary Valve Function

Using mixed effect models, Figure 6.9a shows no change in trans-aortic gradients in the Autograft group up to 13 years after surgery (gradients <10mmHg) versus a steady increase in the Homograft group (*P<0.001*). Figure 6.9b shows time-related changes in aortic regurgitation in the two groups. Overall, actuarial freedom from aortic regurgitation grade 3-4 is 94±3% in the Autograft group versus 82±5% in the Homograft group at 10 years (*P=0.029*). Figure 6.9c depicts the progression of echocardiographically measured transpulmonary gradients across the pulmonary homograft in the Autograft group with a mean value of 25±5mmHg at 13 years.

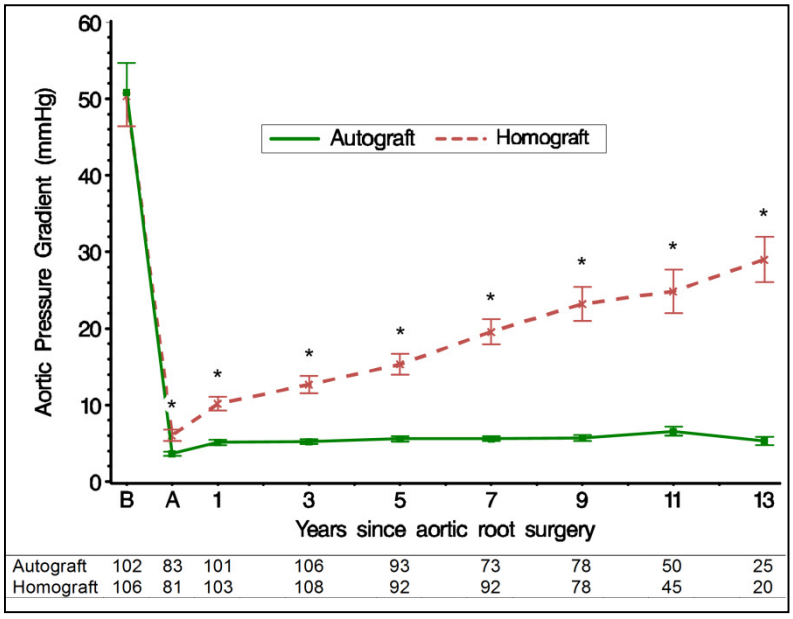

Figure 6.9a Mixed effect models of echocardiographic parameters following Autograft *(green)* versus Homograft *(red)* aortic root replacement looking at the progression of trans-aortic gradients.
**P<0.05 between groups at each given time point.*
B, Preoperative measure; A, 1 month after surgery.

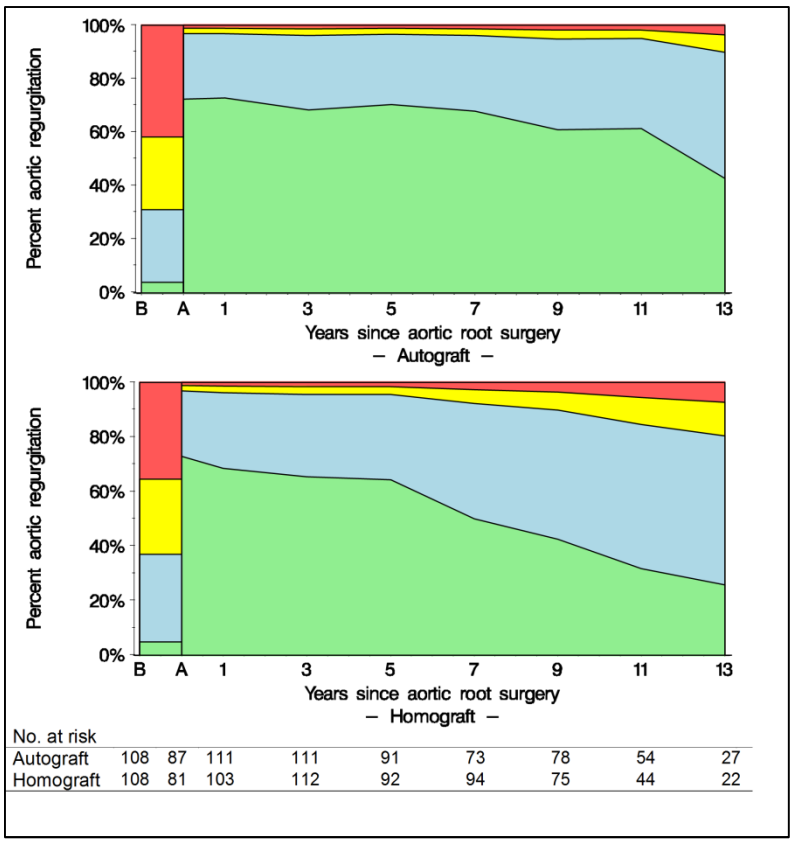

Figure 6.9b Mixed effect models of echocardiographic parameters following Autograft *(upper)* versus Homograft *(lower)* aortic root replacement looking at the progression of aortic regurgitation *(green, grade 1+; blue, grade 2+; yellow, grade 3+; red, grade 4+)*.
**P<0.05 between groups at each given time point.*
B, Preoperative measure; A, 1 month after surgery.

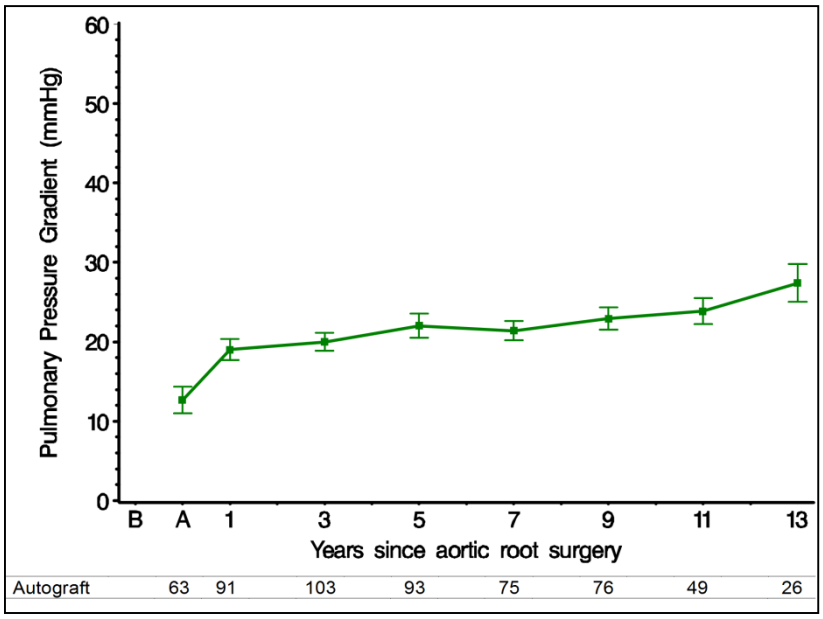

Figure 6.9c Mixed effect models of the progression of transpulmonary gradient by echocardiographic measurement following Autograft root replacement.
B, Preoperative measure; A, 1 month after surgery.

6.3.6.2 Ventricular Function

In both groups, left ventricular end-systolic and end-diastolic dimensions significantly decreased after surgery and remained relatively stable thereafter. No differences were observed between both groups (Figure 10a). Similarly, there was a marked improvement in left ventricular ejection fraction up to 3 years after surgery in both groups which remained stable up to 10 years, followed by a slight decrease (*P=0.047* for change in time for both groups; Figure 10b).

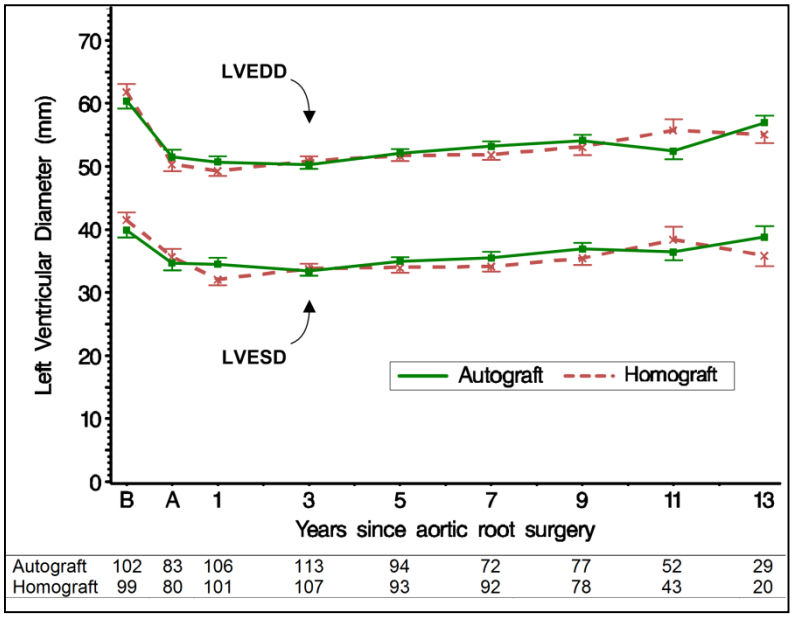

Figure 6.10a Mixed effect models of the echocardiographic changes in left ventricular end-diastolic and end-systolic diameters following Autograft *(green)* versus Homograft *(red)* aortic root replacement.
**P<0.05 between groups at each given time point.*
B, Preoperative measure; A, 1 month after surgery; LVEDD, left ventricular end-diastolic diameter; LVESD, left ventricular end-systolic diameter.

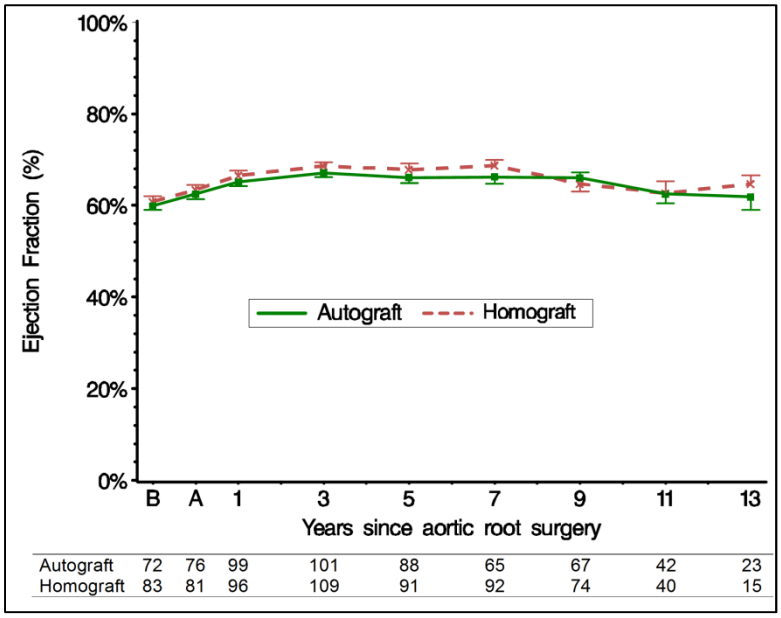

Figure 6.10b Mixed effect models of the echocardiographic changes in ejection fraction following Autograft *(green)* versus Homograft *(red)* aortic root replacement.
**P<0.05 between groups at each given time point.*
B, Preoperative measure; A, 1 month after surgery

6.3.6.3 Autograft Root Dimensions

Figure 6.11 represents changes in echocardiographic aortic root dimensions up to 13 years following surgery. From the outset, autograft roots are slightly larger than homograft roots (*P=0.004*). However, in each group, the diameter remained stable and showed no statistically significant change up to 13 years after surgery (P=0.463 for autografts).

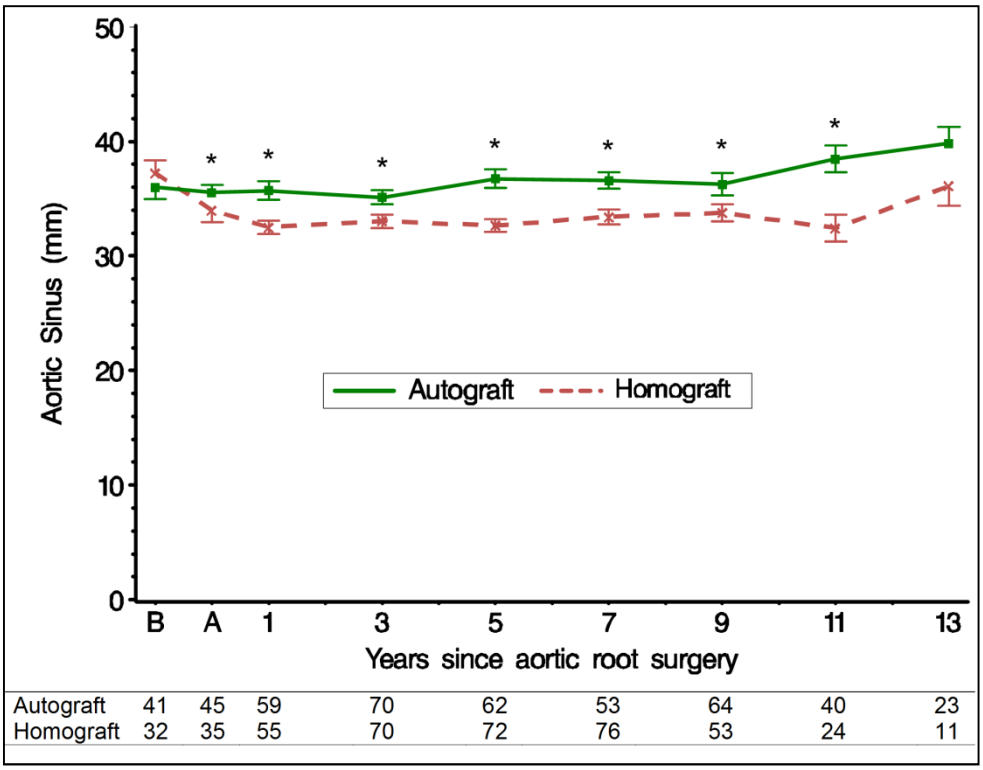

Figure 6.11 Mixed effect models of the echocardiographic changes in aortic sinus diameter following Autograft *(green)* versus Homograft *(red)* aortic root replacement.
**P<0.05 between groups at each given time point.*
B, Preoperative measure; A, 1 month after surgery.

6.3.7 Quality of Life Assessment

Data consistency measured by Cronback's α was >0.8 (range: 0.81-0.93) on all domains, indicating high reliability of the questionnaire. Autograft recipients registered significantly higher scores than Homografts in the physical functioning (51.0 [45.9-56.1] versus 48.5 [38.3-

56.1]; *P=0.041*) and general health domains (51.9 [43.1-55.4] versus 48.0 [35.8-52.9]; *P=0.019,* respectively) (Figure 6.12). This resulted in a significantly higher Physical Component Score in the Autograft compared to the Homograft group (53.5[47.3-56.5] versus 49.1[33.9-54.8]; *P=0.018*).

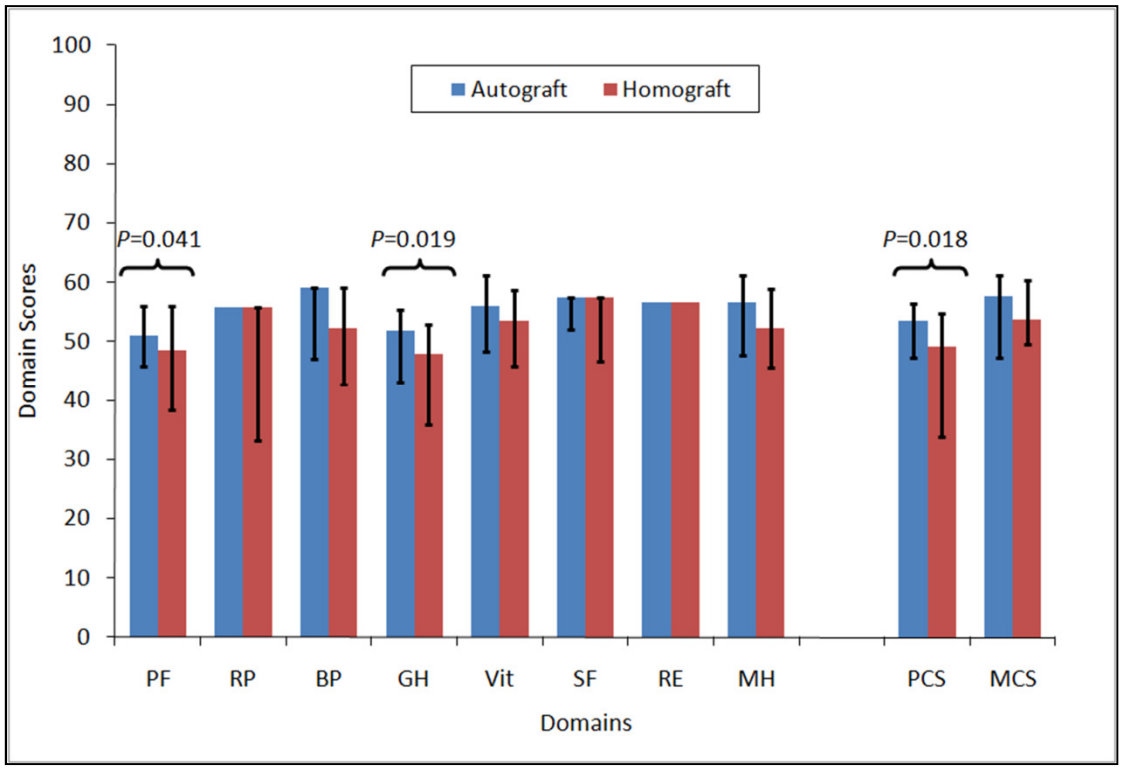

Figure 6.12 Overall results from the SF-36 questionnaire performed on patients following Autograft *(blue)* versus Homograft *(red)* aortic root replacement.
PF, physical functioning; RP, role physical; BP, body pain; GH, general health; Vit, vitality; SF, social functioning; RE, role emotional; MH, mental health; PCS, physical component score; MCS, mental component score.

6.4 Discussion

With the increase in world population and improved access to health care, it is estimated that the number of aortic valve surgeries worldwide will triple within the next 30 years (M. H. Yacoub & Takkenberg, 2005). To date, surgery remains the only effective solution to alter the natural history of the disease; however survival following surgery is often inferior to the general population (Kvidal, Bergstrom, Horte, & Stahle, 2000) and appears to depend on the type of

valve substitute (Svensson, Blackstone, & Cosgrove, 2003). Randomized controlled trials represent the only definitive means of enabling rational, evidence-based decision making regarding the choice of valve substitute. Nevertheless, very few randomized studies have attempted to compare long-term outcomes after different valve replacement procedures in patients with aortic valve disease (Hammermeister et al., 2000; Stassano et al., 2009). Several observational studies have shown excellent pattern of survival after the Ross operation in adults which could have been contributed to by selection bias (Elkins et al., 2008; Sievers et al., 2006; M. H. Yacoub et al., 2006). The current study is the first to show enhanced survival after the Ross procedure in a randomized trial compared to homografts. Survival following the Ross operation was comparable to the general population. The study cohort included patients with endocarditis, poor ventricular function and redo surgery.

The choice of the 2 valve substitutes in this study stems from the fact that both offer excellent hemodynamic function and do not require anticoagulation, with homografts having a long track record (Lund et al., 1999; M. F. O'Brien et al., 2001; Smedira, Blackstone, Roselli, Laffey, & Cosgrove, 2006). Aortic root replacement with implantation of the coronary arteries was used for all patients to maximize aortic orifice area and preserve the exact spatial and functional relationship of the component parts of the aortic valve mechanism (M. H. Yacoub et al., 1999). The Ross procedure is the only operation which guarantees long-term viability of the aortic root which could explain the enhanced survival observed in this study (Mitchell, Jonas, & Schoen, 1998; Rabkin-Aikawa, Aikawa et al., 2004). There is rapidly accumulating evidence that the aortic root performs several sophisticated functions which allow its constituent parts to change their shape and function during the different parts of the cardiac cycle (Dagum et al., 1999; Lansac, Lim, Shomura, Lim, Rice et al., 2002). This can influence left ventricular workload and possibly coronary flow as well as stress distribution on the cusps (J. E. Davies et al., 2008; Katayama et al., 2008). In addition, aortic cusps modify their stiffness in response to humoral and endothelial signals, allowing them to adapt to varying hemodynamic conditions (El-Hamamsy, Balachandran et al., 2009).

Apart from survival, patient quality of life constitutes a major endpoint following valve surgery. In this study, although a number of patients failed to respond to the questionnaire, their quality of life scores were significantly better following the Ross operation. This could be due to the ability of the living valve to rapidly adapt to changing hemodynamic conditions during exercise in addition to the higher rate of reoperations in the Homograft group.

The incidence of progressive autograft root dilatation and neo-aortic regurgitation has been reported in several series following the Ross operation (Tirone E. David et al., 2000; Takkenberg et al., 2006). In contrast, with 97% completeness of follow-up in this series, freedom from aortic root reoperation is 99% at 13 years. Using mixed effects models, no statistically significant change in autograft diameter was observed over the study period. This could be attributable to specific technical elements as well as postoperative management of the patients. Unlike the aortic valve, the pulmonary valve has no fibrous annular support. Therefore, it is critical to trim the infundibular muscle down to 1-2mm below the cusps and to position the root inside the annulus, ensuring adequate fibrous support. Strict blood pressure control (systolic blood pressure ≤100-110mmHg) is critical in the immediate postoperative period and thereafter for 6-12 months to allow adaptive remodelling of the autograft root to systemic pressures.

Pulmonary allograft stenosis has been another area of concern following the Ross procedure. The incidence, pathology and location have previously been described and are characterized by intimal hyperplasia at the distal anastomosis and an inflammatory-mediated external compression by fibrous tissue (Carr-White et al., 2001). Based on this experience, our approach consists of systematic oversizing of the pulmonary homograft, interrupted sutures for the distal anastomosis and the use of anti-inflammatory agents in order to reduce the hemodynamic impact of this inflammatory reaction. In this cohort, mean transpulmonary gradient at 13 years was 25±5mmHg and freedom from pulmonary homograft reoperation was 94%. Combined with the low incidence of autograft reoperation, overall freedom from all

reoperations was 93.7% at 13 years in the Autograft group, which compares favourably to available tissue valve alternatives in a similar patient population (Svensson et al., 2003).

Freedom from the composite endpoint of endocarditis, bleeding, thrombosis and thromboembolism was 97±2% at 10 years in the Autograft group. This compares favourably with published series following aortic valve replacement (Kulik et al., 2006). Nevertheless, freedom from this composite endpoint was 82±3% in the Homograft group, principally due to a higher than anticipated incidence of late endocarditis in these patients.

6.5 LIMITATIONS

In this single-center randomized trial, the number of patients is relatively small. However, sample size was adequate and standardized techniques were used to support the main findings. In addition, very long-term results (beyond 25 years) are not available. Continuing follow-up of our cohort should address this limitation. This study compares autografts to homograft roots only. A comparison of xenogenic tissue valves (both stented and stentless) and mechanical prostheses with autograft implantation needs to be addressed in a future randomized trial.

6.6 CONCLUSION AND FUTURE DIRECTIONS

In conclusion, the Ross procedure results in enhanced survival when compared to homografts following aortic root replacement in young adults. In addition, it is associated with better freedom from reoperation and quality of life. This supports the hypothesis that implanting a living valve in the aortic position can translate into significantly improved clinical outcomes.

VII Discussion

The overarching aim of this thesis was to demonstrate that the aortic valve is a living organ which means that it has a unique and tightly regulated structure and function. It is capable of regulating its own structure both at the cellular and tissue levels and actively responds to its biochemical environment. In addition to regulating its structure in healthy conditions, it is capable of modulating tissue responses to noxious stimuli mimicking pathological conditions. Furthermore, heart valves have the capacity to adapt to changing mechanical and biochemical conditions by adapting their structure (remodelling) to optimize their function. The importance of a living valve was highlighted in patients undergoing aortic root replacement using different valve substitutes. Of those, the Ross procedure is the only operation which guarantees long-term viability of the aortic valve. Our data suggest that active adaptations of the living autograft valve reproduce normal solid and fluid mechanics. Importantly, this translates into clinically relevant endpoints including improved survival and better quality of life.

For a long time, little was known about the complex regulation of the structure and function of heart valves. This stems from the fact that valves initially drew less attention than the myocardium or the coronary arteries. In addition, heart valves were for the most part considered passive structures which open and close as a result of changes in transvalvular pressures and myocardial contraction/relaxation. With the improvement in diagnostic techniques, the advent of echocardiographic screening and the increase in life expectancy, it became apparent that valve disease was a significant source of morbidity and mortality (Ross & Braunwald, 1968). This prompted renewed interest into valve-related research, first from a broad physiological and anatomical point of view (Bellhouse & Bellhouse, 1968; Roberts, 1970; Zimmerman, 1966), leading into more intricate research orientations such as cell physiology, genomics and proteomics. In this thesis, we put a particular emphasis on the biomechanics of aortic valves which represents an essential element towards a better understanding of the complex regulation of these structures.

Aortic valves lie in a unique hemodynamic environment, characterized by a range of stresses - shear stress, bending forces, loading forces and strain – which constantly change in intensity and direction throughout the cardiac cycle. To make matters even more complex, stresses (particularly shear stress) exerted on one side of the valve vary significantly from those on the other side. Yet, aortic valves open and close over 100.000 times a day, and in the majority of human beings, function normally over a lifespan of 70-90 years. This structural and functional longevity requires an ability to withstand these mechanical forces as well as to adapt to changing conditions. It has been shown experimentally and using computer simulations that the flow patterns on either side of the valve result in significant differences in the magnitude and direction of shear stresses on the overlying endothelium. Using high-resolution numerical simulations of the blood flow through a polymeric trileaflet valve, Ge et al. have recently shown that the aortic side of the valve is exposed to disturbed flow patterns and importantly that complicated patterns of flow were observed near the regions where focalized calcium deposits are typically found (Ge & Sotiropoulos, 2010). This highlights the physiological relevance of the valve's mechanical environment in valve pathogenesis. It is a widely accepted concept that areas of low shear stress or complicated patterns of blood flow are at a significantly greater risk of developing atherosclerotic changes. This is thought to be due to endothelial responses to shear stress, the main mechanical stimulus, leading to activation of inflammatory mediators and a cascade of events characterized by expression of adhesion molecules, rolling and penetration of inflammatory cells into the subendothelial cells, followed by interaction with oxidized low density lipoproteins, forming foam cells and leading to hydroxyapatite formation (K. D. O'Brien, 2006). The current work adds a new paradigm to the traditional endothelial activation, inflammation-mediated theory of aortic valve disease which lays the foundation for 2 new important areas of research into aortic valve calcification.

First, from a structural standpoint, using scanning ion conductance microscopy to evaluate endothelial cell biomechanics in situ, we showed that endothelial cells on the ventricular side are significantly stiffer than those on the aortic side. Moreover, cells from either side exhibited different responses to the same vasoactive agents. Cell stiffness represents more than a mere structural characteristic of cells. The degree of cell stiffness (also termed tensegrity) is a product of the particular arrangement of cytoskeletal proteins within that cell (Luo et al., 2008). In cells, "form meets function" (Wang, Tytell, & Ingber, 2009). In other terms, the architectural organization of the cytoskeleton has a direct impact on the biological responses of the cell to mechanical stimuli (mechanotransduction), such as activation or repression of specific genes (Alenghat & Ingber, 2002; Hahn & Schwartz, 2009; White & Frangos, 2007). It remains unclear why cells on the ventricular side of the valve are stiffer than their aortic counterparts. It could in reaction to the higher degrees of shear stress on the ventricular side due to high velocity laminar flow which require stiffer cells to prevent significant structural deformations during systole. It could also be due to the composition of the extracellular matrix in the spongiosa and ventricularis. Indeed, the cytoskeleton is intimately linked to its extracellular environment and can have direct interactions with the various structural proteins such as elastin or collagen as well as microfibrillar proteins such as fibrillin and filamin. The spongiosa is rich in collagen which provides solid tensile strength, whereas the ventricularis is mainly composed of elastin which is less stiff. The stiffer endothelial cells on the ventricular side might be a compensatory response to the softer underlying matrix.

Second, the role of the endothelium in regulating the mechanical properties of the aortic valve by communicating directly with interstitial cells as shown in vitro using a biaxial micromechanical testing system is an area of major interest. It represents the first study to establish a direct functional link between valve endothelial and interstitial cells in situ. Importantly, it suggests that valves are capable of changing and adapting their stiffness in response to their local mechanical, hemodynamic and biochemical environments. This adaptive capacity is probably one of the major reasons explaining the long-term durability of aortic

valves in their highly stressful and dynamic local environment. Changes in the capacity of valves to adjust their mechanical properties causing them to become softer or stiffer are thought to have direct implications in aortic root function as well as valve integrity and durability. The function of the aortic root is to ensure unobstructed unidirectional laminar blood flow through the root in systole while minimizing ventricular workload. Instantaneous movements of the aortic valve and root components are major determinants and partly depend on the mechanical properties of the tissue. In addition, optimal coronary flow is determined by the structure and function of the aortic root. The shape of the root is mainly dependent on the sinuses of Valsalva but also by the underlying aortic valve cusps. Contractile changes or changes in stiffness of up to 30% are likely to affect the patterns of flow generated in the root and the blood recirculation phenomenon. These various implications remain speculative for the moment because of the difficulty in inducing controlled changes in cusp stiffness in vivo while measuring the immediate in vivo effects. Using radiopaque crystals in a close-chest animal model such as performed by the Stanford group (Dagum et al., 1999) combined with functional imaging techniques such as the ones presented in this thesis using 3-dimensional phase contrast-enhanced MRI could provide important answers.

Nevertheless, our findings on the regulation of valve mechanical properties may have important implications in valve pathophysiology. It has been known for a long time that foci of aortic valve calcification mainly occur at sites of high mechanical stresses on the cusps, such as the commissures. This is possibly due to repeated microtrauma exceeding the regenerative capacity of the endothelium or in local activation of inflammatory pathways, which in the long-term result in valve calcification. Therefore, stress distribution along the surface of the cusps is an important determinant of valve durability. Changes in the shape or stiffness of any living structure inevitably results in alterations in local stress maps. The same is likely to hold true for aortic valves with endothelial dysfunction. In addition to changes in stress distribution and potential increased susceptibility to calcification, a recent study by Yip et al. from the University of Toronto suggests an important direct effect of matrix stiffness on valve calcification (Yip et

al., 2009). The authors demonstrated a significant difference in the calcifying potential of aortic valve interstitial cells in vitro when seeded on soft or stiff matrices (Yip et al., 2009). This supports the notion that cells directly interact with their extracellular environment and changes in the stiffness of the matrix can influence cell responses to osteogenic stimuli. It is therefore immediately apparent that dysregulation of the tightly controlled balance of aortic valve stiffness can directly impact cell responses to calcifying stimuli in vivo.

The link between ex vivo and in vivo research on aortic valves remains challenging and elusive. Unlike blood vessels, aortic valves are not tubular structures, the pattern of local flow as discussed is complex and highly variable and no surrogate imaging or biomarkers of whole aortic valve dysfunction or valve endothelial dysfunction have yet been developed. In addition, computer simulations of valve motion based on high resolution imaging techniques also represents a significant challenge because of the highly dynamic nature of the aortic root. The aortic annulus as shown by Dagum et al. undergoes torsional deformations during the cardiac cycle and the annulus undergoes a significant longitudinal excursion during the cycle which makes motion tracking necessary but complex. Thus far, few groups have managed to adjust for dynamic aortic annular motion, led by efforts from research groups at Imperial College. Tracking the cusps on the other hand constitutes an even greater challenge for several reasons: their motion is non-linear, they undergo important conformational changes during the cycle (particularly bending changes) and their movements dictate changes in the volume of blood flowing through them which adds an added element of difficulty. Therefore, descriptive findings on aortic valve physiology inevitably precede in vivo functional validation but offer important clues into the level of detailed imaging required to truly understand valve function in health and disease. Molecular imaging is an exciting area of research which has shown initial promising results in characterizing the early inflammatory changes in diseased vessels (Aikawa, Nahrendorf, Figueiredo et al., 2007; Deguchi et al., 2006). A similar attempt at examining the proteolytic and osteogenic markers in aortic valve disease has also been demonstrated (Aikawa,

Nahrendorf, Sosnovik et al., 2007). This could have important significance in understanding the mechanisms of aortic valve disease.

The ultimate objective behind research on the aortic valve is to alleviate the burden of disease in the population. Aortic valve disease remains a major source of morbidity and mortality in the developed world and is expected to continue increasing in a significant fashion over the next 20-30 years (M. H. Yacoub & Takkenberg, 2005). Clinical trials aimed at improving endothelial function in patients have almost consistently produced little encouragement and have always represented an important gap between laboratory findings and clinical reality. Few studies have however focused on aortic valve disease, partly because for a long time, it was considered a passive, "degenerative", "wear and tear" disease. The largest trials have mainly focused on the role of statins in halting the progression of aortic valve disease but have produced disappointing results, including studies in patients with mild forms of disease. The reasons behind the absence of real observed benefit remains elusive. However, it is now well established that signalling pathways and mechanisms involved in early morphogenesis remain operative in adult life and can contribute to pathophysiology of disease. Therefore the absence of observed benefit with the various therapeutic strategies aimed at improving endothelial function might be directly linked to the timing of treatment initiation. Patients with mild forms of aortic valve disease are currently thought to represent early stages of the disease. Nevertheless, considering the various roles of the endothelium on valve physiology as presented in this thesis (regulation of valve mechanical properties, local differences in single-cell mechanical properties, direct effect of valve interstitial cell calcification), the true impact of these therapies may not be realized unless treatment is administered in very early stages. Of course, this raises important cost and ethical issues which are beyond the scope of this discussion. Nevertheless, if predictive biomarkers or genetic screening tests can identify subjects at a high risk of developing aortic valve disease, the real benefit of medical therapy may only be achieved if administered early to prevent the long-term slow progression of local endothelial and aortic valve dysfunction.

Currently, the only means to alter the natural history of aortic valve disease remains surgical intervention to replace the diseased valve. Studies in patients undergoing aortic valve replacement show an improvement in patient survival which nevertheless does not match that of the general population. The study presented in this thesis represents the first prospective randomized trial to demonstrate restored survival following aortic valve replacement to levels matching an age- and gender-matched population (El-Hamamsy, Eryigit et al., 2010). As previously mentioned, this is thought to be due to the long-term preserved viability of aortic valve cusps, allowing them to adapt to their changing local mechanical and hemodynamic conditions and to ensure long-term valve durability as well as normal root physiology.

VIII Conclusions And Future Directions

In the present thesis, I have attempted to show that the aortic valve is a living structure with unique characteristics and specific intrinsic properties, both at the cellular and tissue levels. I have further tried to demonstrate the clinical relevance of the capacity of an aortic valve to adapt and remodel in response to its local hemodynamic and biochemical environment. The findings support the original hypothesis that the valve has unique structural and functional properties which affect clinically relevant outcomes. At the cellular level, we have shown that aortic valve endothelial cells from either side of the aortic valve have different baseline mechanical properties and, in addition, exhibit different responses to similar stimuli. Furthermore, using a novel technique to separately isolate endothelial cells from both sides of the cusp, we have performed gene expression analyses of primary cultures of aortic- versus ventricular-side endothelial cells, showing differential expression of a range of genes. Unfortunately, until the pig genome is fully characterized, the precise identity of divergent genes remains elusive. Nevertheless, once the genome is published, this will represent a unique set of information and a robust look into potential explanations of the differences in disease expression on both sides of the valve.

The observation that aortic valve calcification occurs almost exclusively on the aortic side of the valve (fibrosa) has always intrigued researchers looking into the pathophysiology of aortic valve calcification, and represents a major hurdle into the understanding and treatment of aortic valve disease. We have postulated that the heterogeneity in endothelial cell properties could have a direct link to differential disease expression. Our findings suggest that endothelial cells from the aortic surface of the valve express less NO than their ventricular counterparts both in static and under physiological flow conditions. Using a custom-developed side-selective tissue culture setup, we have established a firm link between endothelial function as determined by NO production and the formation of calcium nodules in the matrix. Inhibition of NO production using L-NAME resulted in a significant increase in nodule formation, confirming the protective role of NO against valve calcification.

In an attempt to further understand the role of aortic valve endothelium in regulating aortic valve structure and function, we have studied endothelial-dependent regulation of the mechanical properties of aortic valve cusps in vitro. Our findings establish 2 new important findings. First, the endothelium communicates directly with the underlying interstitial cells to control the stiffness of aortic valve cusps. And importantly, different endothelial-dependent signals result in significant changes in the stiffness of the cusps. Considering the highly dynamic environment where aortic valves lie and their constant movement to optimize aortic root function, changes in aortic valve shape and stiffness can have major functional implications.

The implications of a living aortic valve capable of remodelling and adapting to its local milieu was examined in an in vivo human setting by studying aortic root biomechanics and clinical outcomes following different aortic root replacement procedures. The Ross procedure is the only operation which guarantees long-term viability of the aortic valve and root, and therefore serves as the only illustration of the role of a living aortic valve substitute. It was compared to homografts, xenografts and normal individuals with healthy native valves. Our results suggest that a living aortic valve and root substitute most closely reproduces the tissue and fluid mechanics of a normal aortic root. In addition, a living valve translates into clinically relevant endpoints, characterized by restored patient survival to an age- and gender-matched general population as well as improved quality of life. These findings reinforce the need for living tissue engineered heart valve substitutes capable of reproducing the sophisticated structure and function of native heart valves.

8.1 Future Directions

Based on the findings from this work, current and evolving work will focus on several important directions:

1- Further explore the structural and functional intrinsic differences between aortic valve endothelial from both sides of the cusps with particular focus on:
    a. Proteomics
    b. Specific stimuli which cause endothelial dysfunction characterized by a decreased production of NO or dysregulation of their mechanical properties as assessed by SICM
    c. Determining the major stimuli affecting aortic valve endothelial cells, whether it is shear stress, cell stretch, inflammatory mediators etc...
    d. Studying various agents such as statins or NO donors (e.g., tetrahydrobiopterin) which might improve or restore endothelial function following exposure to noxious stimuli.

2- Understand the functional significance of changes in the mechanical properties of aortic valve endothelial cells in response to mechanical (flow, pressure, strain) or biochemical stimuli, by looking at the activated downstream signalling pathways.

3- Work in conjunction with imaging engineers to develop robust and reliable means of examining the instantaneous movements, deformations and stress levels on aortic valve cusps during the cardiac cycle in vivo. Once this has been validated, several avenues need to be explored:
    a. Analyze the changes in stress levels and distribution on aortic valve cusps with changes in the stiffness or shape of the cusps using computer simulation techniques.
    b. Analyze the changes in flow mechanics with a particular focus on aortic root flow dynamics with changes in aortic valve stiffness.
    c. Evaluate the role of circulating mediators (ET-1 or 5-HT) as would be observed in pathological situations (hypertension or carcinoid syndrome) on the

instantaneous movements of aortic valve cusps and stress distribution on the cusps with changes in their mechanical properties.

4- Continue ongoing work aiming at developing a tissue-engineered functional heart valve by elaborating specific protocols to differentiate stems cells into endothelial cells with similar structural and functional properties to valve endothelial cells.

5- From a clinical standpoint, continue ongoing work into the relevance and clinical importance of a living heart valve substitute by comparing various valve replacement procedures in a randomized trial aimed at analyzing biomechanics in a population of patients who are fully comparable.

REFERENCES

Abe, A., & Karaki, H. (1992). Mechanisms underlying the inhibitory effect of dibutyryl cyclic AMP in vascular smooth muscle. *Eur J Pharmacol, 211*(3), 305-311.

Ahlborg, G., & Lundberg, J. M. (1997). Nitric oxide-endothelin-1 interaction in humans. *J Appl Physiol, 82*(5), 1593-1600.

Aicher, D., Urbich, C., Zeiher, A., Dimmeler, S., & Schafers, H. J. (2007). Endothelial nitric oxide synthase in bicuspid aortic valve disease. *Ann Thorac Surg, 83*(4), 1290-1294.

Aikawa, E., Nahrendorf, M., Figueiredo, J. L., Swirski, F. K., Shtatland, T., Kohler, R. H., et al. (2007). Osteogenesis associates with inflammation in early-stage atherosclerosis evaluated by molecular imaging in vivo. *Circulation, 116*(24), 2841-2850.

Aikawa, E., Nahrendorf, M., Sosnovik, D., Lok, V. M., Jaffer, F. A., Aikawa, M., et al. (2007). Multimodality molecular imaging identifies proteolytic and osteogenic activities in early aortic valve disease. *Circulation, 115*(3), 377-386.

Aird, W. C. (2006). Mechanisms of endothelial cell heterogeneity in health and disease. *Circ Res, 98*(2), 159-162.

Alenghat, F. J., & Ingber, D. E. (2002). Mechanotransduction: all signals point to cytoskeleton, matrix, and integrins. *Sci STKE, 2002*(119), PE6.

Bedard, K., & Krause, K. H. (2007). The NOX family of ROS-generating NADPH oxidases: physiology and pathophysiology. *Physiol Rev, 87*(1), 245-313.

Bellhouse, B. J., & Bellhouse, F. H. (1968). Mechanism of Closure of the Aortic Valve. *Nature, 217*(5123), 86-87.

Bellhouse, B. J., Bellhouse, F. H., & Reid, K. G. (1968). Fluid Mechanics of the Aortic Root with Application to Coronary Flow. *Nature, 219*(5158), 1059-1061.

Billiar, K. L., & Sacks, M. S. (2000a). Biaxial mechanical properties of the native and glutaraldehyde-treated aortic valve cusp: Part II--A structural constitutive model. *J Biomech Eng, 122*(4), 327-335.

Billiar, K. L., & Sacks, M. S. (2000b). Biaxial mechanical properties of the natural and glutaraldehyde treated aortic valve cusp--Part I: Experimental results. *J Biomech Eng, 122*(1), 23-30.

Bonow, R. O., Carabello, B. A., Chatterjee, K., de Leon, A. C., Jr., Faxon, D. P., Freed, M. D., et al. (2006). ACC/AHA 2006 Guidelines for the Management of Patients With Valvular Heart Disease: A Report of the American College of Cardiology/American Heart Association Task Force on Practice Guidelines (Writing Committee to Revise the 1998 Guidelines for the Management of Patients With Valvular Heart Disease) Developed in Collaboration With the Society of Cardiovascular Anesthesiologists Endorsed by the Society for Cardiovascular Angiography and Interventions and the Society of Thoracic Surgeons. *J Am Coll Cardiol, 48*(3), e1-148.

Boulanger, C., & Luscher, T. F. (1990). Release of endothelin from the porcine aorta. Inhibition by endothelium-derived nitric oxide. *The Journal of Clinical Investigation, 85*(2), 587-590.

Bozbas, H., Pirat, B., Yildirir, A., Simsek, V., Sade, E., Eroglu, S., et al. (2008). Coronary flow reserve is impaired in patients with aortic valve calcification. *Atherosclerosis, 197*(2), 846-852.

Bozbas, H., Yildirir, A., Demir, O., Cakmak, A., Karacaglar, E., Yilmaz, M., et al. (2008). Serum gamma-glutamyltransferase activity is increased in patients with calcific aortic valve stenosis. *J Heart Valve Dis, 17*(4), 371-375.

Brand, N. J., Roy, A., Hoare, G., Chester, A., & Yacoub, M. H. (2006). Cultured interstitial cells from human heart valves express both specific skeletal muscle and non-muscle markers. *The International Journal of Biochemistry & Cell Biology, 38*(1), 30-42.

Butcher, J. T., & Nerem, R. M. (2006). Valvular endothelial cells regulate the phenotype of interstitial cells in co-culture: effects of steady shear stress. *Tissue Eng, 12*(4), 905-915.

Butcher, J. T., Penrod, A. M., Garcia, A. J., & Nerem, R. M. (2004). Unique morphology and focal adhesion development of valvular endothelial cells in static and fluid flow environments. *Arterioscler Thromb Vasc Biol, 24*(8), 1429-1434.

Butcher, J. T., Tressel, S., Johnson, T., Turner, D., Sorescu, G., Jo, H., et al. (2006). Transcriptional profiles of valvular and vascular endothelial cells reveal phenotypic differences: influence of shear stress. *Arterioscler Thromb Vasc Biol, 26*(1), 69-77.

Carr-White, G. S., Kilner, P. J., Hon, J. K., Rutledge, T., Edwards, S., Burman, E. D., et al. (2001). Incidence, location, pathology, and significance of pulmonary homograft stenosis after the Ross operation. *Circulation, 104*(12 Suppl 1), I16-20.

Carter, S. B. (1967). Effects of cytochalasins on mammalian cells. *Nature, 213*(5073), 261-264.

Charras, G. T., & Horton, M. A. (2002). Determination of Cellular Strains by Combined Atomic Force Microscopy and Finite Element Modeling. *83*(2), 858-879.

Chen, J.-H., Yip, C. Y. Y., Sone, E. D., & Simmons, C. A. (2009). Identification and Characterization of Aortic Valve Mesenchymal Progenitor Cells with Robust Osteogenic Calcification Potential. *Am J Pathol, 174*(3), 1109-1119.

Chenevard, R., Bechir, M., Hurlimann, D., Ruschitzka, F., Turina, J., Luscher, T. F., et al. (2006). Persistent endothelial dysfunction in calcified aortic stenosis beyond valve replacement surgery. *Heart, 92*(12), 1862-1863.

Cheng, A., Dagum, P., & Miller, D. C. (2007). Aortic root dynamics and surgery: from craft to science. *Philos Trans R Soc Lond B Biol Sci, 362*(1484), 1407-1419.

Chester, A. H., Kershaw, J. D., Sarathchandra, P., & Yacoub, M. H. (2008). Localisation and function of nerves in the aortic root. *J Mol Cell Cardiol, 44*(6), 1045-1052.

Chester, A. H., Misfeld, M., & Yacoub, M. H. (2000). Receptor-mediated contraction of aortic valve leaflets. *J Heart Valve Dis, 9*(2), 250-254; discussion 254-255.

Clark-Greuel, J. N., Connolly, J. M., Sorichillo, E., Narula, N. R., Rapoport, H. S., Mohler, E. R., 3rd, et al. (2007). Transforming growth factor-beta1 mechanisms in aortic valve calcification: increased alkaline phosphatase and related events. *Ann Thorac Surg, 83*(3), 946-953.

Clark-Greuel, J. N., Connolly, J. M., Sorichillo, E., Narula, N. R., Rapoport, H. S., Mohler Iii, E. R., et al. (2007). Transforming Growth Factor-[beta]1 Mechanisms in Aortic Valve Calcification: Increased Alkaline Phosphatase and Related Events. *The Annals of Thoracic Surgery, 83*(3), 946-953.

Cloyd, K., El-Hamamsy, I., Sarathchandra, P., Gentleman, E., Yacoub, M. H., Chester, A. H., et al. (2010). *Characterization of In Situ and In Vitro Aortic Valve Nodules Using Bio-Raman Micro-Spectroscopy*. Paper presented at the 4th Biennial Heart Valve Biology and Tissue Engineering Meeting.

Connolly, H. M., Crary, J. L., McGoon, M. D., Hensrud, D. D., Edwards, B. S., Edwards, W. D., et al. (1997). Valvular heart disease associated with fenfluramine-phentermine. *N Engl J Med, 337*(9), 581-588.

Cote, C., Pibarot, P., Despres, J. P., Mohty, D., Cartier, A., Arsenault, B. J., et al. (2008). Association between circulating oxidised low-density lipoprotein and fibrocalcific remodelling of the aortic valve in aortic stenosis. *Heart, 94*(9), 1175-1180.

Cotrufo, M., Della Corte, A., De Santo, L. S., Quarto, C., De Feo, M., Romano, G., et al. (2005). Different patterns of extracellular matrix protein expression in the convexity and the concavity of the dilated aorta with bicuspid aortic valve: preliminary results. *J Thorac Cardiovasc Surg, 130*(2), 504-511.

Dagum, P., Green, G. R., Nistal, F. J., Daughters, G. T., Timek, T. A., Foppiano, L. E., et al. (1999). Deformational dynamics of the aortic root: modes and physiologic determinants. *Circulation, 100*(19 Suppl), II54-62.

David, T. E., Omran, A., Ivanov, J., Armstrong, S., de Sa, M. P. L., Sonnenberg, B., et al. (2000). Dilation of the pulmonary autograft after the Ross procedure. *J Thorac Cardiovasc Surg, 119*(2), 210-220.

David, T. E., Woo, A., Armstrong, S., & Maganti, M. (2010). When is the Ross operation a good option to treat aortic valve disease? *J Thorac Cardiovasc Surg, 139*(1), 68-73; discussion 73-65.

Davies, J. E., Parker, K. H., Francis, D. P., Hughes, A. D., & Mayet, J. (2008). What is the role of the aorta in directing coronary blood flow? *Heart, 94*(12), 1545-1547.

Davies, P. F. (1995). Flow-mediated endothelial mechanotransduction. *Physiol Rev, 75*(3), 519-560.

De Biasi, S., & Vitellaro-Zuccarello, L. (1982). Intrinsic innervation of porcine semilunar heart valves. *Anat Embryol (Berl), 165*(1), 71-79.

de Lange, F. J., Moorman, A. F., Anderson, R. H., Manner, J., Soufan, A. T., de Gier-de Vries, C., et al. (2004). Lineage and morphogenetic analysis of the cardiac valves. *Circ Res, 95*(6), 645-654.

Deck, J. D. (1986). Endothelial cell orientation on aortic valve leaflets. *Cardiovasc Res, 20*(10), 760-767.

Deguchi, J.-o., Aikawa, M., Tung, C.-H., Aikawa, E., Kim, D.-E., Ntziachristos, V., et al. (2006). Inflammation in Atherosclerosis: Visualizing Matrix Metalloproteinase Action in Macrophages In Vivo. *Circulation, 114*(1), 55-62.

Della Corte, A., De Santo, L. S., Montagnani, S., Quarto, C., Romano, G., Amarelli, C., et al. (2006). Spatial patterns of matrix protein expression in dilated ascending aorta with aortic regurgitation: congenital bicuspid valve versus Marfan's syndrome. *J Heart Valve Dis, 15*(1), 20-27; discussion 27.

Della Corte, A., Quarto, C., Bancone, C., Castaldo, C., Di Meglio, F., Nurzynska, D., et al. (2008). Spatiotemporal patterns of smooth muscle cell changes in ascending aortic dilatation with bicuspid and tricuspid aortic valve stenosis: focus on cell-matrix signaling. *J Thorac Cardiovasc Surg, 135*(1), 8-18, 18 e11-12.

Eisenberg, L. M., & Markwald, R. R. (1995). Molecular regulation of atrioventricular valvuloseptal morphogenesis. *Circ Res, 77*(1), 1-6.

El-Hamamsy, I., Balachandran, K., Yacoub, M. H., Stevens, L. M., Sarathchandra, P., Taylor, P. M., et al. (2009). Endothelium-dependent regulation of the mechanical properties of aortic valve cusps. *J Am Coll Cardiol, 53*(16), 1448-1455.

El-Hamamsy, I., Chester, A. H., & Yacoub, M. H. (2010). Cellular regulation of the structure and function of aortic valves. *Journal of Advanced Research, 1*, 5-12.

El-Hamamsy, I., Eryigit, Z., Stevens, L. M., Sarang, Z., George, R., Clark, L., et al. (2010). Long-term outcomes following autograft versus homograft aortic root replacement in adults - a prospective randomized trial. *Lancet, in press*.

El-Hamamsy, I., & Yacoub, M. H. (2009a). Cellular and molecular mechanisms of thoracic aortic aneurysms. *Nat Rev Cardiol, 6*(12), 771-786.

El-Hamamsy, I., & Yacoub, M. H. (2009b). A measured approach to managing the aortic root in patients with bicuspid aortic valve disease. *Curr Cardiol Rep, 11*(2), 94-100.

El-Hamamsy, I., Yacoub, M. H., & Chester, A. H. (2009). Neuronal regulation of aortic valve cusps. *Curr Vasc Pharmacol, 7*(1), 40-46.

Elkins, R. C., Thompson, D. M., Lane, M. M., Elkins, C. C., & Peyton, M. D. (2008). Ross operation: 16-year experience. *J Thorac Cardiovasc Surg, 136*(3), 623-630, 630 e621-625.

Engler, A. J., Sen, S., Sweeney, H. L., & Discher, D. E. (2006). Matrix Elasticity Directs Stem Cell Lineage Specification. *126*(4), 677-689.

Farivar, R. S., Cohn, L. H., Soltesz, E. G., Mihaljevic, T., Rawn, J. D., & Byrne, J. G. (2003). Transcriptional profiling and growth kinetics of endothelium reveals differences between cells derived from porcine aorta versus aortic valve. *Eur J Cardiothorac Surg, 24*(4), 527-534.

Fernández, B., Durán, A. C., Fernández-Gallego, T., Fernández, M. C., Such, M., Arqué, J. M., et al. (2009). Bicuspid Aortic Valves With Different Spatial Orientations of the Leaflets Are Distinct Etiological Entities. *Journal of the American College of Cardiology, 54*(24), 2312-2318.

Flavahan, N. A., & Vanhoutte, P. M. (1990). G-proteins and endothelial responses. *Blood Vessels, 27*(2-5), 218-229.

Flavahan, N. A., & Vanhoutte, P. M. (1995). Endothelial cell signaling and endothelial dysfunction. *Am J Hypertens, 8*(5 Pt 2), 28S-41S.

Fletcher, D. A., & Mullins, R. D. (2010). Cell mechanics and the cytoskeleton. *Nature, 463*(7280), 485-492.

Forstermann, U. (2008). Oxidative stress in vascular disease: causes, defense mechanisms and potential therapies. *Nat Clin Pract Cardiovasc Med, 5*(6), 338-349.

Garg, V., Muth, A. N., Ransom, J. F., Schluterman, M. K., Barnes, R., King, I. N., et al. (2005). Mutations in NOTCH1 cause aortic valve disease. *Nature, 437*(7056), 270-274.

Ge, L., & Sotiropoulos, F. (2010). Direction and magnitude of blood flow shear stresses on the leaflets of aortic valves: is there a link with valve calcification? *Journal of Biomecchanical Engineering, 132*(1), 014505.

Gorelik, J., Ali, N. N., Sheikh Abdul Kadir, S. H., Lab, M., Stojkovic, P., Armstrong, L., et al. (2008). Non-invasive imaging of stem cells by scanning ion conductance microscopy: future perspective. *Tissue Eng Part C Methods, 14*(4), 311-318.

Gorelik, J., Yang, L. Q., Zhang, Y., Lab, M., Korchev, Y., & Harding, S. E. (2006). A novel Z-groove index characterizing myocardial surface structure. *Cardiovasc Res, 72*(3), 422-429.

Grande-Allen, K. J., Cochran, R. P., Reinhall, P. G., & Kunzelman, K. S. (2000). Re-creation of sinuses is important for sparing the aortic valve: a finite element study. *J Thorac Cardiovasc Surg, 119*(4 Pt 1), 753-763.

Grande-Allen, K. J., Cochran, R. P., Reinhall, P. G., & Kunzelman, K. S. (2001). Mechanisms of aortic valve incompetence: finite-element modeling of Marfan syndrome. *J Thorac Cardiovasc Surg, 122*(5), 946-954.

Grande, K. J., Cochran, R. P., Reinhall, P. G., & Kunzelman, K. S. (1998). Stress variations in the human aortic root and valve: the role of anatomic asymmetry. *Ann Biomed Eng, 26*(4), 534-545.

Gustafsson, B. I., Tommeras, K., Nordrum, I., Loennechen, J. P., Brunsvik, A., Solligard, E., et al. (2005). Long-Term Serotonin Administration Induces Heart Valve Disease in Rats. *Circulation, 111*(12), 1517-1522.

Hafizi, S., Taylor, P. M., Chester, A. H., Allen, S. P., & Yacoub, M. H. (2000). Mitogenic and secretory responses of human valve interstitial cells to vasoactive agents. *J Heart Valve Dis, 9*(3), 454-458.

Hahn, C., & Schwartz, M. A. (2009). Mechanotransduction in vascular physiology and atherogenesis. *Nat Rev Mol Cell Biol, 10*(1), 53-62.

Hammermeister, K., Sethi, G. K., Henderson, W. G., Grover, F. L., Oprian, C., & Rahimtoola, S. H. (2000). Outcomes 15 years after valve replacement with a mechanical versus a bioprosthetic valve: final report of the Veterans Affairs randomized trial. *J Am Coll Cardiol, 36*(4), 1152-1158.

Hare, J. M., Givertz, M. M., Creager, M. A., & Colucci, W. S. (1998). Increased Sensitivity to Nitric Oxide Synthase Inhibition in Patients With Heart Failure : Potentiation of ß-Adrenergic Inotropic Responsiveness. *Circulation, 97*(2), 161-166.

Helderman, F., Segers, D., de Crom, R., Hierck, B. P., Poelmann, R. E., Evans, P. C., et al. (2007). Effect of shear stress on vascular inflammation and plaque development. *Curr Opin Lipidol, 18*(5), 527-533.

Hermans, H., Herijgers, P., Holvoet, P., Verbeken, E., Meuris, B., Flameng, W., et al. (2010). Statins for calcific aortic valve stenosis: into oblivion after SALTIRE and SEAS? An extensive review from bench to bedside. *Curr Probl Cardiol, 35*(6), 284-306.

High, F. A., & Epstein, J. A. (2008). The multifaceted role of Notch in cardiac development and disease. *Nat Rev Genet, 9*(1), 49-61.

High, F. A., Zhang, M., Proweller, A., Tu, L., Parmacek, M. S., Pear, W. S., et al. (2007). An essential role for Notch in neural crest during cardiovascular development and smooth muscle differentiation. *J Clin Invest, 117*(2), 353-363.

Hoerstrup, S. P., Zünd, G., Schoeberlein, A., Ye, Q., Vogt, P. R., & Turina, M. I. (1998). Fluorescence activated cell sorting: A reliable method in tissue engineering of a bioprosthetic heart valve. *The Annals of Thoracic Surgery, 66*(5), 1653-1657.

Hokken, R. B., Bartelings, M. M., Bogers, A. J., & Gittenberger-de Groot, A. C. (1997). Morphology of the pulmonary and aortic roots with regard to the pulmonary autograft procedure. *J Thorac Cardiovasc Surg, 113*(3), 453-461.

Hong, D., Mohamad, A., & Chris, R. T. (2007). Oxidative stress and increased eNOS and NADPH oxidase expression in mouse microvessel endothelial cells. *Journal of Cellular Physiology, 212*(3), 682-689.

Horton, M., Charras, G., & Lehenkari, P. (2002). Analysis of ligand-receptor interactions in cells by atomic force microscopy. *J Recept Signal Transduct Res, 22*(1-4), 169-190.

Iivanainen, A. M., Lindroos, M., Tilvis, R., Heikkilä, J., & Kupari, M. (1996). Natural history of aortic valve stenosis of varying severity in the elderly. *The American Journal of Cardiology, 78*(1), 97-101.

Imberti, B., Seliktar, D., Nerem, R. M., & Remuzzi, A. (2002). The response of endothelial cells to fluid shear stress using a co-culture model of the arterial wall. *Endothelium, 9*(1), 11-23.

Itoh, A., Krishnamurthy, G., Swanson, J. C., Ennis, D. B., Bothe, W., Kuhl, E., et al. (2009). Active stiffening of mitral valve leaflets in the beating heart. *Am J Physiol Heart Circ Physiol, 296*(6), H1766-1773.

Jaalouk, D. E., & Lammerding, J. (2009). Mechanotransduction gone awry. *Nat Rev Mol Cell Biol, 10*(1), 63-73.

Janmey, P. A., Euteneuer, U., Traub, P., & Schliwa, M. (1991). Viscoelastic properties of vimentin compared with other filamentous biopolymer networks. *J Cell Biol, 113*(1), 155-160.

Jenkinson, C., Coulter, A., & Wright, L. (1993). Short form 36 (SF36) health survey questionnaire: normative data for adults of working age. *BMJ, 306*(6890), 1437-1440.

Jian, B., Narula, N., Li, Q.-y., Mohler Iii, E. R., & Levy, R. J. (2003). Progression of aortic valve stenosis: TGF-[beta]1 is present in calcified aortic valve cusps and promotes aortic valve interstitial cell calcification via apoptosis. *The Annals of Thoracic Surgery, 75*(2), 457-465.

Jian, B., Xu, J., Connolly, J., Savani, R. C., Narula, N., Liang, B., et al. (2002). Serotonin Mechanisms in Heart Valve Disease I: Serotonin-Induced Up-Regulation of Transforming Growth Factor-{beta}1 via G-Protein Signal Transduction in Aortic Valve Interstitial Cells. *Am J Pathol, 161*(6), 2111-2121.

Jiang, X., Rowitch, D. H., Soriano, P., McMahon, A. P., & Sucov, H. M. (2000). Fate of the mammalian cardiac neural crest. *Development, 127*(8), 1607-1616.

Kaartinen, V., Dudas, M., Nagy, A., Sridurongrit, S., Lu, M. M., & Epstein, J. A. (2004). Cardiac outflow tract defects in mice lacking ALK2 in neural crest cells. *Development, 131*(14), 3481-3490.

Kanno, Y., Into, T., Lowenstein, C. J., & Matsushita, K. (2008). Nitric oxide regulates vascular calcification by interfering with TGF-Î² signalling. *Cardiovascular Research, 77*(1), 221-230.

Karien, J. R., & Kristyn, S. M. (2009). Regulation of valvular interstitial cell calcification by components of the extracellular matrix. *Journal of Biomedical Materials Research Part A, 90A*(4), 1043-1053.

Katayama, S., Umetani, N., Sugiura, S., & Hisada, T. (2008). The sinus of Valsalva relieves abnormal stress on aortic valve leaflets by facilitating smooth closure. *The Journal of Thoracic and Cardiovascular Surgery, 136*(6), 1528-1535.e1521.

Kawano, H., Kawai, S., Shirai, T., & Okada, R. (1993). Morphological study on vagal innervation in human atrioventricular valves using histochemical method. *Jpn Circ J, 57*(8), 753-759.

Kawano, H., Shirai, T., Kawano, Y., & Okada, R. (1996). Morphological study of vagal innervation in human semilunar valves using a histochemical method. *Jpn Circ J, 60*(1), 62-66.

Kennedy, J. A., Hua, X., Mishra, K., Murphy, G. A., Rosenkranz, A. C., & Horowitz, J. D. (2009). Inhibition of calcifying nodule formation in cultured porcine aortic valve cells by nitric oxide donors. *European Journal of Pharmacology, 602*(1), 28-35.

Kim, R. Y., Robertson, E. J., & Solloway, M. J. (2001). Bmp6 and Bmp7 are required for cushion formation and septation in the developing mouse heart. *Dev Biol, 235*(2), 449-466.

Korchev, Y. E., Gorelik, J., Lab, M. J., Sviderskaya, E. V., Johnston, C. L., Coombes, C. R., et al. (2000). Cell volume measurement using scanning ion conductance microscopy. *Biophys J, 78*(1), 451-457.

Kouchoukos, N. T., Davila-Roman, V. G., Spray, T. L., Murphy, S. F., & Perrillo, J. B. (1994). Replacement of the aortic root with a pulmonary autograft in children and young adults with aortic-valve disease. *N Engl J Med, 330*(1), 1-6.

Kouchoukos, N. T., Masetti, P., Nickerson, N. J., Castner, C. F., Shannon, W. D., & Davila-Roman, V. G. (2004). The Ross procedure: long-term clinical and echocardiographic follow-up. *Ann Thorac Surg, 78*(3), 773-781; discussion 773-781.

Ku, C. H., Johnson, P. H., Batten, P., Sarathchandra, P., Chambers, R. C., Taylor, P. M., et al. (2006). Collagen synthesis by mesenchymal stem cells and aortic valve interstitial cells in response to mechanical stretch. *Cardiovasc Res, 71*(3), 548-556.

Kulik, A., Bedard, P., Lam, B. K., Rubens, F. D., Hendry, P. J., Masters, R. G., et al. (2006). Mechanical versus bioprosthetic valve replacement in middle-aged patients. *Eur J Cardiothorac Surg, 30*(3), 485-491.

Kumar, S., Maxwell, I. Z., Heisterkamp, A., Polte, T. R., Lele, T. P., Salanga, M., et al. (2006). Viscoelastic retraction of single living stress fibers and its impact on cell shape, cytoskeletal organization, and extracellular matrix mechanics. *Biophys J, 90*(10), 3762-3773.

Kunzelman, K. S., Grande, K. J., David, T. E., Cochran, R. P., & Verrier, E. D. (1994). Aortic root and valve relationships. Impact on surgical repair. *J Thorac Cardiovasc Surg, 107*(1), 162-170.

Kvidal, P., Bergstrom, R., Horte, L. G., & Stahle, E. (2000). Observed and relative survival after aortic valve replacement. *J Am Coll Cardiol, 35*(3), 747-756.

Lansac, E., Lim, H. S., Shomura, Y., Lim, K. H., Goetz, W., Rice, N. T., et al. (2002). Aortic and pulmonary root: are their dynamics similar? *Eur J Cardiothorac Surg, 21*(2), 268-275.

Lansac, E., Lim, H. S., Shomura, Y., Lim, K. H., Rice, N. T., Goetz, W., et al. (2002). A four-dimensional study of the aortic root dynamics. *Eur J Cardiothorac Surg, 22*(4), 497-503.

Lansac, E., Lim, H. S., Shomura, Y., Lim, K. H., Rice, N. T., Goetz, W. A., et al. (2005). Aortic root dynamics are asymmetric. *J Heart Valve Dis, 14*(3), 400-407.

Latif, N., Sarathchandra, P., Taylor, P. M., Antoniw, J., Brand, N., & Yacoub, M. H. (2006). Characterization of molecules mediating cell-cell communication in human cardiac valve interstitial cells. *Cell Biochem Biophys, 45*(3), 255-264.

Latif, N., Sarathchandra, P., Thomas, P. S., Antoniw, J., Batten, P., Chester, A. H., et al. (2007). Characterization of structural and signaling molecules by human valve interstitial cells and comparison to human mesenchymal stem cells. *J Heart Valve Dis, 16*(1), 56-66.

Laufs, U., La Fata, V., Plutzky, J., & Liao, J. K. (1998). Upregulation of Endothelial Nitric Oxide Synthase by HMG CoA Reductase Inhibitors. *Circulation, 97*(12), 1129-1135.

Laufs, U., & Liao, J. K. (1998). Post-transcriptional Regulation of Endothelial Nitric Oxide Synthase mRNA Stability by Rho GTPase. *Journal of Biological Chemistry, 273*(37), 24266-24271.

Leask, A. (2007). TGFÎ², cardiac fibroblasts, and the fibrotic response. *Cardiovascular Research, 74*(2), 207-212.

Lee, T. C., Zhao, Y. D., Courtman, D. W., & Stewart, D. J. (2000). Abnormal aortic valve development in mice lacking endothelial nitric oxide synthase. *Circulation, 101*(20), 2345-2348.

Lentink, D., Muller, U. K., Stamhuis, E. J., de Kat, R., van Gestel, W., Veldhuis, L. L., et al. (2007). How swifts control their glide performance with morphing wings. *Nature, 446*(7139), 1082-1085.

Liberman, M., Bassi, E., Martinatti, M. K., Lario, F. C., Wosniak, J., Jr., Pomerantzeff, P. M. A., et al. (2008). Oxidant Generation Predominates Around Calcifying Foci and Enhances Progression of Aortic Valve Calcification. *Arterioscler Thromb Vasc Biol, 28*(3), 463-470.

Lincoln, T. M., Komalavilas, P., & Cornwell, T. L. (1994). Pleiotropic regulation of vascular smooth muscle tone by cyclic GMP-dependent protein kinase. *Hypertension, 23*(6 Pt 2), 1141-1147.

Liu, A. C., Joag, V. R., & Gotlieb, A. I. (2007). The emerging role of valve interstitial cell phenotypes in regulating heart valve pathobiology. *Am J Pathol, 171*(5), 1407-1418.

Loeys, B. L., Schwarze, U., Holm, T., Callewaert, B. L., Thomas, G. H., Pannu, H., et al. (2006). Aneurysm syndromes caused by mutations in the TGF-beta receptor. *N Engl J Med, 355*(8), 788-798.

Lopez-Quintero, S. V., Amaya, R., Pahakis, M., & Tarbell, J. M. (2009). The endothelial glycocalyx mediates shear-induced changes in hydraulic conductivity. *Am J Physiol Heart Circ Physiol, 296*(5), H1451-1456.

Lu, Q., Harrington, E. O., Jackson, H., Morin, N., Shannon, C., & Rounds, S. (2006). Transforming growth factor-beta1-induced endothelial barrier dysfunction involves Smad2-dependent p38 activation and subsequent RhoA activation. *J Appl Physiol, 101*(2), 375-384.

Lund, O., Chandrasekaran, V., Grocott-Mason, R., Elwidaa, H., Mazhar, R., Khaghani, A., et al. (1999). Primary aortic valve replacement with allografts over twenty-five years: valve-related and procedure-related determinants of outcome. *J Thorac Cardiovasc Surg, 117*(1), 77-90; discussion 90-71.

Luo, Y., Xu, X., Lele, T., Kumar, S., & Ingber, D. E. (2008). A multi-modular tensegrity model of an actin stress fiber. *J Biomech, 41*(11), 2379-2387.

Luscher, T. F. (1992). Endothelin: systemic arterial and pulmonary effects of a new peptide with potent biologic properties. *Am Rev Respir Dis, 146*(5 Pt 2), S56-60.

Luscher, T. F., Yang, Z., Tschudi, M., von Segesser, L., Stulz, P., Boulanger, C., et al. (1990). Interaction between endothelin-1 and endothelium-derived relaxing factor in human arteries and veins. *Circ Res, 66*(4), 1088-1094.

Marron, K., Yacoub, M. H., Polak, J. M., Sheppard, M. N., Fagan, D., Whitehead, B. F., et al. (1996). Innervation of human atrioventricular and arterial valves. *Circulation, 94*(3), 368-375.

Mathieu, P., Voisine, P., Pepin, A., Shetty, R., Savard, N., & Dagenais, F. (2005). Calcification of human valve interstitial cells is dependent on alkaline phosphatase activity. *J Heart Valve Dis, 14*(3), 353-357.

Matsumoto, Y., Adams, V., Jacob, S., Mangner, N., Schuler, G., & Linke, A. (2010). Regular Exercise Training Prevents Aortic Valve Disease in Low-Density Lipoprotein-Receptor-Deficient Mice. *Circulation, 121*(6), 759-767.

Merryman, W. D., Huang, H. Y., Schoen, F. J., & Sacks, M. S. (2006). The effects of cellular contraction on aortic valve leaflet flexural stiffness. *J Biomech, 39*(1), 88-96.

Merryman, W. D., Youn, I., Lukoff, H. D., Krueger, P. M., Guilak, F., Hopkins, R. A., et al. (2006). Correlation between heart valve interstitial cell stiffness and transvalvular pressure: implications for collagen biosynthesis. *Am J Physiol Heart Circ Physiol, 290*(1), H224-231.

Miller, J. D., Chu, Y., Brooks, R. M., Richenbacher, W. E., Peña-Silva, R., & Heistad, D. D. (2008). Dysregulation of Antioxidant Mechanisms Contributes to Increased Oxidative Stress in Calcific Aortic Valvular Stenosis in Humans. *Journal of the American College of Cardiology, 52*(10), 843-850.

Misfeld, M., Morrison, K., Sievers, H., Yacoub, M. H., & Chester, A. H. (2002). Localization of immunoreactive endothelin and characterization of its receptors in aortic cusps. *J Heart Valve Dis, 11*(4), 472-476; discussion 476-477.

Mitchell, R. N., Jonas, R. A., & Schoen, F. J. (1998). Pathology of explanted cryopreserved allograft heart valves: comparison with aortic valves from orthotopic heart transplants. *J Thorac Cardiovasc Surg, 115*(1), 118-127.

Mohler, E. R., 3rd. (2004). Mechanisms of aortic valve calcification. *Am J Cardiol, 94*(11), 1396-1402, A1396.

Mohler, E. R., 3rd, Chawla, M. K., Chang, A. W., Vyavahare, N., Levy, R. J., Graham, L., et al. (1999). Identification and characterization of calcifying valve cells from human and canine aortic valves. *J Heart Valve Dis, 8*(3), 254-260.

Mookhoek, A., de Heer, E., Bogers, A. J., Takkenberg, J. J., & Schoof, P. H. (2010). Pulmonary autograft valve explants show typical degeneration. *J Thorac Cardiovasc Surg, 139*(6), 1416-1419.

Murad, F. (2006). Shattuck Lecture. Nitric oxide and cyclic GMP in cell signaling and drug development. *N Engl J Med, 355*(19), 2003-2011.

Neptune, E. R., Frischmeyer, P. A., Arking, D. E., Myers, L., Bunton, T. E., Gayraud, B., et al. (2003). Dysregulation of TGF-beta activation contributes to pathogenesis in Marfan syndrome. *Nat Genet, 33*(3), 407-411.

Ngo, D. T. M., Heresztyn, T., Mishra, K., Marwick, T. H., & Horowitz, J. D. (2007). Aortic stenosis is associated with elevated plasma levels of asymmetric dimethylarginine (ADMA). *Nitric Oxide, 16*(2), 197-201.

Ngo, D. T. M., Stafford, I., Kelly, D. J., Sverdlov, A. L., Wuttke, R. D., Weedon, H., et al. (2008). Vitamin D2 supplementation induces the development of aortic stenosis in rabbits: Interactions with endothelial function and thioredoxin-interacting protein. *European Journal of Pharmacology, 590*(1-3), 290-296.

Niessen, K., & Karsan, A. (2008). Notch signaling in cardiac development. *Circ Res, 102*(10), 1169-1181.

Nikolaev, V. O., Moshkov, A., Lyon, A. R., Miragoli, M., Novak, P., Paur, H., et al. (2010). Beta2-adrenergic receptor redistribution in heart failure changes cAMP compartmentation. *Science, 327*(5973), 1653-1657.

Novak, P., Li, C., Shevchuk, A. I., Stepanyan, R., Caldwell, M., Hughes, S., et al. (2009). Nanoscale live-cell imaging using hopping probe ion conductance microscopy. *Nat Methods, 6*(4), 279-281.

O'Brien, K. D. (2006). Pathogenesis of calcific aortic valve disease: a disease process comes of age (and a good deal more). *Arterioscler Thromb Vasc Biol, 26*(8), 1721-1728.

O'Brien, M. F., Harrocks, S., Stafford, E. G., Gardner, M. A., Pohlner, P. G., Tesar, P. J., et al. (2001). The homograft aortic valve: a 29-year, 99.3% follow up of 1,022 valve replacements. *J Heart Valve Dis, 10*(3), 334-344; discussion 335.

ONS. Office of National Statistics Annual Life Tables. 1980-2 to 2005-7, http://www.statistics.gov.uk/StatBase/Product.asp?vlnk=14459.

Osman, L., Chester, A. H., Sarathchandra, P., Latif, N., Meng, W., Taylor, P. M., et al. (2007). A novel role of the sympatho-adrenergic system in regulating valve calcification. *Circulation, 116*(11 Suppl), I282-287.

Osman, L., Yacoub, M. H., Latif, N., Amrani, M., & Chester, A. H. (2006). Role of Human Valve Interstitial Cells in Valve Calcification and Their Response to Atorvastatin. *Circulation, 114*(1_suppl), I-547-552.

Osman, L., Yacoub, M. H., Latif, N., Amrani, M., & Chester, A. H. (2006). Role of human valve interstitial cells in valve calcification and their response to atorvastatin. *Circulation, 114*(1 Suppl), I547-552.

Otto, C. M., Kuusisto, J., Reichenbach, D. D., Gown, A. M., & O'Brien, K. D. (1994). Characterization of the early lesion of 'degenerative' valvular aortic stenosis. Histological and immunohistochemical studies. *Circulation, 90*(2), 844-853.

Pahakis, M. Y., Kosky, J. R., Dull, R. O., & Tarbell, J. M. (2007). The role of endothelial glycocalyx components in mechanotransduction of fluid shear stress. *Biochem Biophys Res Commun, 355*(1), 228-233.

Paranya, G., Vineberg, S., Dvorin, E., Kaushal, S., Roth, S. J., Rabkin, E., et al. (2001). Aortic valve endothelial cells undergo transforming growth factor-beta-mediated and non-transforming growth factor-beta-mediated transdifferentiation in vitro. *Am J Pathol, 159*(4), 1335-1343.

Parkington, H. C., Tonta, M. A., Coleman, H. A., & Tare, M. (1995). Role of membrane potential in endothelium-dependent relaxation of guinea-pig coronary arterial smooth muscle. *J Physiol, 484 (Pt 2)*, 469-480.

Partridge, J., Carlsen, H., Enesa, K., Chaudhury, H., Zakkar, M., Luong, L., et al. (2007). Laminar shear stress acts as a switch to regulate divergent functions of NF-kappaB in endothelial cells. *FASEB J, 21*(13), 3553-3561.

Passerini, A. G., Polacek, D. C., Shi, C., Francesco, N. M., Manduchi, E., Grant, G. R., et al. (2004). Coexisting proinflammatory and antioxidative endothelial transcription profiles in a disturbed flow region of the adult porcine aorta. *Proc Natl Acad Sci U S A, 101*(8), 2482-2487.

Peltonen, T., Taskinen, P., NÃ¤pÃ¤nkangas, J., Leskinen, H., Ohtonen, P., Soini, Y., et al. (2009). Increase in tissue endothelin-1 and ETA receptor levels in human aortic valve stenosis. *European Heart Journal, 30*(2), 242-249.

Perry, G. J., Helmcke, F., Nanda, N. C., Byard, C., & Soto, B. (1987). Evaluation of aortic insufficiency by Doppler color flow mapping. *J Am Coll Cardiol, 9*(4), 952-959.

Poggianti, E., Venneri, L., Chubuchny, V., Jambrik, Z., Baroncini, L. A., & Picano, E. (2003). Aortic valve sclerosis is associatedwith systemic endothelial dysfunction. *Journal of the American College of Cardiology, 41*(1), 136-141.

Rabkin-Aikawa, E., Aikawa, M., Farber, M., Kratz, J. R., Garcia-Cardena, G., Kouchoukos, N. T., et al. (2004). Clinical pulmonary autograft valves: pathologic evidence of adaptive remodeling in the aortic site. *J Thorac Cardiovasc Surg, 128*(4), 552-561.

Rabkin-Aikawa, E., Farber, M., Aikawa, M., & Schoen, F. J. (2004). Dynamic and reversible changes of interstitial cell phenotype during remodeling of cardiac valves. *J Heart Valve Dis, 13*(5), 841-847.

Rabkin, E., Aikawa, M., Stone, J. R., Fukumoto, Y., Libby, P., & Schoen, F. J. (2001). Activated Interstitial Myofibroblasts Express Catabolic Enzymes and Mediate Matrix Remodeling in Myxomatous Heart Valves. *Circulation, 104*(21), 2525-2532.

Rajamannan, N. M., Caplice, N., Anthikad, F., Sebo, T. J., Orszulak, T. A., Edwards, W. D., et al. (2001). Cell proliferation in carcinoid valve disease: a mechanism for serotonin effects. *J Heart Valve Dis, 10*(6), 827-831.

Rajamannan, N. M., Subramaniam, M., Stock, S. R., Stone, N. J., Springett, M., Ignatiev, K. I., et al. (2005). Atorvastatin inhibits calcification and enhances nitric oxide synthase production in the hypercholesterolaemic aortic valve. *Heart, 91*(6), 806-810.

Reynolds, J. L., Joannides, A. J., Skepper, J. N., McNair, R., Schurgers, L. J., Proudfoot, D., et al. (2004). Human vascular smooth muscle cells undergo vesicle-mediated calcification in response to changes in extracellular calcium and phosphate concentrations: a potential mechanism for accelerated vascular calcification in ESRD. *J Am Soc Nephrol, 15*(11), 2857-2867.

Roberts, W. C. (1970). The congenitally bicuspid aortic valve. A study of 85 autopsy cases. *Am J Cardiol, 26*(1), 72-83.

Robicsek, F., & Thubrikar, M. J. (1999). Role of sinus wall compliance in aortic leaflet function. *Am J Cardiol, 84*(8), 944-946, A947.

Ross, J., Jr., & Braunwald, E. (1968). Aortic stenosis. *Circulation, 38*(1 Suppl), 61-67.

Rothman, R. B., Baumann, M. H., Savage, J. E., Rauser, L., McBride, A., Hufeisen, S. J., et al. (2000). Evidence for possible involvement of 5-HT(2B) receptors in the cardiac valvulopathy associated with fenfluramine and other serotonergic medications. *Circulation, 102*(23), 2836-2841.

Roy, A., Brand, N. J., & Yacoub, M. H. (2000). Expression of 5-hydroxytryptamine receptor subtype messenger RNA in interstitial cells from human heart valves. *J Heart Valve Dis, 9*(2), 256-260; discussion 260-251.

Sacks, M. S., & Yoganathan, A. P. (2007). Heart valve function: a biomechanical perspective. *Philos Trans R Soc Lond B Biol Sci, 362*(1484), 1369-1391.

Sanchez, D., Johnson, N., Li, C., Novak, P., Rheinlaender, J., Zhang, Y., et al. (2008). Noncontact measurement of the local mechanical properties of living cells using pressure applied via a pipette. *Biophys J, 95*(6), 3017-3027.

Saura, M., Zaragoza, C., Herranz, B., Griera, M., Diez-Marques, L., Rodriguez-Puyol, D., et al. (2005). Nitric Oxide Regulates Transforming Growth Factor-{beta} Signaling in Endothelial Cells. *Circ Res, 97*(11), 1115-1123.

Selemidis, S., Dusting, G. J., Peshavariya, H., Kemp-Harper, B. K., & Drummond, G. R. (2007). Nitric oxide suppresses NADPH oxidase-dependent superoxide production by S-nitrosylation in human endothelial cells. *Cardiovascular Research, 75*(2), 349-358.

Shimada, T., Murakami, Y., Hashimoto, M., Ishibashi, Y., Inoue, S.-I., Katoh, H., et al. (1999). Impairment of serotonin-mediated nitric oxide release across the coronary bed in patients with coronary spastic angina. *The American Journal of Cardiology, 83*(6), 953-955.

Shimokawa, H. (1998). Endothelial dysfunction in hypertension. *J Atheroscler Thromb, 4*(3), 118-127.

Shyu, K.-G. (2009). Cellular and molecular effects of mechanical stretch on vascular cells and cardiac myocytes. *Clinical Science, 116*(5), 377-389.

Sievers, H. H., Hanke, T., Stierle, U., Bechtel, M. F., Graf, B., Robinson, D. R., et al. (2006). A critical reappraisal of the Ross operation: renaissance of the subcoronary implantation technique? *Circulation, 114*(1 Suppl), I504-511.

Simmons, C. A., Grant, G. R., Manduchi, E., & Davies, P. F. (2005). Spatial heterogeneity of endothelial phenotypes correlates with side-specific vulnerability to calcification in normal porcine aortic valves. *Circ Res, 96*(7), 792-799.

Simmons, C. A., Zilberberg, J., & Davies, P. F. (2004). A rapid, reliable method to isolate high quality endothelial RNA from small spatially-defined locations. *Ann Biomed Eng, 32*(10), 1453-1459.

Smedira, N. G., Blackstone, E. H., Roselli, E. E., Laffey, C. C., & Cosgrove, D. M. (2006). Are allografts the biologic valve of choice for aortic valve replacement in nonelderly patients? Comparison of explantation for structural valve deterioration of allograft and pericardial prostheses. *J Thorac Cardiovasc Surg, 131*(3), 558-564 e554.

Stassano, P., Di Tommaso, L., Monaco, M., Iorio, F., Pepino, P., Spampinato, N., et al. (2009). Aortic valve replacement: a prospective randomized evaluation of mechanical versus biological valves in patients ages 55 to 70 years. *J Am Coll Cardiol, 54*(20), 1862-1868.

Steele, P. A., Gibbins, I. L., & Morris, J. L. (1996). Projections of intrinsic cardiac neurons to different targets in the guinea-pig heart. *J Auton Nerv Syst, 56*(3), 191-200.

Stella, J. A., Liao, J., & Sacks, M. S. (2007). Time-dependent biaxial mechanical behavior of the aortic heart valve leaflet. *J Biomech, 40*(14), 3169-3177.

Stella, J. A., & Sacks, M. S. (2007). On the biaxial mechanical properties of the layers of the aortic valve leaflet. *J Biomech Eng, 129*(5), 757-766.

Sucosky, P., Balachandran, K., Elhammali, A., Jo, H., & Yoganathan, A. P. (2009). Altered shear stress stimulates upregulation of endothelial VCAM-1 and ICAM-1 in a BMP-4- and TGF-beta1-dependent pathway. *Arterioscler Thromb Vasc Biol, 29*(2), 254-260.

Sucosky, P., Padala, M., Elhammali, A., Balachandran, K., Jo, H., & Yoganathan, A. P. (2008). Design of an ex vivo culture system to investigate the effects of shear stress on cardiovascular tissue. *J Biomech Eng, 130*(3), 035001.

Svensson, L. G., Blackstone, E. H., & Cosgrove, D. M. (2003). Surgical options in young adults with aortic valve disease. *Current Problems in Cardiology, 28*(7), 417-480.

Takkenberg, J. J., van Herwerden, L. A., Galema, T. W., Bekkers, J. A., Kleyburg-Linkers, V. E., Eijkemans, M. J., et al. (2006). Serial echocardiographic assessment of neo-aortic regurgitation and root dimensions after the modified Ross procedure. *J Heart Valve Dis, 15*(1), 100-106; discussion 106-107.

Taylor, P. M., Allen, S. P., & Yacoub, M. H. (2000). Phenotypic and functional characterization of interstitial cells from human heart valves, pericardium and skin. *J Heart Valve Dis, 9*(1), 150-158.

Thorin, E., Cernacek, P., & Dupuis, J. (1998). Endothelin-1 regulates tone of isolated small arteries in the rat: effect of hyperendothelinemia. *Hypertension, 31*(4), 1035-1041.

Thorin, E., Nguyen, T. D., & Bouthillier, A. (1998). Control of vascular tone by endogenous endothelin-1 in human pial arteries. *Stroke, 29*(1), 175-180.

Thubrikar, M., & Eppink, R. T. (1982). A method for analysis of bending and shearing deformations in biological tissue. *J Biomech, 15*(7), 529-535.

Thubrikar, M., Skinner, J. R., Aouad, J., Finkelmeier, B. A., & Nolan, S. P. (1982). Analysis of the design and dynamics of aortic bioprostheses in vivo. *J Thorac Cardiovasc Surg, 84*(2), 282-290.

Thubrikar, M. J., Aouad, J., & Nolan, S. P. (1986). Comparison of the in vivo and in vitro mechanical properties of aortic valve leaflets. *J Thorac Cardiovasc Surg, 92*(1), 29-36.

Thubrikar, M. J., Nolan, S. P., Aouad, J., & Deck, J. D. (1986). Stress sharing between the sinus and leaflets of canine aortic valve. *Ann Thorac Surg, 42*(4), 434-440.

Tops, L. F., Wood, D. A., Delgado, V., Schuijf, J. D., Mayo, J. R., Pasupati, S., et al. (2008). Noninvasive evaluation of the aortic root with multislice computed tomography implications for transcatheter aortic valve replacement. *JACC Cardiovasc Imaging, 1*(3), 321-330.

Towler, D. A. (2008). Oxidation, Inflammation, and Aortic Valve Calcification: Peroxide Paves an Osteogenic Path. *Journal of the American College of Cardiology, 52*(10), 851-854.

Tschudi, M., Richard, V., Buhler, F. R., & Luscher, T. F. (1991). Importance of endothelium-derived nitric oxide in porcine coronary resistance arteries. *Am J Physiol, 260*(1 Pt 2), H13-20.

van Geldorp, M. W. A., Eric Jamieson, W. R., Kappetein, A. P., Ye, J., Fradet, G. J., Eijkemans, M. J. C., et al. (2009). Patient outcome after aortic valve replacement with a mechanical or biological prosthesis: Weighing lifetime anticoagulant-related event risk against reoperation risk. *The Journal of Thoracic and Cardiovascular Surgery, 137*(4), 881-886.e885.

Vanhoutte, P. M. (1991). Platelet-Derived Serotonin, the Endothelium, and Cardiovascular Disease. *Journal of Cardiovascular Pharmacology, 17*, S13.

Vasan, R. S., Glazer, N. L., Felix, J. F., Lieb, W., Wild, P. S., Felix, S. B., et al. (2009). Genetic variants associated with cardiac structure and function: a meta-analysis and replication of genome-wide association data. *JAMA, 302*(2), 168-178.

Vollebergh, F. E., & Becker, A. E. (1977). Minor congenital variations of cusp size in tricuspid aortic valves. Possible link with isolated aortic stenosis. *Br Heart J, 39*(9), 1006-1011.

Walker, G. A., Masters, K. S., Shah, D. N., Anseth, K. S., & Leinwand, L. A. (2004). Valvular Myofibroblast Activation by Transforming Growth Factor-{beta}: Implications for Pathological Extracellular Matrix Remodeling in Heart Valve Disease. *Circ Res, 95*(3), 253-260.

Wang, N., Butler, J. P., & Ingber, D. E. (1993). Mechanotransduction across the cell surface and through the cytoskeleton. *Science, 260*(5111), 1124-1127.

Wang, N., Tytell, J. D., & Ingber, D. E. (2009). Mechanotransduction at a distance: mechanically coupling the extracellular matrix with the nucleus. *Nat Rev Mol Cell Biol, 10*(1), 75-82.

Wernersson, R., Schierup, M., Jorgensen, F., Gorodkin, J., Panitz, F., Staerfeldt, H.-H., et al. (2005). Pigs in sequence space: A 0.66X coverage pig genome survey based on shotgun sequencing. *BMC Genomics, 6*(1), 70.

White, C. R., & Frangos, J. A. (2007). The shear stress of it all: the cell membrane and mechanochemical transduction. *Philos Trans R Soc Lond B Biol Sci, 362*(1484), 1459-1467.

Wolinsky, H. (1970). Comparison of medial growth of human thoracic and abdominal aortas. *Circ Res, 27*(4), 531-538.

Wolinsky, H., & Glagov, S. (1967). A lamellar unit of aortic medial structure and function in mammals. *Circ Res, 20*(1), 99-111.

Yacoub, M., & Nerem, R. (2007). Introduction. Bioengineering the heart. *Philos Trans R Soc Lond B Biol Sci, 362*(1484), 1253-1255.

Yacoub, M., Rasmi, N. R., Sundt, T. M., Lund, O., Boyland, E., Radley-Smith, R., et al. (1995). Fourteen-year experience with homovital homografts for aortic valve replacement. *J Thorac Cardiovasc Surg, 110*(1), 186-193; discussion 193-184.

Yacoub, M. H., El-Hamamsy, I., Said, K., Magdi, G., Abul Enein, F., George, R., et al. (2009). The left ventricular outflow in hypertrophic cardiomyopathy: from structure to function. *Journal of Cardiovascular Translational Research, 2*, 510-517.

Yacoub, M. H., Kilner, P. J., Birks, E. J., & Misfeld, M. (1999). The aortic outflow and root: a tale of dynamism and crosstalk. *Ann Thorac Surg, 68*(3 Suppl), S37-43.

Yacoub, M. H., Klieverik, L. M., Melina, G., Edwards, S. E., Sarathchandra, P., Bogers, A. J., et al. (2006). An evaluation of the Ross operation in adults. *J Heart Valve Dis, 15*(4), 531-539.

Yacoub, M. H., & Takkenberg, J. J. (2005). Will heart valve tissue engineering change the world? *Nat Clin Pract Cardiovasc Med, 2*(2), 60-61.

Yanagisawa, M., Kurihara, H., Kimura, S., Tomobe, Y., Kobayashi, M., Mitsui, Y., et al. (1988). A novel potent vasoconstrictor peptide produced by vascular endothelial cells. *Nature, 332*(6163), 411-415.

Yano, K., Gale, D., Massberg, S., Cheruvu, P. K., Monahan-Earley, R., Morgan, E. S., et al. (2007). Phenotypic heterogeneity is an evolutionarily conserved feature of the endothelium. *Blood, 109*(2), 613-615.

Yip, C. Y. Y., Chen, J.-H., Zhao, R., & Simmons, C. A. (2009). Calcification by Valve Interstitial Cells Is Regulated by the Stiffness of the Extracellular Matrix. *Arterioscler Thromb Vasc Biol, 29*(6), 936-942.

Zimmerman, J. (1966). The functional and surgical anatomy of the heart. *Ann R Coll Surg Engl, 39*(6), 348-366.

Annex X Short form (SF-36) quality of life questionnaire sent to patients.

For each of the following questions, please mark with an (X) the best answer that describes your condition

GENERAL HEALTH

1) In general, would you say your health is:

( ) Excellent
( ) Very good
( ) Good
( ) Fair
( ) Poor

2) Compared to one year ago, how would you rate your health in general now?

( ) Much better now than one year ago
( ) Somewhat better now than one year ago
( ) About the same as one year ago
( ) Somewhat worse now than one year ago
( ) Much worse now than one year ago

HEALTH and DAILY ACTIVITES

3) The following questions are about activities you might do during a typical day. Does your health now limit you in these activities? If so, how much?

	Yes, limited a lot	Yes, limited a little	No, not limited at all
• Vigorous activities, such as running, lifting heavy objects, participating in strenuous sports	( )	( )	( )
• Moderate activities, such as moving a table, pushing a vacuum cleaner, bowling, or playing golf	( )	( )	( )
• Lifting or carrying groceries	( )	( )	( )
• Climbing several flights of stairs	( )	( )	( )
• Climbing one flight of stairs	( )	( )	( )
• Bending, kneeling, or stooping	( )	( )	( )

- **Walking more than a mile…….……..( )……..( )…….( )**
- **Walking several hundred yards…….( )……..( )…….( )**
- **Walking one hundred yards……..…….( )……..( )…….( )**
- **Bathing or dressing yourself…..…….( )……..( )…….( )**

4) During the past 4 weeks, have you had any of the following problems with your work or other regular daily activities as a result of your physical health?

	YES	NO
• **Cut down on the amount of time you spent on work or other activities…….……..**	**( )**	**( )**
• **Accomplished less than you would like…….…….....**	**( )**	**( )**
• **Were limited in the kind of work or other activities……**	**( )**	**( )**
• **Had difficulty performing the work or other activities (for example, it took extra effort) ……..……..…….....**	**( )**	**( )**

5) During the past 4 weeks, have you had any of the following problems with your work or other regular daily activities as a result of any emotional problems (such as feeling depressed or anxious)?

	YES	NO
• **Cut down on the amount of time you spent on Work or other activities……**	**( )**	**( )**
• **Accomplished less than you would like…….**	**( )**	**( )**
• **Did work or other activities less carefully than usually……**	**( )**	**( )**

6) During the past 4 weeks, to what extent has your physical health or emotional problems interfered with your normal social activities with family, friends, neighbours, or groups?

( ) Not at all
( ) Slightly
( ) Moderately
( ) Quite a bit
( ) Extremely

7) How much bodily pain have you had during the past 4 weeks?

( ) None
( ) Very mild

( ) Mild
( ) Moderate
( ) Severe
( ) Very severe

8) During the past 4 weeks, how much did pain interfere with your normal work (including both work outside the home and housework)?

( ) Not at all
( ) A little bit
( ) Moderately
( ) Quite a bit
( ) Extremely

9) These questions are about how you feel and how things have been with you during the past 4 weeks. For each question, please give the one answer that comes closer to the way you have been feeling.

10) How much time during the past 4 weeks…..

	All of the time	Most of the time	A good bit of the time	Some of the time	A little of the time	None of the time
• Did you feel full of life?	( )	( )	( )	( )	( )	( )
• Have you been a very nervous person?	( )	( )	( )	( )	( )	( )
• Have you felt so down in the dumps that nothing could cheer you up	( )	( )	( )	( )	( )	( )
• Have you felt calm and peaceful?	( )	( )	( )	( )	( )	( )
• Did you have a lot of energy?	( )	( )	( )	( )	( )	( )
• Have you felt downhearted and blue?	( )	( )	( )	( )	( )	( )
• Did you feel worn out?	( )	( )	( )	( )	( )	( )
• Have you been a happy person?	( )	( )	( )	( )	( )	( )
• Did you feel tired?	( )	( )	( )	( )	( )	( )

11) During the past 4 weeks, how much of the time has your physical health or emotional problems interfered with your social activities (like visiting friends, relatives, etc…)?

( ) All of the time
( ) Most of the time
( ) Some of the time
( ) A little of the time
( ) None of the time

HEALTH in GENERAL

12) How TRUE or FALSE is each of the following statements for you?

	Definitely true	Mostly true	Don't know	Mostly false	Definitely false
• I seem sick a little easier than other people	( )	( )	( )	( )	( )
• I am as healthy as anybody I know	( )	( )	( )	( )	( )
• I expect my health to get worse	( )	( )	( )	( )	( )
• My health is excellent	( )	( )	( )	( )	(

EMPLOYMENT SITUATION

Questions 12 -15 are related to your work and employment status. Please complete these questions to the best of your capability?

12-a) Are you employed?

( ) YES – please go to question 13
( ) NO – please go to question 12b

12-b) Are you not working because of?

( ) Child care reasons
( ) Retired – please go to question 12c
( ) Other – please state reason……

12-c) Are you retired on medical grounds?

( ) YES
( ) NO

13) What is your job?

……...

Are you in?
( ) FULL time employment
( ) PART time employment

14) On average how many hours do you work every week?

( ) 0-10 hours
( ) 10-20 hours
( ) 20-25 hours
( ) 26-30 hours
( ) 30-40 hours
( ) 40+ hours

15) How stressful do you find your job?

( ) Not at all
( ) A little stressful
( ) Moderately stressful
( ) Very stressful
( ) Extremely stressful

MEDICATION

Please list your current medication in the space below along with the doses and the frequency of administration. Please use separate sheet if necessary.

Drug	Dose	Number of times per day
1)……..		
2)……..		
3)……..		
4)……..		
5)……..		
6)……..		
7)……..		
8)……..		
9)……..		
10)……		

End

Thank you for completing these questions